

**MODELING THE BEHAVIOR OF SULFUR MODIFIED  
FOAMED AND EMULSIFIED ASPHALT SOILS MIXES FOR  
LOCAL ROAD APPLICATIONS**

BY

**GAMIL MAHYOUB SAIF ABDULLAH**

A Dissertation Presented to the  
DEANSHIP OF GRADUATE STUDIES

**KING FAHD UNIVERSITY OF PETROLEUM & MINERALS**

DHAHRAN, SAUDI ARABIA

In Partial Fulfillment of the  
Requirements for the Degree of

**DOCTOR OF PHILOSOPHY**

In

**CIVIL ENGINEERING**

MAY, 2014

KING FAHD UNIVERSITY OF PETROLEUM & MINERALS

DHAHRAN- 31261, SAUDI ARABIA

**DEANSHIP OF GRADUATE STUDIES**

This thesis, written by **GAMIL MAHYOUB SAIF ABDULLAH** under the direction his thesis advisor and approved by his thesis committee, has been presented and accepted by the Dean of Graduate Studies, in partial fulfillment of the requirements for the degree of **DOCTOR OF PHILOSOPHY IN CIVIL ENGINEERING.**



Dr. Nedal T. Ratrouf  
Department Chairman

25 MAY 2014



Dr. Salam A. Zummo  
Dean of Graduate Studies

5/6/14  
Date



Dr. Hamad I. Al-Abdul Wahhab  
(Advisor)



Dr. Naser A. Al-Shayea  
(Co-Advisor)



Dr. Sahel N. Abduljawwad  
(Member)



Dr. Husain Jubran Al-Gahtani  
(Member)



Dr. Walid S. Al-Sabah  
(Member)

© GAMIL MAHYOUB SAIF ABDULLAH

2014

***DEDICATED TO THE MOST BELOVED PEOPLE IN MY LIFE WHO  
SUPPORTED AND ENCOURAGED ME AND PRAYED FOR ME  
THROUGHOUT MY STUDY***

***MY LATE FATHER***

***MY MOTHER***

***MY BROTHERS AND SISTERS***

***AND TO MY WIFE AND CHILDRENS***

## **ACKNOWLEDGMENTS**

In the name of Allah, the Most Beneficent, the Most Compassionate and His prayer and peace be upon the last and final Messenger “Mohammed”, his family and companions. All praise and gratitude be to Allah who gave me the power and patience to complete this research successfully.

My deep thanks and appreciations go to Dr. Hamad I. Al-Abdul Wahhab, my main dissertation advisor, for his unlimited help, inspiration and support. Thanks are also extended to my co-advisor Dr. Naser A. A-Shayea and all committee members, Dr. Sahel N. Abduljawwad, Dr. Husain Jubran Al-Gahtani and Dr. Walid S. Al-Sabah for their guidance and encouragement.

My acknowledgment and sincere gratitude are due to the King Fahd University of Petroleum and Minerals for providing me facilities during this research.

I want to acknowledge the assistance I received from all the technicians in Highway Laboratory at King Fahd University of Petroleum and Minerals during this research.

Special and sincere recognition and prayers go to my father, God’s mercy on his soul, who supported and encouraged me to achieve this scientific degree. Thanks and appreciations are extended to my mother, brothers, sisters, wife, children, relatives and my entire family for their patience, encouragement and prayers.

# TABLE OF CONTENTS

ACKNOWLEDGMENTS .....	V
TABLE OF CONTENTS.....	VI
LIST OF TABLES .....	X
LIST OF FIGURES .....	XII
LIST OF ABBREVIATIONS.....	XVII
ABSTRACT.....	XVIII
ملخص الرسالة.....	XX
CHAPTER 1 INTRODUCTION .....	1
1.1 GENERAL.....	1
1.2 PROBLEM STATEMENT .....	2
1.3 SIGNIFICANCE OF THIS STUDY .....	3
1.4 OBJECTIVES .....	3
1.5 METHODOLOGY .....	4
1.6 ORGANIZATION OF THE DISSERTATION.....	5
CHAPTER 2 LITERATURE REVIEW .....	6
2.1 SOIL STABILIZATION .....	6
2.2 FOAMED ASPHALT.....	9
2.3 EMULSIFIED ASPHALT .....	14
2.4 SULFUR EXTENDED ASPHALT (SEA).....	17
2.4.1 Environmental Hazards and Safety Aspects of Using Sulfur-Extended Asphalt ..	22

2.5	MODELING OF PERMANENT DEFORMATION.....	24
CHAPTER 3 EXPERIMENTAL PROGRAM.....		36
3.1	INTRODUCTION .....	36
3.2	MATERIALS COLLECTION.....	38
3.2.1	Preparation of Collected Soils .....	38
3.2.2	Asphalt .....	38
3.3	CHARACTERIZATION OF COLLECTED SOIL SAMPLES.....	39
3.3.1	Mineralogical Analyses .....	39
3.3.2	Specific Gravity Test .....	39
3.3.3	Atterberg Limit Tests.....	40
3.3.4	Grain Size Distribution Test .....	40
3.3.5	Modified Proctor Compaction Test .....	41
3.3.6	Soaked California Bearing Ratio Test (CBR).....	41
3.4	FOAMED AND EMULSIFIED ASPHALT MIX DESIGN.....	42
3.4.1	Foamed Asphalt Mix Design .....	42
3.4.2	Emulsified Asphalt Mix design .....	44
3.5	EVALUATION OF DESIGNED MIXES .....	47
3.5.1	Marshall Stability.....	47
3.5.2	Indirect Tensile Strength Test.....	49
3.5.3	Durability Test .....	50
3.5.4	Resilient Modulus Test ( $M_R$ ) .....	52
3.5.5	Static Triaxial Shear Strength Test .....	54
3.5.6	Dynamic Creep Test (Triaxial).....	57

3.5.7 Accelerated Loaded Wheel Test .....	59
3.5.8 Micro-Characterization Study .....	63
CHAPTER 4 RESULTS AND DISCUSSION .....	64
4.1 Characterization of Soils .....	64
4.1.1 Mineralogical Analyses of Soils .....	64
4.1.2 Specific Gravity .....	67
4.1.3 Atterberg Limits .....	67
4.1.4 Grain Size Distribution and Classification of Soils .....	67
4.1.5 Compaction Test .....	70
4.1.6 California Bearing Ratio (CBR) .....	71
4.2 Asphalt Properties .....	72
4.3 Foamed and Sulfur Modified Foamed Asphalt Mixes Evaluation Results .....	73
4.3.1 Design of Foaming Characteristics .....	73
4.3.2 Mixes Design and Evaluation .....	76
4.4 Emulsified and Emulsified Sulfur Asphalt Mixes Evaluation Results .....	98
4.4.1 Marshall Stability Test Results .....	99
4.4.2 Indirect Tensile Strength Test Results .....	102
4.4.3 Static Triaxial Test (Shear Strength) Results .....	104
4.4.4 Dynamic Resilient Modulus Test Results .....	106
4.4.5 Dynamic Triaxial Test .....	110
4.4.6 Dynamic Triaxial Results of Subgrade Soils .....	116
4.4.7 Wheel Tracking Test Results .....	119
4.5 Micro-Characterization .....	122



4.6 Statistical Analysis Results .....	134
4.6.1 Marshall Stability .....	135
4.6.2 Indirect Tensile Strength (ITS) .....	136
4.6.3 Resilient Modulus (MR) .....	136
CHAPTER 5 PREDICTION OF PERMANENT DEFORMATION .....	140
5.1 Prediction of Permanent Deformation Using VESYS Model.....	140
5.2 Validation and Calibration of Rut Depth Prediction Models.....	148
5.3 Development of Pavement Thickness Design Charts .....	157
5.3.1 Cases Analyzed.....	157
5.3.2 Work Results Limitations .....	166
CHAPTER 6 SUMMARY, CONCLUSIONS AND RECOMMENDATIONS .....	167
6.1 Summary .....	167
6.2 Conclusions.....	168
6.3 Recommendations.....	170
6.4 Future Research .....	170
REFERENCES .....	171
APPENDIX A.....	180
APPENDIX B .....	187
Vitae.....	191

## LIST OF TABLES

Table 2-1: Relationships Describing the Variation of Permanent Axial Deformations $\epsilon_1^p$ with the Number of Load Cycles (Hornych and El Abd, 2004 after Lekarp et al. 2000).....	25
Table 2-2: Relationships Describing the Variation of Permanent Axial Deformations with Applied Stresses (Hornych and El Abd, 2004). ....	28
Table 3-1: Experimental Design Matrix .....	48
Table 3-2: Loading Sequence for Resilient Modulus Test [AASHTO T-307].....	55
Table 4-1: Properties of Asphalt Cement.....	73
Table 4-2: Marshall Stability Test Results.....	80
Table 4-3: Cohesion and Angle of Internal Friction for Soils-FA-SFA Mixes. ....	82
Table 4-4: Regression Models of $M_R$ for Foamed Asphalt Mixes.....	87
Table 4-5: Intercept and Slope Coefficients for Tested Foamed Asphalt Mixes.....	94
Table 4-6: Regression Models of a and b Coefficients for Foamed Asphalt Mixes.....	95
Table 4-7: Cohesion and Angle of Internal friction for Soils-EA-SEA Mixes.....	105
Table 4-8: Regression Models of $M_R$ for Emulsified Asphalt Mixes. ....	110
Table 4-9: Intercept and Slope Coefficients for Tested Emulsified Asphalt Mixes. ....	118
Table 4-10: Regression Models of a and b Coefficients for Emulsified asphalt Mixes. ....	119
Table 4-11: Summury of Chemical Composition of Marl Mixes.....	124
Table 4-12: Result of Marshall Stability ANOVA at 5% Significance Level.....	137
Table 4-13: Result of ITS ANOVA at 5% Significance Level.....	138
Table 4-14: Result of MR ANOVA at 5% Significance Level. ....	139
Table 5-1: Permanent Deformation Parameters for Foamed Asphalt Mixes.....	145

Table 5-2: Permanent Deformation Parameters for Emulsified Asphalt Mixes. ....	146
Table 5-3: Regression Models of $\mu$ and $\alpha$ for Foamed Asphalt Mixes. ....	148
Table 5-4: Regression Models of $\mu$ and $\alpha$ for Emulsified Asphalt Mixes. ....	148
Table 5-5: Calibration Factors for $\alpha$ and $\mu$ . ....	150

## LIST OF FIGURES

Figure 2-1: Accumulated Plastic Strains in Pavements (Asphalt Institute, 1996) .....	24
Figure 2-2: Log-Log Form of Power Model (After Khedr, 1986).....	29
Figure 3-1: Experimental Program Flow Chart. ....	37
Figure 3-2: Laboratory Scale Foamed Asphalt Plant WLB 10.....	42
Figure 3-3: Summary of Mix Design Procedure for Foamed Asphalt Treated Mix [Wirtgen, 2004]. ....	43
Figure 3-4: Marshal Stability Apparatus.....	49
Figure 3-5: Indirect Tensile Strength Test Setup.....	51
Figure 3-6: Vacuum Saturation Apparatus. ....	53
Figure 3-7: Sample Setup for Dynamic Resilient Modulus Test.....	56
Figure 3-8: Static Triaxial Test Setup.....	58
Figure 3-9: Dynamic Triaxial Sample Setup. ....	60
Figure 3-10: Dynamic Triaxial Repeated Load Test Setup .....	60
Figure 3-11: Wessex Engineering Wheel Tracker.....	62
Figure 3-12: Some of Cured Slabs before Testing.....	63
Figure 4-1: X-Ray Diffractogram for Marl Soil. ....	65
Figure 4-2: X-Ray Diffractogram for Sabkha Soil. ....	66
Figure 4-3: X-Ray Diffractogram for Sand Soil. ....	66
Figure 4-4: Grain Size Distribution of Marl Soil.....	69
Figure 4-5: Grain Size Distribution of Sabkha Soil.....	69
Figure 4-6: Grain Size Distribution of Sand Soil.....	70
Figure 4-7: Moisture-Dry Density Relationship for Marl and Sabkha Soils. ....	71

Figure 4-8: Moisture-CBR Relationship for Marl and Sabkha Soils.....	72
Figure 4-9: Determination of Optimum Foaming Water Content of Asphalt at 180 °C...	75
Figure 4-10: Determination of Optimum Foaming Water Content of Sulfur Modified Asphalt at 150 oC.....	76
Figure 4-11: Dry and Soaked ITS for Marl Soil. ....	78
Figure 4-12: Dry and Soaked ITS for Sabkha Soil. ....	78
Figure 4-13: Dry and Soaked ITS for Sand Soil.....	79
Figure 4-14: Index of Retained Strength Variation Versus FA and SFA Contents.....	80
Figure 4-15: Mohr-Coulomb Failure Envelope for Soils-FA-SFA Mixes. ....	83
Figure 4-16: Variation of $M_R$ with Deviator Stress for Foam Soils Mixes at 22 °C.....	85
Figure 4-17: Variation of $M_R$ with Deviator Stress for Soils Mixes at 40 ° C.....	86
Figure 4-18: Dynamic Triaxial Test Results for Marl-FA/SFA Tested at 22 °C.....	89
Figure 4-19: Dynamic Triaxial Test Results for Sabkha-FA/SFA Mixes Tested at 22 °C. .....	89
Figure 4-20: Dynamic Triaxial Test Results for Sand-FA/SFA Mixes Tested at 22 °C...	90
Figure 4-21: Dynamic Triaxial Test Results for Marl-FA/SFA Mixes Tested at 40 °C...	91
Figure 4-22: Dynamic Triaxial Test Results for Sabkha –FA/SFA Mixes Tested at 40 °C. .....	91
Figure 4-23: Dynamic Triaxial Test Results for Sand-FA Mixes Tested at 40 °C.....	92
Figure 4-24: Dynamic Triaxial Test Results for Sand-SFA Mixes Tested at 40 °C.....	92
Figure 4-25: Permanent Deformation in Wheel Tracking of FA/SFA Samples.....	96
Figure 4-26: Results of the Permanent Deformation for the Marl-FA/SFA Mixes Using Wheel Track Machine, Dry at 22 oC. ....	97

Figure 4-27: Results of the Permanent Deformation for the Sabkha-FA/SFA Mixes Using Wheel Track Machine, Dry at 22 oC. ....	97
Figure 4-28: Results of the Permanent Deformation for the Sand-FA/SFA Mixes Using Wheel Track Machine, Dry at 22 oC. ....	98
Figure 4-29: Dry and Soaked Stability for Marl Soil. ....	100
Figure 4-30: Dry and Soaked Stability for Sabkha Soil. ....	100
Figure 4-31: Dry and Soaked Stability for Sand Soil. ....	101
Figure 4-32: Retained Stability Variation Versus Residual Asphalt of EA and SEA. ...	101
Figure 4-33: Dry ITS Results for Marl Soil.....	103
Figure 4-34: Dry ITS Results for Sabkha Soil.....	103
Figure 4-35: Dry ITS Results for Sand Soil.....	104
Figure 4-36: Mohr-Coulomb Failure Envelope for Soils-EA/SEA Mixes. ....	106
Figure 4-37: Variation of $M_R$ with Deviator Stress for Soils Mixes at 22 °C.....	109
Figure 4-38: Variation of $M_R$ with Deviator Stress for Soils Mixes at 40 °C.....	109
Figure 4-39: Dynamic Triaxial Test Results for Marl-EA/SEA Mixes at 22 °C.....	111
Figure 4-40: Dynamic Triaxial Test Results for Sabkha-EA/SEA Mixes at 22 °C.....	112
Figure 4-41: Dynamic Triaxial Test Results for Sand-EA/SEA Mixes at 22 °C.....	112
Figure 4-42: Dynamic Triaxial Test Results for Marl-EA/SEA Mixes at 40 °C.....	114
Figure 4-43: Dynamic Triaxial Test Results for Sabkha-EA/SEA Mixes at 40 °C.....	114
Figure 4-44: Dynamic Triaxial Test Results for Sand-EA/SEA Mixes at 40 °C.....	115
Figure 4-45: Dynamic Triaxial Test Results for Subgrade Soils.....	117
Figure 4-46: Permanent Deformation in Wheel Tracking of EA/SEA Samples .....	120

Figure 4-47: Results of the Permanent Deformation for the Marl-EA/SEA Mixes Using Wheel Track Machine, Dry at 22 oC. ....	121
Figure 4-48: Results of the Permanent Deformation for the Sabkha-EA/SEA Mixes Using Wheel Track Machine, Dry at 22 oC. ....	121
Figure 4-49: Results of the Permanent Deformation for the Sand-EA/SEA Mixes Using Wheel Track Machine, Dry at 22 oC. ....	122
Figure 4-50: SEM and EDX for Marl Soil.....	125
Figure 4-51: SEM and EDX for Marl Treated with 2% Cement.....	127
Figure 4-52: SEM and EDX of Marl Treated with FA + 2 % Cement.....	128
Figure 4-53: SEM and EDX of Marl Treated with SFA + 2 % Cement.....	129
Figure 4-54: SEM and EDX of Sand Treated with SFA + 2 % Cement. ....	130
Figure 4-55: SEM for Sabkha Treated with EA and 2% Cement.....	132
Figure 4-56: SEM for Sabkha Treated with SEA and 2% Cement.....	133
Figure 4-57: SEM of Sand Treated with SEA and 2 % Cement.....	134
Figure 5-1: Calculation of Permanent Deformation Parameters ( $\alpha$ and $\mu$ ). ....	144
Figure 5-2: Model Calibration Flowchart. ....	150
Figure 5-3: Measured and Predicted Rutting for Marl-FA/SFA Mixes.....	151
Figure 5-4: Measured and Predicted Rutting for Sabkha-FA/SFA Mixes.....	152
Figure 5-5: Measured and Predicted Rutting for Sand-FA/SFA Mixes. ....	153
Figure 5-6: Measured and Predicted Rutting for Marl-EA/SEA Mixes. ....	154
Figure 5-7: Measured and Predicted Rutting for Sabkha-EA/SEA Mixes. ....	155
Figure 5-8: Measured and Predicted Rutting for Sand-EA/SEA Mixes. ....	156
Figure 5-9: Case 1: Three Layers System-Marl Subgrade.....	157

Figure 5-10: Case 2: Four Layers System-Sabkha Subgrade. ....	158
Figure 5-11: Case 3: Four Layers System- Sand Subgrade. ....	159
Figure 5-12: Relationship between Marl-Foamed Asphalt Base Thickness and Total Traffic-Case 1.....	161
Figure 5-13: Relationship between Marl-Emulsified Asphalt Base Thickness and Total Traffic-Case 1.....	162
Figure 5-14: Relationship between Marl-Foamed Asphalt Base Thickness and Total Traffic-Case 2.....	162
Figure 5-15: Relationship between Sabkha-Foamed Asphalt Base Thickness and Total Traffic-Case 2.....	163
Figure 5-16: Relationship between Marl-Emulsified Asphalt Base Thickness and Total Traffic-Case 2.....	163
Figure 5-17: Relationship between Sabkha-Emulsified Asphalt Base Thickness and Total Traffic-Case 2.....	164
Figure 5-18: Relationship between Marl-Foamed Asphalt Base Thickness and Total Traffic-Case 3.....	164
Figure 5-19: Relationship between Sabkha-Foamed Asphalt Base Thickness and Total Traffic-Case 3.....	165
Figure 5-20: Relationship between Marl-Emulsified Asphalt Base Thickness and Total Traffic-Case 3.....	165
Figure 5-21: Relationship between Sabkha-Emulsified Asphalt Base Thickness and Total Traffic-Case 3.....	166



## **LIST OF ABBREVIATIONS**

ASTM	: American Society for Testing and Material
AASHTO	: American Association of State Highway and Transportation Officials
ITS	: Indirect Tensile Strength
HMA	: Hot Mix Asphalt
FA	: Foamed Asphalt
SFA	: Foamed Sulfur Asphalt
EA	: Emulsified Asphalt
SEA	: Emulsified Sulfur Asphalt
OMC	: Optimum Moisture Content
CBR	: California Bearing Ratio
$M_R$	: Resilient Modulus
ANOVA	: Analysis of Variance
DT	: Dynamic Triaxial Test
WT	: Wheel Track Test
SEM	: Scanning Electron Microscope
XRD	: X-Ray Diffraction

## **ABSTRACT**

Full Name : GAMIL MAHYOUB SAIF ABDULLAH  
Thesis Title : MODELING THE BEHAVIOR OF SULFUR MODIFIED FOAMED  
AND EMULSIFIED ASPHALT SOILS MIXES FOR LOCAL ROAD  
APPLICATIONS  
Major Field : CIVIL ENGINEERING (GEOTECHNICAL/PAVEMENT)  
Date of Degree : MAY, 2014

The rapidly growing population and expansion of industrial facilities in Saudi Arabia has recently led to the construction of huge industrial cities and associated network of roads and airports. One of the typical problems in the construction of roads along the coastal regions of the Arabian Gulf, the red sea, and northern and southern parts of the country is ascribable to the scarcity of good quality soils. This has led to the increased construction cost of road projects which in turn increased the need to search for alternative methods to modify the quality of the vast local marginal soils to be used in construction projects through various soil treatments.

Sulfur is a by-product of oil and gas production and its rate of production is increasing rapidly every year. Although sulfur is a vital raw material to manufacture a myriad of products, its abundance reduced its price worldwide. The storage of the sulfur will pose an environmental hazard. Since sulfur asphalt has proven its advantage when used to build local roads and was utilized to reduce the required asphalt cement up to 30%, therefore, this study looked into the possible usage of new bituminous materials formed using foamed and emulsified asphalts utilizing 30/70 sulfur asphalt in improving

the engineering properties of local soils in the Eastern Province of the Kingdom of Saudi Arabia.

The main objective of this study was to use foamed and emulsified asphalts utilizing 30/70 sulfur asphalt for the stabilization of local indigenous eastern Saudi soils including marl, sabkha and dune sand. To achieve this objective, the optimum binder content of sulfur foamed/emulsified asphalt was optimized and the produced mixes were evaluated using Marshall stability, split tensile strength, durability, resilient modulus, static and dynamic triaxial and wheel tracking tests, and then compared to those prepared with regular foamed and emulsified asphalts. Permanent deformation of stabilized mixes at optimum binder content was modeled and simulated using dynamic triaxial and wheel tracking tests. The developed models were calibrated to predict rutting using VESYS 5W software and develop design charts for local road applications.

Results indicated that the modified sulfur foamed asphalt (SFA) increased the stability and indirect tensile strength (ITS) of the investigated soils. In addition, SFA mixes enhanced the cohesion of the treated soils and increased the rutting resistance compared to conventional foam asphalt (FA) mixes. On the other hand, sulfur emulsion asphalt (SEA) slightly reduced the stability and increased the ITS of the treated soils. Furthermore, the SEA reduced the shear strength and increased the rutting susceptibility of some soils mixes compared to the regular emulsion asphalt (EA).

## ملخص الرسالة

الاسم الكامل: جميل مهيوب سيف عبدالله

عنوان الرسالة: نمذجة سلوك التربة المعالجة برغوة ومستحلب الاسفلت المحسن بالكبريت لاغراض الطرق المحلية

التخصص: هندسة مدنية (جيو تقنية- طرق)

تاريخ الدرجة العلمية: 2014 م

أدت الزيادة السكانية والتوسع العمراني والصناعي في المملكة العربية السعودية الي انشاء العديد من المدن السكنية والصناعية الضخمة وماتتطلبه هذه المدن من شبكات طرق ومطارات و تعتبر ندرة المواد الانشائية الجيدة و المستخدمة في انشاء الطرق على امتداد الخط الساحلي للخليج العربي والبحر الاحمر وكذلك الاجزاء الشمالية والجنوبية من المملكة من ابرز المشاكل والمعوقات التي تؤدي الي زيادة تكلفة مشاريع الطرق والذي بدوره يتطلب مضاعفة الجهود والبحث عن طرق بديلة لتحسين التربة المحلية الضعيفة لاستخدامها في المشاريع الانشائية.

تنتج مادة الكبريت بكميات كبيرة اثناء عملية انتاج النفط والغاز كمادة ثانوية وتزداد معدلات الانتاج سنويا بشكل ملحوظ. وعلى الرغم من ان الكبريت يعتبر مادة خام تستخدم في تصنيع العديد من المنتجات الا ان وفرته ادى الى انخفاض سعره عالميا. لقد اثبت الكبريت فعالية في الخلطات الاسفلتية المستخدمة في انشاء الطرق حيث يمكن استخدامه للحد من كمية الاسفلت بنسبة تصل الى 30%. ولهذا فان هذه الدراسة بحثت في امكانية انتاج واستخدام رغوة ومستحلب الاسفلت المحسن بالكبريت بنسبة 30% في تثبيت وتحسين الخواص الميكانيكية للتربة المحلية في المنطقة الشرقية للمملكة العربية السعودية مثل التربة الجيرية (المارل) والسبخة والرمل ومقارنتها بخلطات رغوة ومستحلب الاسفلت الاعتيادية.

ولتحقيق هذا الهدف تم استخدام طريقة مارشال لتصميم الخلطات الاسفلتية و ايجاد النسب المثلى لرغوة ومستحلب الاسفلت المحسن بالكبريت والاعتيادي ومن ثم تقييم هذه الخلطات باستخدام عدة اختبارات ميكانيكية شملت اختبار قوة مقاومة الانشطار بالشد ونسبة فقدان القوة نتيجة التعرض للماء و معامل المرونة الديناميكي واختبار قوة القص وزاوية الاحتكاك الداخلي واختبار الزحف ( التحدد او التشوه الدائم). كما تم محاكاة ونمذجة التحدد باستخدام اختبار التحميل الديناميكي الثلاثي واختبار العجل للمحاكاة.

اشارت نتائج الدراسة الى ان رغبة الاسفلت المحسنة بالكبريت حسنت خواص الترب (التربة الجيرية و السبخة و الرمل) وزادت من مقاومتها للتخدد مقارنة بالرغوة الاسفلتية العادية. في المقابل وجد ان مستحلب الاسفلت المحسن بالكبريت قد حسن معامل المرونة الديناميكي ومقاومة الانشطار بالشد بينما زاد من قابلية التخدد مقارنة بمستحلب الاسفلت العادي. كما وجد ان النماذج المطورة والمعايرة قادرة على التنبؤ بمقدار التخدد بدقة عالية.

# **CHAPTER 1**

## **INTRODUCTION**

### **1.1 GENERAL**

Due to the rapid growing population and expansion of industrial facilities, Saudi Arabia has been constructing huge industrial cities and associated network of roads and airports. One of the typical problems in the construction of roads along the coastal areas of the Arabian Gulf, the red sea, and northern and southern parts of the country is ascribable to the scarcity of good quality soils. This has led to the increased construction cost of road, projects which in turn increased the need to look for alternative methods to modify the quality of the huge local marginal soils to be used in construction projects through soil stabilization. Several soil treatment stabilizers have been used including cement, lime, asphalt, cement kiln dust, fly ash, acids, enzymes, polymers, ion-modifiers, etc.(Al-Abdul Wahhab et al., 1989, 1994; Asi et al., 1995, 1999; Aiban et al., 1997, 1999; and Abdullah, 2009). Using soil stabilization is to improve the engineering properties of the soil in order to fulfill the project specifications for the intended use.

Foamed and emulsified asphalt were formulated using local asphalt cement and used environmentally friendly and cost-effective solutions for road building (Abdul Wahhab, 1985, 1992; Al-Abdul Wahhab et al., 2006; Al-Abdul Wahhab and Asi, 1993, 1997; Al-

Abdul Wahhab and Hicks, 1988; Asi et al., 1998, 1999, 2002; KFUPM, 2005, 2008). Sulfur is a by-product of oil and gas production and its rate of production is increasing rapidly every year. Saudi Arabia is one of the largest producers of the sulfur, for example, Saudi Aramco produces sulfur at a rate of approximately 6000 ton/day and it is expected to increase to 10,000 ton/day in few years (Baig et al., 2009). Although sulfur is a vital raw material to manufacture a myriad of products, its abundance reduced its price worldwide. The storage of the sulfur will pose an environmental hazard. Thus, constructional usages should be investigated to utilize this abundant sulfur in a useful, economical, and environmental-friendly way. Sulfur asphalt has proven its advantage when used to build local roads and was used to reduce the required asphalt cement up to 30% (KFUPM, 2008) with no short-term or long-term environmental hazards as indicated by the low emission of hazardous gases at road surface temperature as high as 76°C prevailing in Saudi Arabia (Al-Abdul Wahhab and Baig, 2007; Baig et al., 2009). Similarly, sulfur can be used to reduce the binder content of foamed and emulsified asphalt.

## **1.2 PROBLEM STATEMENT**

Due to the shortage in the good quality of construction materials of roads along the coastal regions of the Arabian Gulf, the red sea, and northern and southern part of the country, there is an increase in the construction cost of road projects which in turn increased the need to search for alternative methods to modify the quality of the vast local marginal soils to be used in construction projects through soil treatment.

Since sulfur asphalt has proven its advantage when used to build local roads and was utilized to reduce the required asphalt cement up to 30%, therefore, this study looked into the possible usage of new bituminous materials formed using foamed and emulsified asphalts utilizing 30/70 sulfur asphalt in improving the engineering properties of local soils in the Eastern Province of the Kingdom of Saudi Arabia.

### **1.3 SIGNIFICANCE OF THIS STUDY**

Since sulfur is considered as a by-product of oil and gas production in many petroleum and chemical plants spreading in Saudi Arabia (i.e. Saudi Aramco) and over the entire world, it would be a noble task if these waste materials are being utilized in structural units such as stabilization of indigenous soils. Therefore, an extensive work was done in this study to investigate the possibility of utilizing 30/70 sulfur asphalt to formulate foamed and emulsified asphalt and using in the stabilization of three selected indigenous eastern Saudi soils (namely, dune sand, marl and sabkha).

### **1.4 OBJECTIVES**

The main objectives of this study are:

- To investigate various properties of local indigenous eastern Saudi soils including marl, sabkha and dune sand stabilized with foamed and emulsified asphalts utilizing 30/70 sulfur asphalt.
- To simulate permanent deformation of stabilized soils mixes using dynamic triaxial and wheel tracking tests.



- To develop a model to predict rutting and construct pavement thickness design charts.
- To calibrate and validate the developed model.

## 1.5 METHODOLOGY

To accomplish the objectives of this study, the following tasks were performed:

**Task 1:** in this task the materials used were collected and characterized.

**Task 2:** mixes were designed using Marshall stability, split tensile strength and durability tests.

**Task 3:** the designed mixes were evaluated using, static and dynamic triaxial shear strength, and wheel tracking tests, and then compared to those prepared with regular foamed and emulsified asphalts. The results of such tests are required for the structural design of layers constructed from sulfur foamed bitumen or sulfur emulsified bitumen treated material.

**Task 4:** statistical analyses were performed to test the significance of many factors on the mechanical properties of the stabilized mixes and regression models were also developed.

**Task 5:** models for prediction the permanent deformation of the stabilized mixes were developed based on the dynamic triaxial test results.

**Task 6:** The developed models were calibrated and validated using wheel tracking test results and the pavement thickness design charts were constructed based on the calibrated models.

## **1.6 ORGANIZATION OF THE DISSERTATION**

The dissertation report consists of six chapters. Chapter one is the introduction, significance and objectives of the study. Chapter 2 presents extensive literature review related to the soil stabilization, foamed stabilization, emulsified stabilization, sulfur extended asphalt and modeling of permanent deformation. The experimental work of the study is explained in Chapter 3 while the results of the experimental program and the analysis of these results are listed in Chapter 4. Chapter 5 contains the modeling of permanent deformation of the stabilized soils mixes and calibrating and validating these models. In addition, pavement thickness design charts are included in Chapter 5. Finally, the summary, conclusions and recommendations are listed in Chapter 6.

## **CHAPTER 2**

### **LITERATURE REVIEW**

#### **2.1 SOIL STABILIZATION**

Due to the tremendous growing and expansion of industrial facilities in Saudi Arabia and Arabian Gulf countries in general especially those located along the coastal line of the Gulf, huge industrial cities and associated network of roads and airports are being built. One of the typical problems in the construction of roads along those coastal regions is ascribable to the scarcity of good quality soils. Thus, soil stabilization plays an important role in the improvement of the engineering properties of weak soils in order to meet the general project specifications for the intended use. Generally, in geotechnical engineering field and particularly in soil stabilization, the parent soils are practically categorized under either cohesionless soils (i.e., sandy and other coarse-grained soils) or cohesive soils (i.e., primarily clay and silt). For clay soil stabilization, lime, sometimes in combination with fly ash and possibly with some Portland cement addition, is considered as the premium material stabilizer (Sreekrishnavilasam et al. 2007). In the case of sandy soils, which are commonly selected in the pavement layers, the usage of Portland cements, cement kiln dust, fly ash, or combination of them and bitumen may provide cementitious materials which enhance their binding characteristics (Abdullah, 2009; Al-Amoudi et al., 2006; Al-Aghbari and Dutta 2008).

Soils used in pavements may be stabilized or modified through the addition of chemicals or bitumen. The principal benefits of stabilization include a reduction in

pavement thickness, provision of a construction platform, decreased swell potential, and reduction of the susceptibility to pumping as well as the susceptibility to strength loss due to moisture.

Numerous chemicals have been used for soil stabilization in many engineering projects. Road way surfacing options catalog stated some of these chemicals such as Chlorides, Salts, Calcium Chloride ( $\text{NaCl}_2$ ), Electrolyte Stabilizers, Ionic Stabilizers, Sulfonated Oils, Electrochemical Stabilizers, Enzymatic Emulsions, Enzymes, Synthetic Polymer Emulsions, Polyvinyl Acetate, Vinyl Acrylic, Tree Resin Emulsions, Tall Oil Emulsions, Pine Tar Emulsions, sodium hydroxide, gypsum, sodium silicate, iron oxides, phosphoric acid, aniline-furfural, lignosulfonate derivatives, and many others have been tried in soil stabilization for different purposes. Amongst those mentioned, the most popular are Organic Petroleum Emulsions, Emulsified Asphalt, Cutback Asphalt, Foamed Asphalt, and Warm Asphalt.

Most suitable soils for bituminous admixtures are sandy gravels, sands, clayey and silty sands and fine-crushed rock. Highly plastic clays can be treated successfully but may require high quantities of bitumen. The performance and properties of bituminous-stabilized silt-clay soils are affected by clay type, type of exchangeable cations present in clay, soil organic matter and bitumen type and composition. Bituminous uses, applicability, testing procedures, construction and characteristics of the mixture have been discussed in many standards and publications such as ASTM and Asphalt Institute (UFC, 2004; McCarthy, 2005).

Stabilization of soils and aggregates with asphalt differs greatly from cement and lime stabilization. The basic mechanism involved in asphalt stabilization of fine-grained soils is waterproofing phenomenon. Soil particles or soil agglomerates are coated with asphalt that prevents or slows the penetration of water which could normally result in a decrease in soil strength. In addition, asphalt stabilization can improve durability characteristics by making the soil resistant to the detrimental effects of water such as volume. In noncohesive materials, such as sands, gravel, crushed gravel, and crushed stone, two basic mechanism are active: waterproofing and adhesion. The asphalt coating on the cohesionless materials provides a membrane which prevents or hinders the penetration of water and thereby reduces the tendency of the material to lose strength in the presence of water. The second mechanism has been identified as adhesion. The aggregate particles adhere to the asphalt and the asphalt acts as a binder or cement. The cementing effect thus increases shear strength by increasing cohesion. Criteria for design of bituminous stabilized soils and aggregates are based on almost entirely on stability and gradation requirements (Christopher et al., 2006; UFC, 2004; McCarthy, 2005).

Bituminous materials have been used in the United States since 1870. Soil and sand-asphalt stabilization projects were constructed in the United States in 1930 (Terrel et al., 1984). Since then, many low traffic roads have utilized mixed-in-place asphalt stabilization. In addition, hot, central plant asphalt stabilization has been used. Asphalts most commonly used are refined from petroleum. Asphalt cement, cutback asphalts and emulsified asphalts have been used in soil stabilization. Asphalt consists of inert mineral particles impregnated or cemented by bitumen. In general, bitumen is taken to include both tar and asphalt and the use of such material is collectively called bituminous

stabilization. Depending on the granulometric composition and the physical properties of the soil, there are four types of bitumen stabilized products: soil bitumen, sand bitumen, waterproofed granular stabilization and oiled earth (Hausmann, 1999). The main objectives of stabilizing soils with bituminous materials are:

- waterproofing fine-grained soils;
- construction expediency;
- upgrading of marginal material;
- reducing dust; and
- providing cohesion to granular material.

## **2.2 FOAMED ASPHALT**

The basic idea of asphalt foaming is to inject a small quantity of cold water (usually with a mass ratio of 1% to 5% to the asphalt binder) together with compressed air into hot asphalt (140°C to 180°C) in a specially designed chamber. The water experiences a sudden temperature increase and becomes steam. When the mixture of asphalt cement, steam and compressed air is injected into the ambient air, asphalt is temporarily expanded into numerous bubbles with greatly increased surface area per unit mass. The purpose of asphalt foaming is to make it easier for asphalt to disperse into cold granular materials at ambient temperature. Foamed asphalt technology was developed more than 30 years ago (Al-Abdul Wahhab et al., 2007, 2012), but it did not gain much acceptance or implementation after its development, mainly because the required equipments were not available at that time to produce or apply the product on a

commercial scale. Recently, due to the advantages of foamed asphalt technology in improved aggregate penetration, coating capabilities, handling, and compaction characteristics, it has progressively gained acceptance as an efficient and economical construction materials improvement and stabilization technique. Saudi Arabia used foamed asphalt application in 1997 in Shaybah oilfield road. The road was constructed using compacted marl base and subbase. Foamed bitumen was used to recycle the top 200 mm of the marl road which in turn graded and compacted to the required profile to produce the foamed asphalt pavement. The foamed asphalt was subsequently surfaced with a slurry seal. The overall assessment of the performance of the road and its condition from the data collected was that the road and the foamed asphalt, in specific, performed very well under the heavy traffic loading and harsh conditions for the proposed design life (Al-Abdul Wahhab et al., 2007, 2012; Asi et al., 2002).

Foamed asphalt technology has been successfully employed in Europe, Africa, and Middle East since the late 1980s and is being increasingly adopted in the U.S., Canada, and Australia as its benefits become widely know (Kendall et al., 2001; Lee, 1981; Muthen, 1998 a and b; Soter International, 1994).

Foamed asphalt has different behavior than regular asphalt during the application process. Foamed asphalt mixture acts like soil treatment rather than asphalt concrete mix. Foamed asphalt is not appropriate for every road due to its moisture sensitivity. The technique did not work on some trial roads because the water table is high or springs flow underneath these roads. There will be a negative effect on the top layer due to the existence of the water table which softens and weakens the subgrade. Foamed asphalt

technology will work well as long as the subgrade is good (Al-Abdul Wahhab et al., 2012; FHWA, 2003).

In Eastern Province of Saudi Arabia, 350 km of access road for Shaybah oil fields was constructed over sabkha subgrade, utilizing marl soils together with foamed asphalt. The road is located in the extremely arid and hot climate of Al-Rub Al-Khali desert (Asi et al., 2002).

Asi et al. (1998, 1999, 2002) carried out several laboratory researches to study the possibility of using foamed asphalt technology in Saudi Arabia to improve the dune sands or sabkha soils for possible use as a base or subbase material in comparison to emulsified asphalt treatment. Several variables were investigated to evaluate the relative improvement of local soils as well as to permit the development of design procedures for the future use of foamed asphalt technology in the harsh climatic conditions of eastern Saudi Arabia. The results were statistically analyzed and employed to verify the effects of foamed asphalt treatment, with and without the addition of Portland cement, on the strength characteristics of the treated mixes. Based on the results displayed, a significant improvement was noticed in the performance of foamed asphalt mixes, as compared to that of the emulsified asphalt mixes.

Al-Abdul Wahhab et al., (2012) have investigated and evaluated the feasible use of foamed asphalt technology for Saudi roads using marginal quality construction materials, marl, and reclaimed asphalt pavement (RAP) materials for local applications. Foamed asphalt mixes were designed for subbase class B (foamed SB) and reclaimed asphalt pavement (foamed RAP) material utilizing low percentage of Portland cement.



They optimized the foamed asphalt mixes to meet dry and wet indirect tensile strength (ITS) requirements. Designed mixes in addition to granular base class A and B were evaluated for CBR, dynamic resilient modulus at 25 °C and wheel tracking test dry at 50 °C and soaked at 22 °C. The results of this study indicated that base class A has the lowest rutting followed by base class B then foamed SB and finally foamed RAP for dry condition at 50 °C, while foamed RAP has the lowest rutting followed by foamed SB then base class B and finally class A for soaked condition at 22 °C. Portland cement was effective in reducing ITS loss of foamed asphalt mixes. Resilient modulus testing indicated that SB mix has behavior comparable to base class A. Foamed RAP mix has shown the best behavior. Saturation has reduced resilient modulus of all mixes significantly. Finally they concluded that foamed asphalt technology can be used successfully to construct road bases from locally available marginal or recycled materials.

He and Wang (2006) investigated decay properties of two foamed bitumens. They carried out foaming tests under various conditions to investigate decay properties of two types of bitumen: Penetration-grade 60 (PG 60) and Penetration-grade 100 (PG 100). It is noticed that water content has a considerable effect on the bitumens decay, and the time at which the maximum expansion ratio appears advances with an increase of temperature. PG 60 achieves the maximum expansion ratio at an earlier time than PG 100.

Huan et al., (2010) reported the preliminary study of the foamed bitumen properties and the mix procedures conducted at Curtin University which simulated the construction of the trial foamed bitumen stabilised project in Western Australia. Based on the results, they found that 2.5% of cold water spraying into 180°C virgin Class 170 bitumen can generate foamed bitumen with a 15 to 20 times expansion rate and 20 s half-

time suitable for foaming aggregates. Both resilient modulus and permanent deformation tests failed to expect an optimum foamed bitumen content when the aggregate was mixed with 1% hydrated lime, compacted at 100% optimum moisture content and plastic sealed curing for 7 days at room temperature. However, the ratio of crushed granite road base to limestone was found to be significant and a mixture consisting of 75% crushed rock base and 25% crushed limestone was calculated as the optimum aggregate proportion, as it showed the best performance in unconfined compressive strength tests and obtained relatively higher values in indirect tensile strength tests. They concluded also that the adding more foamed bitumen to in-situ recycled aggregate reduced the performance of materials.

Different types of rolled asphalt are distinguished according to the process used to bind the aggregate with the asphalt. Hot mix asphalt (HMA) is produced at 160 degrees Celsius. This high temperature serves to decrease viscosity and moisture during the manufacturing process, resulting in a very durable material. HMA is most commonly used for high-traffic areas, such as busy highways and airports. Warm mix asphalt (WMA) reduces the temperature required for manufacture by adding asphalt emulsions, waxes, or zeolites. This process benefits both the environment and the workers, as it results in less fossil fuel consumption and reduced emission of fumes. In cold mix asphalt, the asphalt is emulsified in soapy water before mixing it with the aggregate, eliminating the need for high temperatures altogether. Cold mix plants are lower cost, simpler and more mobile than hot mix plants. However, the asphalt produced is not nearly as durable as HMA or WMA, and cold mix asphalt is typically used for low traffic areas or to patch damaged HMA ([http://en.wikipedia.org/wiki/Asphalt\\_concrete](http://en.wikipedia.org/wiki/Asphalt_concrete)). Robert

et al. (1984) prepared the foamed asphalt mixtures heated and compacted at 160°C and reported that the modulus and density of heated foamed asphalt mixtures were significantly higher than those of cold-mixed foamed asphalt mixtures.

Xiao et al., (2011) have conducted a laboratory investigation of moisture susceptibility and rutting resistance of warm-mix asphalt (WMA) mixtures containing moist aggregates by using a foaming technology. The experimental program included two aggregate moisture contents (0 and 0.5% by weight of the dry mass of the aggregate), two lime contents (1% and 2% lime by weight of dry aggregate), one liquid antistripping agent (ASA) and non-ASA, three foaming water contents (2, 3, and 4%) with control, and two aggregate sources. The results of this study showed that the aggregate source drastically affects the ITS and rutting resistance regardless of the foaming water content, ASA, and aggregate moisture content. Furthermore, the ITS and rut depth of some foamed mixtures containing moist aggregate satisfies the demand of pavement performance without additional treatment, although some mixtures need a completely dry aggregate or additional treatments. Also, it is noticed that the mixture with various hydrated lime contents exhibited similar rutting and moisture resistance under dry and wet conditions. Finally, they stated that the liquid ASA used in this study is not recommended for use in foaming WMA mixtures with moist aggregates, because it is sensitive to moisture.

### **2.3 EMULSIFIED ASPHALT**

Asphalt emulsion is a mixture of asphalt binder and water that includes a small amount of emulsifying agent to cause the asphalt to become mixed with or suspended in the water. Asphalt emulsion may be either anionic with electro-negatively charged

asphalt globules or cationic with electro-positively charged asphalt globules, depending upon the emulsion agent (Kowalski and Starry, 2007).

The usage of asphalt emulsions started in the early part of the 20th century. Nowadays, 5% to 10% of paving-grade asphalt is used in emulsified form, but the degree of emulsion usage varies widely between countries. The United States is the world's largest producer of asphalt emulsion. Asphalt emulsion has some advantages compared to hot asphalt and cut back binders, such as low application temperature, compatibility with other water-based binders like rubber latex and cement, and low-solvent content (James A., 2006).

Moore (1982) studied the use of bituminous emulsion to stabilize lime-treated clays. The effect of lime content, molding moisture content, modification curing time, emulsion type and curing temperature on the unconfined compressive strength of the stabilized material was investigated. He reported that the unconfined compressive strength increases with the increase of lime content, molding moisture content and curing temperature. However, the effect of modification curing time is dependent on the soil type and percentage of emulsion used. The effect of emulsion type depends on whether rapid-set or slow-set emulsion is used and on the type of treated soil.

Al-Abdul Wahhab and Asi (1995) investigated using of slow setting emulsified asphalt and medium curing cutback asphalt to stabilize marl and sand obtained from the Eastern Province of Saudi Arabia. The addition of 2% and 4% lime and Portland cement was applied to the stabilized soils to accelerate curing process and to reduce stability loss due to water damage. The results of this research indicated that the stabilizing agent have

both enhanced strength and resistance of the analyzed soils to water damage. Cement additive was found to be more effective than lime.

Oruc et al. (2007) studied the addition of Portland cement on emulsified asphalt mixtures by changing the percentage of this additive from 0% to 6% as mineral filler. Moisture-damage performance was evaluated using the ratio of measuring resilient modulus of mixtures, before and after soaking in water. Mixtures without the addition of cement failed after six hours of conditioning. However, emulsified asphalt mixtures with cement showed better water resistance and an increase in the resilient modulus.

Al-Khashab and Al-Hayalee (2008) investigated the possibility of the stabilization of expansive clayey soil pre-treated by lime, with an emulsified asphalt addition. The soil was classified as medium to high expansiveness in naturally. The pre-treatment of soil was accomplished with (0.5, 1.0, and 1.5%) lime addition by weight. After short period, emulsified asphalt was added with different dosages namely (2, 4, 6 and 8) by weight, for optimum percentages of an emulsified asphalt to give the most useful stabilization aspects. The result of adding lime alone indicated that there was a significant reduction in soil plasticity, 1.5% of lime addition changed the clayey soil towards non-plastic types. The emulsified asphalt addition to the mixture, resulted in slight increase in the plasticity but, their values in the whole, remained below the value of the natural soil. Results also showed decrease in the specific gravity with the emulsified asphalt addition as well as, a general reduction, compatible with the increase in the optimum moisture contents. The absorption values of the treated soil with the emulsified asphalt showed consequent reduction as compared with the original one. A significant reduction in swelling pressure and swelling percent were noticed as well as an improvement in some values of the

unconfined compressive strength at low percentages of emulsified asphalt addition, compatible with reduction in values of the high percent additions.

Kavussi and Modarres (2010) have reported the effect of cement on the fatigue properties of cold recycled mixes with bitumen emulsion (CRME). To build up fatigue models for these mixes, extensive indirect tensile fatigue and resilient modulus tests were conducted at different temperatures (varying from -10 to 25°C) and curing times (varying from 7 to 120 days). The results of this study indicated that the effects of cement on fatigue life of mixes are related to the initial strain level assumed in testing. Finally based on their laboratory testing results, distinct models were established for different boundary strain levels.

Bunga et al., (2011) have investigated the stabilization of sandy loam clay by using emulsified asphalt as a stabilizer material. The soil samples were collected from Manuju village, Gowa regency, South Sulawesi province, Indonesia. They obtained emulsified asphalt type CSS-15 from PT. Widya Sapta Colas. The emulsified asphalt concentrations were 1.5%, 3.0%, and 4.5%. The results of the investigation showed the physical, chemical, and mechanical characteristics of sandy clay loam are improved due to using emulsified asphalt. It was also noticed that chemical bindings occurred among the soil minerals and emulsified asphalt. Finally, plasticity and shear strength of soil increased in a linear relationship with the increase of emulsified asphalt concentration.

## **2.4 SULFUR EXTENDED ASPHALT (SEA)**

“The term sulfur extended asphalt (SEA) applied to a paving binder, paving mixture, or pavement, denotes a replacement of a significant portion of the

conventionally used asphalt with element sulfur. Typically, 20 to 40 percent by weight of the asphalt is replaced with sulfur” (Beatty et al., 1987). The optimum sulfur content in sulfur-extended asphalt binders is found somewhere between 20 and 30 wt%. Below the former, no hardening effect is obtained. Above the latter the improvement of mix workability is reduced (Kennepohl et al., 1975; Celard, 1978).

Lewandowski (1994) stated that the main reasons to use additives with bituminous materials could be summarized as follows:

- To get softer blends at low service temperatures and decrease cracking,
- To reach stiffer blends at high temperatures and reduce rutting,
- To increase the stability and the strength of mixtures,
- To enhance fatigue resistance of blends,
- To decrease structural thickness of pavements.

In the 1970s, concern began growing in the use of SEA. Many laboratory test programs were established to study the use of sulfur in asphalt mixtures. In addition, field experiments were established to test the long-term performance characteristics of SEA pavements. The enormous majority of published literature on the use of SEA occurred from 1974 to 1986 (Timm et al., 2009).

Federal Highway Administration (FHWA), in 1987, conducted a field study to compare the performance of SEA to the conventional asphalt pavements (Beatty et al., 1987). In this study, they noticed that there was no difference in overall performance

between SEA pavement and the conventional sections. In 1990, FHWA conducted a complementary laboratory investigation and the results supported that of the field study. They had seen that sulfur decrease the resistance to moisture susceptibility in the laboratory and there were minor trends that sulfur may reduce the susceptibility to rutting and increase the susceptibility to fatigue cracking with some mixtures (Stuart, 1990).

In general, the expected benefits of the use sulfur extended asphalt may be summarized as follows (AI, 2007):

- Decreased cost for hot- mix asphalt (HMA).
- Saving and conservatory of asphalt binder resources.
- Comparable pavement performance.
- Reduced tendency to rut due to the stiffening effect of sulfur on asphalt.
- Fuel saving due to lower mix temperatures, a result of the lower equiviscous properties of SEA.

Strickland and coworkers (2008) studied the performance of sulfur-modified mixtures in the laboratory. Rutting performance of the prepared mixtures was evaluated using the asphalt pavement analyzer (APA) test at 58°C, and the mixture stiffness modulus was measured at a temperature ranging from -10 to 30°C. Additionally, the low temperature performance was evaluated by using the Thermal Stress Restraining Specimen Test (TSRST). Results of this study showed that the rutting resistance and stiffness modulus of the mixture are improved. In addition, the modified sulfur additive improved the elongation properties of the mix at low temperatures.



Timm et al. (2009) have conducted a complete experimental program to investigate the moisture resistance and dynamic modulus of sulfur-modified asphalt mixtures. Results indicated that sulfur-modified asphalt mixture had a lower tensile-strength ratio (TSR) after curing but greater dynamic moduli for all combinations of test temperatures and frequencies.

Cooper et al., (2011) have studied the effects of sulfur-modified warm mix asphalt (WMA) on the predicted performance from the Mechanistic-Empirical Pavement Design Guide (MEPDG) and assessed the life cycle costs of pavement structures constructed with this sustainable alternative. To achieve this objective, three typical pavement structures were analyzed at three traffic levels (low, medium, and high). Based on the results of the analysis, the use of sulfur-modified WMA improved the predicted rutting and fatigue performances and the overall pavement service lives over conventional mixtures at all traffic levels. The results also showed that sulfur modification has the potential to decrease production and life cycle costs when compared to a conventional asphalt mixture made with the same binder grade (Cooper et al. 2011).

Cooper et al., (2011) also compared the laboratory mechanistic properties of sulfur-modified warm-mix asphalt (WMA) with conventional asphalt mixtures. Three mixtures, two hot-mix asphalt (HMA) and one WMA were prepared. Mixture One used an unmodified asphalt binder classified as PG 64-22, Mixture Two used a styrene-butadiene-styrene elastomeric modified binder classified as PG 70-22, and Mixture Three was a WMA that incorporated a sulfur-based mix additive and a PG 64-22 binder. A suite of tests was performed to evaluate the rutting performance, moisture resistance, fatigue endurance, fracture resistance, and thermal cracking resistance of the three mixtures.

Results of the experimental program showed that the rutting performance of sulfur-modified WMA was comparable or superior to conventional mixes prepared with polymer-modified and unmodified asphalt binders. Results of the modified Lottman test showed that the moisture resistance of the sulfur-modified mixture was comparable to conventional mixes. Results of the fracture tests showed that sulfur-modified WMA is more susceptible to cracking than conventional mixes, given its stiff characteristics. However, given these stiff properties, the higher modulus of sulfur-modified mixtures will reduce the magnitude of strain induced in the pavement. Thermal stress restrained specimen test results showed that the sulfur-modified WMA had greater fracture stress than the polymer-modified mixture.

Baig et al., (2009) investigated the feasibility of using sulfur as an additive for local asphalt concrete mixtures at KFUPM. They also studied many cases of using sulfur modified asphalt in road construction including the field trial at Khursaniyah and the concerns related to air pollution due to sulfur containing gases. Sulfur-asphalt concrete consists of testing local sulfur, Shell Canada sulfur-extended asphalt modifier (SEAMTM), with local asphalt-concrete mixes was studied to assess the effect of sulfur and modified sulfur materials by comparing the performance of these paving mixes. Based on laboratory and field trials results, they reported that SEAMTM and sulfur modified asphalt concrete can be produced, hauled, placed and compacted easily with conventional methods and equipment. There will be no constructability problem with the use of sulfur or SEAMTM binder. They also stated that the use of asphalt with SEAMTM or sulfur material at 30% replacement could be more economical as compared to regular asphalt as the amount of required asphalt will be reduced in proportion to the

SEAMTM/sulfur percentages used. The environmental impact of the sulfur-asphalt technology was assessed through the field tests and the results indicated that there is no long-term hazard for mixes as showed by acceptable values of emission of hazardous gases such as  $\text{H}_2\text{S}$  and  $\text{SO}_2$  ( $<1$  PPM at  $76^\circ\text{C}$ ). However, precautions must be taken during preparation and laying of mixes at  $145^\circ\text{C}$ .

Based on the brief previous literature review on the using of sulfur modifier with asphalt in the world and Gulf in particular, there is no any indication of using sulfur with foamed or emulsified asphalt. Thus, this study investigated the feasibility of producing sulfur foamed/emulsified asphalt and using this production in stabilization of three local soils in the Eastern Province of Saudi Arabia, namely, sand, sabkha, and marl.

#### **2.4.1 Environmental Hazards and Safety Aspects of Using Sulfur-Extended Asphalt**

Gawel (2000) reported that, no problems should come out unless the temperature of  $140^\circ\text{C}$  is exceeded during the production of sulfur-extended asphalt mixes (warm mixes) and their utilization in pavement construction. Below this temperature the formation of hydrogen sulphide and sulfur dioxide is negligible.

Al-Abdul Wahhab and Baig (2007) concluded that, there is no short-term or long-term environmental hazard for sulfur-asphalt mixes prepared using sulfur-extended asphalt modifier (SEAM) as indicated by the low emission of hazardous gases at road surface temperature as high as  $76^\circ\text{C}$  prevailing in Saudi Arabia nor during field construction.

Baig et al., (2009) reported that there are no major safety concerns with regard to careful monitoring of mixing and handling of hot sulfur asphalt mix and sulfur should be used in

both wearing course and base course layers with strict quality control to avoid undesirable performance due to layers stiffness compatibility.

Asphalt institute (2007) characterized the challenges to the use of sulfur-extended asphalt as data gap, in whole or in part and summarized them as follows:

- Nuisance odors.
- Potential for increased emissions of  $\text{H}_2\text{S}$ ,  $\text{SO}_2$ , acid mists, and particulate (elemental) sulfur at high temperatures.
- Potential worker exposure to increased emission of  $\text{H}_2\text{S}$ ,  $\text{SO}_2$ , and particulate with no information related to severity or nature of exposure.
- Potential fire and explosion hazard (in confined spaces).
- Recyclability of pavements containing sulfur-extended asphalt, which must be processed at lower temperatures to prevent increased levels of emissions.
- Potential for corrosion of structural and/or emissions handling materials.

In this study, the application of sulfur foamed asphalt would be at temperatures equal or lower than  $150^\circ\text{C}$ , which is considered as a warm asphalt mix, and during a very short period. Similarly, sulfur-emulsified asphalt was produced and applied at very low temperatures. Based on the previous literature, there is no any problem of hazardous

fumes and sulfur asphalt technology can be used successfully with current road construction technology and expertise.

## 2.5 MODELING OF PERMANENT DEFORMATION

Permanent deformation in asphalt (flexible) pavements, commonly referred to as rutting, usually consists of longitudinal depressions in the wheel paths, which are an accumulation of small amounts of unrecoverable deformation caused by each load application as shown in Figure 2.1 (Asphalt Institute, 1996).

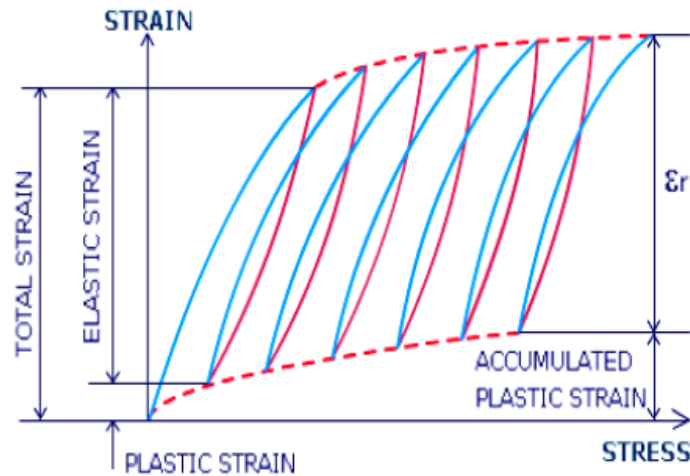


Figure 2-1: Accumulated Plastic Strains in Pavements (Asphalt Institute, 1996)

Existing permanent deformation models are mostly based on cyclic load triaxial testing, and are of two main types (Hornych and El Abd, 2004):

- Empirical laws, describing the variation of permanent strains with the number of load cycles and the maximum applied stresses.
- Incremental models, generally based on the theory of elasto-plasticity.

A summary of various empirical relationships describing the variation of permanent deformations of unbound granular materials (generally only axial deformations) with the number of load cycles  $N$ , partly based on a literature review made by Lekarp et al. (2000), is presented in Table 2.1.

Table 2-1: Relationships Describing the Variation of Permanent Axial Deformations  $\epsilon_1^p$  with the Number of Load Cycles (Hornych and El Abd, 2004 after Lekarp et al. 2000).

Author	Relationship	Parameters
Barksdale [1972]	$\epsilon_1^p = a + b \log(N)$	$a, b$
Khedr [1985]	$\frac{\epsilon_1^p}{N} = A \cdot N^{-b}$	$A, b$
Paute and al [1988]	$\epsilon_1^{p*} = \frac{A \sqrt{N}}{\sqrt{N} + D}$	$\epsilon_1^{p*}$ permanent deformation after the first 100 cycles $A, D$ parameters function of stress level
Tseng and Lytton [1989]	$\epsilon_1^p(N) = \epsilon_0 \cdot e^{-\left(\frac{p}{N}\right)^\beta}$	$\epsilon_0, p, \beta$
Sweere [1990]	$\epsilon_1^p = a N^b$	$a, b$
Hornych et al. [1993]	$\epsilon_1^{p*} = A \left( 1 - \left( \frac{N}{100} \right)^{-B} \right)$	$\epsilon_1^{p*}$ permanent axial strain after the first 100 cycles $A, B$
Vuong [1994]	$\epsilon_1^p = \epsilon_1^r \left( \frac{a}{b} \right) N^c$	$\epsilon_1^r$ resilient axial strain $a, b, c$
Wolff and Visser [1994]	$\epsilon_1^p = (cN + a)(1 - e^{-bN})$	$a, b, c$
Huurman [1997]	$\epsilon_1^p(N) = A \cdot \left( \frac{N}{1000} \right)^B + C \cdot (e^{\frac{D \cdot N}{1000}} - 1)$	$A, B, C, D$ parameters function of the level of stress

Hornych and El Abd (2004) reported that the relationships describing the variation of permanent deformations with the number of load cycles presented above cannot be

applied to the prediction of permanent deformations in pavement structures, because they do not take into account the applied stresses. They also presented the work of other researchers who have followed another approach, trying to relate the permanent deformation after a given number of cycles to the applied stresses (generally the maximum stresses). Relationships of this type are listed in Table 2.2. Some of these relationships also try to couple the effects of both stresses and number of load cycles, but they are only very few of them (see Table 2.2).

The NCHRP 1-26 study (Barenberg and Thompson, 1990) recommended the use of the permanent strain accumulation model developed at Ohio State University (Majidzadeh et al. 1981). This strain model predicts total rutting, considers the rutting rate of the pavement as indicated by the following equation:

$$\epsilon_p / N = A(N)^m$$

where

$\epsilon_p$  = permanent strain

$N$  = number of load application

$A$  = Experimental constant (depends on material type and stress state)

$m$  = Experimental constant (depends on material type)

Equation above is valid for describing the progression of rutting in pavement layers, asphalt surface and base courses, granular base and subbase courses, and subgrade soils (Majidzadeh, et al 1981).

Several material permanent strain accumulation models have been developed so far to predict the permanent deformation in AC pavement layers. Pavement system rutting models were also evaluated in the NCHRP 1-26 (Barenberg and Thompson 1990). The study have revealed that those models which are related to log of permanent strain to the log of load repetition appear to be the most appropriate and versatile for practical use. This power model is often fitted to the accumulated permanent deformation curve. It is probably the most commonly used permanent deformation equation. The power model plots as straight line on log-log scale. It has also been thought that the slope and intercept of this model when plotted on log-log scale may be used as indicators of rutting resistance (Garba, 2002). The basic permanent strain to load repetition model expressed as:

$$\epsilon_p = aN^b$$

It was initially proposed for subgrade and unbound materials by Monismith (1976); and initially used for asphalt concrete mixes by (Khedr, 1986). Later on, various researchers used the same model for asphaltic concrete (Diylajee and Raymond, 1982), (Vuong and Armstrong 1991), (Behzadi and Yandell, 1996). Where a and b are intercept and slope coefficients and N is the load repetition. The curve of power model on log-log scale between load repetition and permanent strain can be expressed in graphical form in Figure 2.2.



Table 2-2: Relationships Describing the Variation of Permanent Axial Deformations with Applied Stresses (Hornych and El Abd, 2004).

Author	relationship	Parameters
Lashine et al. [1971]	$\varepsilon_1^p = a \frac{q}{\sigma_3}$	a, $\sigma_3$ confining stress, q deviator stress
Barksdale [1972]	$\varepsilon_1^p = \frac{q/a\sigma_3^b}{1 - \left[ \frac{R_f \cdot q \cdot (1 - \sin\phi)}{2(C \cdot \cos\phi + \sigma_3 \sin\phi)} \right]}$	a, b , $R_f$ = ratio of applied deviator stress q to deviator stress at failure $q_f$ . $\phi$ friction angle, C cohesion
Shenton [1974]	$\varepsilon_1^p = K \left( \frac{q_{\max}}{\sigma_3} \right)^a$	K ,a , $q_{\max}$ maximum applied deviatoric stress
Pappin [1979]	$\varepsilon_s^p = f_n(N) \cdot L \cdot \left( \frac{q}{p} \right)^{2,8}$	$\varepsilon_s^p$ permanent shear strain, $f_n(N)$ shape function, depending on the number of cycles N, p mean normal stress, $L = \sqrt{p^2 + q^2}$
Lentz and Baladi [1981]	$\varepsilon_1^p = \varepsilon_{0,95S} \ln(1 - q/S)^{-0,15} + \left[ \frac{n(q/S)}{1 - m(q/S)} \right] \ln(N)$	$\varepsilon_{0,95S}$ axial strain at 95% of the deviatoric stress at failure, n , m slope of the failure line, S deviatoric stress at failure
Paute et al. [1994]	$\varepsilon_1^{p*} = f(N) \frac{\frac{q}{(p + p^*)}}{b \left( m - \frac{q}{(p + p^*)} \right)}$	$\varepsilon_1^{p*}$ permanent axial strain after the first 100 cycles b,p*, m slope of failure line in p,q space f(N) function of the number of cycles N
Nishi [1994]	$\varepsilon_1^{p,ult} = k \frac{q^a}{p^b}$	k, a, b $\varepsilon_1^{p,ult}$ ultimate permanent axial strain
Lekarp and Dawson. [1998]	$\frac{\varepsilon_1^p(N_{ref})}{(L/p_0)} = a \left( \frac{q}{p} \right)^b$	a,b $\varepsilon_1^p(N_{ref})$ : permanent strain after a reference number of cycles $N_{ref} > 100$ $L = \sqrt{p^2 + q^2}$ $p_0$ reference mean stress

According to VESYS, 1990 progressing of rutting with load repetition can be measured using layer elastic and viscoelastic theory, where in all layers can be modeled using a constitutive model in the form given in following equation (partial differentiation form).

$$\frac{\partial \varepsilon_p}{\partial N} = \varepsilon_{pn} = \frac{\partial (aN^b)}{\partial N}$$

$$\varepsilon_{pn} = abN^{(b-1)}$$

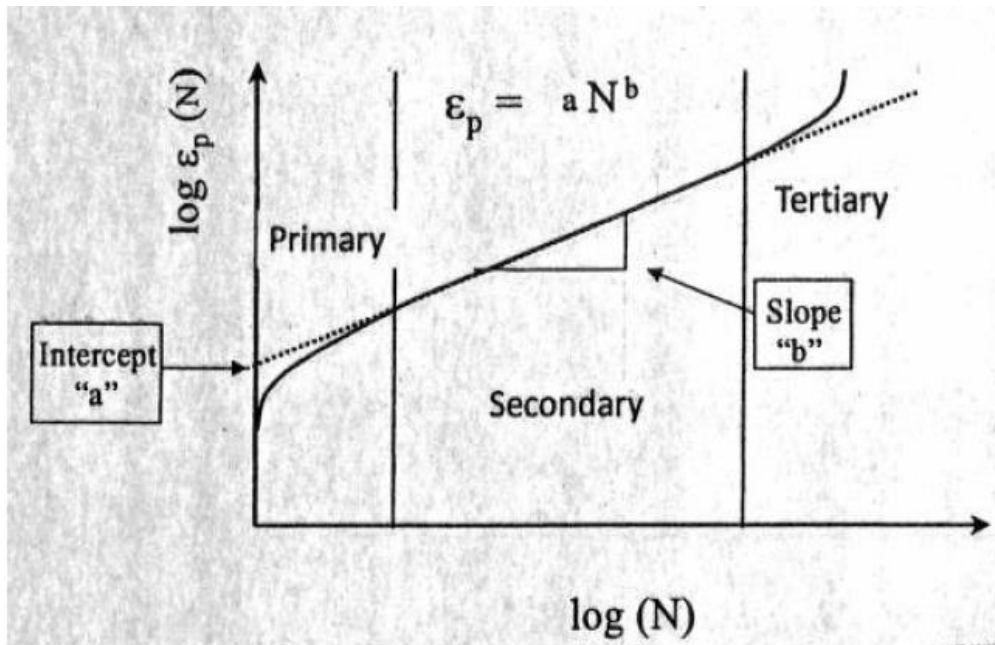


Figure 2-2: Log-Log Form of Power Model (After Khedr, 1986)

The resilient strain ( $\varepsilon_r$ ) is assumed to be independent of load repetition. The ratio of plastic to resilient strain can thus be defined as:

$$\frac{\varepsilon_{pn}}{\varepsilon_r} = \left( \frac{ab}{\varepsilon_r} \right) N^{b-1} = \mu_N^{-\alpha}$$

where

$$\mu = \frac{ab}{\varepsilon_r} \quad \alpha = 1 - b$$

$\varepsilon_p$  = Permanent Strain (rut value)

N = Number of Load Application

a = Intercept Coefficient; and

b = Slope Coefficient

$\mu$  = ratio of plastic to elastic response

$\alpha$  = rate of change of the plastic response

In order to get the cumulated permanent strain in each layer, we have to integrate the above equation with respect to N as follows:

$$\varepsilon_p = \int_0^N \varepsilon_p \partial N = \int_0^N \mu \varepsilon N^{-\alpha} \partial N$$

The integration yields the following equation:

$$\varepsilon_p = \frac{\varepsilon_r \mu}{1 - \alpha} (N)^{1-\alpha}$$

Thus the total rut depth can now be calculated as:

$$RD = \sum_{i=1}^n (\varepsilon_{pi} \times h_i)$$

where

$h_i$  = thickness of the layer.

In order to predict the rut depth using the model above we have to find model parameters experimentally and the resilient strain for all the layers of pavement structure in algorithm using suitable finite element method program.

Alpha and mu according to Sullivan (2002) are the stress and temperature dependent non linear parameters and can be used for modelling permanent deformation of mixes:

$$\alpha = 1.748418 - 0.446558 \log T - 2.65284 \frac{\log \sigma_D}{34.03532 - 0.253679T}$$

$$\mu = 1.663759 - 0.438729 \log T - 1.25191 \frac{\log \sigma_D}{1.918523 + 0.066875T}$$

where, T = Temperature, F°; and

$\sigma_D$  = Deviator stress (equal to  $\sigma_1 - \sigma_3$ ), psi.

Hu et al. (2011) presented a new Mechanistic-Empirical (*M-E*) rutting model developed for hot-mix asphalt (HMA) overlay thickness design and analysis adapting VESYS model with minor modification. Additionally, the proposed *M-E* HMA overlay rutting model was calibrated using 8 test sections of the National Center for Asphalt Technology (NCAT) Test Track 2006, and the calibrated model was further validated using two sets

of independent rutting data: 3 test sections of the NCAT Test Track 2000 and 4 test sections of SPS5 on US175, Texas. Overall, the *M-E* rutting model proposed in this paper offers greater potential for rationally modeling and accurately predicting the HMA overlay rutting.

The current MEPDG incorporates a power model for generating rutting predictions for asphalt concrete. Rutting model developed from laboratory uniaxial repeated load strain tests as provided in MEPDG in the following form has been used as basis to estimate the relationships between the predictor variables and the permanent deformation parameters (Stephen et. al 2007):

$$\frac{\varepsilon_p}{\varepsilon_r} = a_1 T^{a_2} N^{a_3}$$

Where,  $\varepsilon_p$ ,  $\varepsilon_r$ , are the plastic and elastic strains respectively, at N repetitions of load and  $a_i$  are the non linear regression coefficient.

AASHTO 2002 design guide developed M-E models for predicting permanent deformation in asphalt mixtures and unbound materials. The final model of permanent deformation for asphalt mixtures is:

$$\frac{\varepsilon_p}{\varepsilon_r} = k_1 * 10^{-3.4488} T^{1.5606} N^{0.479244}$$

$$k_1 = (C_1 + C_2 * depth) * 0.328196^{depth}$$

$$C_1 = -0.1039 * h_{ac}^2 + 2.4868 * h_{ac} - 17.342$$

$$C_2 = 0.0172 * h_{ac}^2 - 1.7331 * h_{ac} + 27.428$$

where,

$\epsilon_p$  = accumulated plastic strain at N repetitions of load (in/in)

$\epsilon_r$  = resilient strain of the asphalt material as a function of mix properties, temperature and time rate of loading (in/in)

T = number of load repetitions

T = temperature (deg F)

$k_1$  = function of total asphalt layers thickness ( $h_{ac}$ , in) and depth ( $depth$ , in) to computational point, to correct for the confining pressure at different depths.

Furthermore, the final calibrated model for the unbound granular base is as follows:

$$\delta_a(N) = \beta_{GB} \left( \frac{\epsilon_0}{\epsilon_r} \right) e^{-\left(\frac{\rho}{N}\right)^\beta} \epsilon_v h$$

with the national calibration factor of  $\beta_{GB} = 1.673$  being determined and the final calibrated model for the unbound granular base is as follows:

$$\delta_a(N) = \beta_{GB} \left( \frac{\epsilon_0}{\epsilon_r} \right) e^{-\left(\frac{\rho}{N}\right)^\beta} \epsilon_v h$$

with the national calibration factor of  $\beta_{SG} = 1.35$  being determined.

where:

$\delta_a$  = Permanent deformation for the layer/sublayer (in).

$N$  = Number of traffic repetitions.

$\epsilon_o$ ,  $\beta$ , and  $\rho$  = Material properties.

$\epsilon_r$  = Resilient strain imposed in laboratory test to obtain the above listed material properties,  $\epsilon_o$ ,  $\beta$ , and  $\rho$  (in/in).

$\epsilon_v$  = Average vertical resilient strain in the layer/sublayer as obtained from the primary response model (in /in)

$h$  = Thickness of the layer/sublayer (in).

$$\left( \frac{\epsilon_o}{\epsilon_r} \right) = \frac{\left( 0.15 * e^{(\rho)^\beta} \right) + \left( 20 * e^{\left( \frac{\rho}{10^9} \right)^\beta} \right)}{2}$$

where:

$$\log \beta = -0.61119 - 0.017638 W_c$$

$$\rho = 10^9 \left( \frac{-4.89285}{\left[ 1 - (10^9)^\beta \right]} \right)^{\frac{1}{\beta}}$$

$$W_c = 51.712 * CBR^{-0.3586 * GWT^{0.1192}}$$

$$CBR = \left( \frac{M_r}{2555} \right)^{(1/0.64)}$$

where:

$W_c$  = Water content (%).

$M_r$  = Resilient modulus of the layer/sublayer (psi).

GWT = Ground water table depth (ft).

In pavement analysis, analytical solutions (e.g., Burmister's three-layer system solutions) can be obtained often by assuming that the pavement is constructed with homogeneous, isotropic, linear elastic materials and is subjected to a monotonic load. These assumptions oversimplify the complex nature of pavement structures and materials. With the fast development of high-speed computers today, numerical methods, especially FEM, have been extensively used in pavement analysis. Compared to analytical solutions, FEM pavement analysis provides better simulation of material behaviors, wheel configurations, and environmental conditions. We can conclude that pavement response can be determined using the multi-layered elastic program (e.g., BISAR, CHEV, and ELSYM5), multi-layered program based on the viscoelastic calculation approach (e.g., VESYS, MICH-PAVE), and finite element method (FEM). Among these tools FEM is a powerful one since it could account for the sophisticated boundary conditions. Based on the previous literature, VESYS model was adopted in modeling and predicting the permanent deformation of asphalt mixtures and unbound material in this study.



## **CHAPTER 3**

### **EXPERIMENTAL PROGRAM**

#### **3.1 INTRODUCTION**

The work in this study consists of five main phases; the first one comprised of materials collection including dune sand, marl, sabkha, asphalt cement, sulfur, and emulsifying agents. In the second phase, physical properties and characterization of the collected materials were conducted. Marshall mix design were applied to design foamed and emulsified asphalt mixes with and without sulfur extender in the third phase. In the fourth phase, designed mixes were evaluated using a set of mechanical tests. These tests include marshal stability, indirect tensile strength, durability, resilient modulus and static triaxial test. Optimum mixes were subjected to dynamic triaxial and wheel tracking tests for the modeling and verification of permanent deformation. Finally, results analysis and rutting modeling were accomplished in the fifth phase. Figure 3.1 shows the flow chart of the sequence of the experimental program.

The main objective of this chapter is to outline the methods and procedures which were followed to conduct the experimental programs. The following paragraphs describe the steps in details.

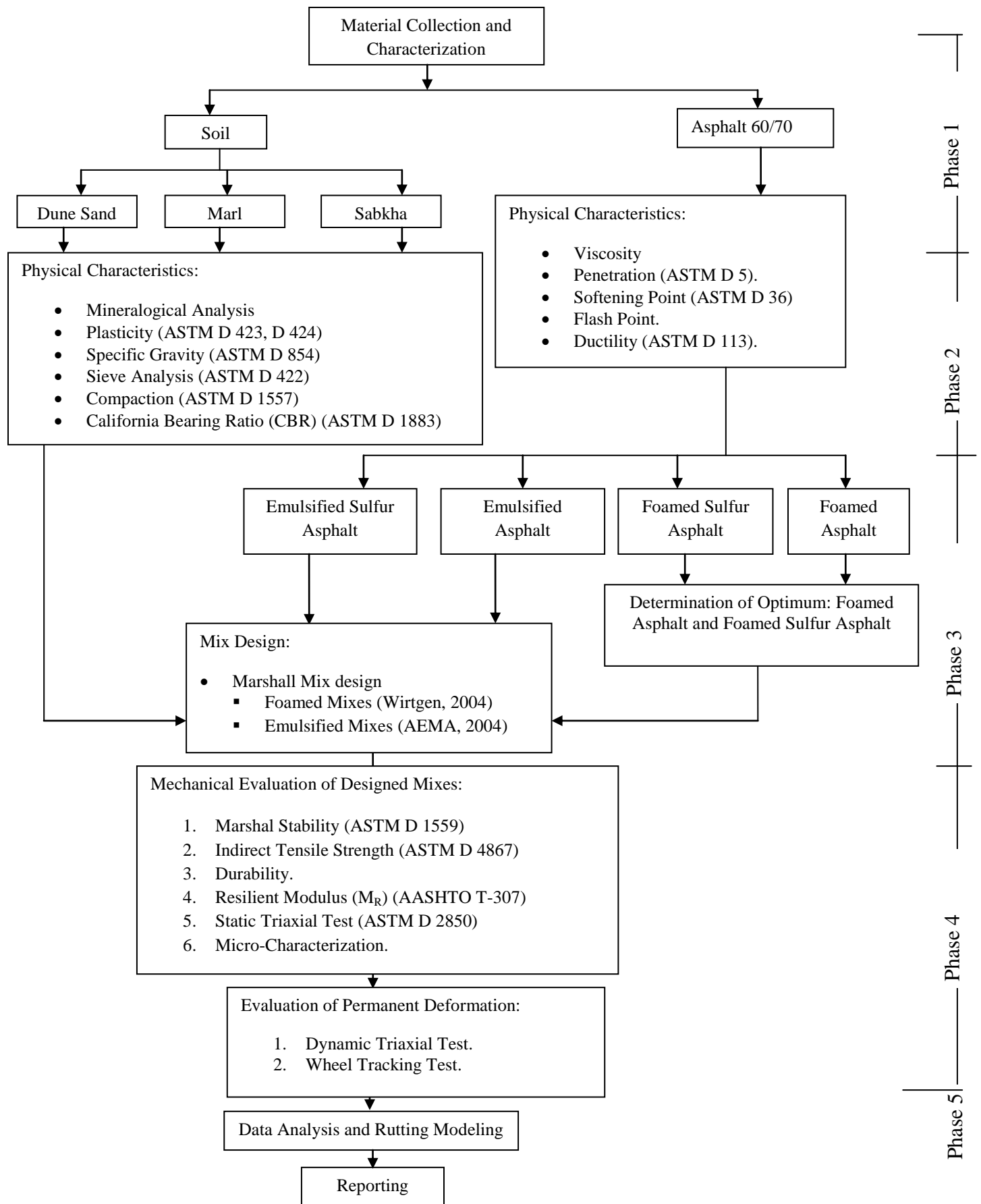


Figure 3-1: Experimental Program Flow Chart.

## **3.2 MATERIALS COLLECTION**

One of the typical problems in the construction of roads along the coastal regions of the Arabian Gulf, the red sea, and northern and southern parts of the Kingdom of Saudi Arabia is ascribable to the scarcity of good quality soils. Marginal soils cover most areas of the eastern province of Saudi Arabia. In order to investigate the possible treatment of these marginal soils and use in the construction of road projects, required quantities for the experimental program of this research including sand, marl and sabkha were collected, subjected to basic characterization and then stored for the use in the experiments. Asphalt cement, sulfur, and emulsifying agent, were also collected from the eastern province of Saudi Arabia, subjected to basic characterization and then stored for the use in the experiments.

### **3.2.1 Preparation of Collected Soils**

The soil samples were brought to the laboratory, thereafter, sabkha and sand soils were sieved through ASTM Sieve #4 whereas marl soil was sieved through ASTM Sieve #  $\frac{3}{4}$  and then air dried. The soil materials were then thoroughly mixed and stored in plastic drums till testing.

### **3.2.2 Asphalt**

Asphalt cement used in this study was obtained from Saudi-Aramco Ras-Tannurah refinery. The grade of the utilized asphalt was 60/70, because this grade is the best grade that widely used in all road projects in the Kingdom. Several ASTM tests were conducted on asphalt cement 60/70 to evaluate its basic physical properties such as, viscosity, penetration, softening point, flash point and ductility.

### **3.3 CHARACTERIZATION OF COLLECTED SOIL SAMPLES**

The basic engineering properties of the soils were assessed by conducting preliminary characterization tests. These preliminary tests included mineralogical analysis, specific gravity, plasticity and grain size distribution tests. In addition, the compaction and strength characteristics were investigated by using modified Proctor compaction and California bearing ratio tests.

#### **3.3.1 Mineralogical Analyses**

Knowledge of the mineralogical composition of a material helps in predicting its behavior and reaction under different environmental conditions. The mineralogical analyses of the soils were performed at the Research Institute (RI), KFUPM.

The soils samples were initially air dried, sieved using sieve #10 and thoroughly mixed well for homogenization. They were then pulverized and sieved using sieve #200. Thereafter, the pulverized soil samples were oven dried at 70 °C for 72 hours [Conklin, 2005; Brady and Weil, 2010]. Finally, about 10 grams of each soil sample was utilized for the mineralogical analyses. The mineralogical composition of the soils was determined by X-ray diffraction method. The x-ray diffractometer used in this investigation was RIGAKU ULTIMA IV X-RAY DIFFRACTOMETER. The generator settings were 40 kV and 40 mA at an angle between 6 and 90° (2 $\theta$ ).

#### **3.3.2 Specific Gravity Test**

Specific gravity is a very important parameter used in determination of soil properties such as unit weight, void ratio, volume-weight relationship of soil and soil particle size analysis. The test was conducted in accordance with ASTM D 854. The test

was conducted on two representative "disturbed" samples from each soil and the average value of the two samples was taken as the specific gravity value.

### **3.3.3 Atterberg Limit Tests**

All soils (i.e. marl, sabkha, and sand) reflect a sandy nature because it was not possible to get the required number of blows for the liquid limit test and cannot be rolled to a thread of 1/8 in. (3.18 mm) when conducting the liquid limit and plastic limit tests on the material passing ASTM sieve # 40 using distilled water according to ASTM D 423 and ASTM D 424, respectively. Therefore, the liquid limit was reported as "not defined" and the plastic limit as "non-plastic" for all the three soils.

### **3.3.4 Grain Size Distribution Test**

It is a fundamental test for any soil classification and investigation. In this test, both dry and washed sieving techniques were performed for the three types of soils in accordance with ASTM D 422. Washed sieving with distilled water was done for marl and sand soils, however, sabkha soils was washed with sabkha brine and distilled water. In the wet sieving method, a representative soil sample was taken and washed through a set of sieves including ASTM No. 3/4, 4, 10, 20, 40, 80 and 200 sieves until the water passing through each sieve was clear. The soil portion retained on each sieve as well as that passing through No. 200 sieve were dried in the oven and then weighed. The difference in weights of the (sieves + dry soils) and the (empty sieves) was used to determine the percentage passing for each sieve.

### **3.3.5 Modified Proctor Compaction Test**

The relationship between moisture contents and dry density can be established using compaction test. Based on the results of this test, the optimum water content at which the maximum dry density of the soil is attained can be determined. In this study, the modified Proctor compaction test (ASTM D 1557) was used. In this test, the required amount of soil was placed in Hobart mixer ( $0.3 \text{ m}^3$  capacity). Mixing was, thereafter, started in a dry state for half a minute, the water was then added to the mixture and mixing was continued for about another half a minute till the whole mixture was totally mixed and the final product was homogeneous. Compaction was made in five layers in the CBR mold. The CBR mold has a height of 5 in (127 mm) and a diameter of 6 in (152 mm) and the number of blows per layer was 25.

### **3.3.6 Soaked California Bearing Ratio Test (CBR)**

The suitability of a soil to be used as a subgrade material in pavement structure should be evaluated using California bearing ratio (CBR) test which was originally evolved in California, USA for this purpose. CBR, thereafter, was adapted by the engineering communities as a test to empirically measure the strength of soil under controlled moisture and density conditions and can easily be used to quantify the material for use in pavement construction. In this study, CBR tests were conducted according to ASTM D 1883. All samples prepared for moisture-density relationship was subjected to soaked CBR testing procedure and the relationship between soaked CBR values and moisture contents was established. Sabkha soil specimens were soaked in sabkha brine.

### 3.4 FOAMED AND EMULSIFIED ASPHALT MIX DESIGN

#### 3.4.1 Foamed Asphalt Mix Design

Laboratory scale foamed asphalt plant WLB 10 shown in Figure 3.2 was calibrated to produce foamed asphalt and 30/70 sulfur foamed asphalt. First, the flow rate of water and asphalt cement or sulfur/asphalt cement for the plant was calibrated, and then the expansion ratio and half life for the foamed asphalt was determined at different operating temperatures (130° to 180° C). Expansion ratio is defined as the ratio of the maximum volume of the asphalt in its foamed state to the volume of the asphalt once the foam has completely subsided while half life is defined as the time in seconds required for the foam asphalt to settle to one-half of the maximum volume attained after foaming. The temperature that gave the highest half life without causing sulfur fumes was adopted for the research. The laboratory mix design procedure was carried out based on the cited literature (Wirtgen, 2004) as outlined in the Wirtgen Cold Recycling Manual and summarized in Figure 3.3. 2% cement was added to all mixes after adding foamed asphalt to prevent affecting the optimum moisture content [Al-Abdul Wahhab et al., 2012].



Figure 3-2: Laboratory Scale Foamed Asphalt Plant WLB 10.

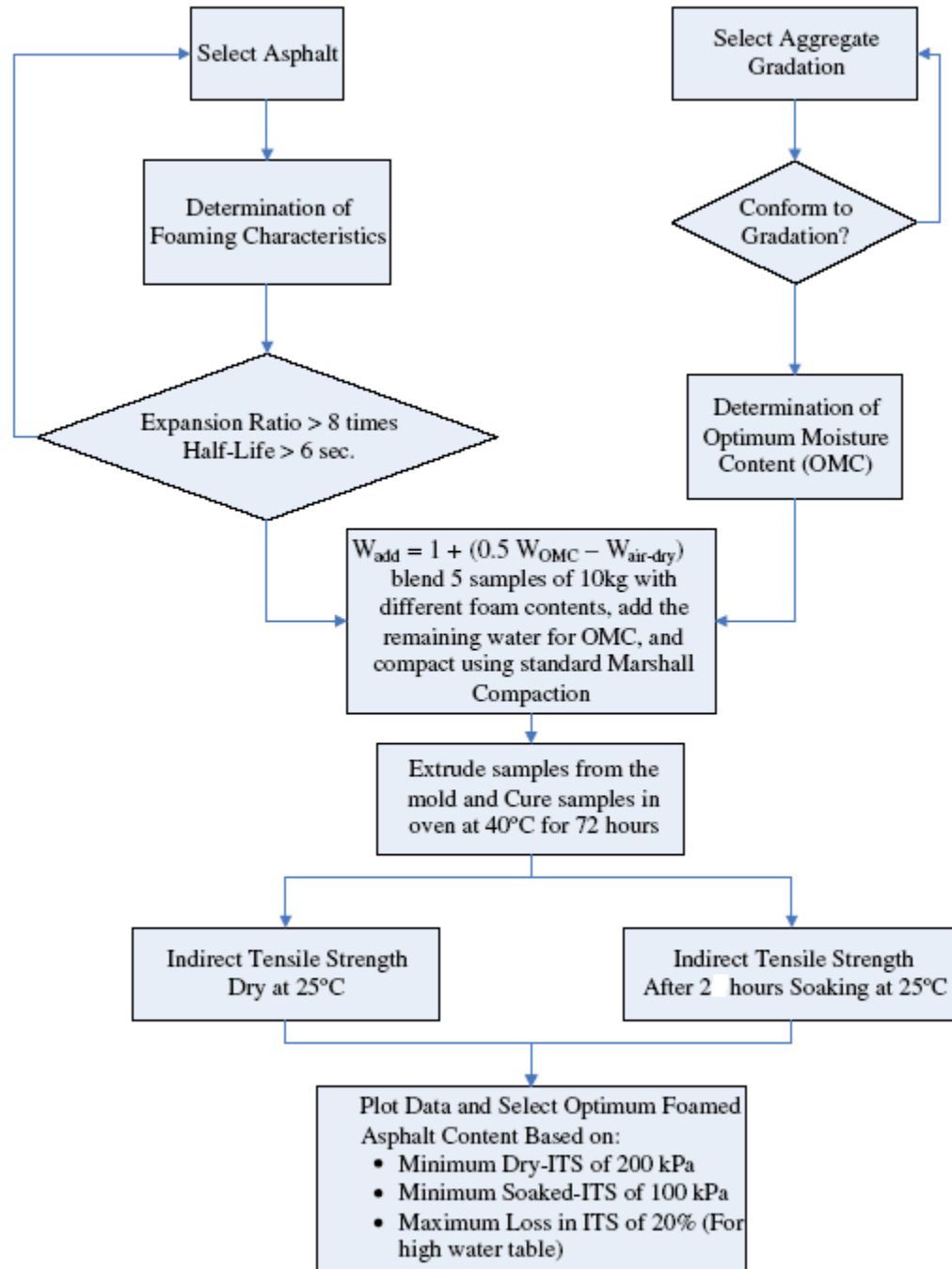


Figure 3-3: Summary of Mix Design Procedure for Foamed Asphalt Treated Mix [Wirtgen, 2004].



### **3.4.2 Emulsified Asphalt Mix design**

Slow setting cationic sulfur asphalt emulsion was produced by using emulsified asphalt plant available in Highway Laboratory at King Fahd University of Petroleum and Minerals. The flow rates of water and sulfur asphalt (30/70) were calibrated and several trials were carried out to determine the best emulsifying agent and production variables.

In the emulsification process, heated sulfur asphalt was pumped into the colloid mill where it was divided into tiny droplets. At the same time, water contained the emulsifying agent was pumped into the colloid mill. The sulfur asphalt entered the colloid mill was heated to a low viscosity, and the water temperature was also adjusted to optimize emulsification. It is recommended to do not use extremely high asphalt temperatures because the temperature of the emulsion leaving the mill must be below the boiling point of water, unless a heat exchanger is used to cool the emulsion (AEMA, 2004).

Cold emulsion technology is based on a polar (surface charge) of asphalt emulsion and aggregate, therefore, they have to be matched. Thus, for soils which have a negatively charged surface, a cationic emulsion (positive charge) was used in which the positively charged droplets of emulsion asphalt are attracted to the negatively charge surface of the soils and begin to break.

In cold bituminous emulsion mixtures, many design procedures among research organizations and road authorities are based on the Asphalt Institute or AASHTO with some modifications. In general, determination of suitable aggregate gradations, optimum water content at compaction, and the determination of optimum residual bitumen content

should be covered by any design procedure used. There is no universally accepted asphalt emulsion-aggregate mix design method for either dense or open-graded cold mixtures. However, the Federal Highway Administration recently attempted to develop and standardize two design methods for use with asphalt emulsion cold mixtures. One method is for the design of mixes having dense-graded aggregate and the second for mixes having open-graded aggregate. In this study, dense-graded aggregate mix design method was adopted. The main steps of this method are (AEMA, 2004);

#### **3.4.2.1 Aggregate and Emulsion Selection**

In dense graded aggregate mix design, the gradation of aggregate used (soils in this study) should meet the requirements specified by the method. Furthermore, the types of asphalt emulsion used for producing dense-graded emulsion cold mixtures are either anionic slow setting (SS) or medium setting (MS). Slow setting (SS) emulsion was used in this study due to its suitability for soil stabilization.

#### **3.4.2.2 Determination of Premixing and Added Water Contents**

Good distribution of the emulsified asphalt over the soils particles depends on the sufficient amount of mixing water. The total water content of soil- emulsion mixes was kept constant as determined from the Proctor compaction tests. Premixing water contents required for marl, sabkha and sand soils were found to be about 4, 3 and 2 %, respectively [Al-Abdul Wahhab, 1985; Arabiyat, 1985 and Al-Halhouli, 1986]. The amount of water presents in emulsion was considered in the mixes design .Thus, the amount of water required to be added to keep the total water quantity of the mix constant as predetermined from compaction test was varied and depended on the used emulsion asphalt percentage.

### **3.4.2.3 Determination of Initial Emulsion Content**

Several procedures are available to determine the trial emulsion or residual asphalt content of a mix. In a dense graded design mix method, two simple formulas are used, one for base mixtures and another one for surface mixtures. The formulas are based on the percentage of aggregate passing the 4.75 mm (No. 4) sieve and in most cases will give a satisfactory starting point. In this study, preselected ratios of emulsion were used (i.e 3, 6, 9, 12 and 15%) as shown in the experimental design presented in Table 3.1. Thus, no need to determine the initial emulsion content.

### **3.4.2.4 Preparation of Test Specimens**

A set of test specimens of height  $63.5 \pm 6$  mm and diameter 101.6 mm were prepared over a range of residual asphalt content. Test mixtures were prepared in increments of residual asphalt contents; using the previously determined premix water and optimum water content required for mixing and compaction. Prepared mixtures were compacted in Marshal mold with 75 blows for each side. After that, the molds containing the compacted specimen were placed on a perforated shelf in a 60 °C (140 °F) forced draft oven for 48 hours. In order to simulate the traffic action on the specimens, the design procedure stated that samples after curing should be removed from the oven and while still at 60 °C (140 °F), a static load of 178 kN (40,000 lbs.) should be applied on the specimen by the double plunger method where a free-fitting plunger is positioned at both the bottom and top of the specimen in the mold. Apply the load at a rate to give about 1.3 mm/min. (0.05 in./min.) of compression and maintain the full load for one minute and then release. Finally, let the compacted specimen to cool in the mold for a minimum of one hour prior to extracting the specimen for testing. Details of specimen

preparation and compaction are found in the basic asphalt emulsion manual (AEMA, 2004). specimens were soaked under 50 mm Hg vacuum in water for one hour and without vacuum for another hour and then tested for soaked stability. Based on the results, a relationship between soaked stability and residual asphalt content is plotted and the optimum residual asphalt content which provides the maximum soaked stability is determined.

### **3.5 EVALUATION OF DESIGNED MIXES**

Designed mixes of sulfur modified foamed/emulsified asphalt were evaluated using a set of mechanical tests shown in Table 3.1. Similarly, regular mixes of foamed and emulsified asphalt were subjected to the same tests for comparison purposes. Following is a brief description of these tests;

#### **3.5.1 Marshall Stability**

Marshall stability test is used to determine the stability (maximum load of failure) in N or kN and flow (deformation in mm at peak strength) for the designed mixes. The procedure followed in conducting this test was in accordance with ASTM D 1559 and the samples were tested at room temperature instead of 60° C as is common for the hot mixtures [MPW-RI, 1990 and Thanaya, 2003]. Marshall samples of size about 101mm diameter by approximately 63.5mm height were formed, using 75 blows of a standard Marshall hammer per face. These samples were then cured (72 h in the mold at 40 °C for foamed asphalt mixes and 48 h at 60 °C for emulsified asphalt mixes). For soaked stability, specimens were soaked in water at 25°C under a vacuum pressure of 50-mm mercury for one hour. The vacuum is slowly released and the specimen is left to soak in water for another one hour. The specimen is then removed from the water, towel dried

and weighed in air. The cured samples were then subjected to soaked and unsoaked Marshall stability. Specimens are loaded along a diameter at a constant rate of compression of 51mm/minute. Figure 3.4 below shows the Marshal apparatus used.

Table 3-1: Experimental Design Matrix

Soil Type	Test	Asphalt Type															
		Foamed Asphalt				Foamed Sulfur Asphalt				Emulsified Asphalt				Emulsified Sulfur Asphalt			
		3%	6%	9%	12%	3%	6%	9%	12%	3%	6%	9%	12%	3%	6%	9%	12%
Marl	Marshall Stability																
	Split Tensile Strength																
	Durability																
	Resilient Modulus																
	Static Triaxial																
	Dynamic Triaxial	At optimum				At optimum				At optimum				At optimum			
	Wheel Tracking	At optimum				At optimum				At optimum				At optimum			
Sand	Marshall Stability																
	Split Tensile Strength																
	Durability																
	Resilient Modulus																
	Static Triaxial																
	Dynamic Triaxial	At optimum				At optimum				At optimum				At optimum			
	Wheel Tracking	At optimum				At optimum				At optimum				At optimum			
Sabkha	Marshall Stability																
	Split Tensile Strength																
	Durability																
	Resilient Modulus																
	Static Triaxial																
	Dynamic Triaxial	At optimum				At optimum				At optimum				At optimum			
	Wheel Tracking	At optimum				At optimum				At optimum				At optimum			



Figure 3-4: Marshal Stability Apparatus.

### 3.5.2 Indirect Tensile Strength Test

Split tensile strength (ITS) test was conducted in accordance with ASTM D 4867 to test treated Marshall specimens under both dry and soaked conditions. The split tensile strength is determined by measuring the ultimate load to failure of a specimen that is subjected to a constant deformation rate of 50.8 mm/minute on its diametrical axis. Tensile strength can be related to HMA crack resistance, especially at low temperatures. The test is normally conducted at room temperature using a Marshall loading frame fitted with 12.5 mm wide concave surface loading strips below and above the Marshall sized bituminous sample, as shown in Figure 3.5. The horizontal tensile stress at the center of the test specimen is calculated using Equation (3.2).

$$\text{Horizontal Tensile Stress} = \sigma = \frac{2P}{\pi dt} \quad (3.2)$$

where,

d = specimen diameter

P = applied load

t = thickness of the specimen

Tensile strength and tensile strain at failure are very useful prosperities for bituminous mixtures characterization, in which tensile strength is used in evaluating mixtures for water susceptibility and the tensile strain is useful for predicting cracking potential. These two properties are provided by indirect tensile strength test [Thanaya, 2003].

### **3.5.3 Durability Test**

Durability of asphalt pavement structure materials is defined as the ability of these materials to resist the effect of environmental conditions such as aging, temperature and water variation without any considerable deterioration during the design life period for a given amount of traffic loading [Scholtz and Brown, 1996]. Damage of bituminous mixtures due to water (moisture damage) is the major factor affecting the durability. There are two mechanisms by which water can damage the structural integrity of the bitumen aggregate interface, firstly loss of cohesion (strength) and stiffness of the bitumen are lost by water and secondly, the adhesive bond between the bitumen and the aggregate in the mixture (stripping) is disintegrated by water attacks. These two water

damage mechanisms result in decreasing the strength of the pavement layer [Scholtz and Brown, 1996].



Figure 3-5: Indirect Tensile Strength Test Setup.

Water damage for a certain asphaltic mixture can be tested after following a specified moisture conditioning procedure and is expressed in terms of retained mechanical property such as the ratio of strength of the mix after and before the conditioning



procedure. Marshal stability test or indirect tensile strength test is commonly used to get the retained strength of the tested mixes. Many moisture conditioning procedures for asphaltic mixtures are reported in the literature, however, here we have selected which is suitable for warm and cold asphalt mixes such as capillary soaking and vacuum saturation. In this study, vacuum saturation was adopted as a moisture conditioning procedure.

#### **3.5.3.1 Vacuum Saturation**

In this method, tested specimen is placed in a plastic drum and completely covered with water and then put in the vacuum apparatus as shown in Figure 3.6. The dessicator is evacuated at 50 mm of Hg and held under vacuum for one hour. The vacuum is slowly released and the specimen is allowed to soak in water for another one hour. The specimen is then removed from the water, towel dried, weighed in air and then tested for its strength (ITS for foam mixes and Marshall stability for emulsion mixes) [Asphalt Institute, 1989].

#### **3.5.4 Resilient Modulus Test ( $M_R$ )**

Stress-strain relationship, as characterized by elastic or resilient modulus, is an important characteristic. The stiffness moduli for treated mixtures were found by conducting resilient modulus test.

Resilient modulus is simply the ratio of the dynamic deviatoric stress to the recovered strain under a standard haversine pulse loading. Resilient modulus is considered as an important design input parameter and it is required to determine structural layer thickness and the overall system response to traffic loads.



(a) Samples Covered with Water



(b) Samples in the Vacuum Saturation Apparatus

Figure 3-6: Vacuum Saturation Apparatus.

Different test methods and equipments have been developed and employed to measure  $M_R$ . Some of the tests employed are triaxial tests (repeated cyclic loads), cyclic flexural test and dynamic diametral tests. Resilient modulus measured in the indirect tensile mode (ASTM D 4123) has been used by many engineers as a method to determine the resilient modulus of asphalt mixes, however, it is not suitable to quantify the effects of confining pressure which is a main influencing factor on the  $M_R$ . Therefore, the dynamic triaxial test approach was adopted in this study.

Dynamic resilient modulus for treated mixes was measured using the dynamic triaxial test and following the procedure standardized in 1999 as AASHTO T-307. The test is conducted by applying axial haversine pulse compressive loading to cylindrical specimen (4-inch diameter by 8-inch height) as shown in Figure 3.7. The specimens were prepared at optimum water and asphalt contents for each asphalt type and compacted to the same density as Marshall specimens. Table 3.2 presents the loading sequences required for tested samples. To minimize the effects of initially imperfect contact between the sample cap and loading ram, in addition to the base plate and the specimen, conditioning loading was introduced by applying 1000 loading cycles at confining pressure of 15 psi and maximum deviator stress of 20 psi [AASHTO T-307, 1999].

### **3.5.5 Static Triaxial Shear Strength Test**

To construct the Mohr-Coulomb failure envelope and to measure the angle of internal friction and cohesion of the treated mixes, static triaxial shear strength test (ASTM D 2850) was conducted on specimens (2 in. diameter and 4 in. height) compacted at their optimum residual asphalt and optimum water content.

Table 3-2: Loading Sequence for Resilient Modulus Test [AASHTO T-307]

Phase	Combination	Confining Pressure (psi)	Deviator Stress (psi)
Specimen Conditioning	0	15	20
Testing	1	3.0	5.0
	2		7.0
	3		9.0
	4	5.0	5.0
	5		10.0
	6		14.9
	7	10.0	5.0
	8		10.0
	9		20.0
	10		30.0
	11	14.9	10.0
	12		20.0
	13		30.0
	14		40.0
	15	20.0	10.0
	16		15.0
	17		20.0
	18		30.0
	19		40.0



Figure 3-7: Sample Setup for Dynamic Resilient Modulus Test.

Trial and error was applied to get the number of layers and blows required for the compacted mixes in this small size molds to achieve the same maximum Marshall density corresponding to their optimum residual asphalt and water contents. Figure 3.8 clarify the static triaxial test configuration and setup. To construct the Mohr-Coulomb failure envelope of treated mixes, three levels of confinement were required, in which, specimen was subjected to a static confining stress and a deviator stress that gradually increased until it fails due to shear. The shear strength parameters ( $c$  and  $\phi$ ) of mixes were determined from the Mohr-Coulomb failure envelope model:

$$\tau = c + \sigma \tan \phi \quad (3.3)$$

where,

$\tau$  = shear strength

$\sigma$  = normal stress

$c$  = cohesion

$\phi$  = angle of internal friction

### **3.5.6 Dynamic Creep Test (Triaxial)**

Using dynamic triaxial test, many parameters of designed mixes can be calculated such as resilient modulus, poison's ratio and permanent deformation. Permanent deformation response for regular and sulfur modified foamed and emulsified asphalt mixes were characterized using dynamic triaxial repeated load test on (4-inch diameter by 8-inch height) sample size. Specimens were compacted using a kneading compactor in three layers. Several trials of compaction were done to find the number of tamps and compaction pressures required producing uniform specimens at their maximum dry Marshall density. Samples were subjected to a curing regime in which they were put in an oven at 40 °C for 72 hr for foamed mixes and at 60 °C for 48 hr for emulsified mixes. Moreover, samples were allowed to cool down in a dissicator for 24 hrs. After that they were covered by a rubber membrane and placed on the base plate of the triaxial cell and then secured at the bottom and top using rubber O-rings as shown in Figure 3.9.

To avoid friction and the associated restraining effect at samples ends, two soft filter fabric papers were positioned between the samples ends and the bottom and top loading plates. The specimens were tested under 10 psi confining pressure and a range of deviator stress 276 to 552 kPa (40-80 psi) to simulate the traffic loading that the granular base and subbase materials are subjected to in the road.

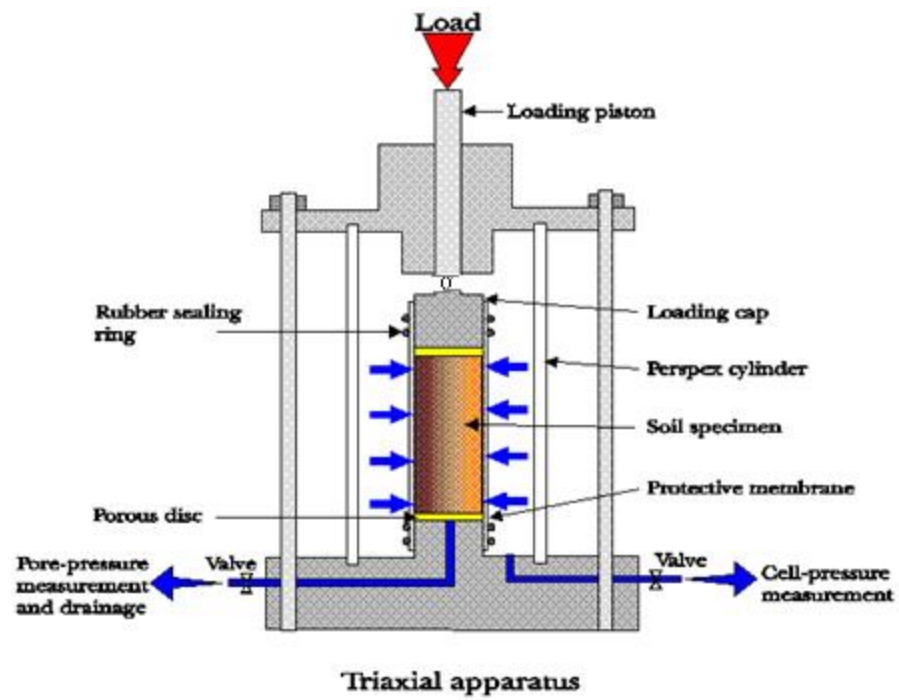


Figure 3-8: Static Triaxial Test Setup.

The deviatoric stress was applied in the form of a sinusoidal (haversine) wave pulse with loading time of 0.1 second followed by reset period of 0.9 second. Linear Variable Differential Transducers (LVDT) were used to measure the axial deformation (creep). Figure 3.10 below shows the dynamic triaxial load test setup.

Repeated load tests were applied for treated mixes samples at two different temperatures (laboratory temperature, 22°C and 40° C) and with three levels of deviator stress 275, 345 and 414 kPa (40, 50 and 60 psi) for low stiffness mixes and 414, 483 and 552 kPa (60, 70 and 80 psi) for high stiffness mixes. Thermally controlled triaxial cell was used and cell temperature was set at 40 °C. Specimens were conditioned at 40 °C at least 6 hours before conducting the test.

### **3.5.7 Accelerated Loaded Wheel Test**

In recent years, the increase of wheel loads and tire pressures has led to the increase in pavement stresses which in turn decreases the useful life of the pavements. Rutting occurs as longitudinal depressions in wheel path due to the repeated application of high stress on the pavement structure or by inadequate shear strength of pavement materials. Permanent deformation might be caused by inadequate structure or weakened subgrade. The low shear strength of the pavement materials such as hot mix asphalt results in a permanent deformation due to the accumulation of unrecoverable strain resulting from applied wheel loads. This results in a combination of consolidation and/or lateral movement of the hot mix asphalt under traffic. Shear failure (or lateral movement) in a hot mix asphalt pavement generally occurs in the top 10 cm of the pavement. Thus, in order to identify the hot mix asphalt that prone to rutting, loaded wheel simulators have been used.





Figure 3-9: Dynamic Triaxial Sample Setup.



Figure 3-10: Dynamic Triaxial Repeated Load Test Setup

In this study, Wessex engineering wheel tracker shown in Figure 3.11 (a) and (b) was used to identify and simulate the permanent deformation behavior of the tested materials.

In this simulator, a loaded wheel is run over a slab sample. Two slabs for each mix were

compacted at the optimum residual asphalt and water contents to the same maximum dry density of the dynamic triaxial samples. Twenty four slabs, 45 cm x 22 cm x 10 cm thick, were prepared from the three treated soils (marl, sabkha, and sand) at the optimum contents of foamed asphalt (FA), sulfur foamed asphalt (SFA), emulsified asphalt (EA), and sulfur emulsified asphalt (SEA) and were compacted to the optimum density using dynamic compaction . The slabs were then cured at 40 °C for 72 h for foamed mixes and at 60 °C for 48 h for emulsified mixes and tested in a dry condition under a wheel load of 552 kPa (80 psi) at a laboratory temperature of 22 °C. Figure 3.12 shows some of the cured slabs before testing. The slabs of sabkha soil mixes were sealed after curing by using plastic sheets to prevent the ambient humidity effect on the slabs before testing. The device applies a vertical force through contact surface of c. It has a dual wheel assembly that accommodates testing of two specimens simultaneously. The self-weight of each wheel is 18 kg. The required contact pressure is provided by a static weight of steel plates (4.5 kg each). In other word, we need to put 8 steel plates (4.5 kg each) on each wheel so that the weight of these plates in addition to the self weight of the wheel divided by the contact area ( $1000 \text{ mm}^2$ ) gave the required load for testing (552 kPa). Samples were placed inside stainless steel sample molds and mounted on a stainless steel bracket. Slabs are loaded with 50 mm wide steel wheels with a 12.5 mm thick rubber contact surface that translates a horizontal distance of 230 mm. The rate of loading corresponds to 54 wheel passes per minute. The deformation of the tested slabs with the number of load repetitions was recorded by permanent deformation recording unit shown in Figure 3.11(b). The test was ended when the deformation of the specimen reached 20 mm or at 100,000 load repetitions.



a)



b)

Figure 3-11: Wessex Engineering Wheel Tracker.

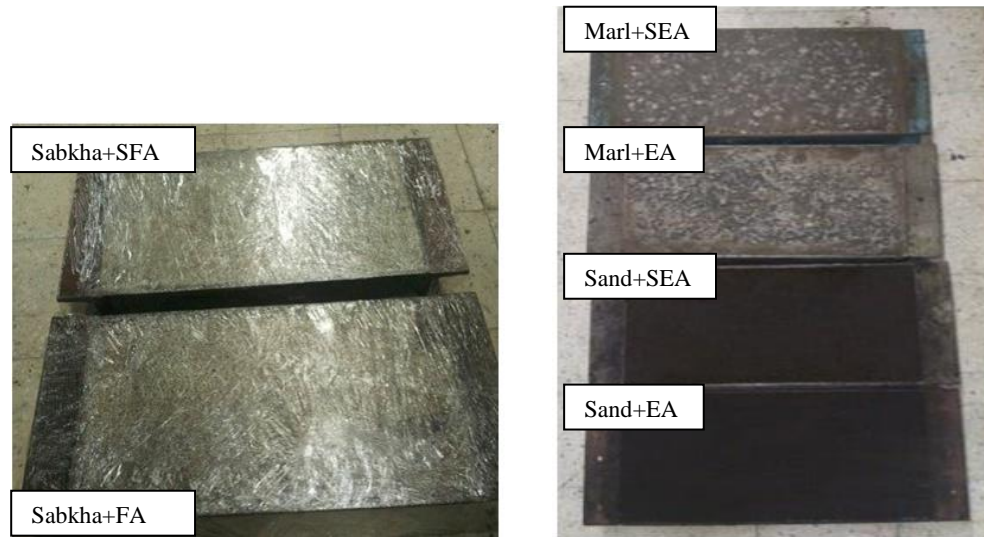


Figure 3-12: Some of Cured Slabs before Testing.

### 3.5.8 Micro-Characterization Study

For the micro-characterization studies, scanning electron microscopy (SEM) was utilized to study the morphology of some investigated soils mixtures. A JEOL 500LV scanning electron microscope utilizing the secondary electron mode was used. Specimens of about 10 mm in diameter and 5 mm in height were carefully cut from the tested specimens using a sharp knife and submitted to the Research Institute at KFUPM for testing. The specimens were coated using gold (Au), to eliminate the conductivity of the specimen, before testing. SEM with energy dispersive X-ray analysis was conducted for each specimen.

## **CHAPTER 4**

### **RESULTS AND DISCUSSION**

In this chapter, the experimental program results are presented and discussed to explain the behavior of the evaluated mixes and the reasoning of such behavior. The results are presented in three sections. In the first section, general characterization of the materials used in this study is presented. The foamed asphalt mixes evaluation results are explained in the second section while the emulsified asphalt mixes evaluation results are discussed in the third section.

#### **4.1 Characterization of Soils**

In this section, characterization tests of the marl, sabkha, and sand soils included mineralogical analyses, specific gravity of solid grains, grain size distribution, Atterberg limits, compaction, and California bearing ratio tests were conducted according to the relevant of ASTM and AASHTO standards and the results are presented in the following sections.

##### **4.1.1 Mineralogical Analyses of Soils**

X-ray diffraction (XRD) technique was used to perform the mineralogical composition of the marl, sabkha, and sand soils used in this study. XRD analyses for these soils are shown in Figures 4.1 through 4.3.

Figure 4.1 shows the x-ray diffractogram for marl and the peaks reveal the presence of about 60% dolomite [ $\text{CaMg}(\text{CO}_3)_2$ ], 30% quartz ( $\text{SiO}_2$ ) and 6% calcite ( $\text{CaCO}_3$ ) in

addition to traces of other minerals. The relatively high percentage of calcite and quartz is responsible for the non-plastic and fine-grained nature of this type of marl [Al-Amoudi et al., 2010].

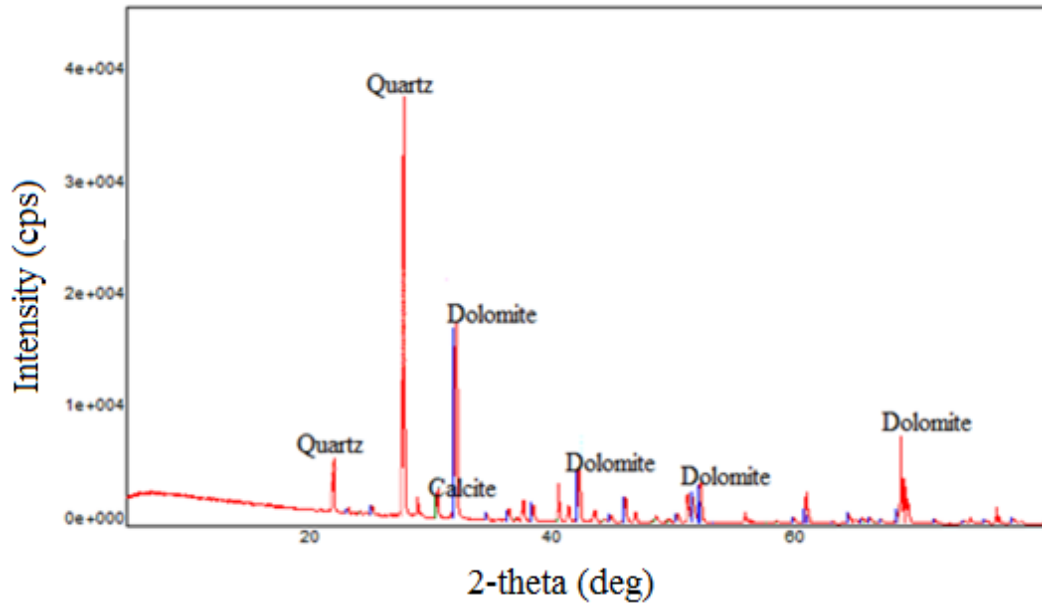


Figure 4-1: X-Ray Diffractogram for Marl Soil.

The x-ray diffractogram for sabkha soil is shown in Figure 4.2. Peaks for quartz (75%), gypsum (12%) and halite (10%) were noted in addition to traces of other minerals. The high percentage of quartz is responsible for the non-plastic and fine-grained nature of this type of sabkha [Al-Amoudi et al., 2010].

Figure 4.3 presents the x-ray diffractogram for sand. The peaks for quartz were noted in this diffractogram. Quartz ( $\text{SiO}_2$ ) constitutes about 100% of the sand soil.

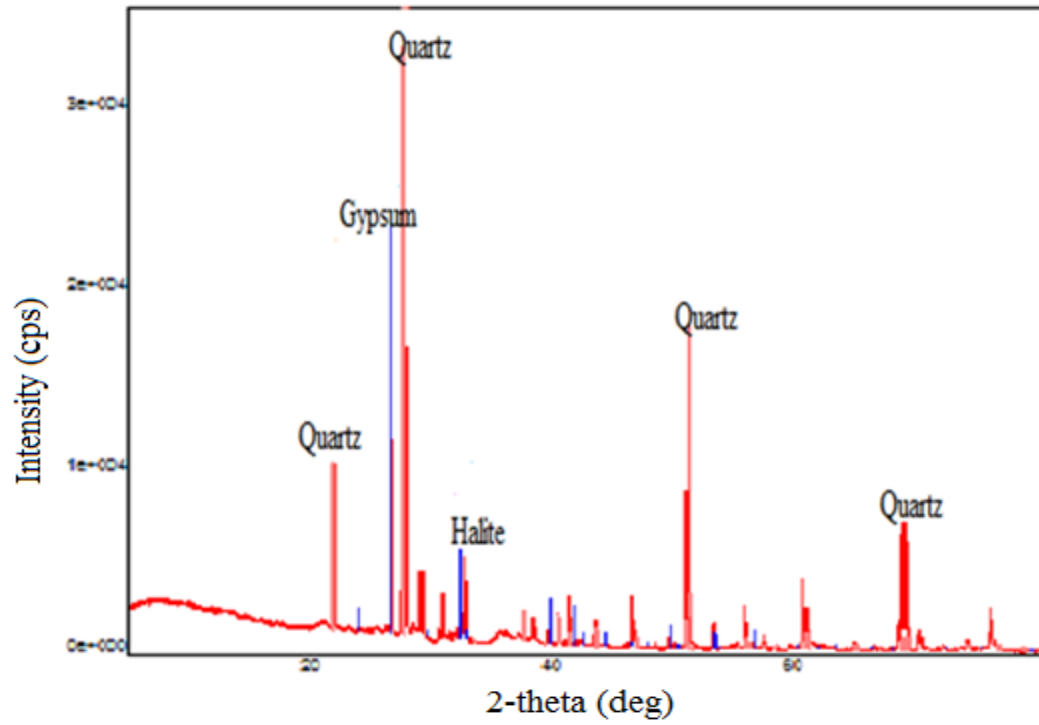


Figure 4-2: X-Ray Diffractogram for Sabkha Soil.

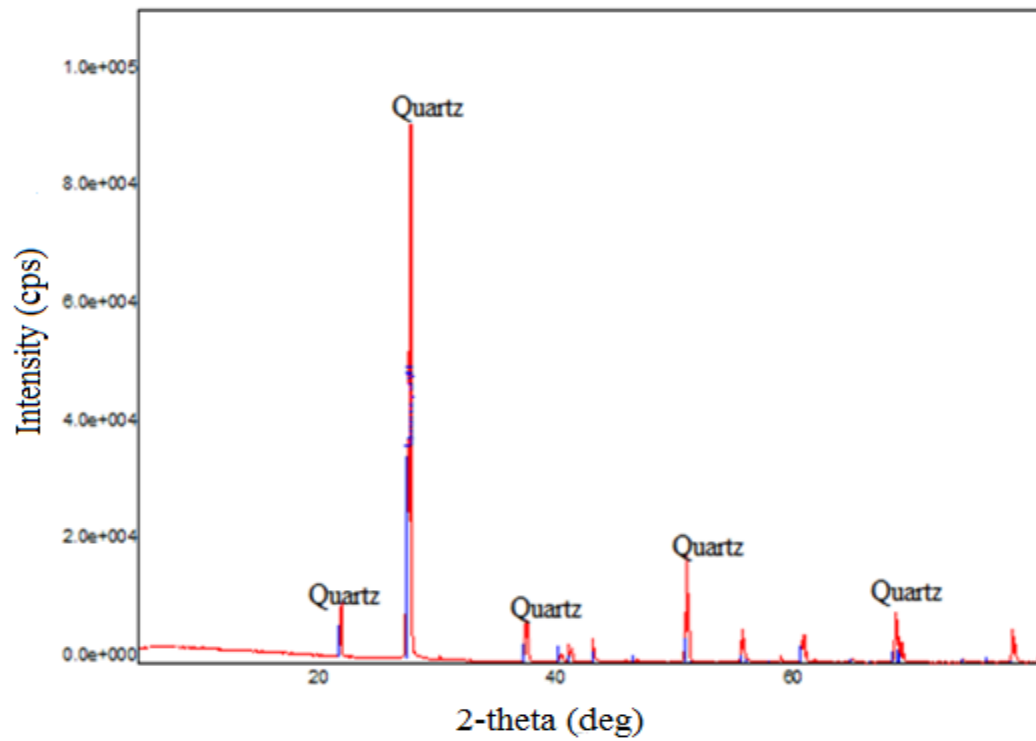


Figure 4-3: X-Ray Diffractogram for Sand Soil.

#### **4.1.2 Specific Gravity**

Two samples from each soil were subjected to the specific gravity test and the average value was taken. The specific gravity values of the marl, sabkha, and sand soils were 2.69, 2.71 and 2.63, respectively. The values of the specific gravity of all soils fall within the range of eastern Saudi soils as reported by many researchers [Ahmed, 1995; Amin, 2004; Al-Amoudi, 1994; Al-Guniayan 1998].

#### **4.1.3 Atterberg Limits**

Liquid and plastic limit tests were done on marl and sabkha samples in accordance with ASTM D 423 and ASTM D 424, respectively, and it was difficult to find the required moisture contents for the 25 blows. Thus, the two soils were reported as “not defined”. In addition, the two soil samples also could not be rolled to a thread of 1/8-in (3.18 mm). Therefore, the investigated soils were classified as "non-plastic".

#### **4.1.4 Grain Size Distribution and Classification of Soils**

The dry and wet grain size distribution curves for marl, sabkha and sand soils are shown in Figures 4.4 to 4.6, respectively. Wet sieving of sabkha was done with sabkha brine rather than distilled water in order to simulate the field conditions. It can be seen from Figure 4-4 that the marl soil passing sieve ASTM #200 is 22 and 28%, respectively, when dry and wet sieving methods were used. The soil can be classified as SM or SC if the material passing #200 is more than 12%. However, since the investigated soil was non-plastic, the soil is classified as SM and A-3 according to the USCS and AASHTO soil systems, respectively, based on both dry and wet sieving methods.



Based on the grain size distribution curves of sabkha soil shown in Figure 4.5 the soil passing Sieve #200 was 8.14% and 15.8% for dry and wet sieving with sabkha brine methods, respectively. Since the material passing sieve #200 is less than 50%, the soil can be classified as SM or SC according to USCS system. However, the collected sabkha is non-plastic, therefore, it can be classified as SM according to the USCS system and as A-3 according to the AASHTO system for dry sieving.

The material passing sieve # 200 by wet sieving is 15.8%, (greater than 12%). Therefore, the wet sabkha can be classified as SM or SC. But the collected sabkha is non-plastic, hence, the wet sabkha is classified SM according to the USCS system and A-3 according to the AASHTO system.

According to the grain size distribution curves of sand (Figure 4.6), it can be noticed that the material passing #200 for the dry and wet materials was less than 5%, it could be classified as SW or SP, according to the USCS. The coefficients of uniformity (Cu) determined by dry and wet sieving methods is almost the same, 3.1. Therefore, sand soil is classified as SP. Moreover; since the sand is non-plastic in nature, it can be classified as A-3 according to the AASHTO system.

It is clear from dry and wet sieve analysis curves for marl and sabkha soils that the wet sieving curve is always above dry curve and this is ascribed to the fact that water tends to dissolve the salts between particles of the soil, thus, the proportion of wet materials passing a particular sieve is consistently more than that for dry sieving. This difference would be higher if sabkha was sieved with distilled water instead of sabkha brine. However, in sand soil, it can be seen that there is almost no variation between grain

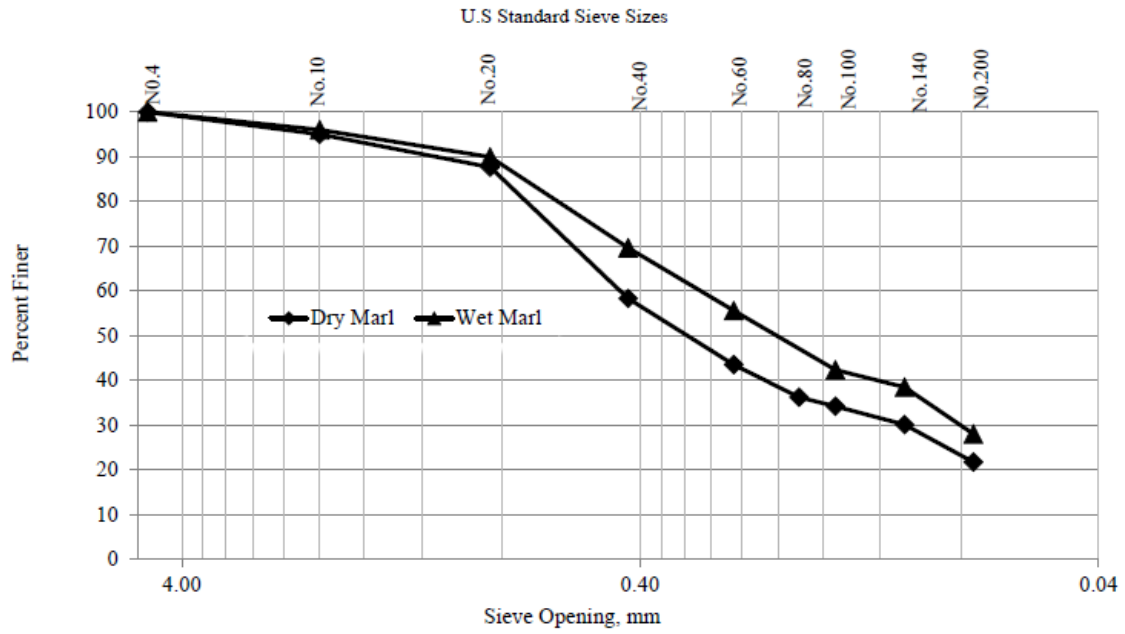


Figure 4-4: Grain Size Distribution of Marl Soil.

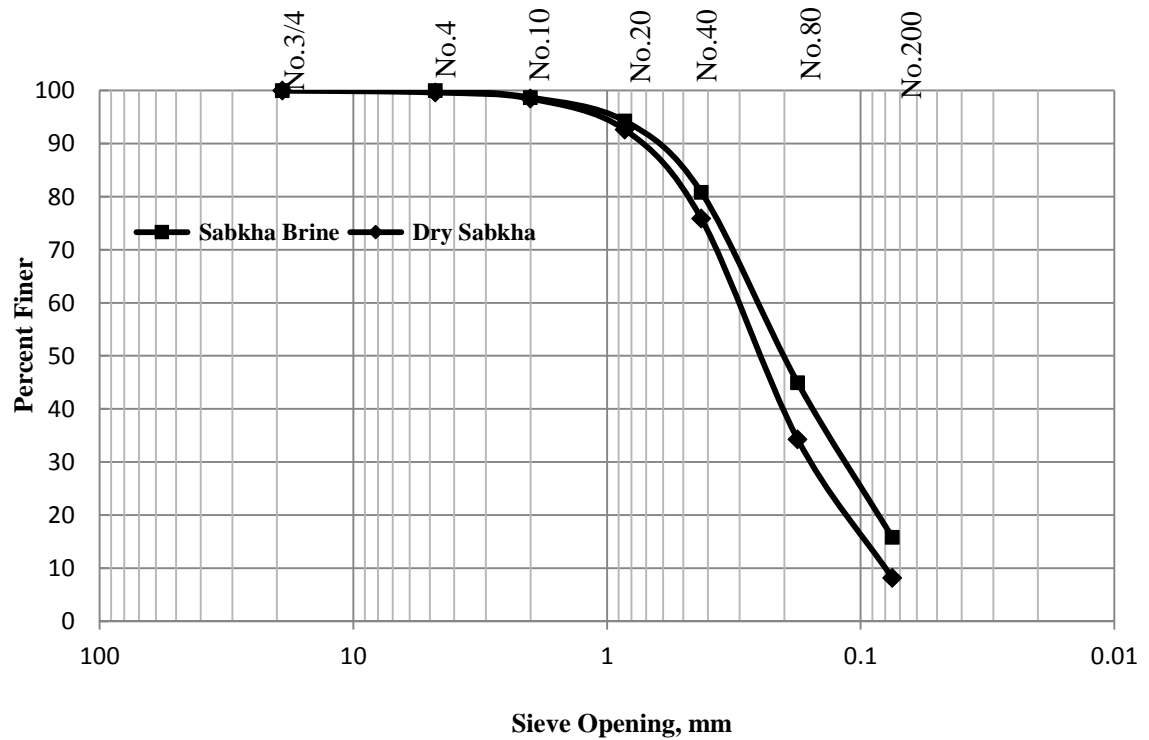


Figure 4-5: Grain Size Distribution of Sabkha Soil.

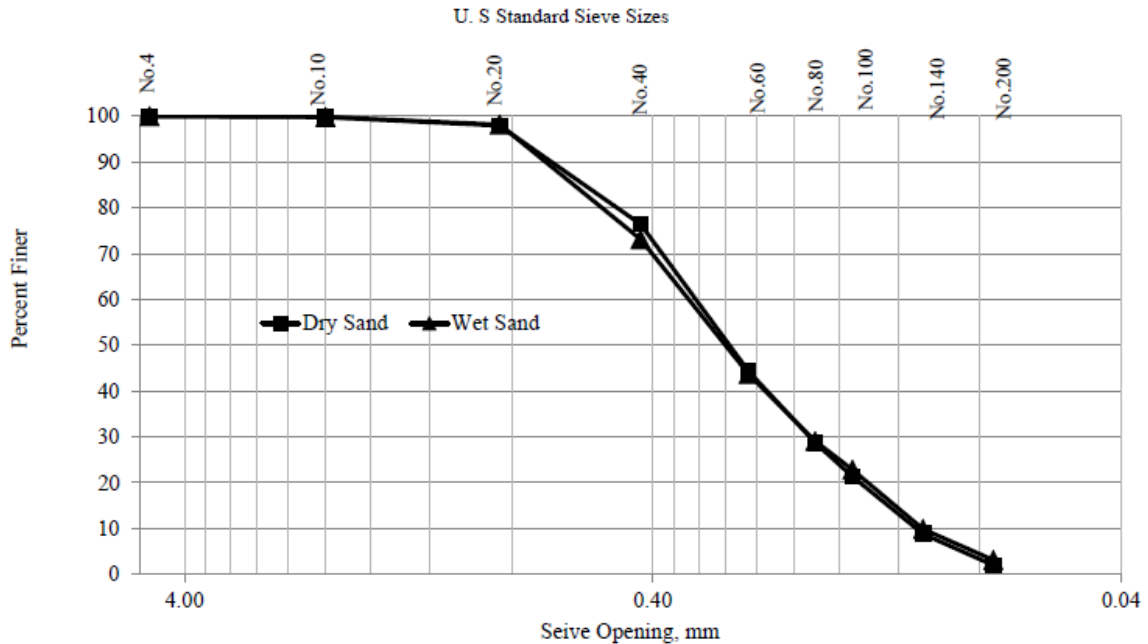


Figure 4-6: Grain Size Distribution of Sand Soil.

size distributions calculated by both the dry and wet sieving methods. This is ascribed to the fact that sand is made up of quartz which is not affected much by washing.

#### 4.1.5 Compaction Test

The relationships between moisture content and dry density for marl and sabkha, soils are shown in Figure 4.7. Compaction was conducted on plain soils using the modified Proctor compaction test in accordance with ASTM D 1557. It is clear from the figure that the maximum dry density of the marl soil was  $1.86 \text{ g/cm}^3$  at an optimum moisture content of 13% whereas for the sabkha soil it was  $1.75 \text{ g/cm}^3$  at 12% optimum moisture content. The water used in compaction test of sabkha soil was sabkha brine to simulate the field conditions of this soil. Regarding the sand soil, it was difficult to conduct the compaction test and get the moisture-density relationship curve so relative

density experiment was done to get the minimum and maximum density and they were  $1.63 \text{ g/cm}^3$  and  $1.84 \text{ g/cm}^3$ , respectively.

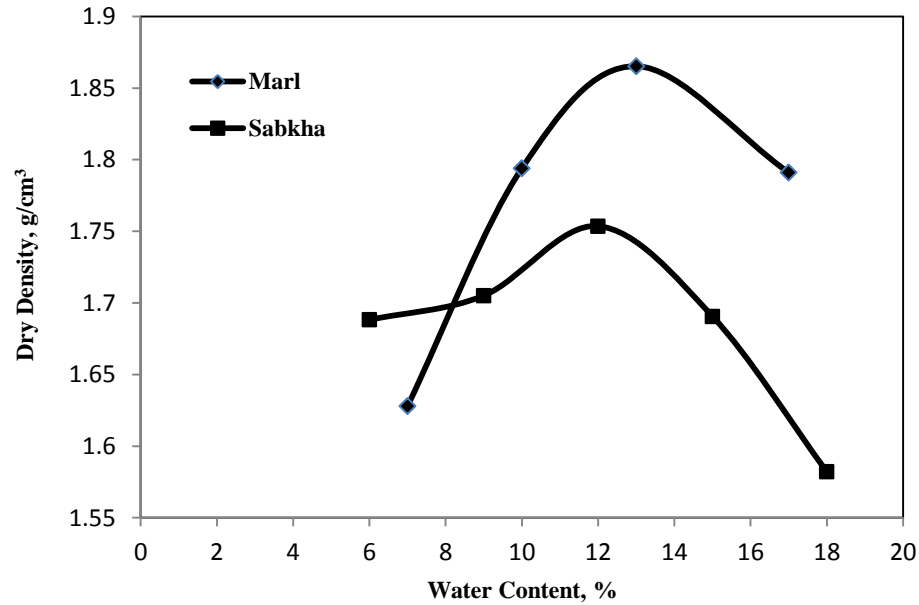


Figure 4-7: Moisture-Dry Density Relationship for Marl and Sabkha Soils.

#### 4.1.6 California Bearing Ratio (CBR)

The evaluation of soils to be used as a subgrade material in pavement structures is done by conducting CBR test. Figure 4.8 shows the relationships between water content and CBR value for marl and sabkha soils. It is seen that the maximum CBR value for the marl soil was 24.7% at a moisture content of 12% whereas it was 25% for sabkha soil at water content of 10%. The results indicated that the moisture content for maximum CBR is less than the optimum moisture content obtained from the dry unit weight-moisture content relationship. This is in agreement with the findings that have been reported in the literature for [Al-Amoudi et al., 1992a and Aiban et al., 1995]. The CBR value for the

sabkha soil is almost equal that for the marl soil and this is attributed to the submerging of sabkha soil samples in saline water rather than distilled water which reduced the dissolved salts that is responsible of particles bonding in sabkha soil. The reported CBR value in the literature for weak sabkha is around 10%.

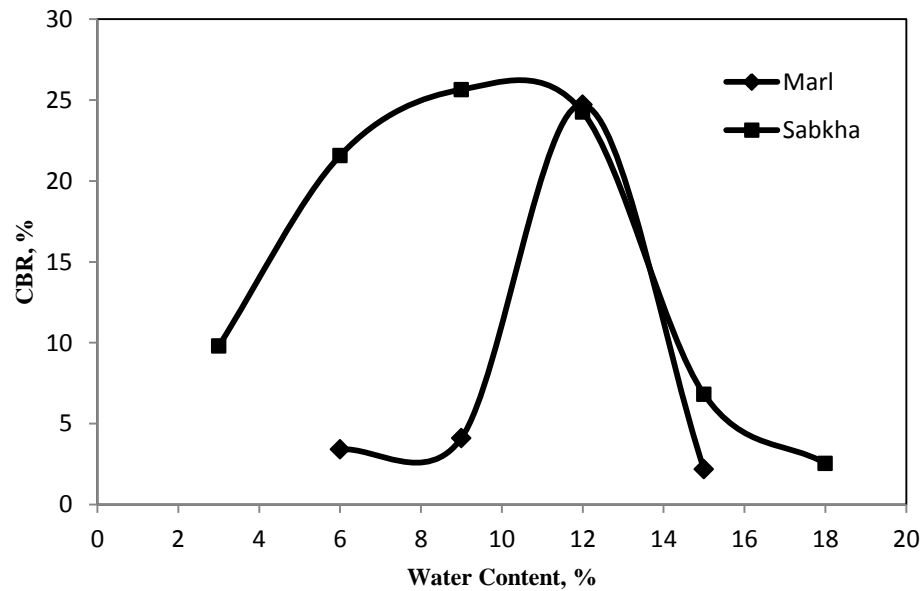


Figure 4-8: Moisture-CBR Relationship for Marl and Sabkha Soils.

The CBR test of the sand soil was done on samples compacted to at least 95% of the maximum density achieved in relative density test and the value of CBR was found to be 15%.

## 4.2 Asphalt Properties

Several ASTM tests were performed on asphalt cement 60/70 to evaluate its basic physical properties. The results of these tests are listed in Table 4.1, along with ASTM specifications. The results indicated that the utilized asphalt has a penetration value of 67.6 dmm, a softening point of 52.3 °C and a flash point of 340 °C and they are in the

range specified by ASTM. In addition, results show that asphalt has a rational viscosity of 571.75 centi-poise at 135 °C and a ductility of 150+ at 25 °C.

Table 4-1: Properties of Asphalt Cement.

Physical Properties	Utilized Asphalt	ASTM
Penetration at 25 °C (dmm) (ASTM D 5)	67.6	60-70
Rotational viscosity at 135 °C (centi-poise)	571.75	-
Softening point (°C) (ASTM D 36)	52.3	49-54
Flash point, Cleveland Open Cup (°C)	340	223 min.
Ductility at 25 °C (cm) (ASTM D 113)	150+	-

### **4.3 Foamed and Sulfur Modified Foamed Asphalt Mixes Evaluation Results**

#### **4.3.1 Design of Foaming Characteristics**

Laboratory mix designs and foamed asphalt producing were carried out using Laboratory scale WLB 10 foamed asphalt plant built by Wirtgen Gmbh Company which produces foamed asphalt that closely simulates full-scale production, as described in Chapter 3. The unit essentially consists of a kettle to heat the asphalt and calibrated systems for asphalt, water, and air. It enables predetermined volumes of asphalt, water, and air to be injected into the expansion chamber where the asphalt cement is formed and is then discharged through a nozzle. The expansion ratio and half-life of the foam can be manipulated by altering the proportion of water that is added to the asphalt and the optimum addition of water is determined [Writgen, 2004]. Once the design of the foam has been completed, the required volume of foamed asphalt is discharged directly into a sample of aggregate while it is being agitated in a laboratory mixer. Normally five

samples are produced in this way, with varying asphalt contents. In order to bring a material to its optimum moisture content for compaction, water prior to mixing was determined and added as follows [Writgen, 2004]:

$$W_{\text{added}} = 1 + (0.5W_{\text{OMC}} - W_{\text{air-dry}}) \quad (4-1)$$

Where,

$W_{\text{added}}$  is the pre-mixing water to be added to the sample;

$W_{\text{OMC}}$  is the optimum moisture content and

$W_{\text{air-dry}}$  is the moisture content in air dried sample.

2% of cement was added to all mixes after adding foamed asphalt to prevent affecting the optimum moisture content. The addition of 2% of cement has been found more economical and significantly improved the soaked ITS [Al-Abdul Wahhab et al., 2012]. The flow rate of the asphalt at different temperatures and water ratios at a specific pressure were determined after calibration of the Laboratory foaming machine WLB 10 which was used to produce the foamed asphalt. In this study, the asphalt flow rate was determined at different temperatures in a range of 160 °C to 180 °C. It is noticed that as the temperature increased, the asphalt flow rate increased. Furthermore, the amount of foaming water was varied at each temperature. For each water content, the expansion ratio and half-life were measured and found to increase with the increase in temperature. Based on comparison of the foaming characteristic at the three temperatures, it was clear that the normal asphalt (0% sulfur) produced the best foaming characteristics at 180 °C. Figure 4.9 shows the variation of the expansion ratio and half-life at this temperature.

Similarly, the procedure was repeated at different temperatures ranging from 140 °C to 150 °C for modified sulfur asphalt (30/70) to get the best foaming characteristics which were attained at 150 °C. The selection of lower temperatures (140 and 150 °C) was to avoid producing sulfur fumes and sulfur hydroxide (H<sub>2</sub>S) which are harmful gases. Figure 4.10 shows the variation of the expansion ratio and half-life at temperature of 150 °C for the modified sulfur asphalt. The optimum water content was selected to provide the minimum expansion ratio of eight times and minimum half-life of 6 sec. as explained in Figures 4.9 and 4.10 [Wirtgen, 2004]. The optimum water content was found to be 3.85 and 3.4% at 180 °C and 150 °C for the asphalt and the sulfur modified asphalt, respectively. The water flow rates were set at 24 l/h and 19 l/h for asphalt and sulfur modified asphalt, respectively.

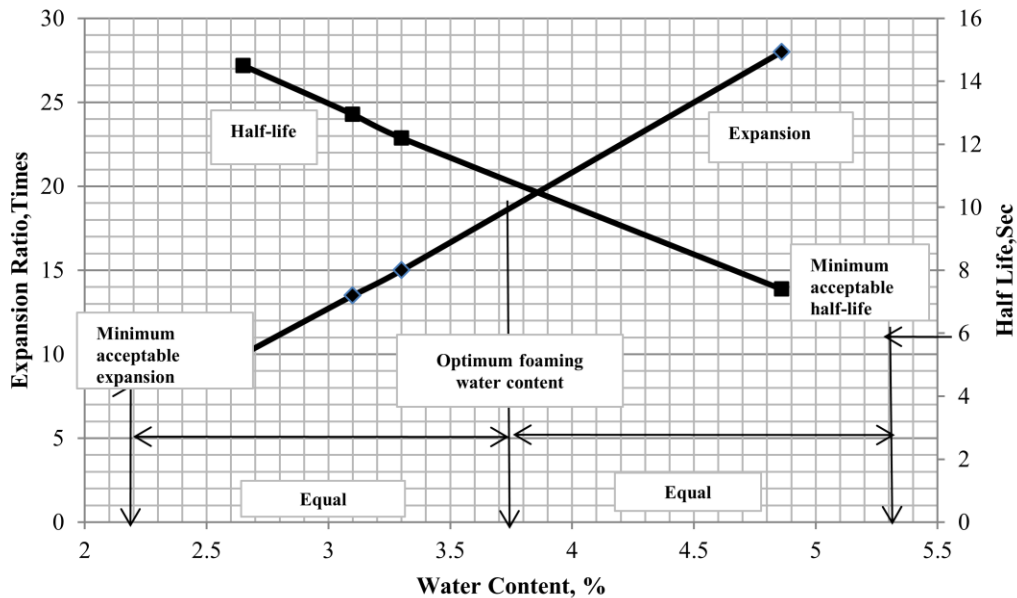


Figure 4-9: Determination of Optimum Foaming Water Content of Asphalt at 180 °C



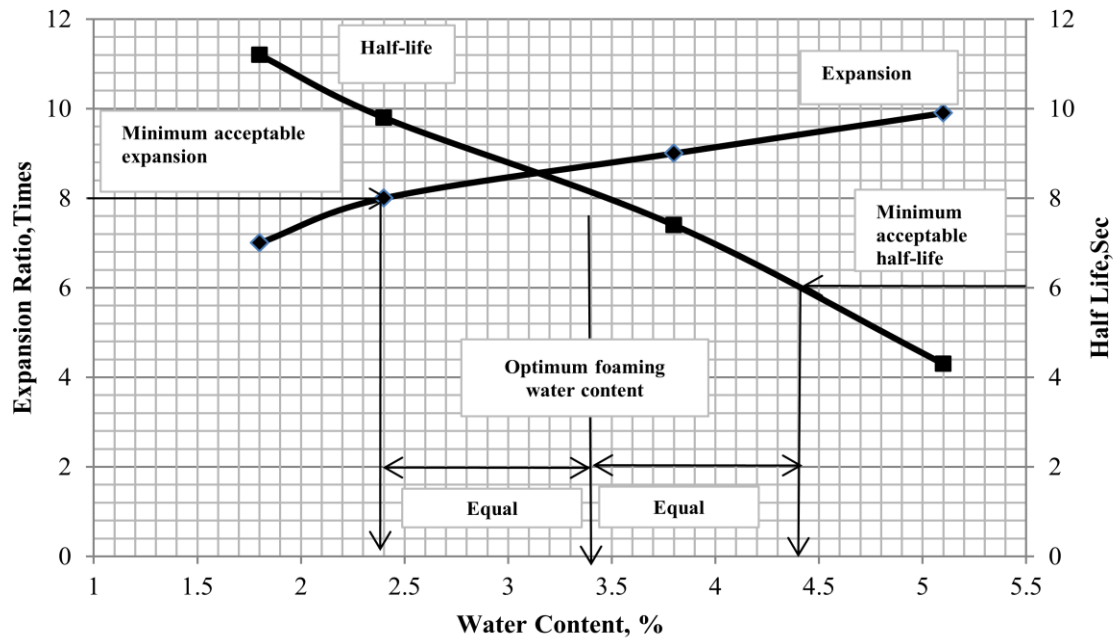


Figure 4-10: Determination of Optimum Foaming Water Content of Sulfur Modified Asphalt at 150 °C.

#### 4.3.2 Mixes Design and Evaluation

Three different soils, namely, marl, sabkha, and sand having gradation curves as shown in Figures 4.4 through 4.6 were treated with foamed and sulfur foamed asphalt to be used as a base in flexible pavements structure. After optimizing the foaming characteristics for the required water content and flow rate at which the maximum expansion ratio and half-life were attained, the selected soils were mixed with different foamed asphalt and sulfur foamed asphalt percentages (i.e. 3, 6, 9, 12, and 15%) to find the optimum foamed asphalt and sulfur asphalt contents. Foamed asphalt mixes were used as a reference in comparison results. Portland cement was added at a ratio of 2% to all mixes. The soils-foamed asphalt and sulfur asphalt mixes were compacted by using 75 blows of Marshall hammer into standard four-inch samples. The compacted specimens,

after curing for 72 hrs in an oven at 40 °C, were tested using indirect tensile strength test (ITS) at 25 °C for dry samples and after soaking for 2 hrs at 25 °C for wet samples to determine mix durability. Soaking was done in water at 25 °C under a vacuum pressure of 50-mm mercury for one hour. The vacuum is then slowly released and the specimen is left to soak in water for another one hour before testing.

#### **4.3.2.1 Indirect Tensile Strength (ITS) Results**

Figures 4.11 through 4.13 show the results of ITS of dry and soaked specimens for the marl, sabkha and sand soils mixed with foamed asphalt and sulfur foamed asphalt at the prescribed foam ratios. Optimum binder content should be selected at the maximum soaked ITS. From figures, it can be seen that the optimum foamed asphalt contents for the marl, sabkha, and sand soils were 9, 8, and 7%, respectively. However, the optimum contents for sulfur foamed asphalt were 9, 7, and 8% for the same soils, respectively.

Based on the ITS test results, it is concluded that marl soil exhibits higher values of ITS than sabkha and sand soils. Furthermore, the retained strength of the marl is higher than sabkha and sand soil either for foamed asphalt (FA) or sulfur foamed asphalt (SFA) mixes as shown in Figure 4.14. It can also be noticed that, although the indirect tensile strength values are reduced for the sulfur foamed asphalt (SFA) mixes, especially for sabkha, the strength loss for all soils mixed with SFA is less than that of the normal foamed asphalt mixes (FA). This leads to conclude that the addition of sulfur makes the mixes more stiff and resistant to the water effect. The index of retained strength for the three soils mixed with FA and SFA shown in Figure 4.14.

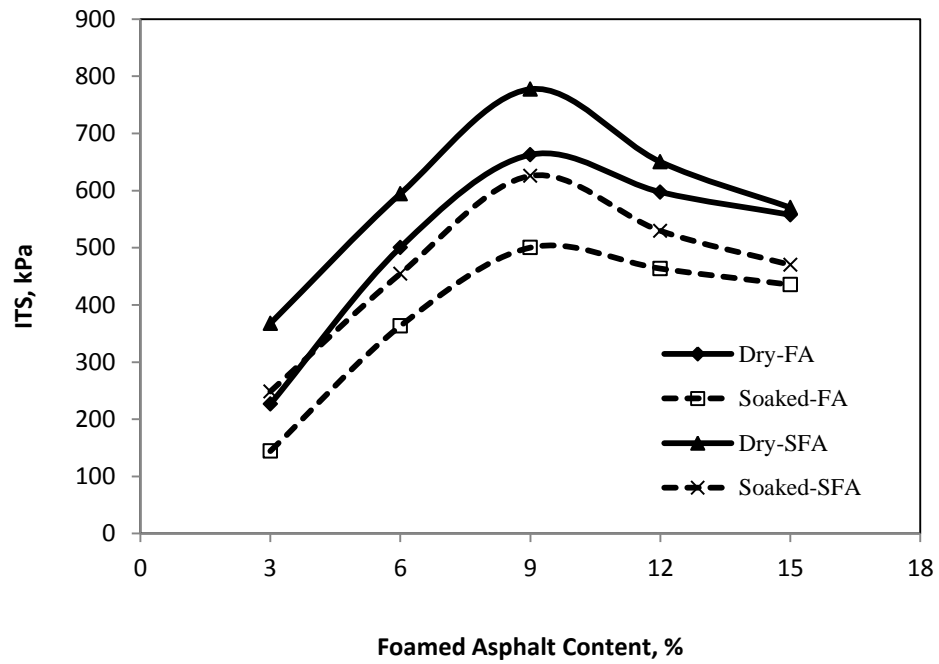


Figure 4-11: Dry and Soaked ITS for Marl Soil.

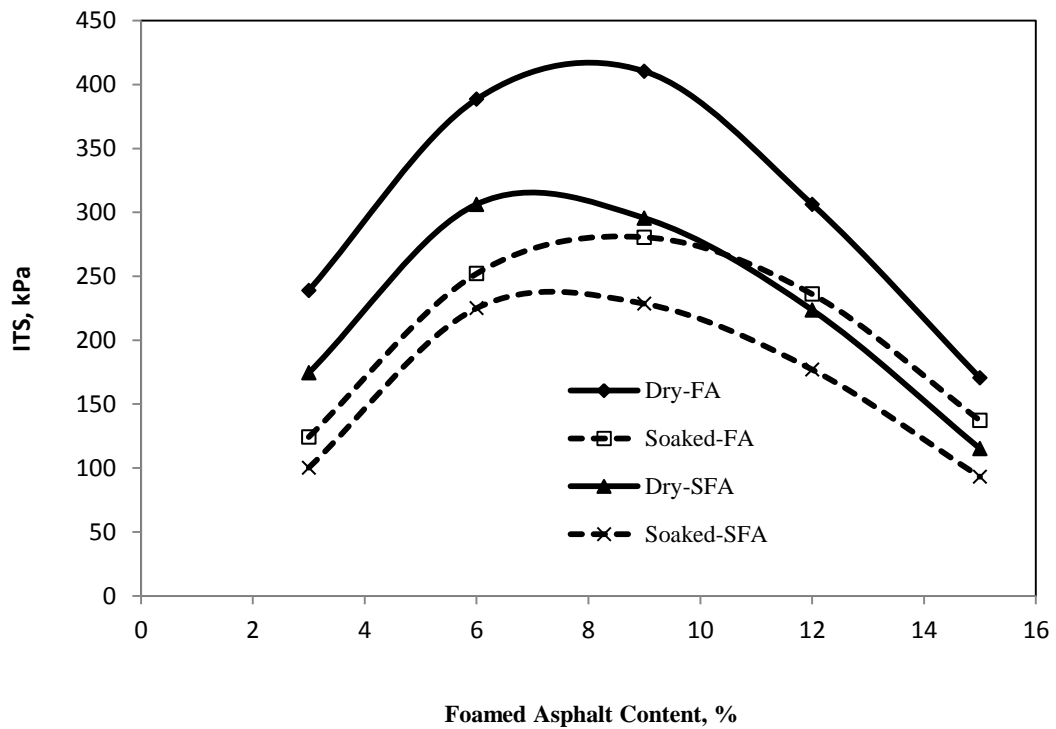


Figure 4-12: Dry and Soaked ITS for Sabkha Soil.

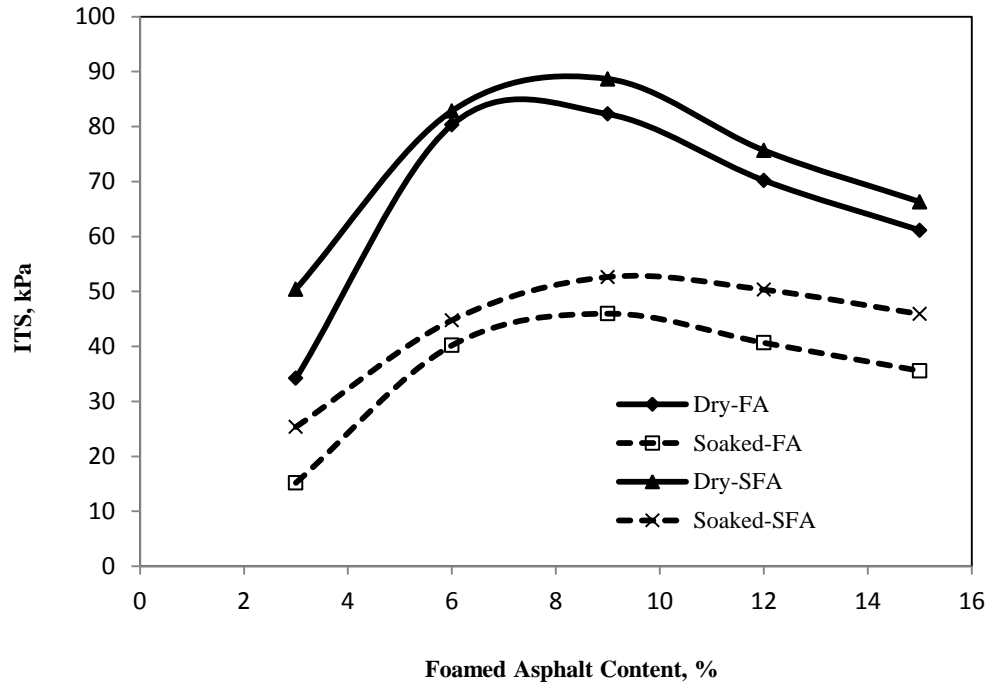


Figure 4-13: Dry and Soaked ITS for Sand Soil.

Recommendations from experts in the Australian Road Research Board (ARRB) are that the dry indirect tensile strength should be at least 200 kPa and the soaked tensile strength be at least 100 kPa for base course layer in the pavement structure [SABITA, 1998]. The design binder content should be selected at the maximum soaked ITS. For use as a base course layer in the pavement structure, where the water table is close to the surface, it is believed that an ITS of more than 200 kPa together with more than 80% retained strength of ITS will perform adequately [SABITA, 1998]. The results of ITS show that marl and sabkha mixes passed the requirements at the dry and soaked conditions as shown previously in Figures 4.11 and 4.12. However, sand mixes failed to pass these requirements as shown in Figure 4.13.

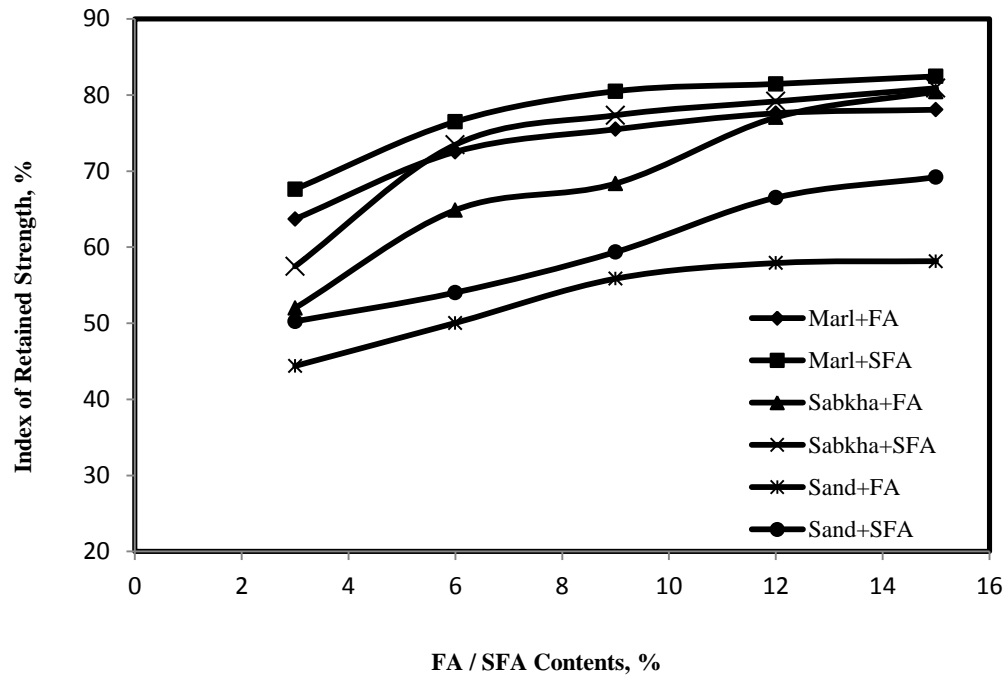


Figure 4-14: Index of Retained Strength Variation Versus FA and SFA Contents.

#### 4.3.2.2 Marshall Stability Test Results

Dry and soaked Marshall stability tests were conducted as per the standard test procedure ASTM D 1559 on the three soils (marl, sabkha, and sand) mixed at the optimum percentages of FA and SFA. The results are tabulated in Table 4.2.

Table 4-2: Marshall Stability Test Results.

Soil	Binder Type	Optimum Content, %	Dry Stability (kN)	Soaked Stability (kN)	Stability Loss (%)
Marl	FA	9	30	22.1	26.4
	SFA	9	34.2	27	21
Sabkha	FA	8	21.41	12.77	40
	SFA	7	21	13.8	34
Sand	FA	7	7.52	4.1	45.5
	SFA	8	8.5	5.04	41

It has been found that a stability value of 2224 N (500 lbs) or greater is considered satisfactory for most pavements with low to medium traffic volume [AEMA, 2004]. It is seen from the Table 4.1 that all soils mixes have stability (dry or soaked) greater this value and they passed the Asphalt Institute requirement. Furthermore, the stability loss of the soils-SFA mixes is lower than that of soils-FA mixes which is consistent with retained strength trend and clearly shows that addition of sulfur enhances the durability of mixes against water damage.

#### **4.3.2.3 Static Triaxial Test (Shear Strength) Results**

The triaxial shear strength test was performed in accordance with ASTM D 2850 on the three soils mixes (marl, sabkha, and sand) prepared at the optimum water, FA and SFA contents. 2 % cement was added to the mixes. The specimens have a size of 2 in. diameter and 4 in. height, were compacted to the optimum density using dynamic compactor. The number of blows and layers were determined to get the same density of Marshall specimens. Thereafter, samples were cured for 72 hrs at 40°C and then tested for the static triaxial test. The test was conducted at three different confining pressures up to failure. The test results were used to construct the Mohr-Coulomb failure envelope as presented in Figure 4.15. The angle of internal friction and cohesion were calculated and are summarized in Table 4.3.

It is clear from the results shown in Figure 4.15 and Table 4.3 that the highest shear strength is achieved by marl soil followed by sabkha soil and finally by sand soil. In addition to that, the soils-SFA mixes have a higher shear strength compared to the soils-FA mixes.

Table 4-3: Cohesion and Angle of Internal Friction for Soils-FA-SFA Mixes.

Soil Type	Binder Type	C (kPa)	$\phi$ (degree)
<b>Marl</b>	FA	121.9	22
	SFA	286.4	32
<b>Sabkha</b>	FA	104.4	27
	SFA	184.2	27
<b>Sand</b>	FA	18.8	27
	SFA	65.8	27

The strength parameter cohesion (C) increases sharply (more than 100 %) when soils are treated with sulfur foamed asphalt rather than normal foamed asphalt. However, the internal friction angle ( $\phi$ ) remains the same except for the marl soil. This means a structure with better bond is developed. For marl, larger interlocking grains are produced resulting in higher internal friction angle. The fine fraction plays a fundamental role in generating the cohesive properties and the more effective these materials the higher the particles contacts are and this justifies the high values of cohesion in marl and sabkha soils. Thus, it is expected that the sulfur foamed mixes will show superior rutting resistance than the standard mixes.

The general regression model with a high correlation ( $R^2 = 99.5\%$ ) for the shear strength was developed using Minitab version (16) software and reported as follows:

$$\tau = 317 - 23.4 x_1 - 7.4 x_2 + 12.5 x_3 + 0.509 \sigma_n + 1.13 C - 12.4 \phi \quad (R^2 = 99.5\%) \quad (4-2)$$

Where,

$\tau$  = shear strength in kPa;

$x_1 = 1$  (marl) or  $x_1 = 0$  (otherwise);

$x_2 = 1$  (sabkha) or  $x_2 = 0$  (otherwise);

$x_3 = 1$ (FA) or  $x_3 = 0$  (otherwise);

$\sigma_n$  = normal stress in kpa;

$C$  = cohesion in kPa, and

$\phi$  = Angle of internal friction in degree.

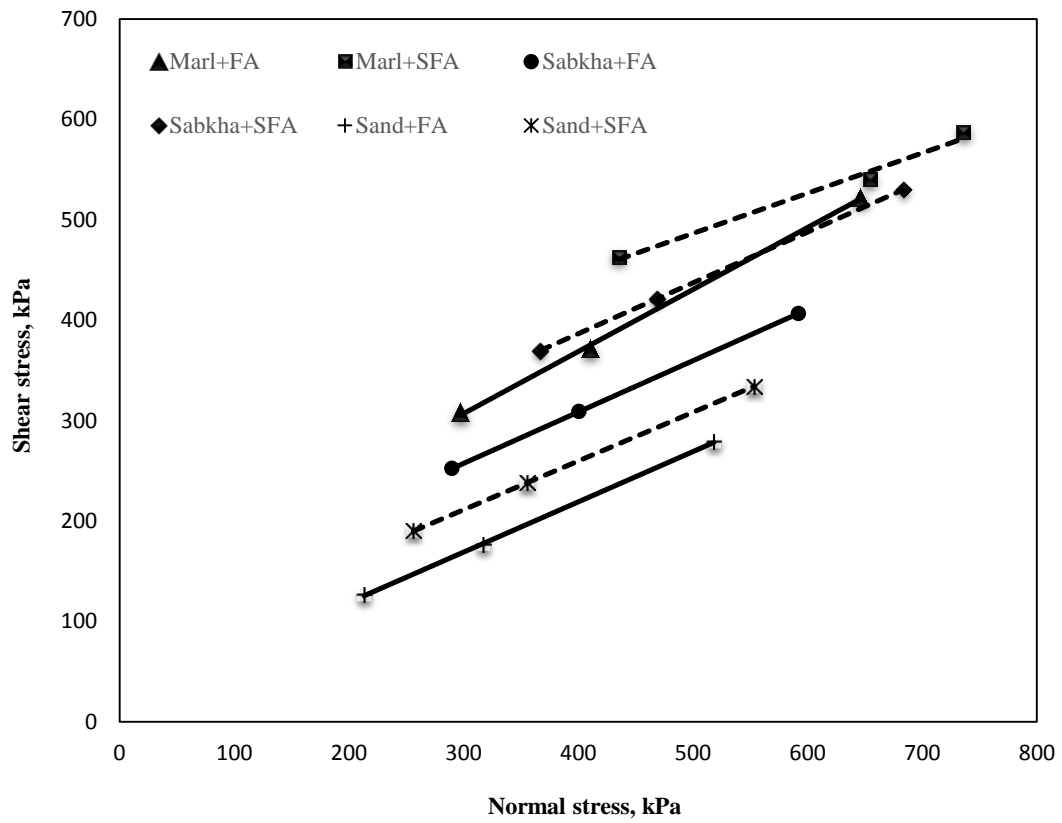


Figure 4-15: Mohr-Coulomb Failure Envelope for Soils-FA-SFA Mixes.



#### 4.3.2.4 Dynamic Resilient Modulus

Dynamic triaxial test was conducted at 22 °C and 40 °C to measure the dynamic resilient modulus at these two temperatures for the three soils, namely, marl, sabkha, and sand mixed with FA and SFA. The dynamic resilient modulus was measured according to the AASHTO T-307 procedure. The specimens were tested under different combinations of confined pressure, 21 to 138 kPa (3-20 psi) and deviator stress, 34 to 276 kPa (5-40 psi) as shown in Table 3.2 to simulate the traffic loading that the granular base and subbase materials are subjected to in the road structures. The variations of the resilient modulus with the deviator stress for all soils-FA/SFA mixes at 22 °C are presented in Figure 4.16. The results in Figure 4.16 and the statistical analysis presented in the end of this chapter show that there is a significant effect of the confining pressure variation in resilient modulus for all mixes either for FA or SFA mixes. In addition to that, the effect of deviator stress is clearly shown. At each confining pressure the resilient modulus increased greatly with the increase in the deviator stress. These findings are consistent with the results reported by [Li and Liu, 2010]. Furthermore, the marl soil mixed with FA or SFA have the highest resilient modulus values, followed by sabkha and lastly by sand mixes, however, SFA mixes have less resilient modulus values than that for the FA mixes.

Similarly, FA and SFA mixes were tested for resilient modulus at 40 °C and the relationships between the resilient modulus and the deviator stress are shown in Figure 4.17. From the figure, it can be seen that, upon testing at 40, the resilient modulus values dropped by magnitude of 30% for FA mixes, while, significant was noticed in the resilient modulus values for the SFA mixes. This insignificant reduction in the resilient

modulus of FA and SFA mixes under increased temperature could be attributed to the fact that the bond between particles of the mixes are improved due to small dispersed droplets of asphalt formed as a result of foaming and mixing process. Thus, at low temperature stiffness increased at the points where mineral particles are bounded by asphalt droplets while where are no asphalt droplets, the connection between particles did not change much when temperature dropped [Li and Liu, 2010]. Thus, due to increased temperature, only the asphalt bounded particles are affected, which are less comparing with normal soil grains.

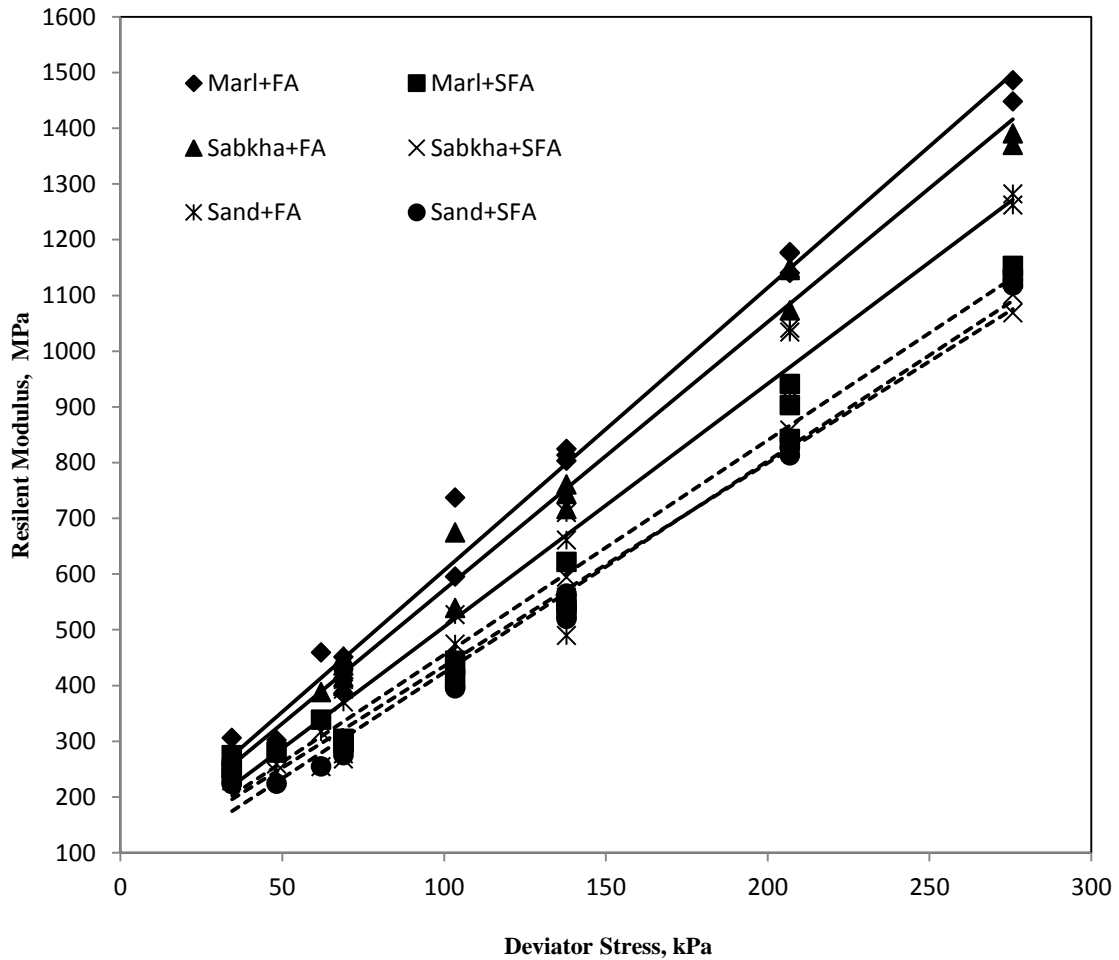


Figure 4-16: Variation of  $M_R$  with Deviator Stress for Foam Soils Mixes at 22 °C.

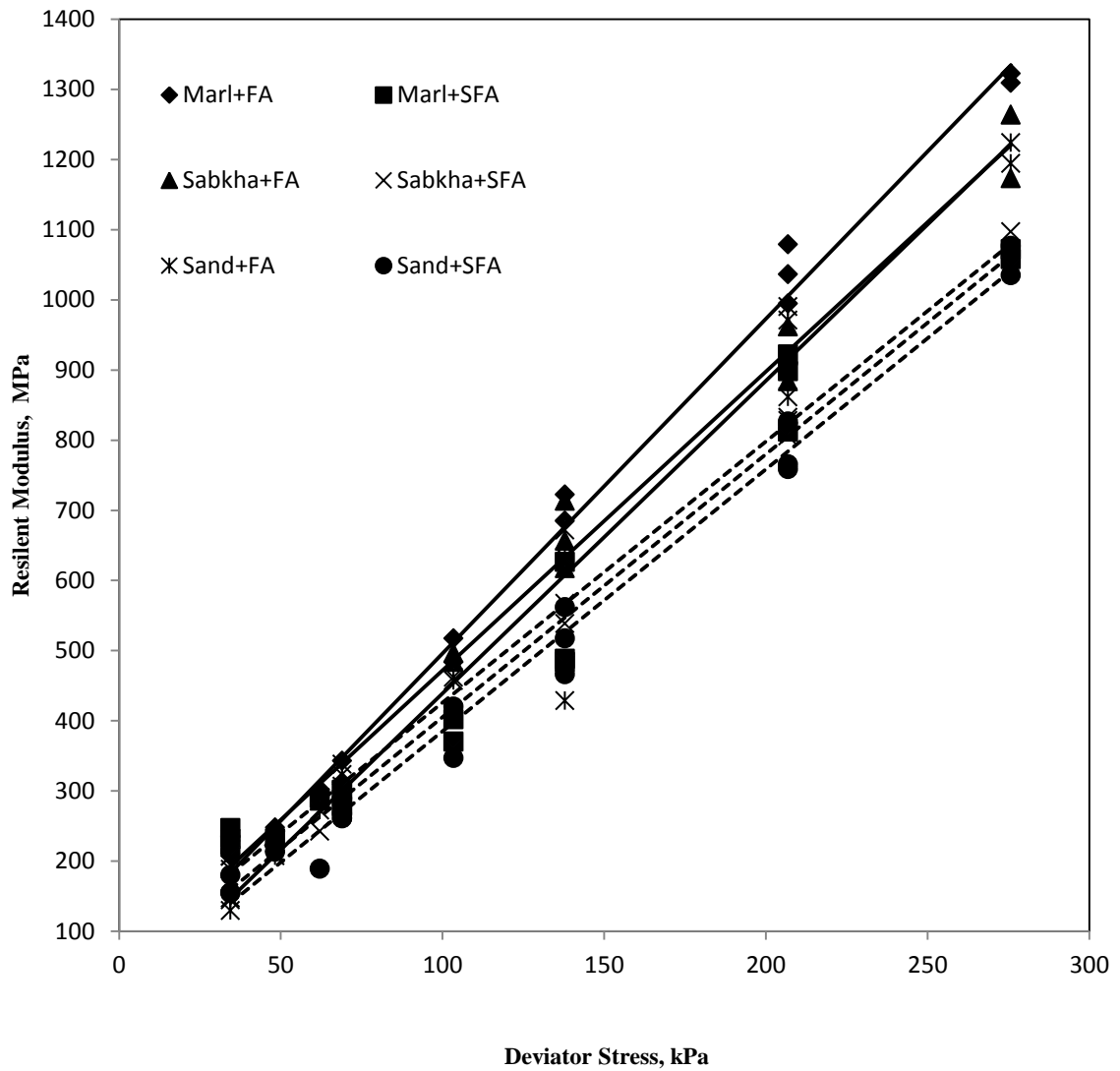


Figure 4-17: Variation of  $M_R$  with Deviator Stress for Soils Mixes at 40 ° C.

Furthermore, since the sulfur modified mixes have a higher strength compared to conventional mixes, as seen in the static triaxial test results, so they are stiff mixes and that might justify their lower sensitivity to temperature variation.

Table 4.4 shows regression models with high correlation of the resilient modulus in terms of deviator stress, confining pressure and temperatures. The general regression model of  $M_R$  that performed high correlation ( $R^2 = 96.9\%$ ) is as follows:

$$M_R = 83.2 + 63.1 x_1 + 33.3 x_2 - 3.62 T + 111 x_3 - 0.203 \sigma_c + 4.25 \sigma_d \quad (4-3)$$

Where,

$M_R$  = resilient modulus in MPa

$x_1 = 1$  (marl) or  $x_1 = 0$  (otherwise);

$x_2 = 1$  (sabkha) or  $x_2 = 0$  (otherwise);

$x_3 = 1$  (FA) or  $x_3 = 0$  (otherwise);

$T$  = temperature in degree

$\sigma_c$  = confining pressure in kPa

$\sigma_d$  = deviator stress in kPa

Table 4-4: Regression Models of  $M_R$  for Foamed Asphalt Mixes.

Material Type	Type of Additive	$M_R$	$R^2$
Marl	FA	$M_R = 260 - 6.47 T + 0.004 \sigma_c + 4.92 \sigma_d$	0.989
	SFA	$M_R = 147 - 1.77 T - 0.692 \sigma_c + 4.00 \sigma_d$	0.982
Sabkha	FA	$M_R = 256 - 6.16 T + 0.079 \sigma_c + 4.51 \sigma_d$	0.986
	SFA	$M_R = 115 - 1.53 T - 0.393 \sigma_c + 3.82 \sigma_d$	0.988
Sand	FA	$M_R = 135 - 3.57 T + 0.152 \sigma_c + 4.36 \sigma_d$	0.977
	SFA	$M_R = 112 - 2.20 T - 0.371 \sigma_c + 3.88 \sigma_d$	0.991

#### **4.3.2.5 Dynamic Triaxial Test**

Dynamic triaxial repeated load test was conducted on specimens of size (100 mm diameter by 200 mm height) prepared at the optimum water and asphalt contents (FA, and SFA) and compacted to the maximum dry density. The specimens were tested under 10 psi confining pressure and a range of deviator stress (40-80 psi) (276- 552 kPa) to simulate the traffic loading that the granular base and subbase materials are subjected to in the road. The deviatoric stress was applied in the form of a sinusoidal (haversine) wave pulse with loading time of 0.1 second followed by reset period of 0.9 second. Repeated load tests were applied for treated mixes samples at two different temperatures (lab temperature 22°C and 40° C) and with three levels of deviator stress (60, 70 and 80 psi) (414, 483, and 552 kPa) for stiff materials and (40, 50 and 60 psi) (276, 345, and 414 kPa) for less stiffness materials.

The results of the dynamic triaxial tests for the soils (marl, sabkha and sand) treated at the optimum percentages with FA and SFA and tested at 22°C are presented through Figure 4.18 to Figure 4.20. It is clear from the figures that the marl soil has a high resistance to rutting, followed by sabkha soil and then by sand soil. Furthermore, the SFA mixes, except sand soil, reflect a high rutting resistant in comparison to the normal FA mixes which is considered a great advantage for the new investigated material (SFA). However, for the sand soil the difference is not so much and the permanent deformation is high either for the standard mixes (FA) or the modified mixes (SFA). The increase in

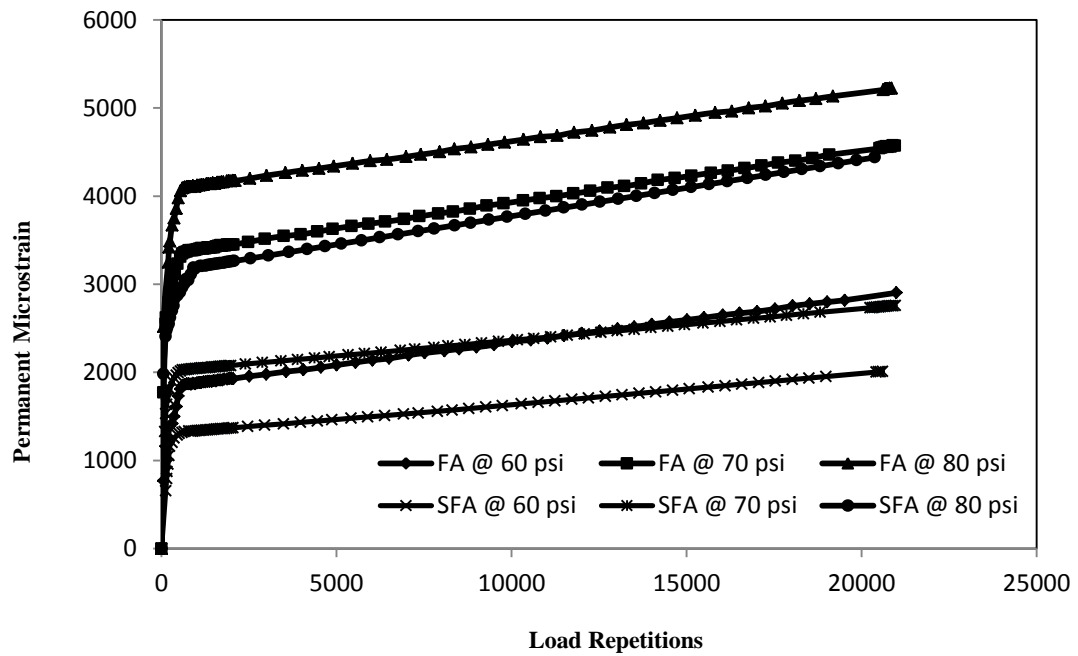


Figure 4-18: Dynamic Triaxial Test Results for Marl-FA/SFA Tested at 22 °C.

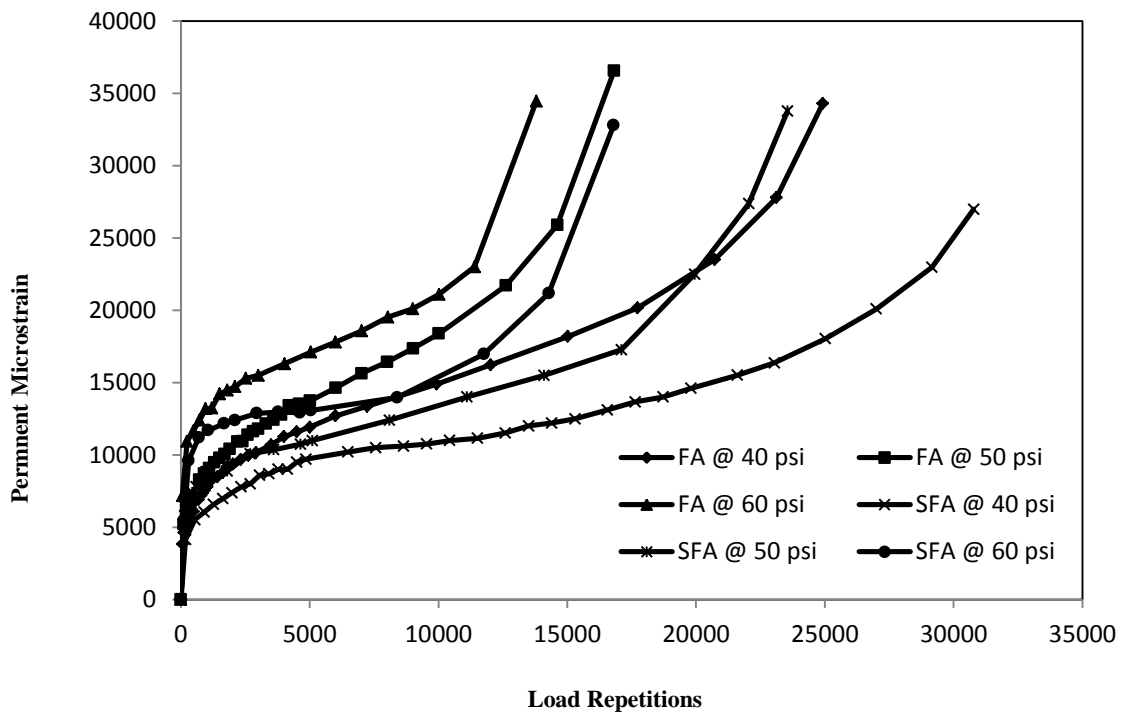


Figure 4-19: Dynamic Triaxial Test Results for Sabkha-FA/SFA Mixes Tested at 22 °C.

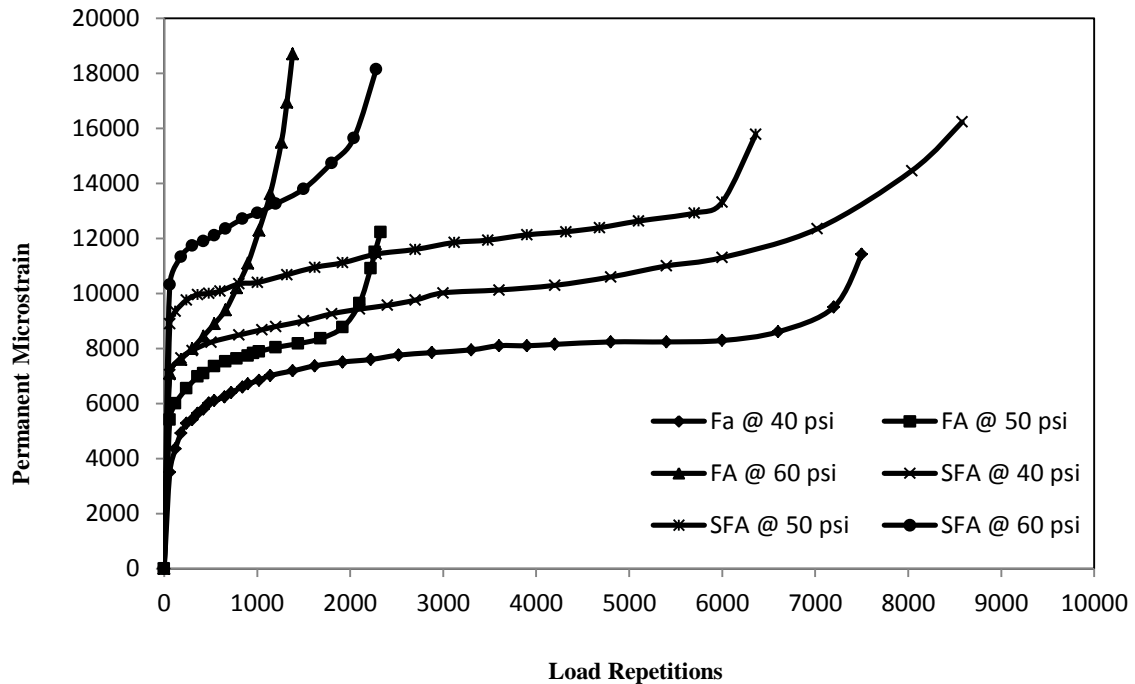


Figure 4-20: Dynamic Triaxial Test Results for Sand-FA/SFA Mixes Tested at 22 °C.

the resistivity of the sulfur modified mixes to the permanent deformation may be ascribed to the high shear strength of these mixes as it is clear from the results of the static triaxial test in which there was a sharp increase in the shear strength parameters  $C$  and  $\phi$ , particularly  $C$  when soils are treated with sulfur foamed asphalt.

Similarly, Figures 4.21 to 4.24 show the results of the dynamic triaxial test for the same soils tested at 40 °C. It can be seen that, the same trend as before (at 22 °C) is noticeable for the sabkha soil and marl in which SFA mixes have higher resistance to permanent deformation. In addition to that and based on the results of the sand mixes shown in Figure 4.23 and Figure 4.24, in spite of the weakness of the sand mixes, the SFA mix are more resistant to permanent deformation than FA mix when tested at higher temperature (40 °C), particularly under low to medium loading stresses.

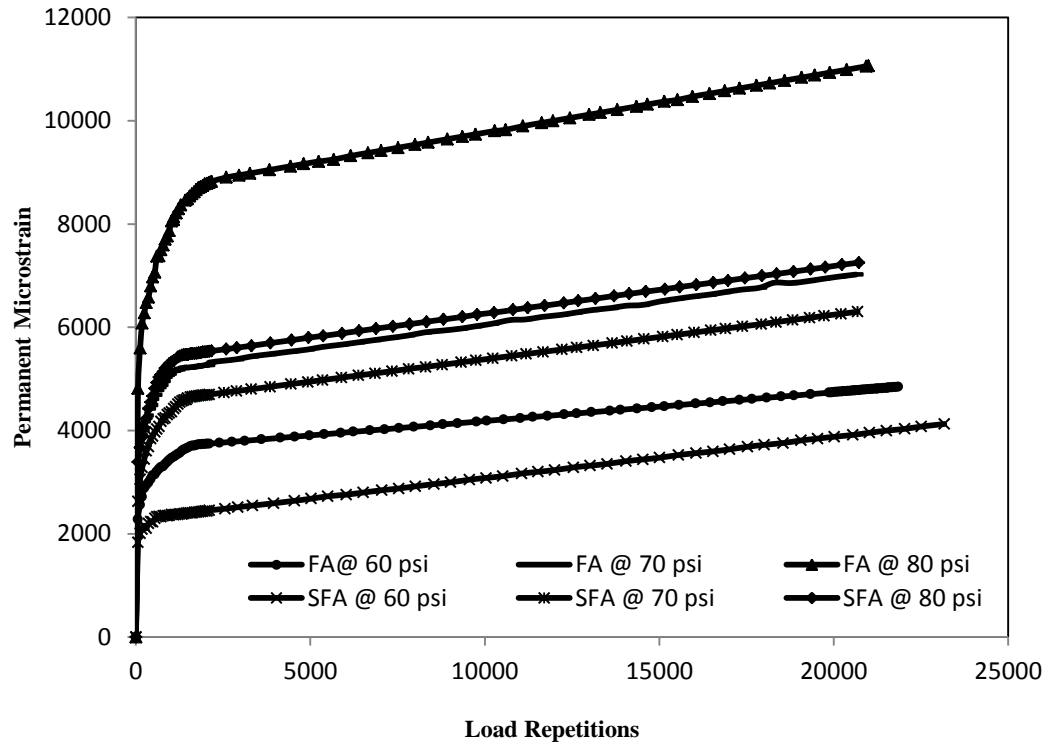


Figure 4-21: Dynamic Triaxial Test Results for Marl-FA/SFA Mixes Tested at 40 °C.

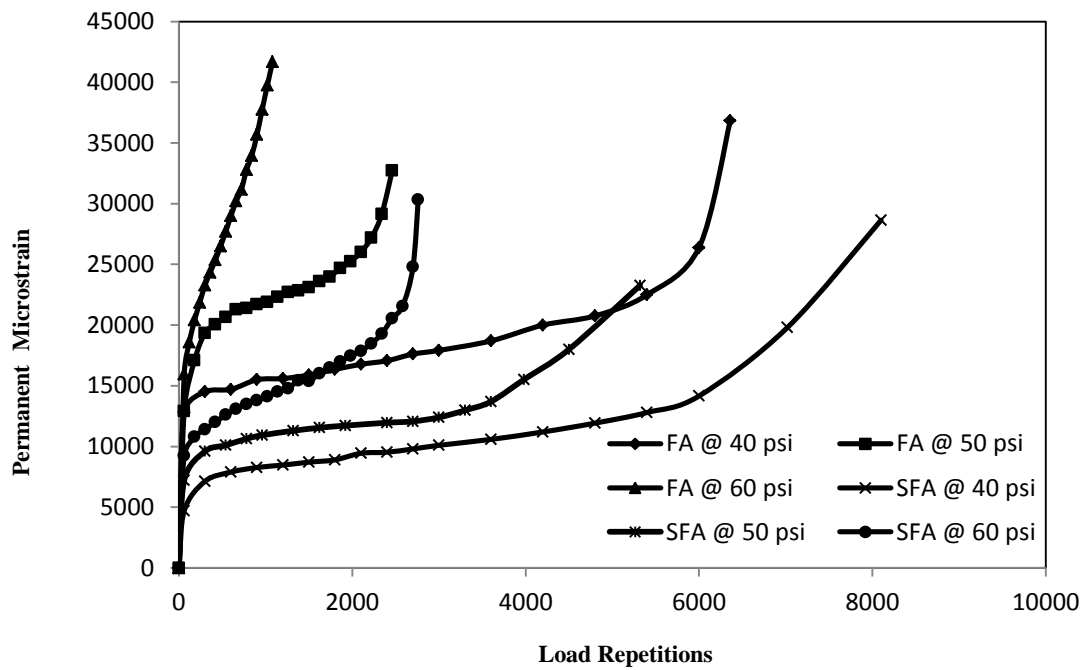


Figure 4-22: Dynamic Triaxial Test Results for Sabkha –FA/SFA Mixes Tested at 40 °C.



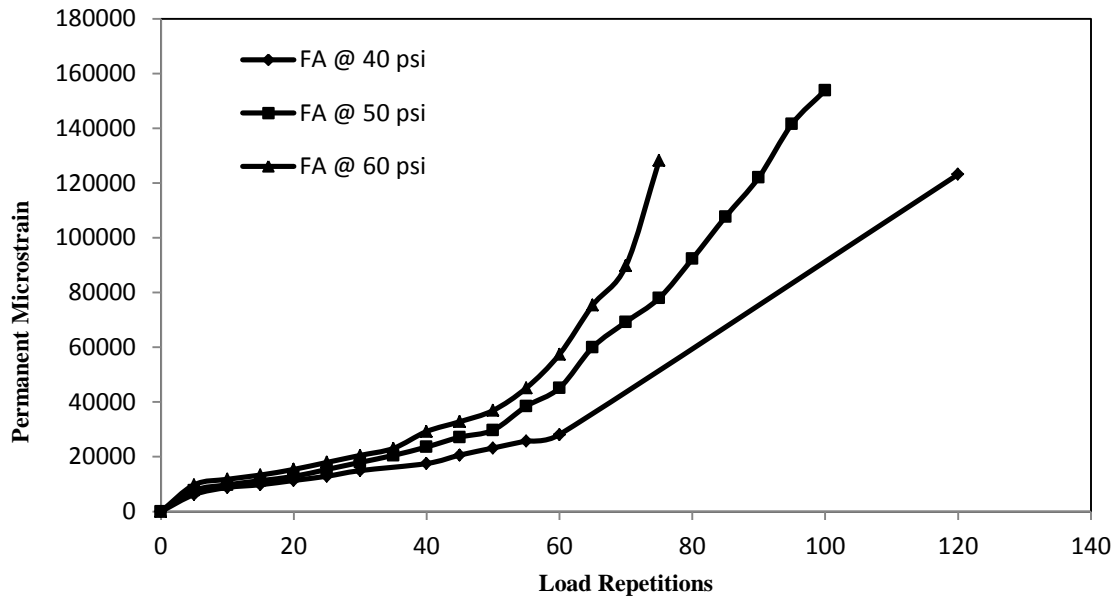


Figure 4-23: Dynamic Triaxial Test Results for Sand-FA Mixes Tested at 40 °C.

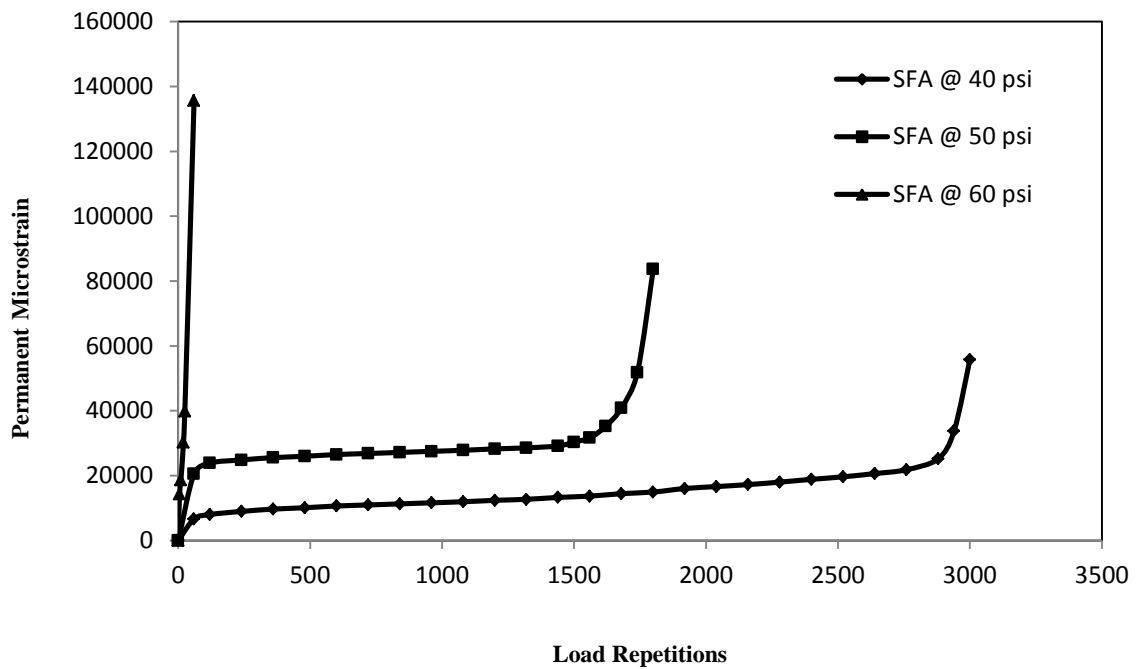


Figure 4-24: Dynamic Triaxial Test Results for Sand-SFA Mixes Tested at 40 °C.

Table 4.5 shows calculated intercept coefficient (a) and slope coefficient (b) of the regression curves fitting to the log permanent strain ( $\epsilon_p$ ) – log load repetitions ( $N$ ) for all mixes under different stress levels and at different temperatures (22 °C and 40 °C).

Regression models of these parameters in terms of temperature and deviator stress were developed using Minitab 16 software for all mixes and are listed in Table 4.6. The general regression models are as follows:

$$a = 362 - 4399 x_1 - 1944 x_2 - 627 x_3 + 42.7 T + 8.69 \sigma_d \quad (R^2 = 63.4\%) \quad (4-4)$$

$$b = 0.028 - 0.148 x_1 - 0.0262 x_2 + 0.0211 x_3 + 0.00331 T + 0.000316 \sigma_d \quad (R^2 = 32.3\%) \quad (4-5)$$

Where,

a and b = intercept and slope coefficients (permanent deformation regression coefficients)

$x_1 = 1$  (marl) or  $x_1 = 0$  (otherwise);

$x_2 = 1$  (sabkha) or  $x_2 = 0$  (otherwise);

$x_3 = 1$ (FA) or  $x_3 = 0$  (otherwise);

T = temperature in degree.

$\sigma_d$  = deviator stress in kPa.

It is clear that the general models of a and b coefficients have low correlation compared with the models listed in Table 4.6 even when we tried stepwise regression (foreword regression) and removed insignificant factors the correlation did not change much, hence,

Table 4-5: Intercept and Slope Coefficients for Tested Foamed Asphalt Mixes.

Soil Type	Temp. °C	Treatment Type	$\sigma_c$ (psi)	$\sigma_d$ (psi)	$\sigma_d$ (kPa)	a	b	R <sup>2</sup>
Marl	22	FA	10	60	413.69	436	0.103	0.951
			10	70	482.60	1260	0.125	0.918
			10	80	551.60	1808	0.185	0.91
		SFA	10	60	413.69	347	0.122	0.912
			10	70	482.60	780	0.140	0.916
			10	80	551.60	1060	0.171	0.938
	40	FA	10	60	413.69	407	0.100	0.931
			10	70	482.60	1881	0.128	0.915
			10	80	551.60	2551	0.183	0.931
		SFA	10	60	413.69	1144	0.141	0.975
			10	70	482.60	993	0.170	0.976
			10	80	551.60	1312	0.184	0.976
Sabkha	22	FA	10	40	275.79	350	0.220	0.991
			10	50	344.74	1012	0.240	0.964
			10	60	413.69	2658	0.250	0.96
		SFA	10	40	275.79	1262	0.200	0.924
			10	50	344.74	1604	0.220	0.829
			10	60	413.69	1631	0.220	0.862
	40	FA	10	40	275.79	4679	0.210	0.916
			10	50	344.74	3931	0.220	0.865
			10	60	413.69	3017	0.230	0.939
		SFA	10	40	275.79	1945	0.207	0.905
			10	50	344.74	4717	0.230	0.889
			10	60	413.69	2264	0.240	0.955
Sand	22	FA	10	40	275.79	2548	0.141	0.967
			10	50	344.74	3180	0.130	0.978
			10	60	413.69	3523	0.147	0.933
		SFA	10	40	275.79	4076	0.110	0.923
			10	50	344.74	5734	0.130	0.918
			10	60	413.69	7543	0.330	0.89
	40	FA	10	40	275.79	2783	0.480	0.96
			10	50	344.74	2486	0.598	0.939
			10	60	413.69	3566	0.220	0.83
		SFA	10	40	275.79	3439	0.177	0.98
			10	50	344.74	6656	0.164	0.964
			10	60	413.69	6861	0.374	0.969

we recommend using material and stabilizer specific models shown in Table 4.6 instead of the general models above.

Table 4-6: Regression Models of a and b Coefficients for Foamed Asphalt Mixes.

Material Type	Type of Additive	a	R <sup>2</sup>	b	R <sup>2</sup>
Marl	FA	$a = -5529 + 24.7 T + 12.7 \sigma_d$	0.926	$b = -0.15 - 0.000073 T + 0.000598 \sigma_d$	0.95
	SFA	$a = -1326 + 23.4 T + 3.19 \sigma_d$	0.8	$b = -0.0419 + 0.00115 T + 0.000334 \sigma_d$	0.974
Sabkha	FA	$a = -2567 + 141 T + 2.34 \sigma_d$	0.704	$b = 0.195 - 0.000926 T + 0.000181 \sigma_d$	0.962
	SFA	$a = -1165 + 82.0 T + 2.49 \sigma_d$	0.426	$b = 0.132 + 0.000685 T + 0.000192 \sigma_d$	0.872
Sand	FA	$a = 1056 - 7.7 T + 6.37 \sigma_d$	0.703	$b = 0.098 + 0.0163 T + 0.00092 \sigma_d$	0.712
	SFA	$a = -2665 - 7.4 T + 25.0 \sigma_d$	0.887	$b = -0.398 + 0.00287 T + 0.00151 \sigma_d$	0.759

#### 4.3.2.6 Wheel Tracking Test Results

Wheel tracking test is considered one of the most important tests simulating the field conditions. Thus, rutting behavior of compacted base mixes was simulated using Wessex engineering wheel track tester. Two slabs for each mix were compacted to their maximum dry density (the same density as in the dynamic triaxial test specimens) using dynamic compaction. Twelve slabs, 45 cm x 22 cm x 10 cm thick, were prepared from the three soils (marl, sabkha and sand) mixed with FA and SFA. The slabs were then cured at 40 °C for 72 hours and tested dry under a wheel load of 80 psi (552 kPa) at the lab temperature (22 °C). Figure 4.25 shows samples of the tested slabs of marl soil where high rutting resistance is clearly shown.

The results shown in Figures 4.26 to 4.28 are the measured rut depth for the foamed (FA and SFA) treated slabs for the marl, sabkha and sand soils, respectively. Results clearly show the same ranking obtained from the dynamic triaxial test in which marl soil has the highest rutting resistance followed by sabkha and then by sand soil. Furthermore, the sulfur modified foam asphalt mixes have less rutting susceptibility than

the conventional foam mixes. Results also show that the sand treated with FA or SFA is very sensitive to the rutting and exhibited higher permanent deformation ( $> 15$  mm within first thousand load repetition) compared to the others mixes (marl and sabkha). The test section was considered failed when the vertical deformation was equal or more than 25mm (1 in.).



Figure 4-25: Permanent Deformation in Wheel Tracking of FA/SFA Samples.

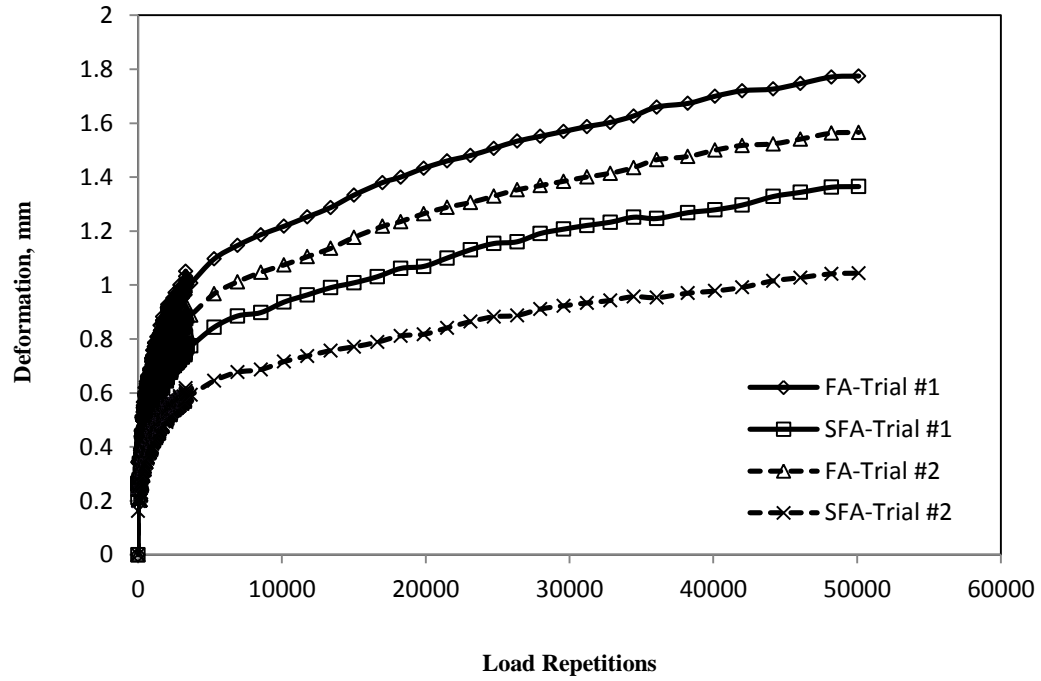


Figure 4-26: Results of the Permanent Deformation for the Marl-FA/SFA Mixes Using Wheel Track Machine, Dry at 22 °C.

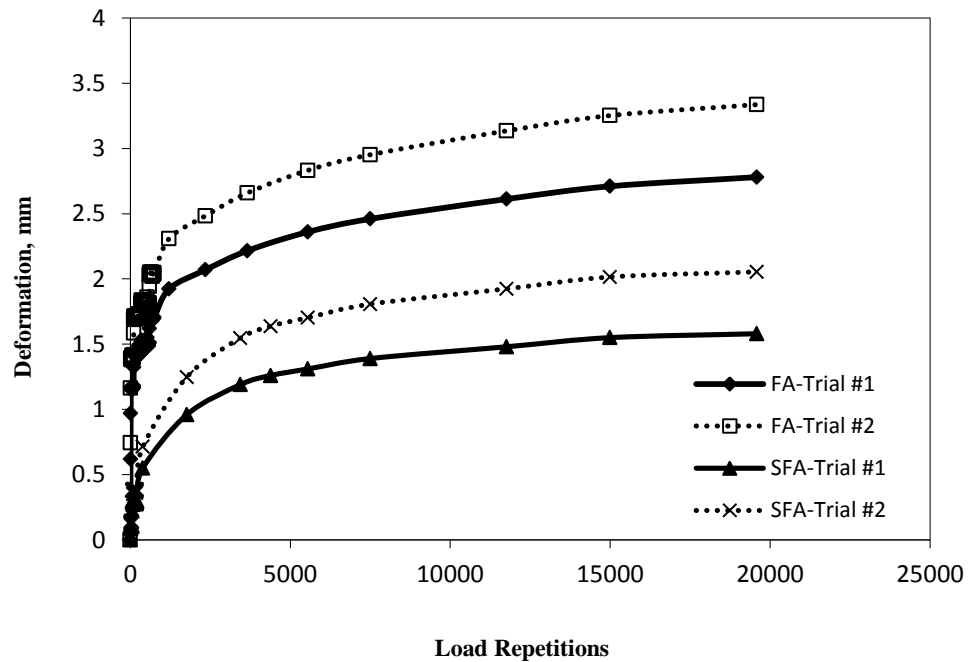


Figure 4-27: Results of the Permanent Deformation for the Sabkha-FA/SFA Mixes Using Wheel Track Machine, Dry at 22 °C.

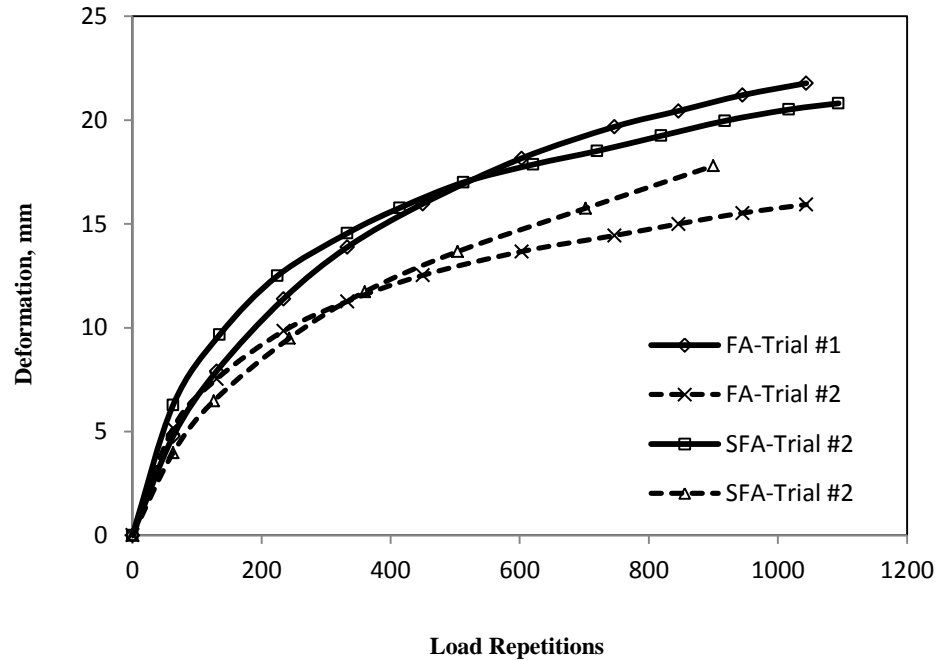


Figure 4-28: Results of the Permanent Deformation for the Sand-FA/SFA Mixes Using Wheel Track Machine, Dry at 22 °C.

## 4.4 Emulsified and Emulsified Sulfur Asphalt Mixes Evaluation

### Results

Emulsified asphalt plant available in Highway Laboratory at KFUPM was used to produce slow setting cationic sulfur asphalt emulsion. Samples from marl, sabkha, and sand soils were prepared and mixed with various percentages (i.e. 3, 6, 9, 12, and 15%) of emulsified and sulfur emulsified asphalt according to the procedures described in Chapter 3 (AEMA, 2004). To get the optimum residual asphalt the prepared mixtures were compacted in Marshall mold with 75 blows for each side. After that, the molds containing the compacted specimen were placed on a perforated shelf in a 60 °C (140 °F) forced draft oven for 48 hours. After curing, the specimens were subjected to dry and soaked Marshall test and the optimum residual asphalt was obtained based on the maximum

soaked Marshall stability. Furthermore, the mixes specimens were evaluated for dry indirect tensile strength.

#### **4.4.1 Marshall Stability Test Results**

The prepared specimens of size about 101mm diameter by approximately 63.5mm high for the soils treated with the normal emulsified asphalt and sulfur modified emulsified asphalt were subjected to dry and soaked Marshall stability test in accordance to ASTM D 1559 and the results are shown in Figures 4.29 to 4.31. It is seen from the figures that the optimum residual asphalt contents (OAC), based on the attained maximum soaked stability, are 8.1, 4, and 5.4% for the marl, sabkha, and sand treated with emulsion asphalt (EA), respectively, while, the OAC are 7.2, 3.6, and 5.4% for the same soils treated with sulfur modified asphalt (SEA), respectively. It can also be seen that, the sulfur modified emulsion decreases the stability of the treated soils comparing to the conventional emulsion asphalt. The optimum residual asphalt contents at which the maximum stabilities were attained for the SEA mixes were less than that for the EA mixes, except sand mixes.

The durability of the treated soils with EA and SEA were assessed by following the procedure reported in Chapter three Sec. 3.5.3 for soaking the specimens and then testing for the soaked stability. Figure 4.32 shows the variation of retained stability with residual asphalt contents of EA and SEA. From the figure, it is seen that SEA mixes, except sand soil, have higher retained stabilities than those of EA which indicated that the addition of sulfur modified emulsion asphalt enhance the water resistance of the mixes. Based on the results of Marshall stability, it is clear that the marl soil have the highest stability, then followed by the sabkha soil, and finally by the sand soil.



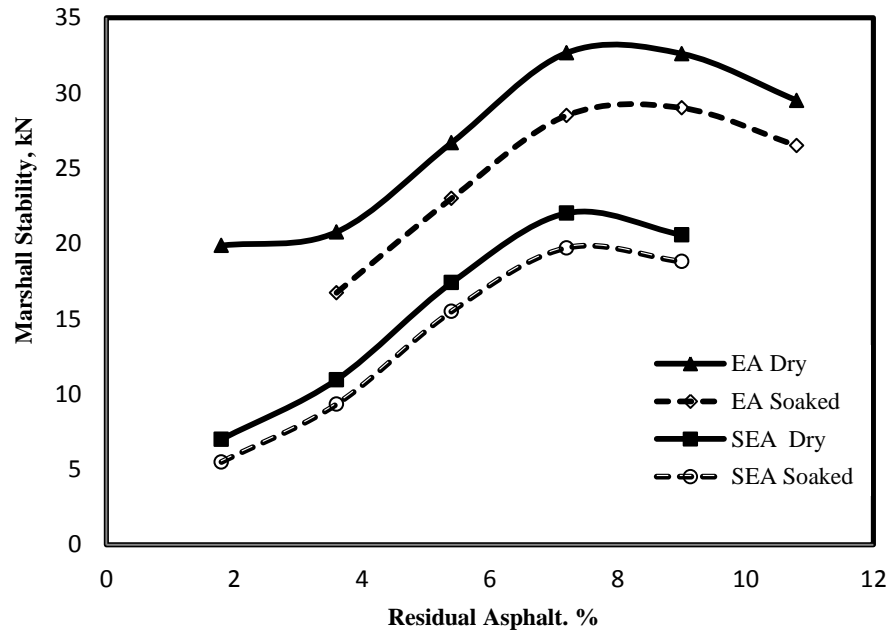


Figure 4-29: Dry and Soaked Stability for Marl Soil.

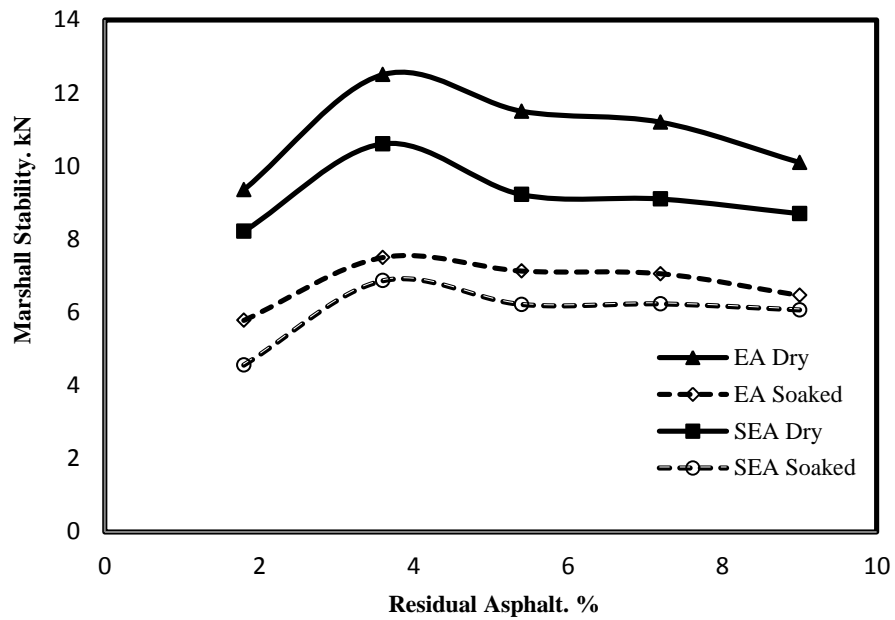


Figure 4-30: Dry and Soaked Stability for Sabkha Soil.

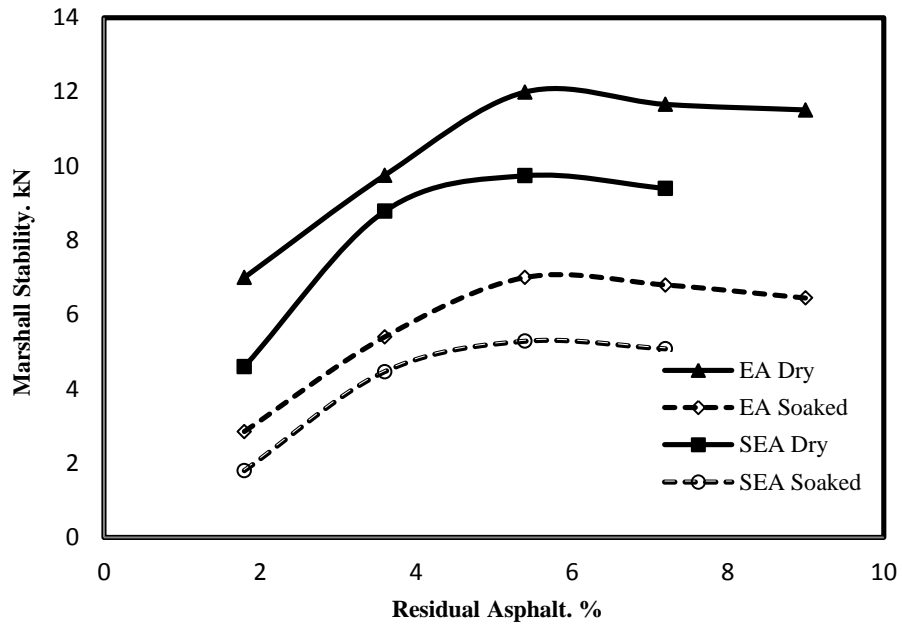


Figure 4-31: Dry and Soaked Stability for Sand Soil.

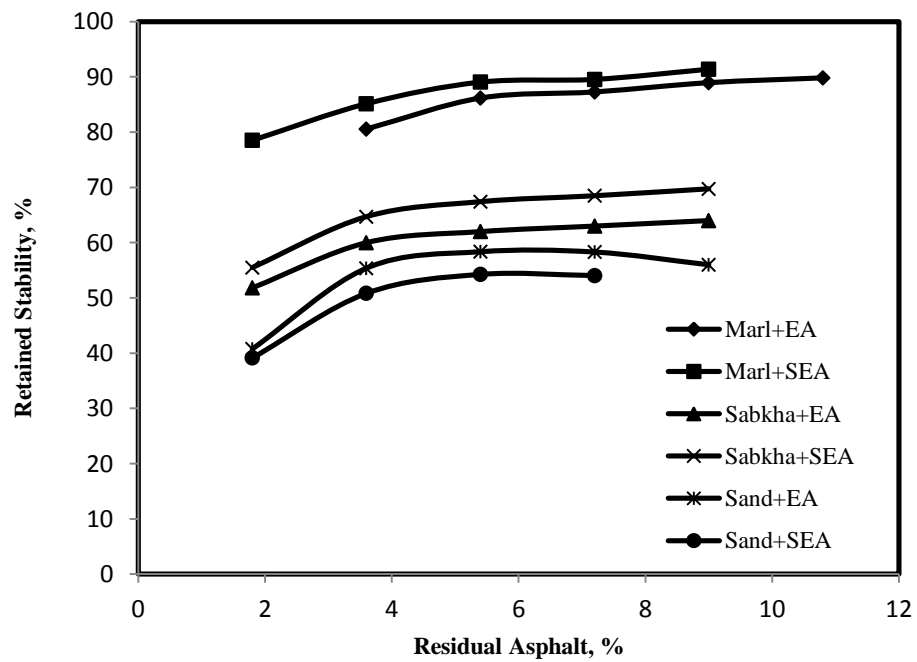


Figure 4-32: Retained Stability Variation Versus Residual Asphalt of EA and SEA.

The stabilities for all stabilized soils mixed with EA and SEA satisfy the requirement (2.24 kN) which is considered satisfactory for most pavements with low to medium traffic volume [AEMA, 2004]. Although sand-EA and sand-SEA mixes have stability higher than required for light and medium traffic volume, these mixes are very sensitive to water effects.

#### **4.4.2 Indirect Tensile Strength Test Results**

Figures 4.33 through 4.35 show the results of dry indirect tensile strength for the marl, sabkha, and sand soils mixed with various percentages of EA and SEA. It is clear from the figures that the ITS results follow the same trend of the stability results and the maximum ITS was attained at approximately the same optimum residual asphalt for the maximum Marshall stability. The results show that marl and sabkha soils treated with SEA exhibit a little bit higher ITS values compared to the same soils treated with EA, whereas, for the sand soil the inverse is correct. Recommendations from experts in the Australian Road Research Board (ARRB) are that the dry indirect tensile strength should be at least 200 kPa and the soaked tensile strength be at least 100 kPa for base course layer in the pavement structure [SABITA, 1998]. For the treated materials to be used as a base course layer in the pavement structure, where the water table is close to the surface, it is believed that an ITS of more than 200 kPa together with more than 80% retained strength of ITS will perform adequately [SABITA, 1998]. The results show that all soils mixes combinations except sand soil passed the requirements at the dry condition.

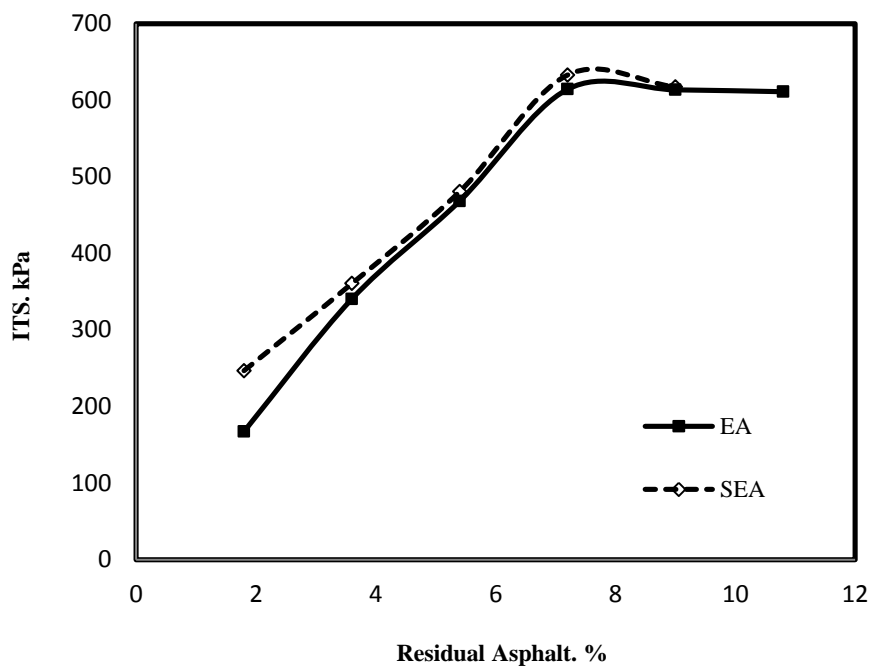


Figure 4-33: Dry ITS Results for Marl Soil.

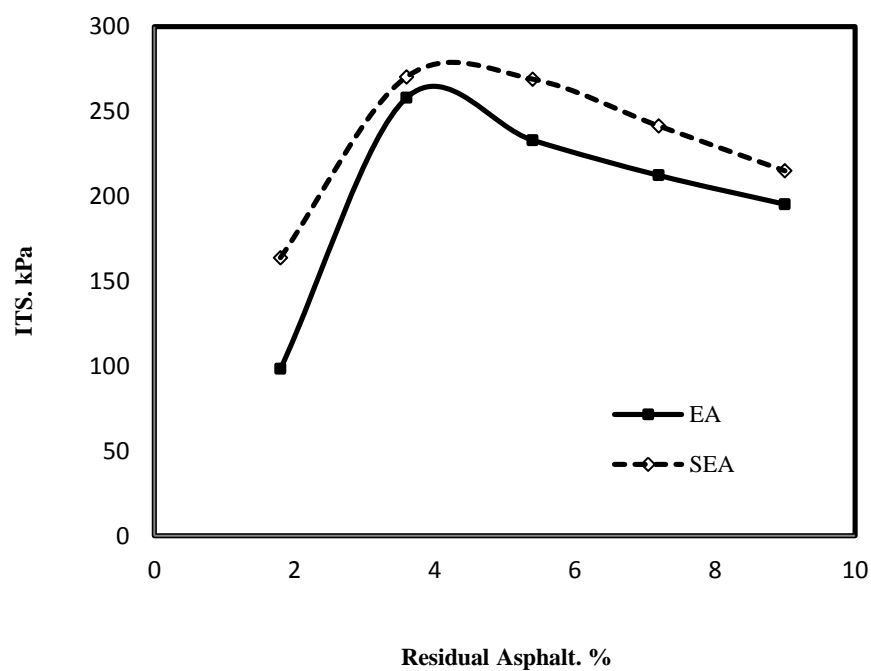


Figure 4-34: Dry ITS Results for Sabkha Soil.

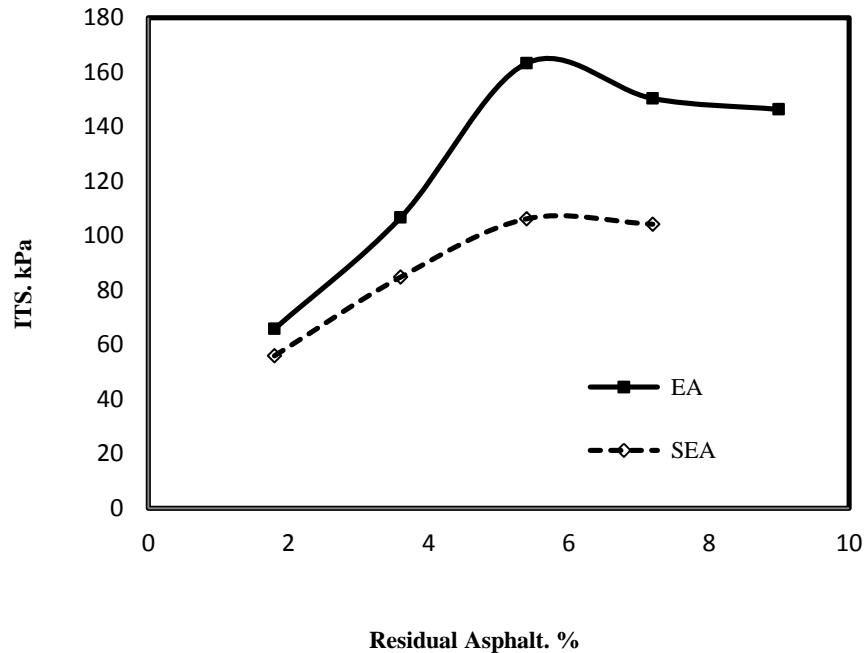


Figure 4-35: Dry ITS Results for Sand Soil.

#### 4.4.3 Static Triaxial Test (Shear Strength) Results

Specimens have a size of 2 in. diameter and 4 in. height, were prepared from the marl, sabkha, and sand soils at the optimum moisture, EA, and SEA contents and compacted to the optimum density using dynamic compactor. 2% cement was also added to the mixtures. In order to get the same Marshall density, the required number of layers and blows were determined. The prepared specimens were, then cured for 48 hrs at 60 °C. After curing, the specimens were subjected to the static triaxial test in a compliance with ASTM D 2850 to get the shear strength parameters  $C$  and  $\phi$ . To construct the Mohr-Coulomb failure envelope, tests were done at three different confining pressures up to failure. Figure 4.36 shows the Mohr-Coulomb failure envelopes for all mixes and the angle of internal friction and cohesion were calculated and are listed in Table 4.7.

Table 4-7: Cohesion and Angle of Internal friction for Soils-EA-SEA Mixes.

Soil Type	Binder Type	C (kPa)	$\phi$ (degree)
<b>Marl</b>	EA	280.66	31
	SEA	133.93	32
<b>Sabkha</b>	EA	20	32
	SEA	12.22	30
<b>Sand</b>	EA	25.11	30
	SEA	14.4	31

The results shown in Figure 4.36 and Table 4.7 indicate that, marl-EA mix has the highest cohesion value and this value dropped when the marl treated with SEA. Sabkha and sand soils have shown very close strength parameters to each other and again there is a reduction in the cohesion when they were treated with SEA. The values of cohesion reveal that EA mixes have better coating, while, SEA mixes have less effective coating.

The general regression model with a high correlation ( $R^2 = 99.6\%$ ) for the shear strength was developed using Minitab 16 software and reported as follows:

$$\tau = -304 + 55.2 x_1 + 0.99 x_2 + 8.41x_3 + 0.588 \sigma_n + 0.63 C + 10.51\phi \quad (R^2 = 99.6\%) \quad (4-6)$$

Where,

$\tau$  = shear strength in kPa;

$x_1 = 1$  (marl) or  $x_1 = 0$  (otherwise);

$x_2 = 1$  (sabkha) or  $x_2 = 0$  (otherwise);

$x_3 = 1$ (EA) or  $x_3 = 0$  (otherwise);

$\sigma_n$  = normal stress in kPa;

$C$  = cohesion in kPa, and

$\phi$  = angle of internal friction in degree.

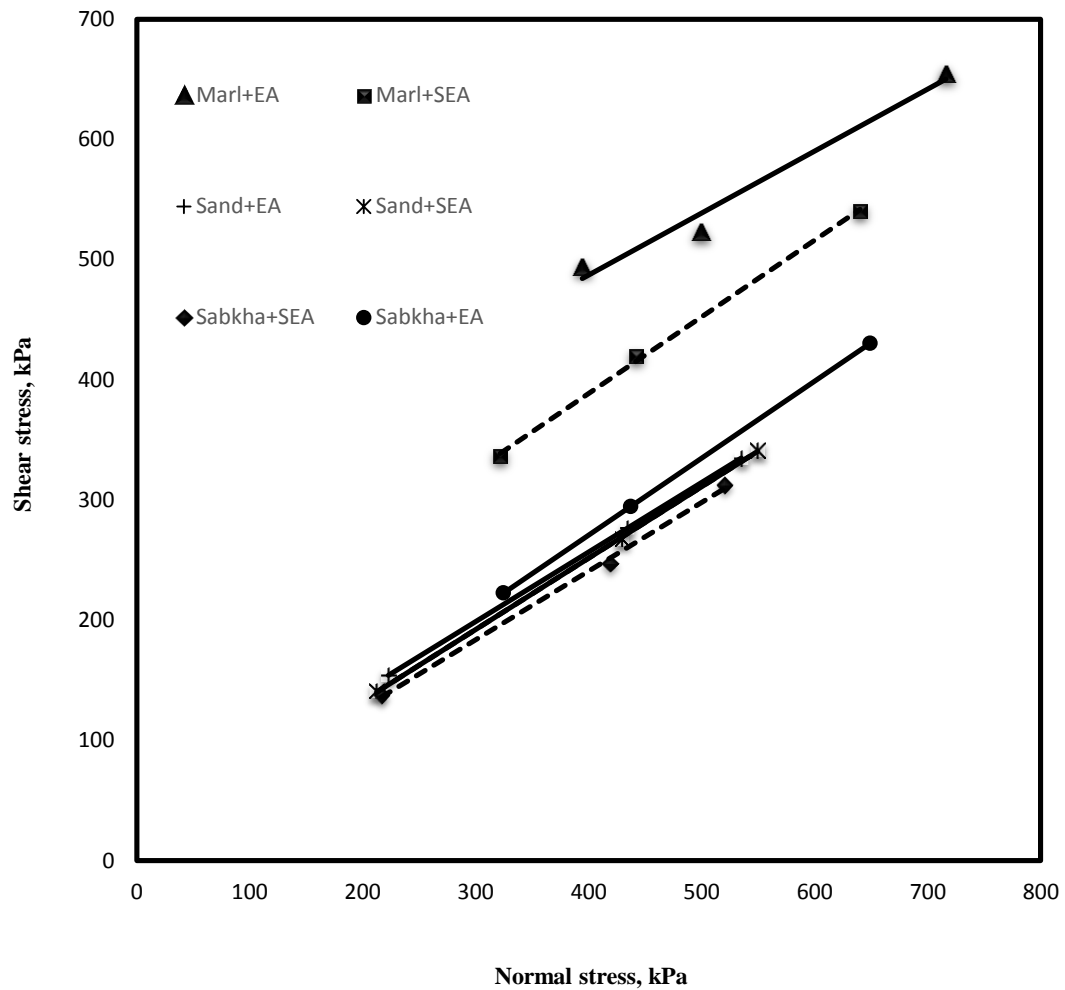


Figure 4-36: Mohr-Coulomb Failure Envelope for Soils-EA/SEA Mixes.

#### 4.4.4 Dynamic Resilient Modulus Test Results

The dynamic resilient modulus for the marl, sabkha, and sand soils stabilized with EA and SEA was measured according to the AASHTO T-307 procedure. The specimens

of a size 4 inch diameter and 8 inch height were prepared at the optimum moisture, EA, and SEA contents and compacted to the maximum density. Thereafter, they were tested under different combinations of confined pressure 21-138 kPa (3-20 psi) and deviator stress 34-276 kPa (5-40 psi) as shown in Table 3.2 to simulate the traffic loading that the granular base and subbase materials are subjected to in the road structures. The variations of the resilient modulus with the deviator stress for all soils mixed with EA and SEA at 22 °C are shown in Figure 4.37.

The results in Figure 4.37 and the statistical analysis presented at the end of this chapter clearly show that there is a significant effect of the variation of the confining pressure on the resilient modulus. Furthermore, the effect of deviator stress is clearly shown. At each confining pressure the resilient modulus increased greatly with the increase in the deviator stress. It can be seen that the marl soil, treated with EA or with SEA, has the highest resilient modulus, followed by the sabkha, and lastly by the sand soils treated with the same stabilizers. The difference, however, is insignificant.

Figures 4.38 presents the variation of the resilient modulus, measured at 40 °C, for the same soils mixed with EA and SEA. Again there is significant effect of the confining pressure variation on the resilient modulus results and the effect of deviator stress variation is very clear. Under the same confining pressure, the resilient modulus increased greatly with the increase in the applied deviator stress and this is the same trend noticed for the resilient modulus measured at 22 °C. The results also show that there is a drop in the resilient modulus values measured at 40 °C compared to those measured at 22 °C. This reduction in the  $M_R$  values appeared to be small in the SEA mixes compared to



the EA mixes. Thus, the sulfur modified emulsified asphalt (SEA) mixes are less sensitive to the temperature effect which is considered as a great advantage.

In comparison between the resilient moduli for the emulsified asphalt and emulsified sulfur asphalt mixes, it is seen that the moduli for the marl-SEA and sabkha-SEA are slightly higher than those for the marl-EA and sabkha-EA mixes, whereas, the inverse is true for the sand soil.

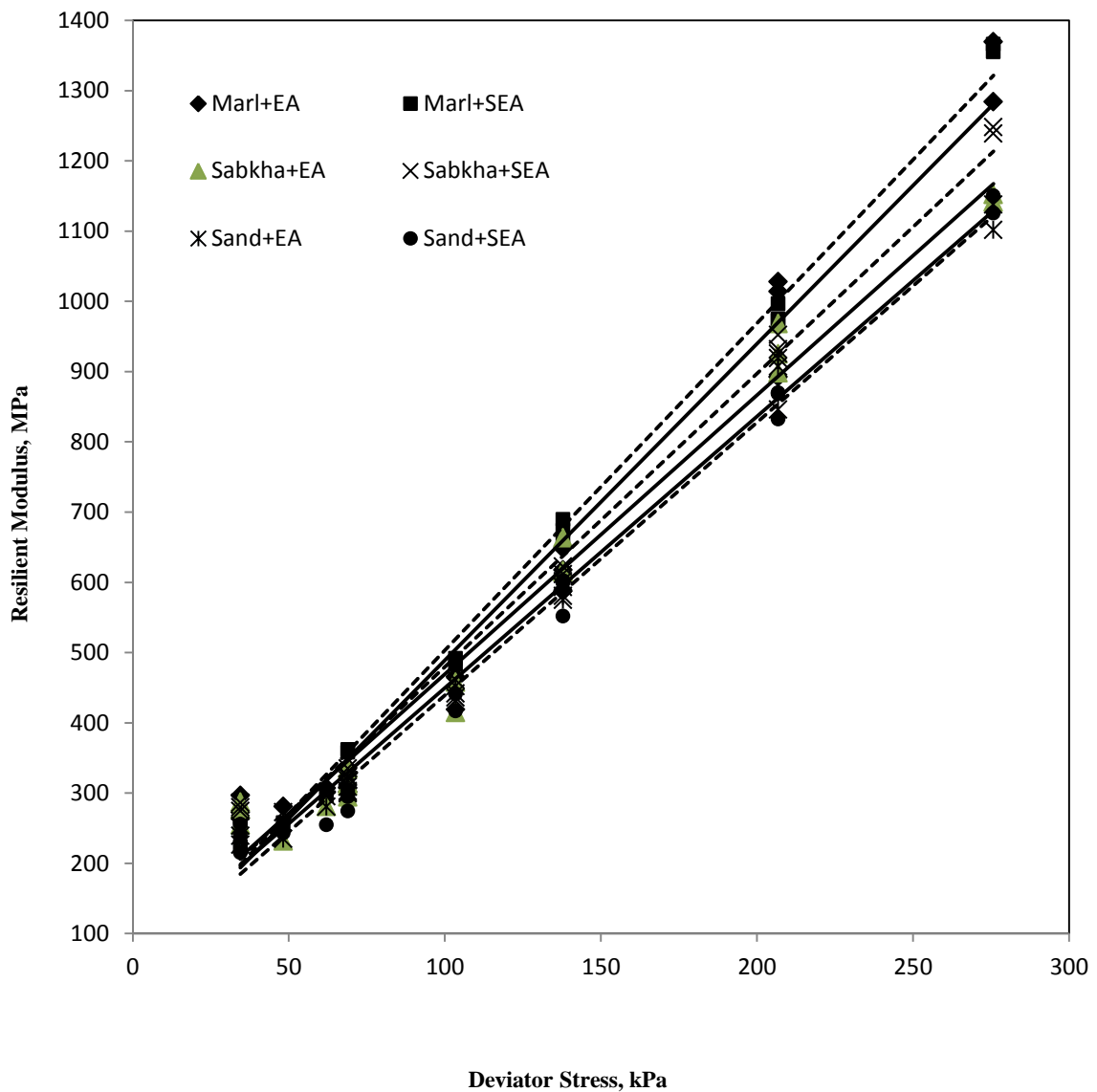


Figure 4-37: Variation of  $M_R$  with Deviator Stress for Soils Mixes at 22 °C.

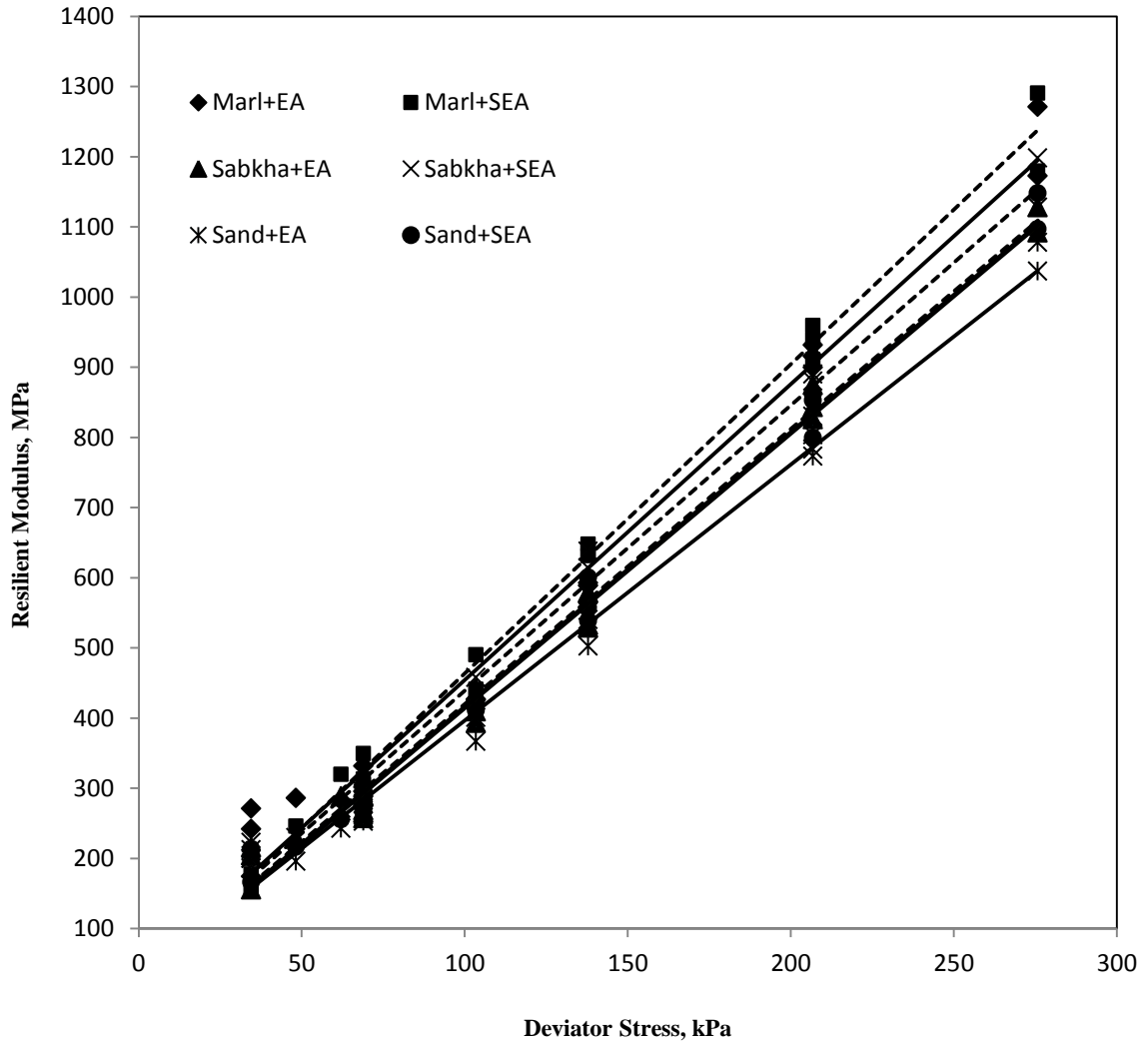


Figure 4-38: Variation of  $M_R$  with Deviator Stress for Soils Mixes at 40 °C.

Table 4.8 shows regression models with high correlation of the resilient modulus in terms of deviator stress, confining pressure and temperatures. The general regression model of  $M_R$  that performed high correlation ( $R^2 = 98.4\%$ ) is as follows:

$$M_R = 107 + 63.5 x_1 + 28.5 x_2 - 2.41 T - 15.2 x_3 - 0.326 \sigma_c + 4.20 \sigma_d \quad (4-7)$$

Where,

$M_R$  = resilient modulus in MPa

$x_1 = 1$  (marl) or  $x_1 = 0$  (otherwise);

$x_2 = 1$  (sabkha) or  $x_2 = 0$  (otherwise);

$x_3 = 1$  (EA) or  $x_3 = 0$  (otherwise);

$T$  = temperature in degree

$\sigma_c$  = confining pressure in kPa

$\sigma_d$  = deviator stress in kPa

Table 4-8: Regression Models of  $M_R$  for Emulsified Asphalt Mixes.

Material Type	Type of Additive	$M_R$	$R^2$
Marl	EA	$M_R = 128 - 2.26 T - 0.513 \sigma_c + 4.52 \sigma_d$	0.98
	SEA	$M_R = 119 - 2.49 T - 0.257 \sigma_c + 4.61 \sigma_d$	0.993
Sabkha	EA	$M_R = 158 - 3.07 T - 0.346 \sigma_c + 4.05 \sigma_d$	0.988
	SEA	$M_R = 139 - 2.39 T - 0.417 \sigma_c + 4.25 \sigma_d$	0.99
Sand	EA	$M_R = 151 - 3.21 T - 0.093 \sigma_c + 3.79 \sigma_d$	0.99
	SEA	$M_R = 86.1 - 1.05 T - 0.329 \sigma_c + 4.01 \sigma_d$	0.992

#### 4.4.5 Dynamic Triaxial Test

The dynamic triaxial tests were conducted, in a manner as discussed in Chapter 3, on soils, namely, marl, sabkha and sand treated at the optimum contents with emulsified asphalt (EA) and sulfur emulsified asphalt (SEA) at two different temperatures (22 °C and 40 °C). The results of the test at 22 °C are presented through Figures 4.39 to 4.41.

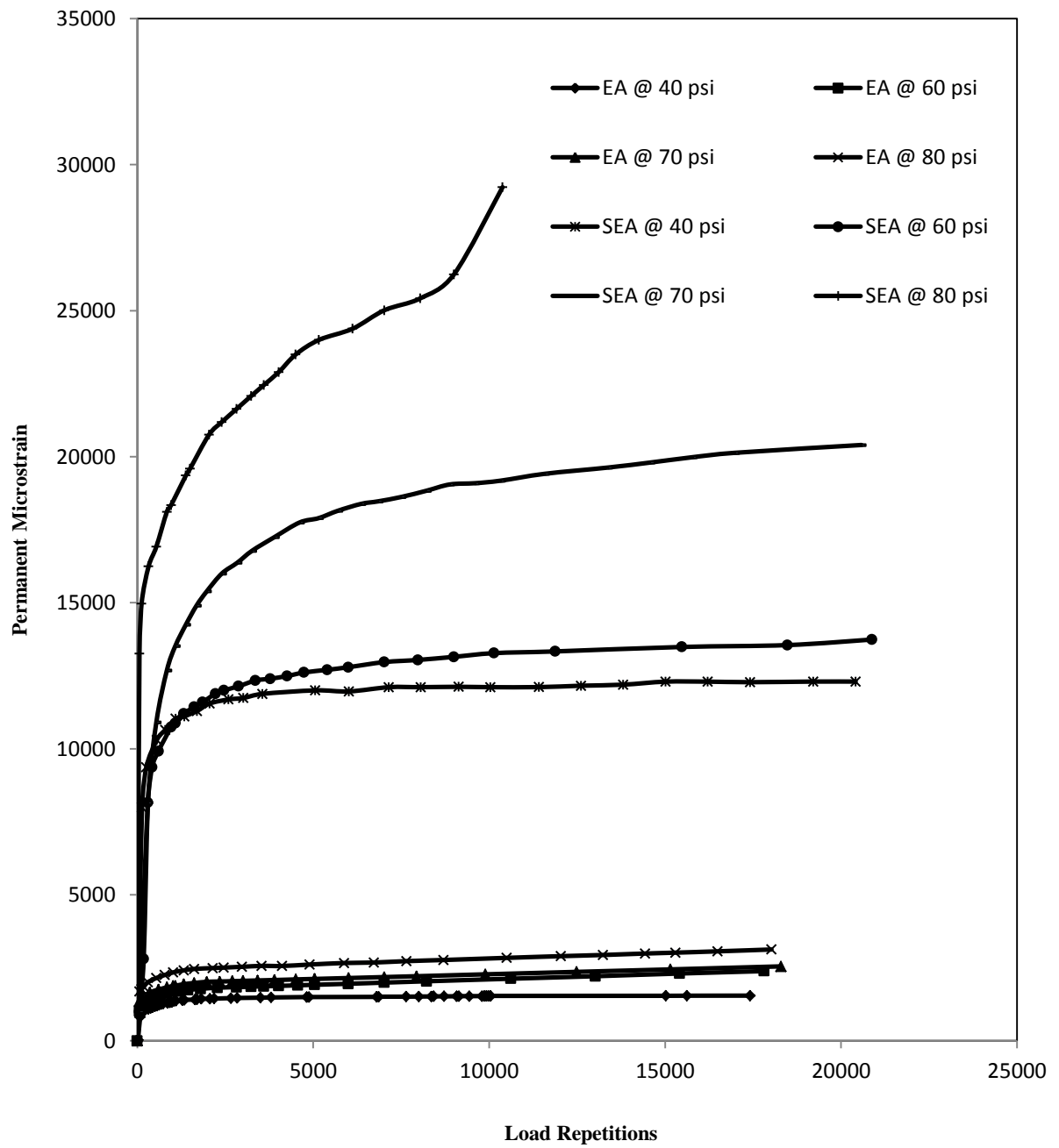


Figure 4-39: Dynamic Triaxial Test Results for Marl-EA/SEA Mixes at 22 °C.

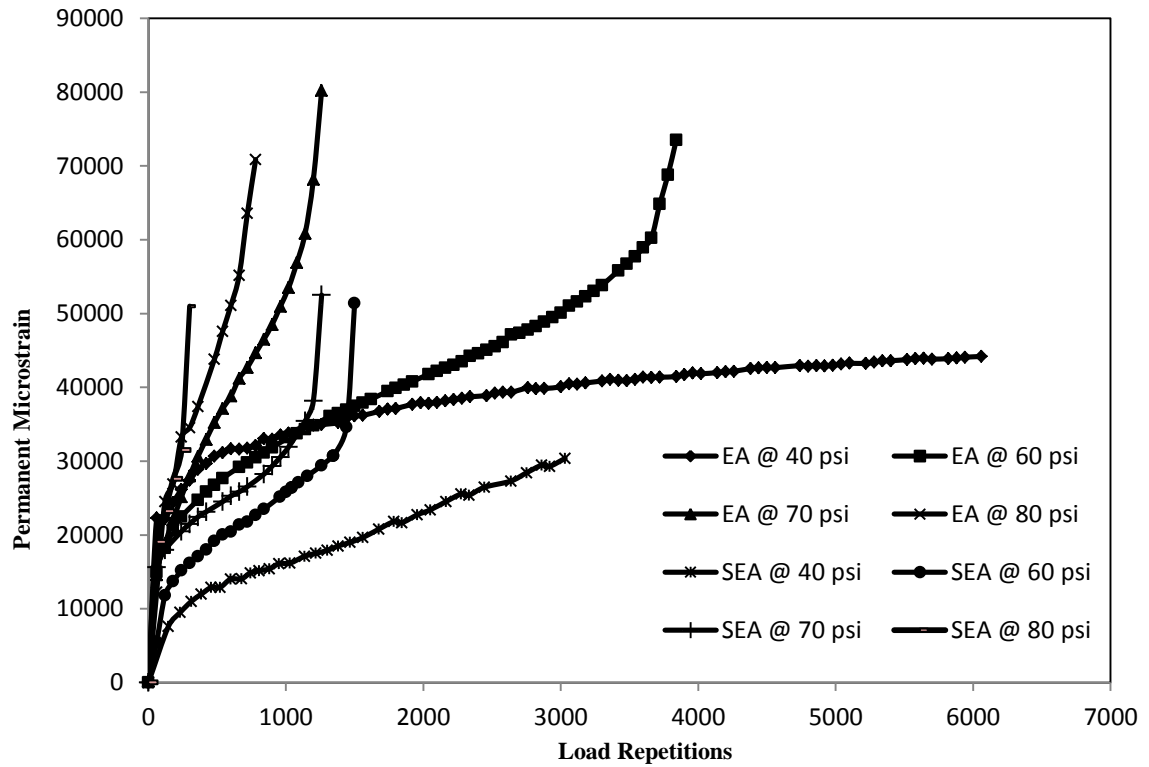


Figure 4-40: Dynamic Triaxial Test Results for Sabkha-EA/SEA Mixes at 22 °C.

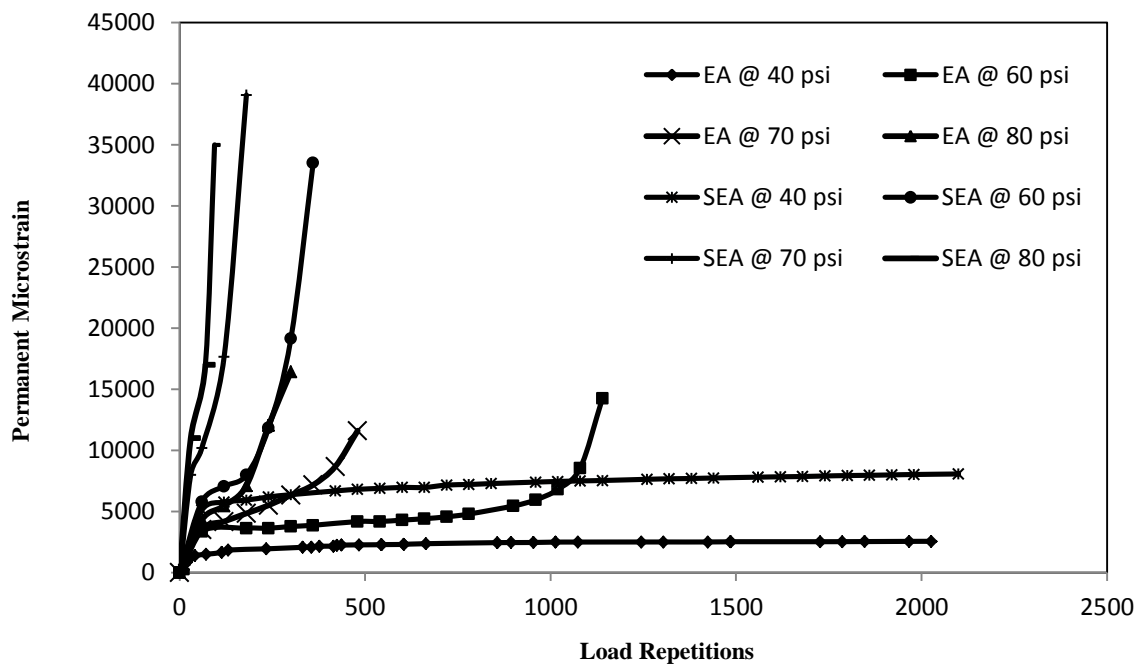


Figure 4-41: Dynamic Triaxial Test Results for Sand-EA/SEA Mixes at 22 °C.

On the contrary to the foamed mixes, the addition of the modified sulfur emulsion asphalt (SEA) to the soils increased the possibility of rutting especially for marl and sand soils as it is clear from the results presented in Figure 4.39 and Figure 4.41. However, in the sabkha soil the SEA mixes show less permanent deformation than the standard mixes (EA) but they reached to the third stage (failure stage) earlier than EA mixes, particularly at high stress levels. Such behavior could be attributed to the reduction in the shear strength parameters ( $C$  and  $\phi$ ) of the soils when treated with SEA rather than conventional EA and this is obvious in the results of the static shear triaxial test in Chapter 4 for both conventional and modified mixes.

Figures 4.42 to 4.44 show the dynamic triaxial test results for the same three soils tested at 40 °C. Based on the results shown in Figure 4.42 for the marl soil, the same trend as in testing at 22 °C is clearly present but, here the mixes remained in the second stage of the creep curve and did not reach to the third stage (failure stage) as happened when testing at 22 °C and under 80 psi loading which means that sulfur mixes performed very well at higher temperatures.

On the other hand, sabkha and sand soils show the inverse trend in which SEA mixes are less sensitive to rutting in comparison to the conventional mixes which failed rapidly as shown in Figure 4.43 and Figure 4.44. Furthermore, the materials did not reach to the failure stage, particularly at low to medium loading for sand and for all levels of loading in case of the sabkha soil. In addition to that, the slope ( $b$ ) and intercept ( $a$ ) of the permanent deformation curves are low which leads to have a high ALPHA ( $\alpha$ ) and low GNU ( $\mu$ ) (rutting model parameters) and then low rutting prediction.

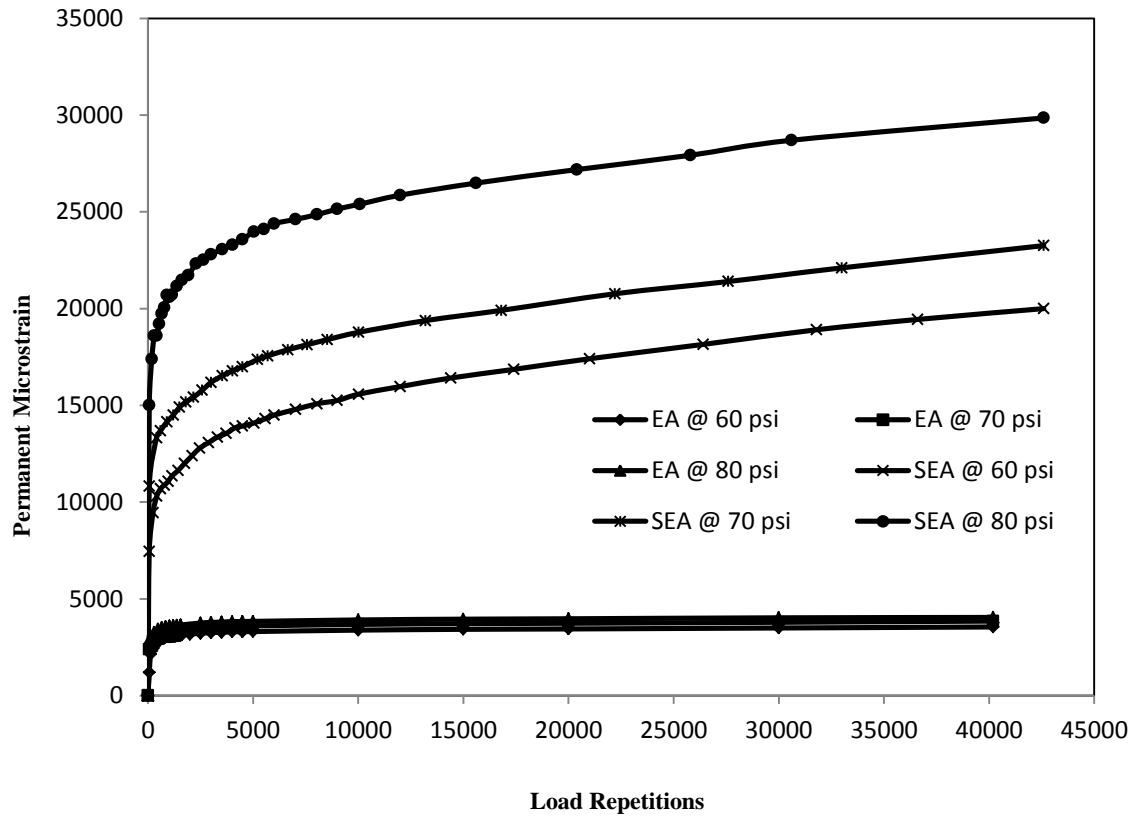


Figure 4-42: Dynamic Triaxial Test Results for Marl-EA/SEA Mixes at 40 °C.

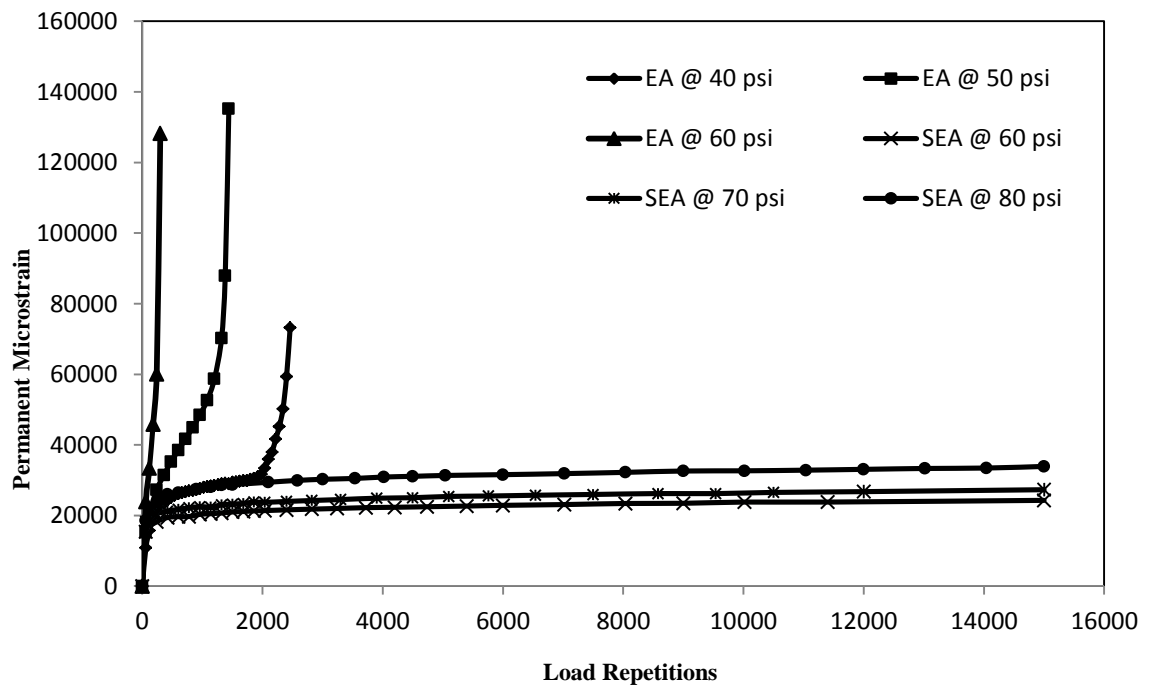


Figure 4-43: Dynamic Triaxial Test Results for Sabkha-EA/SEA Mixes at 40 °C.

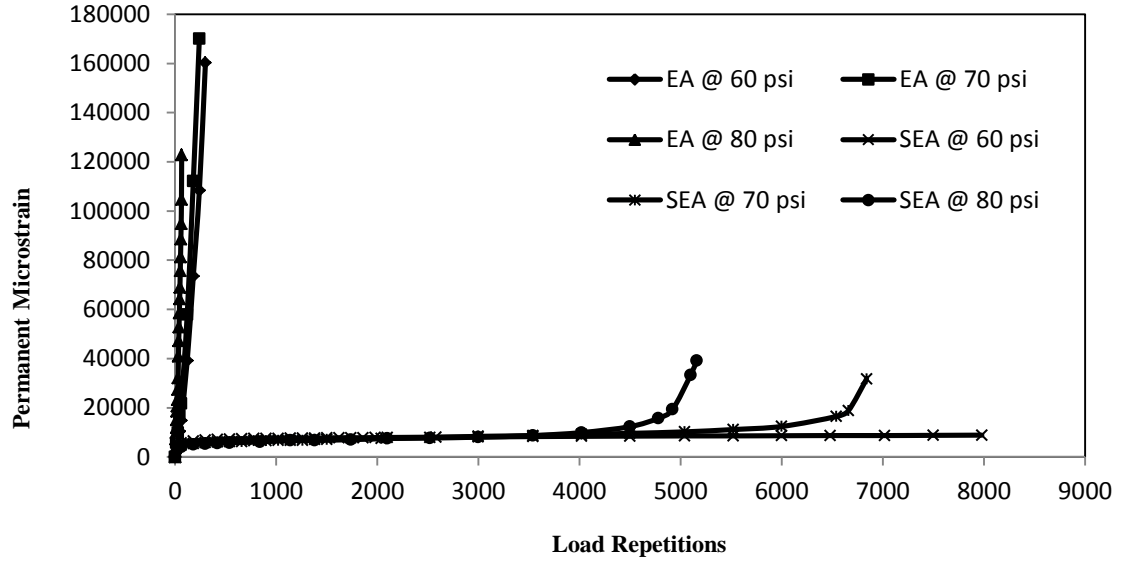


Figure 4-44: Dynamic Triaxial Test Results for Sand-EA/SEA Mixes at 40 °C.

Hence, we can end up with the clue that the sulfur modified emulsion mixes have higher ability to resist permanent deformation (rutting) and lower temperature susceptibility than conventional mixes.

Table 4.9 shows calculated intercept coefficient (a) and slope coefficient (b) of the regression curves fitting to the log permanent strain ( $\epsilon_p$ ) – log load repetitions ( $N$ ) for all emulsion mixes tested under different stress levels and at different temperatures (22 °C and 40 °C).

Regression models of these parameters in terms of temperature and deviator stress were developed using Minitab version (16) software for all mixes and are listed in Table 4.10. The general regression models are as follows:

$$a = -362 + 2468 x_1 + 4612 x_2 - 4370 x_3 + 134 T + 0.92 \sigma_d \quad (R^2 = 56.8\%) \quad (4-8)$$

$$b = 0.042 - 0.278 x_1 - 0.0441 x_2 + 0.137 x_3 - 0.00006 T + 0.000561 \sigma_d \quad (R^2 = 47\%) \quad (4-9)$$



Where,

a and b = intercept and slope coefficients (permanent deformation regression coefficients)

$x_1 = 1$  (marl) or  $x_1 = 0$  (otherwise);

$x_2 = 1$  (sabkha) or  $x_2 = 0$  (otherwise);

$x_3 = 1$ (EA) or  $x_3 = 0$  (otherwise);

T = temperature in degree.

$\sigma_d$  = deviator stress in kPa.

It is clear that the general models of a and b coefficients have low correlation compared with the models listed in Table 4.10 even after we did a forward regression and tried to remove the insignificant factors, the correlations still low, hence, we recommend using material and treatment specific models shown in Table 4.10 instead of the general models above.

#### **4.4.6 Dynamic Triaxial Results of Subgrade Soils**

Dynamic triaxial repeated load test was also conducted on three types of soils, which might be found in the field as a subgrade. These soils are marl, sabkha and sand. The dynamic triaxial test was conducted on soils specimens having a size of 100 mm in diameter and 200 mm in height, prepared at their optimum moisture contents and compacted to the maximum dry density as determined by compaction test. The test was applied with a confining pressure of 5 psi and a deviatoric stress of 10 psi. These stresses are the most likely subgrade subjected to as determined by analyzing the proposed

pavement sections under standard axle load (18 kip). Figure 4.45 shows the results of this test on the three soils. The Soaked CBR values for marl, sabkha and sand are 25, 10 and 15%, respectively. The soaked CBR value (10%) for the sabkha soil represents a weak sabkha, while, the CBR value for the sabkha compacted and soaked with sabkha brine was found to be around 24%.

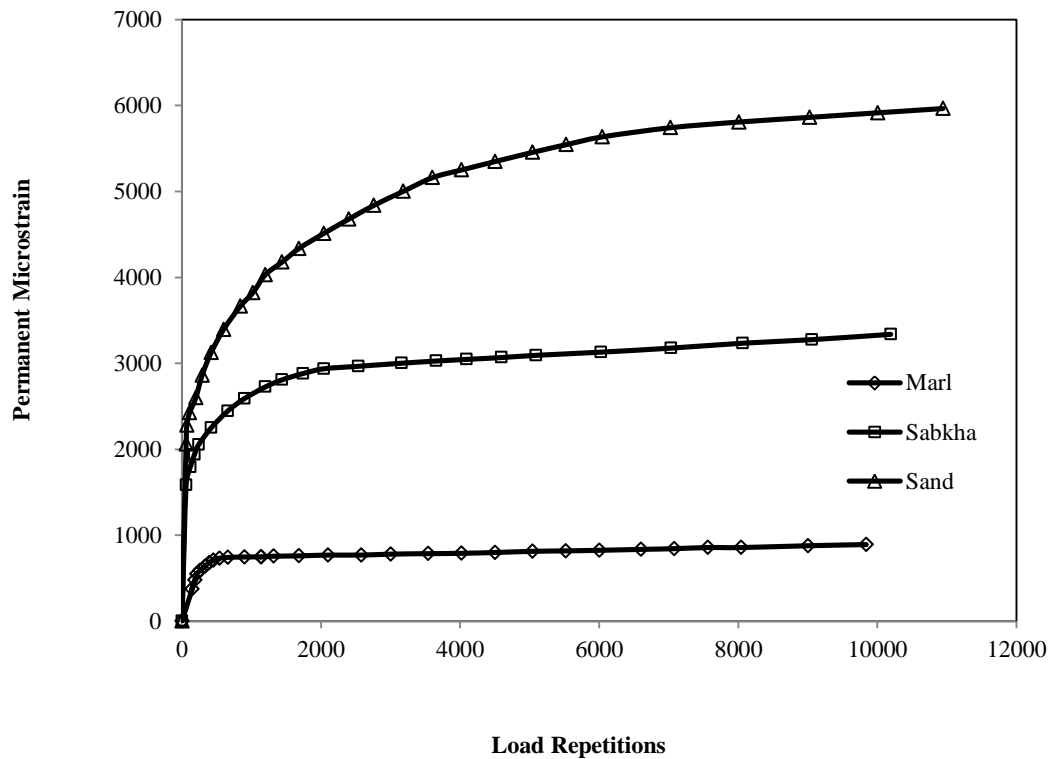


Figure 4-45: Dynamic Triaxial Test Results for Subgrade Soils

Table 4-9: Intercept and Slope Coefficients for Tested Emulsified Asphalt Mixes.

Soil Type	Temp. °C	Treatment Type	$\sigma_c$ (psi)	$\sigma_d$ (psi)	$\sigma_d$ (kPa)	a	b	R <sup>2</sup>
Marl	22	EA	10	40	275.80	1130.00	0.031	0.88
			10	60	413.69	788.60	0.106	0.931
			10	70	482.60	983.50	0.091	0.926
			10	80	551.60	1262.00	0.087	0.929
		SEA	10	40	275.80	8904.00	0.033	0.572
			10	60	413.69	7002.00	0.068	0.955
			10	70	482.60	5757.00	0.130	0.961
			10	80	551.60	6320.00	0.155	0.986
	40	EA	10	60	413.69	2283.00	0.033	0.962
			10	70	482.60	2558.00	0.039	0.964
			10	80	551.60	2860.00	0.042	0.971
		SEA	10	60	413.69	3837.00	0.096	0.991
			10	70	482.60	6130.00	0.121	0.982
			10	80	551.60	10485.00	0.152	0.996
Sabkha	22	EA	10	60	413.69	3922.00	0.311	0.99
			10	70	482.60	1839.00	0.479	0.997
			10	80	551.60	3155.00	0.422	0.973
		SEA	10	60	413.69	2106.00	0.357	0.989
			10	70	482.60	5584.00	0.240	0.968
			10	80	551.60	4298.00	0.359	0.985
	40	EA	10	60	275.79	4844.00	0.420	0.888
			10	70	344.74	2689.00	0.450	0.988
			10	80	413.69	2168.00	0.581	0.983
		SEA	10	60	413.69	13817.00	0.058	0.995
			10	70	482.60	15238.00	0.059	0.993
			10	80	551.60	19768.00	0.054	0.947
Sand	22	EA	10	40	275.80	1475.00	0.120	0.768
			10	60	413.70	1948.00	0.122	0.886
			10	70	482.60	690.00	0.442	0.965
			10	80	551.60	795.30	0.354	0.967
		SEA	10	40	275.80	3290.00	0.116	0.978
			10	60	413.70	828.00	0.290	0.845
			10	70	482.60	1091.00	0.570	0.952
			10	80	551.60	1888.00	0.518	0.999
	40	EA	10	60	413.70	1189.00	0.539	0.999
			10	70	482.60	704.30	0.775	0.999
			10	80	551.60	1567.00	0.839	0.987
		SEA	10	60	413.70	4843.00	0.064	0.946
			10	70	482.60	3079.00	0.150	0.972
			10	80	551.60	2365.00	0.180	0.988

Table 4-10: Regression Models of a and b Coefficients for Emulsified asphalt Mixes.

Material Type	Type of Additive	a	R <sup>2</sup>	b	R <sup>2</sup>
Marl	EA	$a = -2728 + 86.4 T + 3.81 \sigma_d$	0.999	$b = 0.181 - 0.00315 T - 0.000036 \sigma_d$	0.957
	SEA	$a = -4640 + 25 T + 21.6 \sigma_d$	0.386	$b = -0.139 + 0.000296 T + 0.000518 \sigma_d$	0.916
Sabkha	EA	$a = 10779 - 81.1 T - 12.5 \sigma_d$	0.483	$b = -0.335 + 0.0120 T + 0.000986 \sigma_d$	0.722
	SEA	$a = -25258 + 682 T + 29.5 \sigma_d$	0.965	$b = 0.642 - 0.0145 T - 0.000007 \sigma_d$	0.917
Sand	EA	$a = 2488 + 0.5 T - 2.81 \sigma_d$	0.411	$b = -1.13 + 0.0229 T + 0.00193 \sigma_d$	0.906
	SEA	$a = 1110 + 120 T - 5.14 \sigma_d$	0.691	$b = 0.258 - 0.0182 T + 0.00125 \sigma_d$	0.896

#### 4.4.7 Wheel Tracking Test Results

Rut depth measurement of EA and SEA mixes was carried out in the same manner discussed in Chapter 3 in which twelve slabs of size 45 cm x 22 cm x 10 m thick (two slabs for each mix) for the marl, sabkha and sand were prepared at the density corresponding to the dynamic triaxial specimens density. Thereafter, the slabs were cured at 60 °C for 48 hours and tested dry under the same wheel load used for foam slabs testing (552 kPa) and at the lab temperature (22 °C). Figure 4.46 shows some of tested slabs where a severe rut is obviously shown in some slabs (sand mixes), whereas, some other slabs show less rutting susceptibility (marl mixes).

The results shown through Figures 4.47 to 4.49 are the measured rut depth for EA and SEA mixes for marl, sabkha and sand, respectively. Again the same trend and ranking as in the dynamic triaxial is observed in which marl soil has the highest rutting resistance followed by sabkha and then by sand soil. This means that rutting can be predicted from any of the test method and can be compared reasonably well with one another. Results also indicate that the sulfur emulsion mixes show lower rutting resistance than the normal emulsion mixes. In comparison to foamed mixes either normal or sulfur modified,

emulsified mixes are less resistant to permanent deformation than foamed mixes. Results also show that the sand treated with EA or SEA is very sensitive to the rutting and exhibited higher permanent deformation ( $> 15$  mm within first thousand load repetition) compared to the others mixes (marl and sabkha).

In general, the relative performance ranking of accelerated pavement tests (APT), represented here by loaded wheel tracking test, and dynamic triaxial repeated load tests is found to be the same for all investigated mixes in this study.

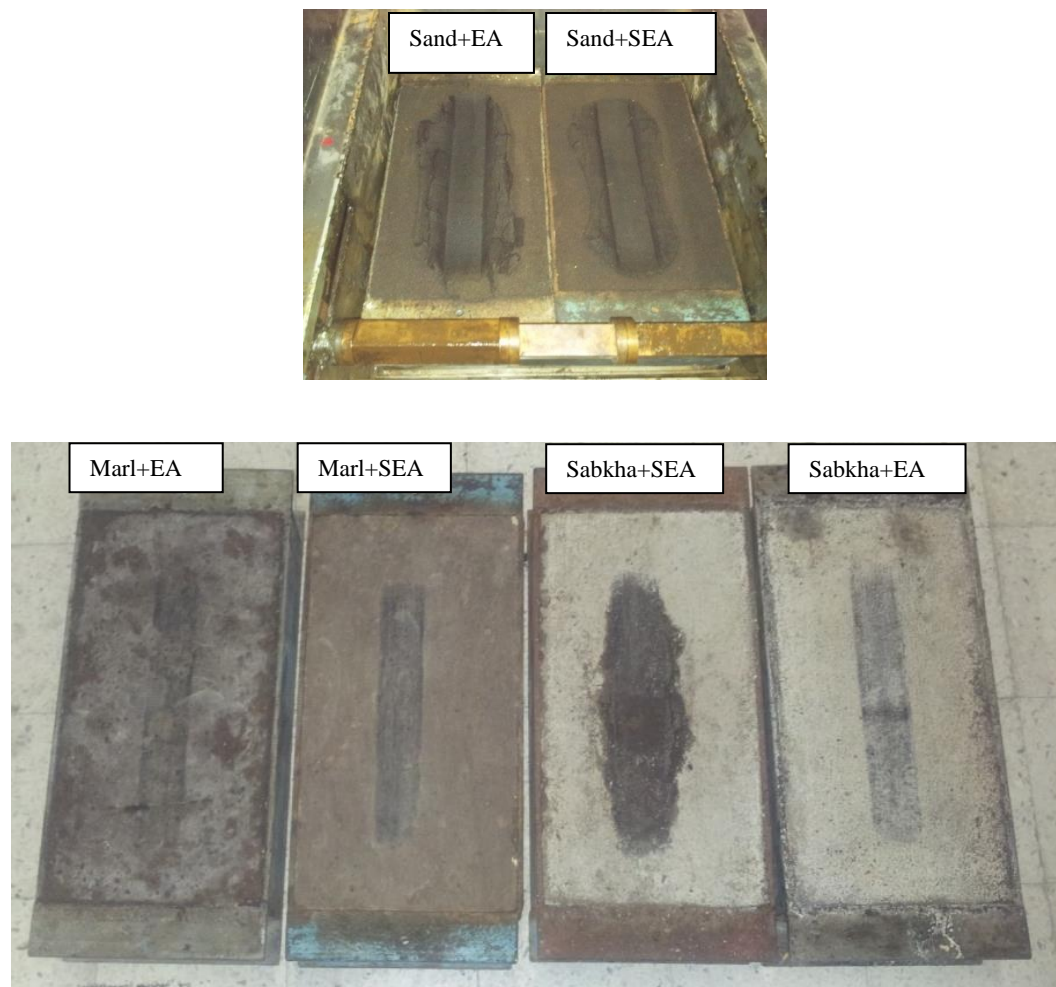


Figure 4-46: Permanent Deformation in Wheel Tracking of EA/SEA Samples

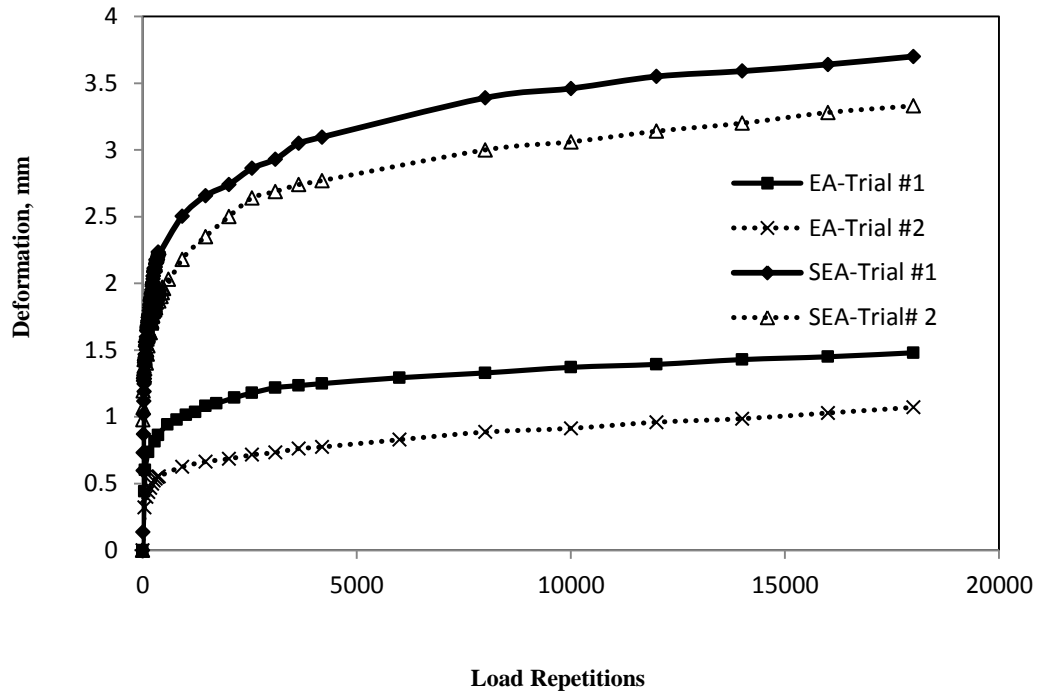


Figure 4-47: Results of the Permanent Deformation for the Marl-EA/SEA Mixes Using Wheel Track Machine, Dry at 22 °C.

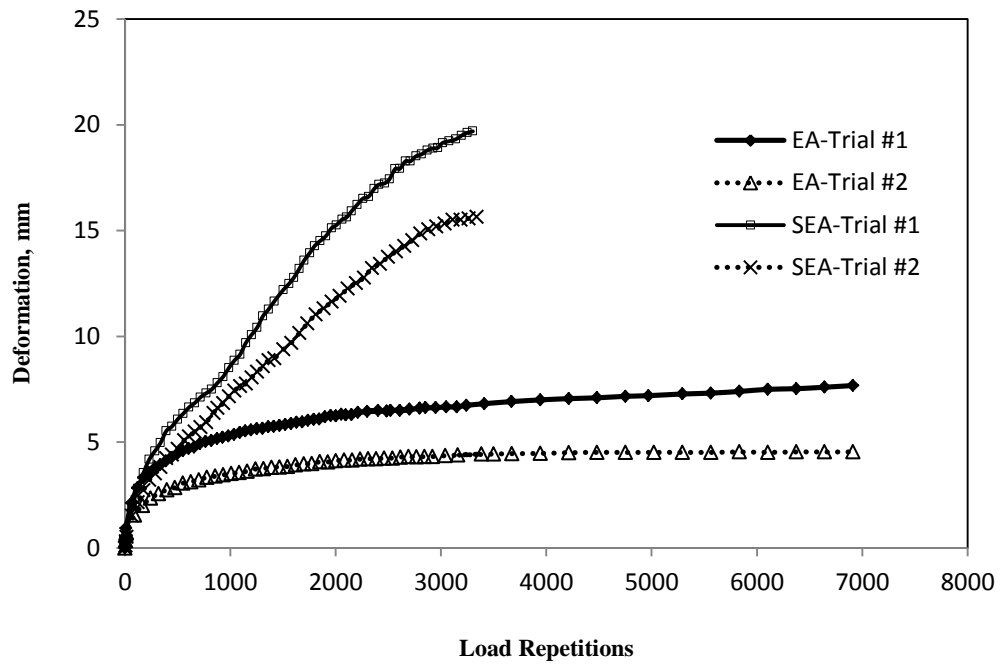


Figure 4-48: Results of the Permanent Deformation for the Sabkha-EA/SEA Mixes Using Wheel Track Machine, Dry at 22 °C.

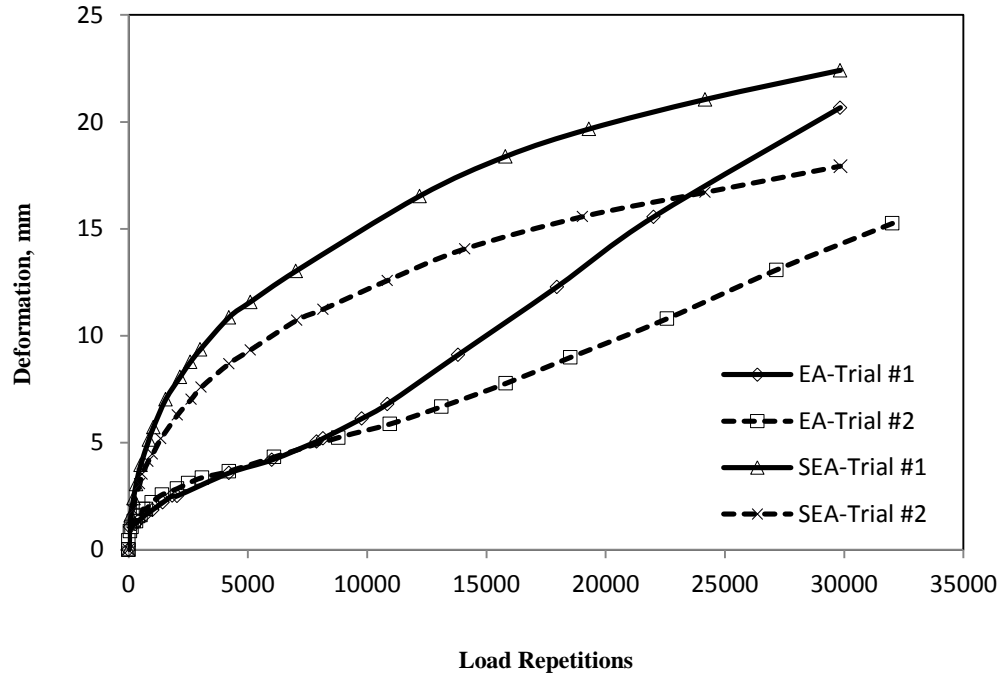


Figure 4-49: Results of the Permanent Deformation for the Sand-EA/SEA Mixes Using Wheel Track Machine, Dry at 22 °C.

#### 4.5 Micro-Characterization

The SEM micrograph of marl soil is shown in Figure 4.50 (a). A porous morphology and large voids are clearly shown in the soil structure. Furthermore, the grain size distribution is clearly shown in which large grains are present with some fines materials filled some of interparticles voids. The EDX shown in Figure 4.50 (b) implies the presence Mg, Si, K, Ca and Fe with about 10.67, 3.56, 0.62, 19.66 and 1.14 % by weight, respectively.

Figure 4.51 (a) shows the SEM of marl soil treated with 2 % cement. The SEM micrograph indicates a porous morphology and lack of cementing gel due to the low percentage of cement used. The EDX shown in Figure 4.51 (b) indicated the presence of

Mg, Al, Si, K, Ca, and Fe with about 8.38, 2.47, 10.4, 1.15, 20.36 and 1.02 % by weight, respectively. These are mainly contributed by the marl soil and cement. The increase in Ca and Si was due to the addition of 2% cement and formation of calcium silicate hydrate C-S-H.

Figure 4.52 (a) shows the SEM of marl treated with normal foamed asphalt in addition to 2 % cement. The structure is denser due to the presence of foamed asphalt droplets which coat and joint some grains of the marl soil. The EDX, Figure 4.52 (b), shows that C, Mg, Si, K, Ca, and Fe elements form 12.97, 2.04, 12.22, 0.51, 10.51 and 0.66 % by weight, respectively.

Figure 4.53 (a) shows the SEM of marl treated with foamed sulfur asphalt in addition to 2 % cement. The structure is too dense compared to the normal FA mix. The EDX is shown in Figure 4.53 (b) where C, Na, Mg, Al, Si, S, K, Ca and Fe form 9.4, 1.49, 1.85, 1.48, 17.48, 1.3, 1.27, 15.85 and 0.99 % by weight, respectively. Ca and Si are responsible for the formation of calcium –silicate-hydrate gel (C-S-H) and it is seen that these elements are present with higher percentage compared with the normal FA mix in Figure 4.52 (b) which means higher strength would be gained. The percent of carbon (C) is noticed to be less than in conventional foamed mixes because of the replacement of asphalt by 30% sulfur. Sulfur is also shown with a significant percent (1.3%) in the EDX results. Thus, one can say that, the gain in strength have come from the increase in the stiffness of asphalt binder due to the presence of sulfur.

Table 4.11 summarizes the percents by weight of the chemical elements for all mixes discussed in the previous paragraphs.



Table 4-11: Summary of Chemical Composition of Marl Mixes.

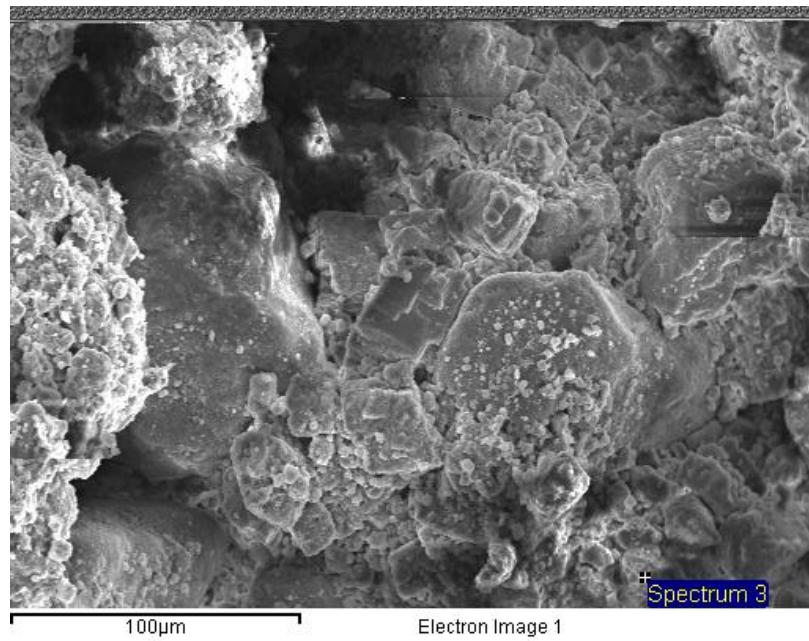
Element	Marl (% weight)	Marl+2% C (% weight)	Marl+2% C+FA (% weight)	Marl+2% C+SFA (% weight)
C	-	-	12.97	9.4
Na	-	-	-	1.49
Mg	10.67	8.38	2.04	1.85
Al	-	2.47	-	1.48
Si	3.56	10.4	12.22	17.48
K	0.62	1.15	0.51	1.27
Ca	19.66	20.36	10.51	15.85
Fe	1.14	1.02	0.66	0.99
S	-	-	-	1.3

Mahoney et al., (1982) reported that when sulfur are heated and combined with asphalt, three different reactions may occur:

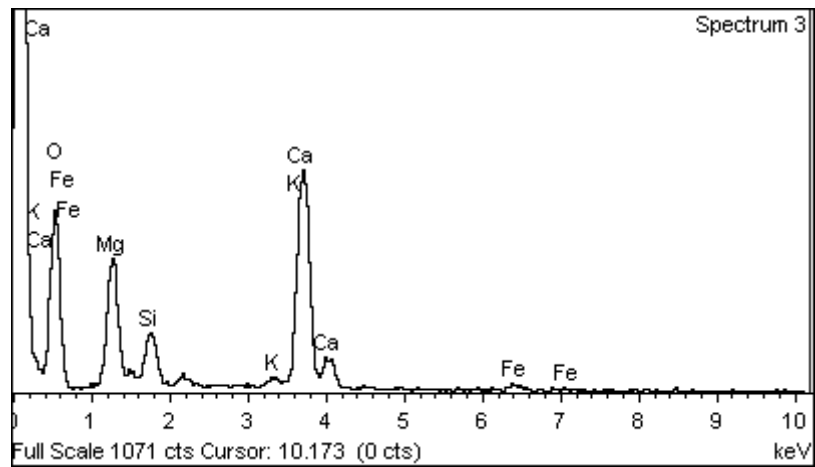
1. Sulfur can react chemically with the bitumen and result in dehydrogenation. This becomes important at temperatures above about 152°C.
2. Sulfur can be dissolved in the bitumen.
3. Sulfur in the crystalline form can remain in suspension in the bitumen.

The sulfur that does not chemically combine with the bitumen may be dissolved in true solution, dispersed as a colloid, or appeared in the asphaltic mixture as crystalline sulfur.

Recent study [Masegosa et al., 2012] reported that 70% of the sulfur in the blend remained in an immiscible crystalline form, with the remainder 30% being amorphous. The larger the amount of added sulfur to a bitumen, the larger the amount of sulfur that ends up not in solution and hence existing in a crystalline state.



a) SEM



b) EDX

Figure 4-50: SEM and EDX for Marl Soil.

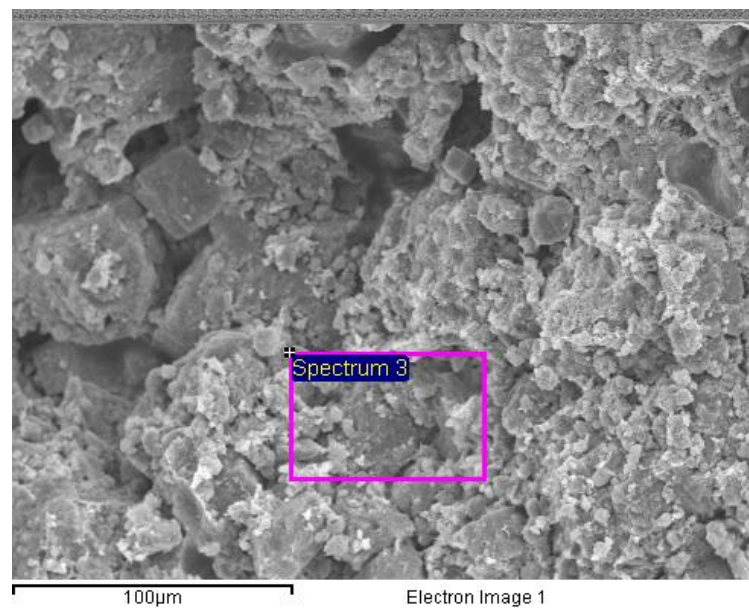
The result is large amounts of crystalline sulfur existing in the paving mixture generally as “needle-like” structures. Scanning electron microscopy analysis has shown that sulfur crystals were more abundant in the voids than in the binder itself, thus the more voids in a particular asphalt mixture, the more crystals [Mahoney et al., 1982].

Since SFA was produced at a temperature of 150 °C that gave the best foaming characteristic without causing sulfur fumes, thus sulfur were dissolved in the bitumen or existed in a needle-like crystalline form as shown in the Figure 4.53 (a), Figure 4.54 (a) and Figure 4.57.

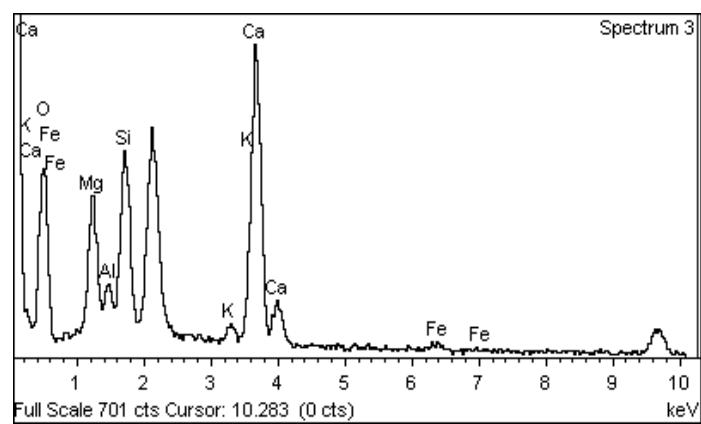
The higher strength of marl-SFA could be attributed to the presence of the sulfur crystals in the voids of the mixture and due to the increased stiffness of sulfur asphalt binder. The needle like crystals formed as a result to the addition of sulfur are also shown clearly for the sand soil treated with SFA and 2 % cement in Figure 4.54. The presence of calcium and silicon with 8.4 and 16.71%, respectively, indicated the component of the C-S-H gel which is evident in the same SEM micrograph.

Figure 4.55 show the SEM for sabkha treated with emulsion asphalt in addition to 2 % cement. The smooth areas are certainly bitumen and the different phases of recrystallized cement are also seen. Moreover, the characteristics of ettringite, calcium hydroxide and calcium silicate are presents, similar to that found in the normal hardened concrete. In addition to the crystals, pores are also formed due to the gas bubbles or evaporation of water droplets. Some of these pores are evident in the mixture shown in Figure 4.55 (a) and (c). Image in Figure 4.55 (c) shows that the cementitious phase is

dispersed within the bituminous binder. This could have the additional effect of stiffening the organic binder.

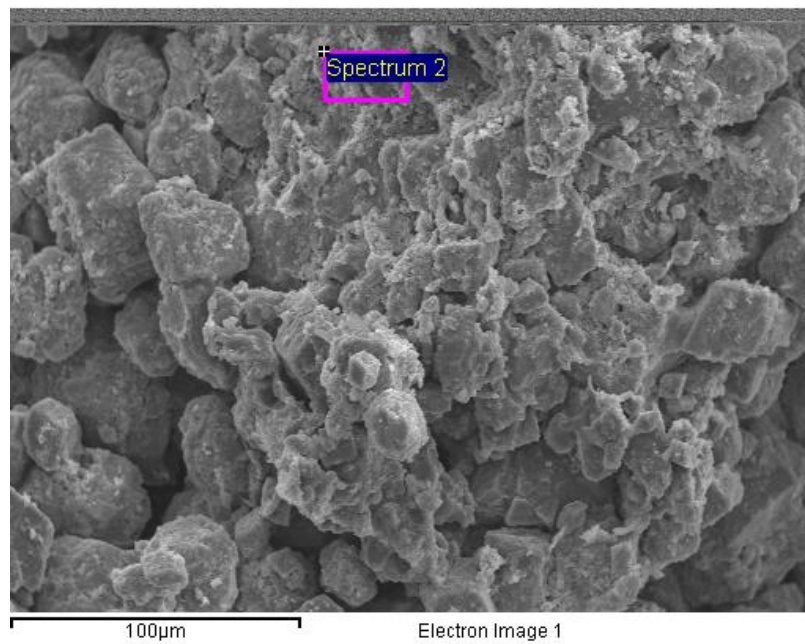


a) SEM

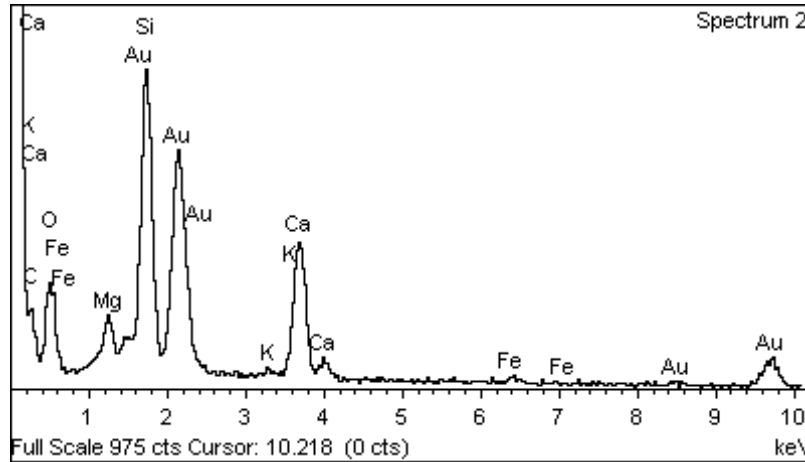


b) EDX

Figure 4-51: SEM and EDX for Marl Treated with 2% Cement.

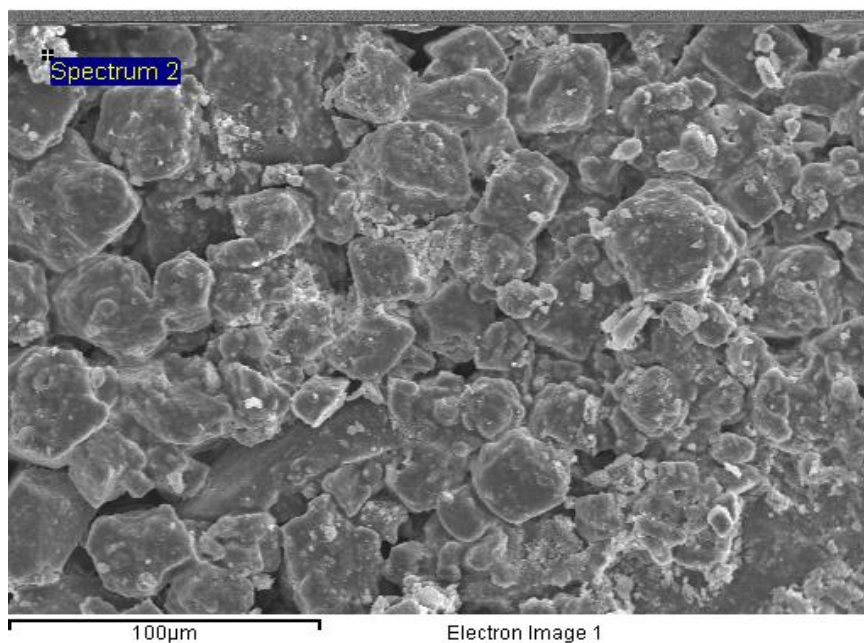


a) SEM

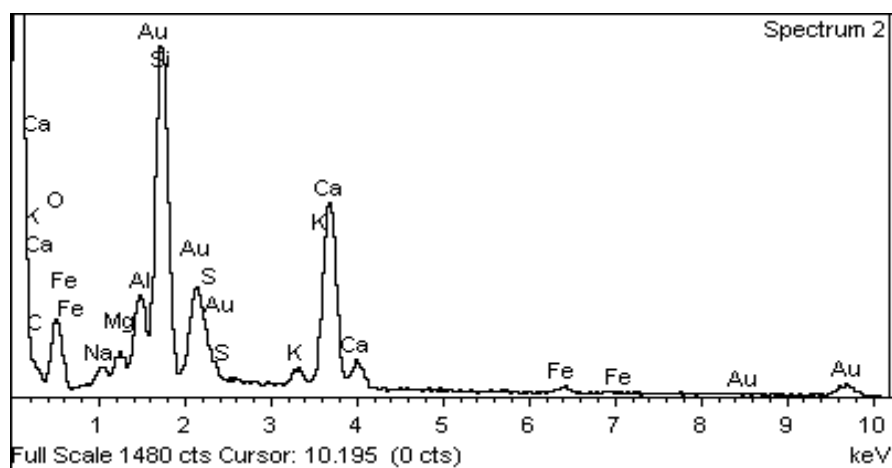


b) EDX

Figure 4-52: SEM and EDX of Marl Treated with FA + 2 % Cement.

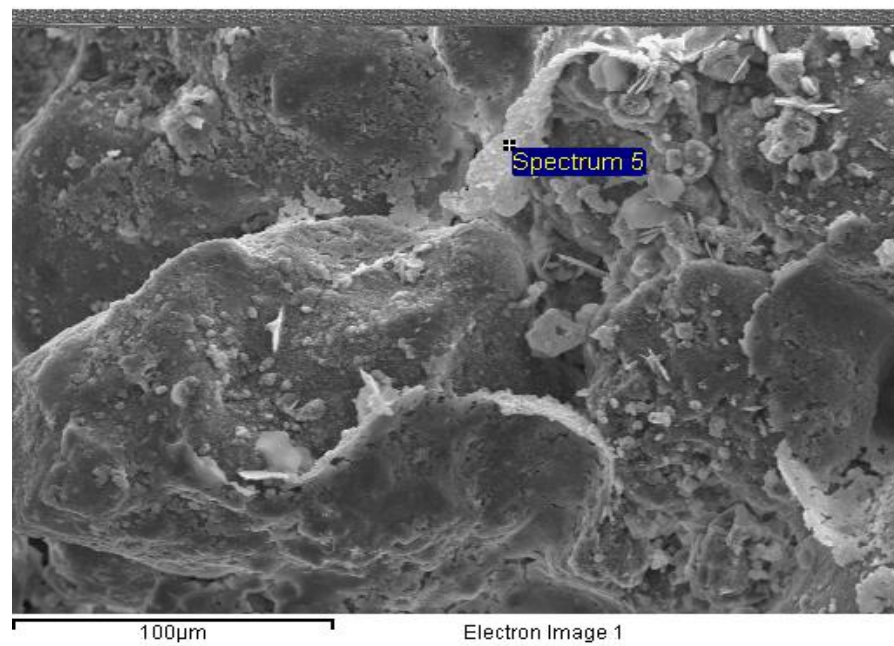


a) SEM

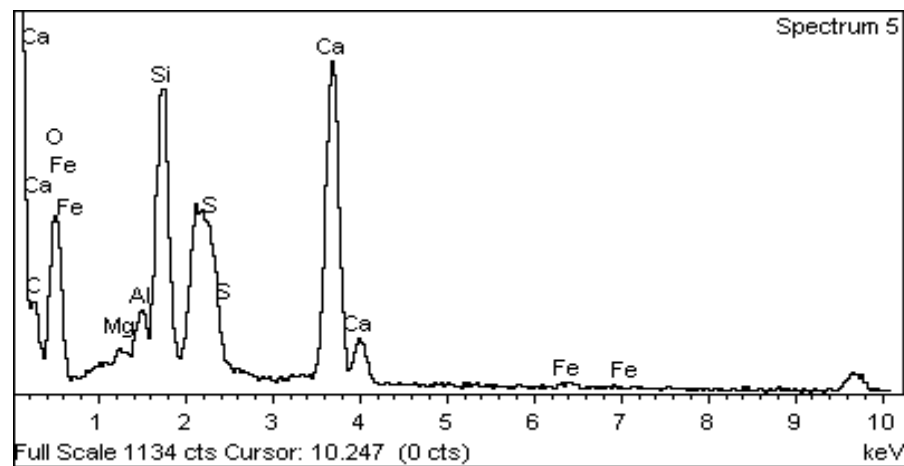


b) EDX

Figure 4-53: SEM and EDX of Marl Treated with SFA + 2 % Cement.



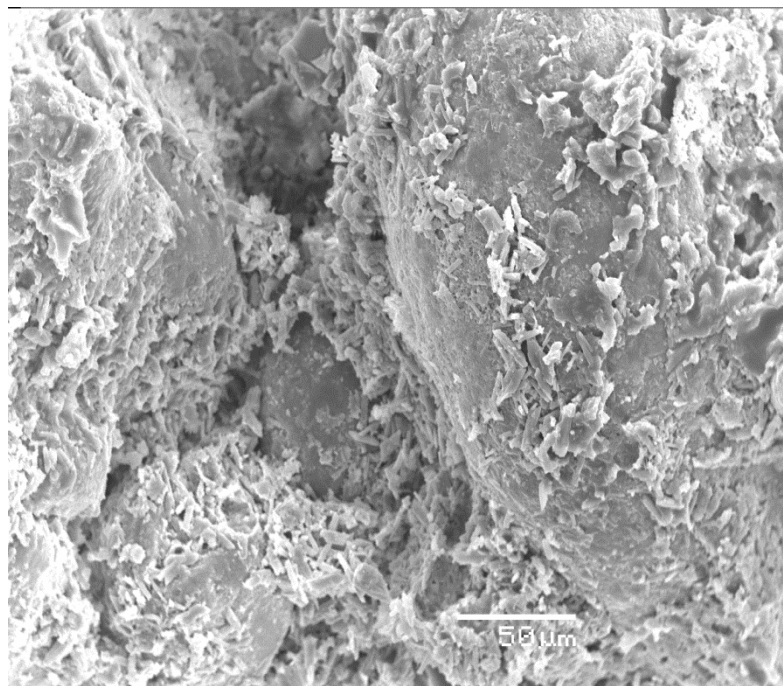
a) SEM



b) EDX

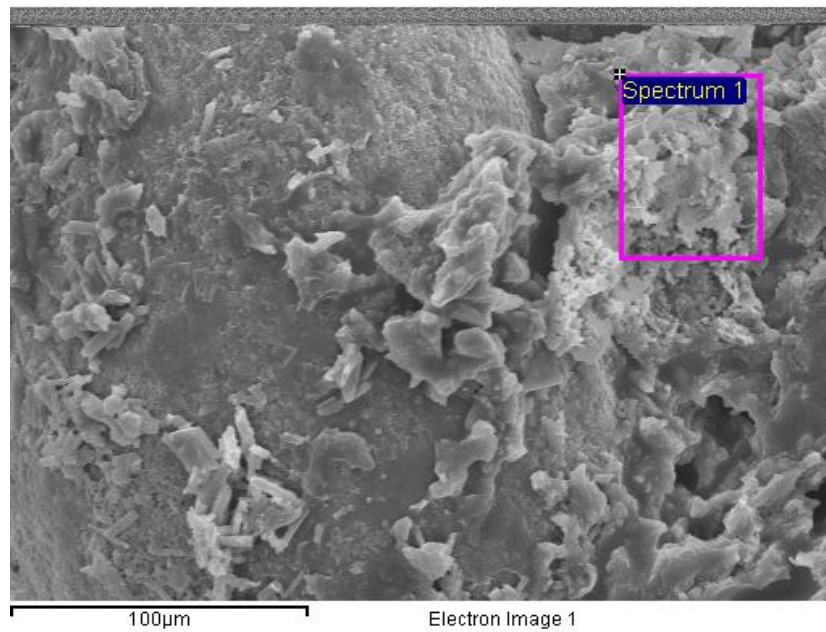
Figure 4-54: SEM and EDX of Sand Treated with SFA + 2 % Cement.

The presence of halite and gypsum in sabkha has reduced the quality and strength of the C-S-H gel. Though the presence of gypsum increases the amount of C-S-H gel, the quality of the gel is weak. Furthermore, the presence of gypsum in the sabkha lead to the formation of ettringite which in turn contributed to the lower quality of C-S-H gel, thus leading to reduction in strength as compared with the strength of emulsion-cement-marl specimens.

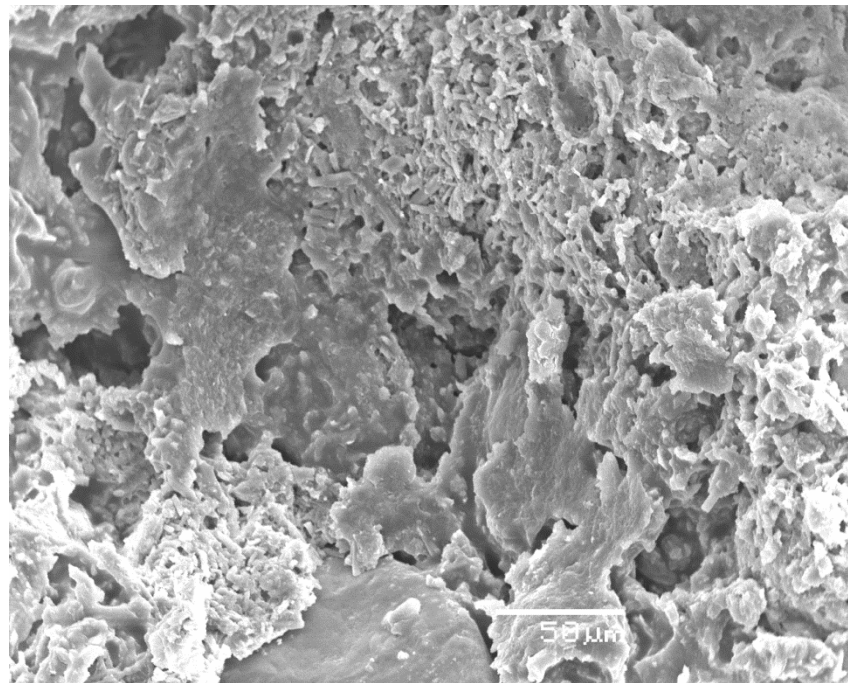


a) CH Crystals





b) Ettringite



C) C-S-H Crystals.

Figure 4-55: SEM for Sabkha Treated with EA and 2% Cement.

Similarly, Figures 4.56 and 4.57 show the SEM for the sabkha and sand treated with SEA and 2 % cement, respectively. The same morphology was observed as in the normal emulsion-cement-soils mixes except that the colloids and the needle-like crystals of sulfur are evident in the voids between the soil particles. Moreover, characteristics of calcium hydroxide and calcium silicate are presents. Although water in emulsion mixtures is a vital ingredient of the process, it becomes a problem in terms of inhibiting compaction and delaying strength gain and this might justify the low stiffness of some emulsion mixes, particularly sulfur modified emulsion mixes where the sulfur crystals formed in voids of the mixtures delay water evaporation to some extent. Thus, to gain the final strength, sulfur modified emulsion mixtures should be cured longer than regular EA mixes. Figure 4.56 also show a more voids which might be behind the weakness of the mixture.

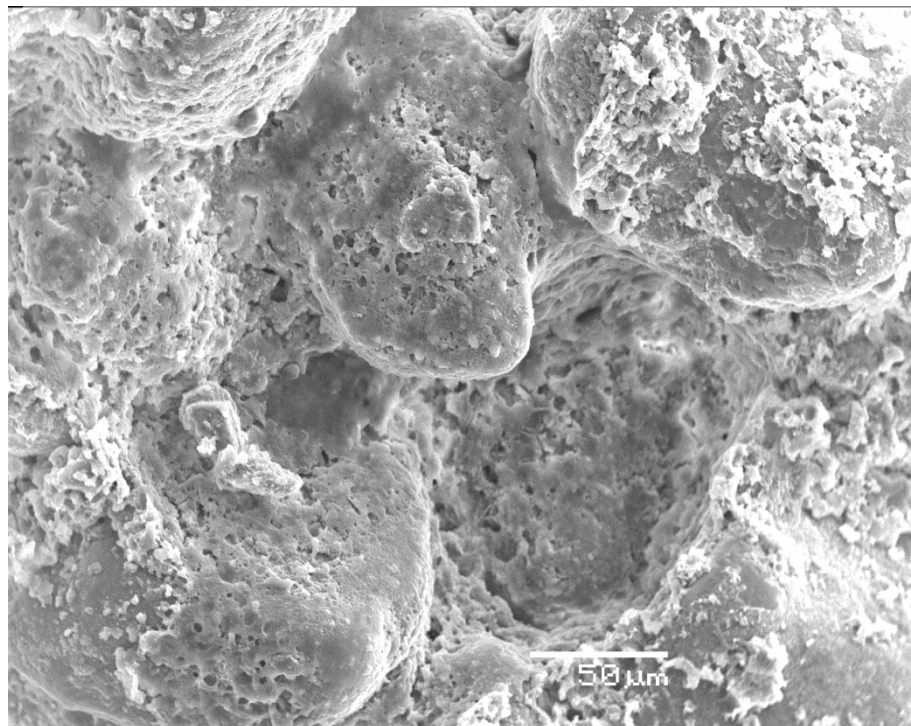


Figure 4-56: SEM for Sabkha Treated with SEA and 2% Cement.

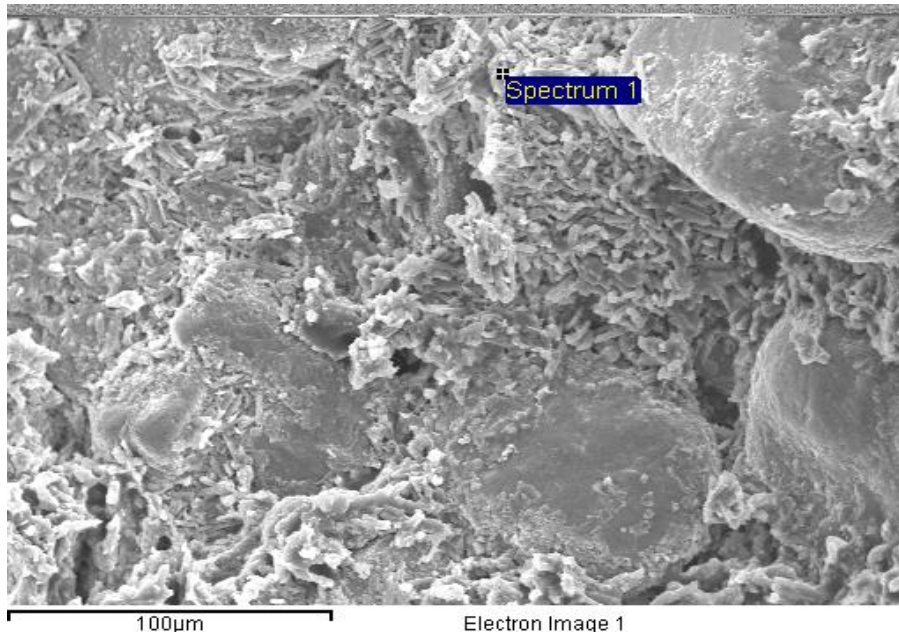


Figure 4-57: SEM of Sand Treated with SEA and 2 % Cement.

#### 4.6 Statistical Analysis Results

The effect of binder type (i.e. FA, SFA, EA and SEA) on the mechanical and engineering properties of the soils, namely, marl, sabkha and sand soils were statistically analyzed using the data obtained from the different laboratory tests conducted on the soil mixes. Furthermore, the effect of temperature, stresses either confined or deviatoric, on some of these engineering properties such as resilient modulus were also analyzed. Since residual asphalt percentages are not always the same for the tested mixes, so the experiment design should involved two factors (i.e. additive type and percentage of residual asphalt) when testing for Marshall stability and indirect tensile strength. In the resilient modulus results analysis, however, all tested mixes were at optimum residual asphalt content so we ignored this factor.

Analyses were done for the null hypothesis “Ho: the data obtained has equal means”. The alternative hypothesis (Ha) is that at least one population means is significantly different from the others. The null hypothesis is rejected if P-value is less than  $\alpha = 0.05$  (95 % confidence level) implying that the data do not support the null hypothesis. Due to the nature of the experimental design and the number of treatment involved in each test, the hypotheses were tested using a two-way and general linear model analysis of variance (ANOVA) by Minitab (version 16) software. The model adequacy check was performed before conducting ANOVA analysis. To ensure the relevance and appropriateness of the selected test method, equality of variance test and normality check test were carried out first. The results of these tests indicated that the observations independency assumption was satisfied and the normality and equal variance checks also shows the data to be normally distributed with more or less equal variance for each level of treatment. The abstract of the ANOVA results are shown in Table 4.12 through Table 4.14 and the complete Minitab print out is presented in Appendix A.

#### **4.6.1 Marshall Stability**

Table 4.12 shows the abstract of the ANOVA results of Marshall stability (dry and soaked) for foamed and emulsion mixes, as well. The analysis of data by ANOVA technique shows that the additive types (FA and SFA) and residual asphalt have a significant effect only on the dry stability in marl mixes whereas there is a slight effect (insignificant) on the stability in the sabkha and sand mixes either dry or soaked. On the other hand, the additive types EA and SEA have a significant effect on the dry and soaked stability in the all three soils mixes. Furthermore, the residual asphalt has a significant impact on the stability.

#### **4.6.2 Indirect Tensile Strength (ITS)**

Abstract of the statistical analysis results for dry and soaked split tensile strength for foamed mixes and only dry ITS for emulsified mixes is shown in Table 4.13. The results reveal that the null hypothesis “additive types and residual asphalt have equal means” can be rejected indicating that there is a significant effects of additive type as well as residual asphalt on both dry and soaked ITS in soils-FA/SFA mixes. However, for emulsified asphalt-soils mixes, the ANOVA results reveal that the additive type has insignificant effect on ITS in marl soil mix but it has a significant effect on the sabkha and sand soils mixes.

#### **4.6.3 Resilient Modulus (MR)**

Since the effect of four factors that are, temperature, additive type, confining pressure and deviator stress on the resilient modulus should be statistically analyzed, the general linear model under ANOVA technique was used. Table 4.14 shows abstract of the ANOVA results for foamed and emulsified soils mixes. Based on the results of the foam mixes in Table 4.14, it is clearly shown that, the null hypothesis can be rejected since there is a significant effect for all factors on the resilient modulus in the marl, sabkha and sand soil mixes. The low values of p-value imply that the data do not support the null hypothesis and thus the alternative hypothesis is accepted. Similarly, results for emulsified-soils mixes shown in the same table reveal that all the factors have a significant effect on the resilient modulus except the additive type which reflects insignificant effect in the three soils mixes.

Table 4-12: Result of Marshall Stability ANOVA at 5% Significance Level.

Mix Type	Test Condition	Material Type	Factors	Calculated $F_{\text{value}}$	P-value	Comments
Foamed Asphalt	Dry	Marl	Additive Type	48	0.020	Significant
			Residual Asphalt	134.33	0.007	Significant
		Sabkha	Additive Type	0.00	0.972	Insignificant
			Residual Asphalt	0.25	0.799	Insignificant
		Sand	Additive Type	0.02	0.892	Insignificant
			Residual Asphalt	1.5	0.400	Insignificant
	Soaked	Marl	Additive Type	0.27	0.652	Insignificant
			Residual Asphalt	0.31	0.765	Insignificant
		Sabkha	Additive Type	0.02	0.910	Insignificant
			Residual Asphalt	1.00	0.499	Insignificant
		Sand	Additive Type	0.05	0.850	Insignificant
			Residual Asphalt	0.16	0.865	Insignificant
Emulsified Asphalt	Dry	Marl	Additive Type	372.23	0.000	Significant
			Residual Asphalt	64.84	0.000	Significant
		Sabkha	Additive Type	67.22	0.001	Significant
			Residual Asphalt	19.06	0.007	Significant
		Sand	Additive Type	56.25	0.002	Significant
			Residual Asphalt	45.77	0.001	Significant
	Soaked	Marl	Additive Type	96.25	0.001	Significant
			Residual Asphalt	19.31	0.007	Significant
		Sabkha	Additive Type	33.45	0.004	Significant
			Residual Asphalt	23.96	0.005	Significant
		Sand	Additive Type	63.49	0.001	Significant
			Residual Asphalt	59.91	0.001	Significant

Table 4-13: Result of ITS ANOVA at 5% Significance Level.

Mix Type	Test Condition	Material Type	Factors	Calculated F <sub>value</sub>	P-value	Comments
Foamed Asphalt	Dry	Marl	Additive Type	13.29	0.022	Significant
			Residual Asphalt	38	0.002	Significant
		Sabkha	Additive Type	61.53	0.001	Significant
			Residual Asphalt	63.26	0.001	Significant
		Sand	Additive Type	9.23	0.038	Significant
			Residual Asphalt	42.68	0.002	Significant
	Soaked	Marl	Additive Type	28.95	0.006	Significant
			Residual Asphalt	62.85	0.001	Significant
		Sabkha	Additive Type	36.16	0.004	Significant
			Residual Asphalt	78.11	0.000	Significant
		Sand	Additive Type	52.91	0.002	Significant
			Residual Asphalt	79.05	0.000	Significant
Emulsified Asphalt	Dry	Marl	Additive Type	3.84	0.107	Insignificant
			Residual Asphalt	144.49	0.000	Significant
		Sabkha	Additive Type	12.55	0.024	Significant
			Residual Asphalt	26.07	0.004	Significant
		Sand	Additive Type	17.06	0.014	Significant
			Residual Asphalt	9.59	0.025	Significant

Table 4-14: Result of MR ANOVA at 5% Significance Level.

Mix Type	Material Type	Factors	Calculated $F_{value}$	P-value	Comments
Foamed Asphalt	Marl	Temperature	9.6	0.003	Significant
		Type of Additive	31.18	0.000	Significant
		Confining Pressure	26.36	0.000	Significant
		Deviator Stress	121.16	0.000	Significant
	Sabkha	Temperature	10.32	0.002	Significant
		Type of Additive	30.32	0.000	Significant
		Confining Pressure	30.27	0.000	Significant
		Deviator Stress	130.64	0.000	Significant
	Sand	Temperature	7.33	0.009	Significant
		Type of Additive	17.81	0.000	Significant
		Confining Pressure	42.71	0.000	Significant
		Deviator Stress	161.59	0.000	Significant
Emulsified Asphalt	Marl	Temperature	4.18	0.045	Significant
		Type of Additive	0.54	0.467	Insignificant
		Confining Pressure	36.30	0.000	Significant
		Deviator Stress	167.04	0.000	Significant
	Sabkha	Temperature	7.18	0.009	Significant
		Type of Additive	1.27	0.264	Insignificant
		Confining Pressure	38.94	0.000	Significant
		Deviator Stress	179.51	0.000	Significant
	Sand	Temperature	4.53	0.037	Significant
		Type of Additive	0.28	0.598	Insignificant
		Confining Pressure	38.02	0.000	Significant
		Deviator Stress	162.82	0.000	Significant



## **CHAPTER 5**

### **PREDICTION OF PERMANENT DEFORMATION**

One of the major distresses in the flexible pavement is rutting, as indicated by the permanent deformation or rut depth along the wheel paths. Many factors affect the width and depth of the rut, such as, structural characters of the pavement layers (thickness and material quality), traffic loads and environmental conditions. It is known that surface rutting forms as a result of the accumulation of the load-induced permanent deformation developed from all individual pavement layers, including the subgrade. Moreover, when the surface layer is thin, large percentage of the total rutting will mostly come from the underneath layers of pavement such as, base, subbase and subgrade. Thus, in order to predict the total permanent deformation of a pavement structure, one has to get the properties of the material in each layer and predict the layer rut. VESYS model is adopted in this study since it is considered suitable to predict a layer rut depth and the total rut depth of the pavement structure. The model parameters depend on the results of the experimental work on the material for each layer. Therefore, the dynamic triaxial repeated load test, which is suitable lab tests to get the VESYS model parameters, was conducted on the investigated materials and the results were presented in Chapter 4.

#### **5.1 Prediction of Permanent Deformation Using VESYS Model**

VESYS model includes two different flexible pavement rutting models: system rutting and layer rutting model. One of the advantages of the layer rutting model is its capability to predict both surface rutting and the permanent deformation in each layer of

the pavement structure. The permanent deformation in each finite layer can be estimated as the product of the layer material permanent deformation law associated with that layer and the elastic compression at that layer which in layer theory is given by the difference in deflections of the top and bottom of the layer. Thus, the rut depth in any finite layer can be calculated from the following equation [Zhou and Scullion, 2002]:

$$R_D(N) = (W^+ - W^-) * \frac{\mu_i}{1 - \alpha_i} N^{(1 - \alpha_i)} \quad (5-1)$$

Where,

$R_D$  = the permanent deformation (rutting) level after N load repetitions;

$W^+$ ,  $W^-$  = the elastic deflection amplitudes of the top and bottom surfaces of the layer, respectively;

$\mu_i$ ,  $\alpha_i$  = the laboratory permanent deformation parameters for the each layer (i) material;

$$\mu = \frac{ab}{\epsilon_r}, \quad \alpha = 1 - b \quad (5-2)$$

a = intercept coefficient of accumulated permanent strain vs. number of load repetitions curve on log-log scale;

b = slope coefficient of accumulated permanent strain vs. number of load repetitions curve on log-log scale; and

$\epsilon_r$  = resilient strain

For the subgrade layer which is considered as a semi-infinite layer, Equation 5-1 becomes:

$$R_{\text{sub}}(N) = W_{\text{sub}}^+ * \frac{e_t}{e_s} * \frac{\mu_{\text{sub}}}{1-\alpha_{\text{sub}}} N^{(1-\alpha_{\text{sub}})} \quad (5-3)$$

Where,

$\mu_{\text{sub}}$  and  $\alpha_{\text{sub}}$  = permanent deformation parameters of the subgrade material;

$W_{\text{sub}}^+$  = the deflection at top of subgrade due to single axle load;

$e_t$  = the strain at top of subgrade due to the axle group; and

$e_s$  = the strain at top of subgrade due to single axle.

To predict the total rut depth for a pavement structure, the above model parameters for each layer need to be calculated. Two software packages that can model the rutting of individual pavement layers are available. Zhou and Scullion (2005) developed a convenient pre- and post-processor for the classical VESYS program originally developed by Kenis (1977) called VESYS 5W. VESYS 5W software program is short for Visco - Elastic Pavement System Analysis Program [Kenis et. al., 1982 and FHWA, 2003]. Tirado et al. (2006) developed an advanced version of VESYS 5W called TxIntPave which addresses some of the well-known limitations of VESYS 5W and can be used to estimates the rutting of each individual layer of in a flexible pavement with the number of truck passes. In this study, VESYS 5W software was used to analyze the pavement structure and perform analysis. Some of the model requirements above are directly calculated by the software itself. The two main input parameters in the VESYS 5W rutting model are permanent deformation parameters,  $\alpha$  and  $\mu$  for each layer. These parameters should be calculated using Eq. 5.2 and input into the software.

One of the most primary important parameters required for the pavement analysis and performance is resilient modulus ( $M_R$ ) for each layer of the pavement structure. To obtain the accurate values of the resilient modulus for the treated base materials, the base layer was divided into sub-layers and starting with assumed initial values of resilient modulus based on the results of resilient modulus test presented in Chapter 4 for all treated soil mixes. Thereafter, the 3D move analysis software was used to compute the stress state in each sub-layer and then the average stress was used to calculate the subsequent resilient modulus value. The process continued for a number of iteration until the difference between the assumed and calculated  $M_R$  was less than 1%. The resilient strain for a layered elastic system then can be approximated as [Gautam et al., 2009]:

$$\varepsilon_r = \frac{\sigma_d}{M_R} \quad (5-4)$$

The results of the dynamic triaxial tests for the soils (marl, sabkha and sand) alone as a subgrade and treated with FA, SFA, EA, and SEA as a base were presented in Chapter 4. Based on these results, one can calculate the permanent deformation parameters ( $\alpha$  and  $\mu$ ) for each mix by presenting the accumulated permanent strain versus number of load repetitions curve on a log-log scale as explained in Chapter 4. Figure 5.1 shows how these two parameters were calculated where  $\sigma_d$  is a deviator stress. An example showing how to calculate these parameters is presented in Appendix B. Table 5.1 presents the VESYS layer rutting parameters,  $\mu$  and  $\alpha$  for subgrade soils and foamed mixes, while, Table 5.2 presents  $\mu$  and  $\alpha$  parameters for emulsion mixes.

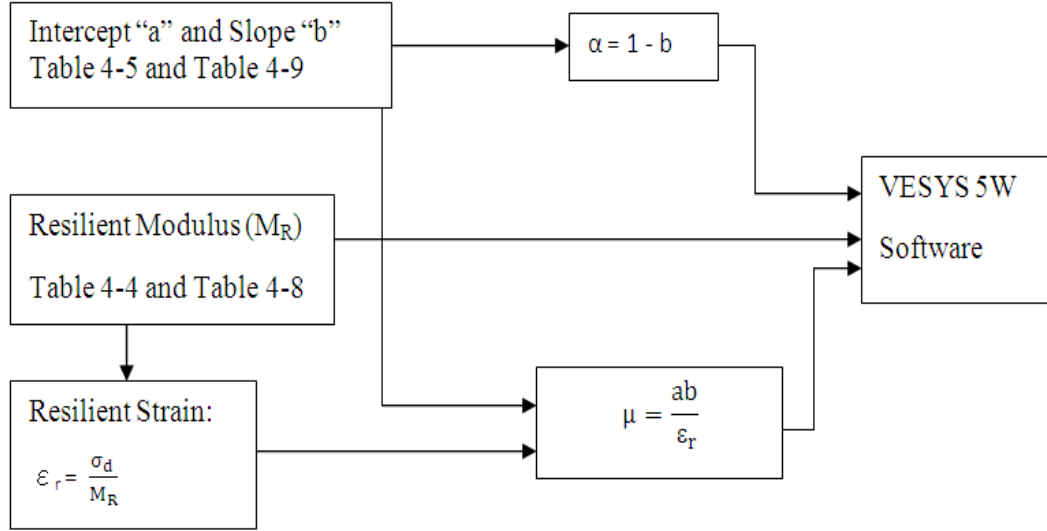


Figure 5-1: Calculation of Permanent Deformation Parameters ( $\alpha$  and  $\mu$ ).

The total rut depth for any pavement structure is the summation of the rut depth for each layer in addition to the rut depth of the subgrade. To compute the rut depth for the investigated materials which will be used as a base course, we used the VESYS layer rutting model:

$$R_D = (W^+ - W^-) * \frac{\mu_i}{1 - \alpha_i} N^{(1 - \alpha_i)} \quad (5-5)$$

In which  $\alpha$  and  $\mu$  are stress and temperature dependent. Based on the results on Table 5.1 and Table 5.2,  $\alpha$  and  $\mu$  were analyzed and regression models were created using Minitab version 16 to express these two parameters as functions of stress levels and temperature as shown in Table 5.3 and Table 5.4.

Table 5-1: Permanent Deformation Parameters for Foamed Asphalt Mixes.

Soil Type	Temp. °C	Treatment Type	$\sigma_c$ (psi)	$\sigma_d$ (psi)	$\sigma_d$ (kPa)	$\alpha$	$\mu$
Marl	22	No Treatment	5	10	69.00	0.91	0.07
Sabkha			5	10	69.00	0.85	0.20
Sand			5	10	69.00	0.80	0.43
Marl	22	FA	10	60	413.69	0.90	0.24
			10	70	482.60	0.88	0.84
			10	80	551.60	0.82	1.78
		SFA	10	60	413.69	0.88	0.18
			10	70	482.60	0.86	0.45
			10	80	551.60	0.83	0.74
	40	FA	10	60	413.69	0.90	0.20
			10	70	482.60	0.87	1.20
			10	80	551.60	0.82	2.33
		SFA	10	60	413.69	0.86	0.65
			10	70	482.60	0.83	0.71
			10	80	551.60	0.82	1.01
Sabkha	22	FA	10	40	275.79	0.78	0.77
			10	50	344.74	0.76	1.64
			10	60	413.69	0.75	2.48
		SFA	10	40	275.79	0.80	0.70
			10	50	344.74	0.78	1.50
			10	60	413.69	0.78	1.52
	40	FA	10	40	275.79	0.79	1.85
			10	50	344.74	0.78	2.15
			10	60	413.69	0.77	3.60
		SFA	10	40	275.79	0.79	1.00
			10	50	344.74	0.77	1.50
			10	60	413.69	0.76	2.32
Sand	22	FA	10	40	275.79	0.86	1.61
			10	50	344.74	0.87	1.84
			10	60	413.69	0.85	2.28
		SFA	10	40	275.79	0.89	1.75
			10	50	344.74	0.91	1.93
			10	60	413.69	0.67	2.17
	40	FA	10	40	275.79	0.73	5.56
			10	50	344.74	0.64	6.78
			10	60	413.69	0.68	8.05
		SFA	10	40	275.79	0.82	2.40
			10	50	344.74	0.94	4.44
			10	60	413.69	0.63	11.52

Table 5-2: Permanent Deformation Parameters for Emulsified Asphalt Mixes.

Soil Type	Temp. °C	Treatment Type	$\sigma_c$ (psi)	$\sigma_d$ (psi)	$\sigma_d$ (kPa)	$\alpha$	$\mu$
Marl	22	EA	10	40	275.80	0.97	0.16
			10	60	413.69	0.89	0.38
			10	70	482.60	0.91	0.41
			10	80	551.60	0.91	0.50
		SEA	10	40	275.80	0.97	1.36
			10	60	413.69	0.93	2.17
			10	70	482.60	0.87	3.39
			10	80	551.60	0.85	4.42
	40	EA	10	60	413.69	0.97	0.33
			10	70	482.60	0.96	0.44
			10	80	551.60	0.96	0.52
		SEA	10	60	413.69	0.90	1.64
			10	70	482.60	0.88	3.29
			10	80	551.60	0.85	7.06
Sabkha	22	EA	10	60	413.70	0.69	2.75
			10	70	482.60	0.52	4.23
			10	80	551.60	0.58	4.63
		SEA	10	60	413.70	0.64	3.19
			10	70	482.60	0.76	5.65
			10	80	551.60	0.64	6.46
	40	EA	10	40	275.80	0.58	3.52
			10	50	345.00	0.55	4.95
			10	60	413.70	0.42	5.01
		SEA	10	60	413.70	0.94	3.32
			10	70	482.60	0.94	3.71
			10	80	551.60	0.95	4.39
Sand	22	EA	10	40	275.80	0.88	0.47
			10	60	413.70	0.87	0.93
			10	70	482.60	0.56	1.15
			10	80	551.60	0.65	1.05
		SEA	10	40	275.80	0.88	1.57
			10	60	413.70	0.71	2.07
			10	70	482.60	0.43	2.50
			10	80	551.60	0.48	1.71
	40	EA	10	60	413.70	0.46	2.06
			10	70	482.60	0.23	1.39
			10	80	551.60	0.16	3.95
		SEA	10	60	413.70	0.93	1.36
			10	70	482.60	0.85	1.51
			10	80	551.60	0.82	1.38

The general regression models for the material properties ( $\mu$  and  $\alpha$ ) were also developed for foam and emulsion mixes as follows:

Foamed asphalt mixes:

$$\mu = -3.96 - 5.24 x_1 - 2.44 x_2 + 0.483 x_3 + 0.101 T + 0.0138 \sigma_d \quad (R^2 = 64.4\%) \quad (5-6)$$

$$\alpha = 1.03 + 0.134 x_1 - 0.0142 x_2 - 0.0106 x_3 - 0.00205 T - 0.000508 \sigma_d \quad (R^2 = 42.4\%) \quad (5-7)$$

Emulsified asphalt mixes:

$$\mu = -0.54 + 0.213 x_1 + 2.68 x_2 - 1.06 x_3 + 0.0117 T + 0.00524 \sigma_d \quad (R^2 = 59.4\%) \quad (5-8)$$

$$\alpha = 0.954 + 0.280 x_1 + 0.0454 x_2 - 0.137 x_3 + 0.00003 T - 0.000553 \sigma_d \quad (R^2 = 47.5\%) \quad (5-9)$$

Where;

$\mu$  and  $\alpha$  = permanent deformation properties of the materials

$x_1 = 1$  (marl) or  $x_1 = 0$  (otherwise);

$x_2 = 1$  (sabkha) or  $x_2 = 0$  (otherwise);

$x_3 = 1$  (FA or EA) or  $x_3 = 0$  (otherwise);

$T$  = temperature in degree

$\sigma_d$  = deviator stress in kPa

The performance and correlations of the above general models of the permanent deformation parameters are very low compared with the models shown in Tables 5.3 and 5.4. Thus, it is recommended to use developed models in terms of temperature and



deviator stress (Tables 5.3 and 5.4) for modeling, since they have high correlations, instead of the general models above.

Table 5-3: Regression Models of  $\mu$  and  $\alpha$  for Foamed Asphalt Mixes.

Soil Type	Stabilizer	$\mu$	$R^2$	$\alpha$	$R^2$
Marl	FA	$\mu = -5.81 + 0.0161 T + 0.0133 \sigma_d$	0.97	$\alpha = 1.15 + 0.000037 T - 0.000598 \sigma_d$	0.95
	SFA	$\mu = -1.53 + 0.0189 T + 0.00325 \sigma_d$	0.934	$\alpha = 1.04 - 0.00115 T - 0.000334 \sigma_d$	0.974
Sabkha	FA	$\mu = -3.80 + 0.0502 T + 0.0125 \sigma_d$	0.95	$\alpha = 0.805 + 0.000926 T - 0.000181 \sigma_d$	0.962
	SFA	$\mu = -1.88 + 0.0204 T + 0.00776 \sigma_d$	0.882	$\alpha = 0.865 - 0.000741 T - 0.000181 \sigma_d$	0.892
Sand	FA	$\mu = -14.7 + 0.345 T + 0.0261 \sigma_d$	0.85	$\alpha = 1.93 - 0.0247 T - 0.00154 \sigma_d$	0.902
	SFA	$\mu = -15.1 + 0.232 T + 0.0346 \sigma_d$	0.678	$\alpha = 1.37 - 0.00148 T - 0.00149 \sigma_d$	0.505

Table 5-4: Regression Models of  $\mu$  and  $\alpha$  for Emulsified Asphalt Mixes.

Soil Type	Stabilizer	$\mu$	$R^2$	$\alpha$	$R^2$
Marl	EA	$\mu = -0.113 - 0.00005 T + 0.00113 \sigma_d$	0.914	$\alpha = 0.812 + 0.00326 T + 0.00004 \sigma_d$	0.949
	SEA	$\mu = -10.9 + 0.037 T + 0.0278 \sigma_d$	0.826	$\alpha = 1.14 - 0.000296 T - 0.000518 \sigma_d$	0.916
Sabkha	EA	$\mu = -3.31 + 0.0247 T + 0.0137 \sigma_d$	0.867	$\alpha = 1.17 - 0.00444 T - 0.000979 \sigma_d$	0.715
	SEA	$\mu = -0.91 - 0.0719 T + 0.0157 \sigma_d$	0.811	$\alpha = 0.341 + 0.0146 T + 0.000036 \sigma_d$	0.915
Sand	EA	$\mu = -5.63 + 0.107 T + 0.00897 \sigma_d$	0.714	$\alpha = 2.17 - 0.0280 T - 0.00178 \sigma_d$	0.918
	SEA	$\mu = -2.51 - 0.0454 T + 0.0124 \sigma_d$	0.706	$\alpha = 0.735 + 0.0181 T - 0.00123 \sigma_d$	0.895

## 5.2 Validation and Calibration of Rut Depth Prediction Models

Simulation in accelerated pavement tests (APT) such as wheel tracking (WT) test is the most effective manner to test the impact of traffic loading and environmental conditions on pavement configurations. Recently, these tests are called Hamburg wheel test and used for superpave evaluation process. As mentioned before the rutting prediction models derived in this study are based on the dynamic triaxial test which is different than WT in many aspects such as boundary conditions and traffic loading, etc.

However, both methods remain only a simulation of actual behavior of the material [Hussain et al., 2013]. The effect of the boundary conditions on the results of the dynamic triaxial tests models developed in this study is obvious which in turn would be reflected by the developed models behavior. Thus, it is necessary to verify and calibrate these models with the results of the wheel tracking test which presents a better simulation to actual field.

Figure 5.2 shows the procedure of the calibration process. First, the permanent deformation properties of the materials ( $\alpha'$  and  $\mu'$ ) calculated from the developed triaxial models at a temperature of 22 °C and under a deviator stress of 552 kPa (as in WT test) for each mix were entered into VESYS 5W software and rut depths were predicted. The predicted rut depths were compared with the rut depths measured using WT tests. If the predicted rut depth is similar to the measured rut depth within 90%, then, no need for calibration and the model can be used for rutting prediction, otherwise,  $\alpha'$  and  $\mu'$  were multiplied by the ratio of the recent predicted rut depth ( $R_{D+1}$ ) to the rut depth predicted in the previous step ( $R_D$ ) and called  $\alpha'_{i+1}$  and  $\mu'_{i+1}$  as shown in the flowchart.  $\alpha'_{i+1}$  and  $\mu'_{i+1}$  were reentered into the VESYS 5W software and the process was repeated till the predicted rut depth is close to the WT-measured rut depth within 90%. Finally, calibration factors for the permanent deformation properties ( $\alpha'$  and  $\mu'$ ) for each mix were determined and are listed in Table 5.5. Figures 5.3 to 5.8 show the WT- measured and VESYS 5W- predicted rut depth curves for the marl, sabkha and sand treated with FA, SFA, EA and SEA, respectively. It is clear from the figures that the calibrated models have predicted the rutting values close to that measured using wheel tracking test.

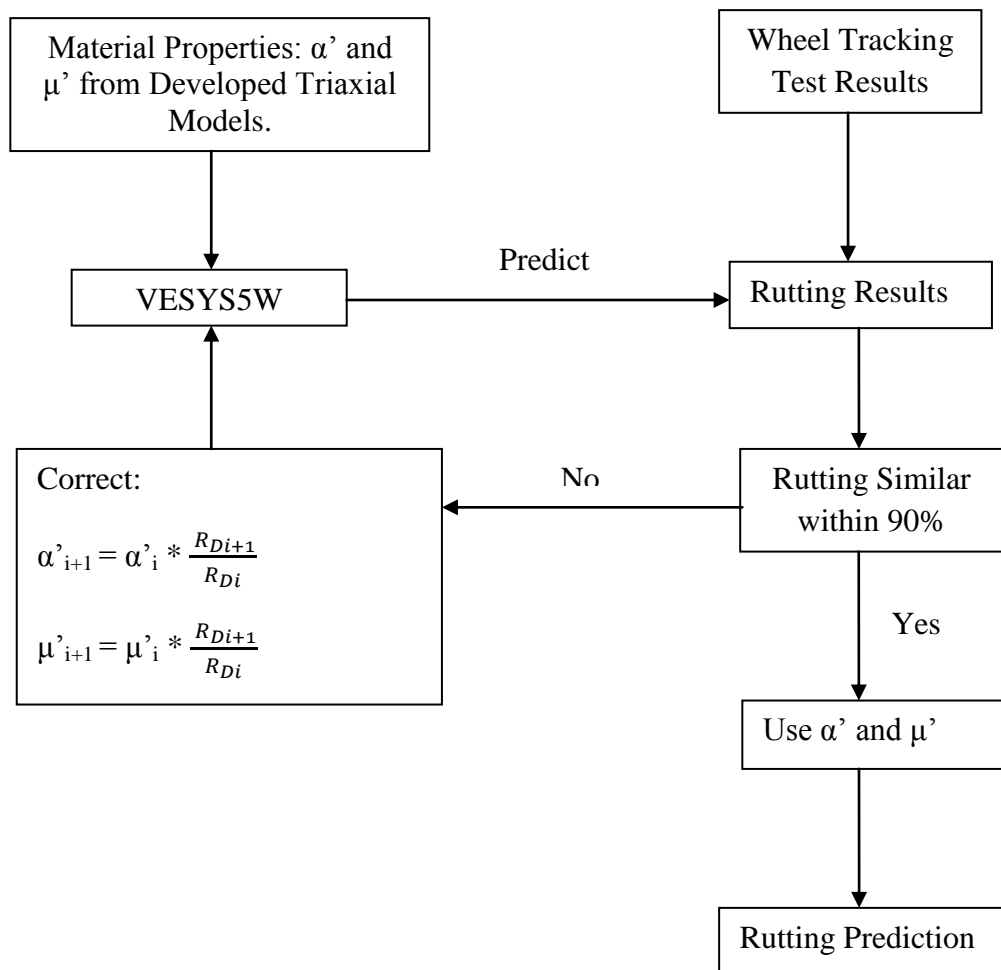
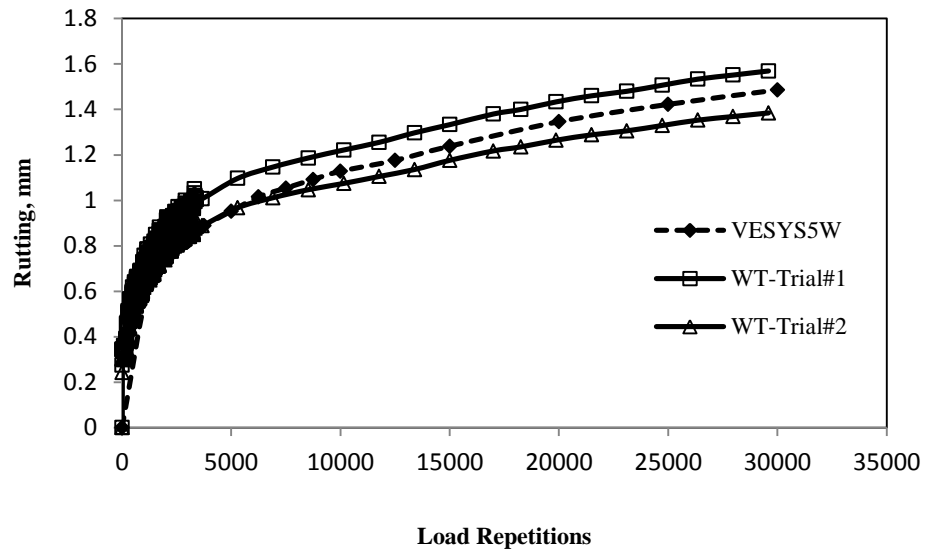


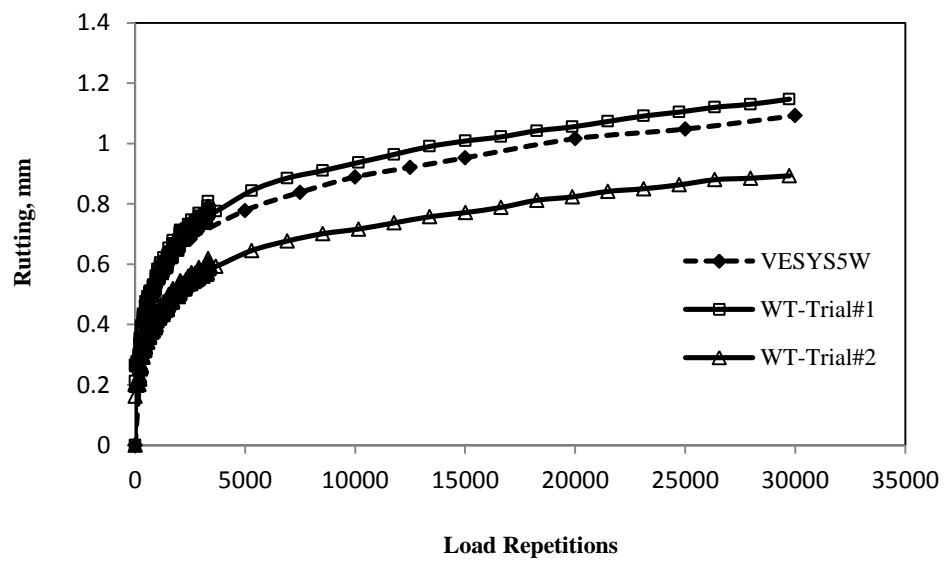
Figure 5-2: Model Calibration Flowchart.

Table 5-5: Calibration Factors for  $\alpha$  and  $\mu$ .

Soil Type	Treatment Type	$\alpha_{CF}$	$\mu_{CF}$
Marl	FA	0.8904	1.058
	SFA	0.9638	2.50
Sabkha	FA	1.0959	1.429
	SFA	0.8267	0.351
Sand	FA	0.6604	1.16
	SFA	0.7843	1.098
Marl	EA	0.7912	2.941
	SEA	0.9412	1.331
Sabkha	EA	1.321	1.77
	SEA	0.60	0.903
Sand	EA	0.93	1.191
	SEA	1	0.749

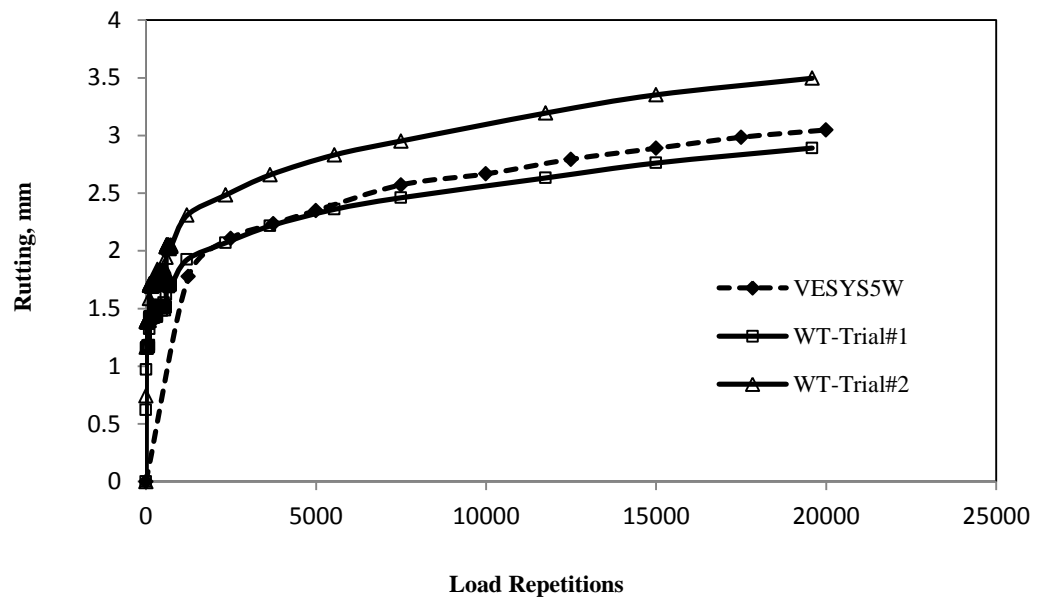


a) FA

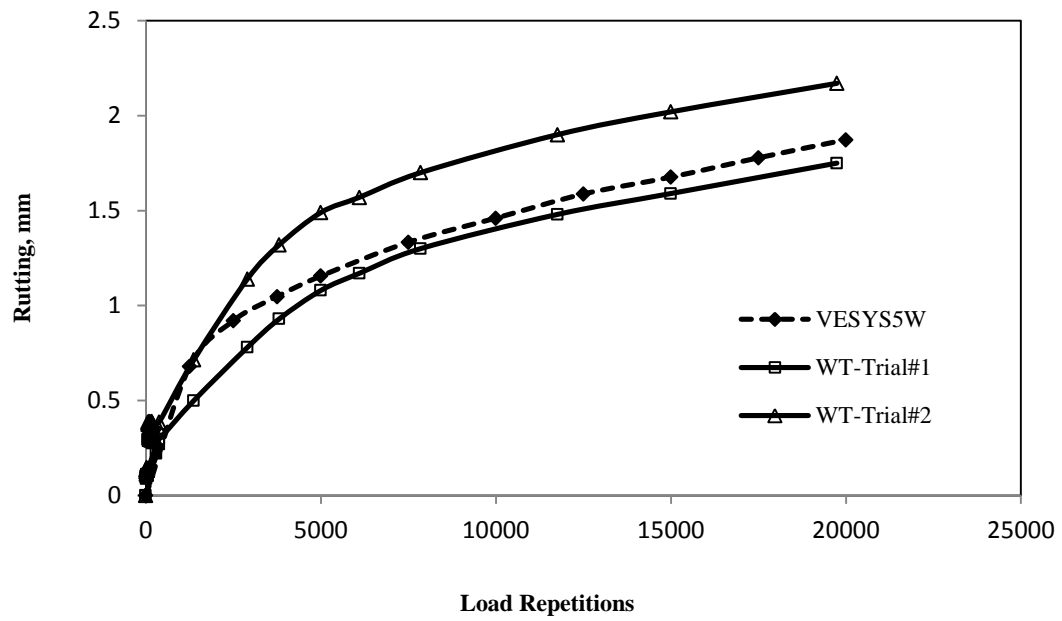


b) SFA

Figure 5-3: Measured and Predicted Rutting for Marl-FA/SFA Mixes.

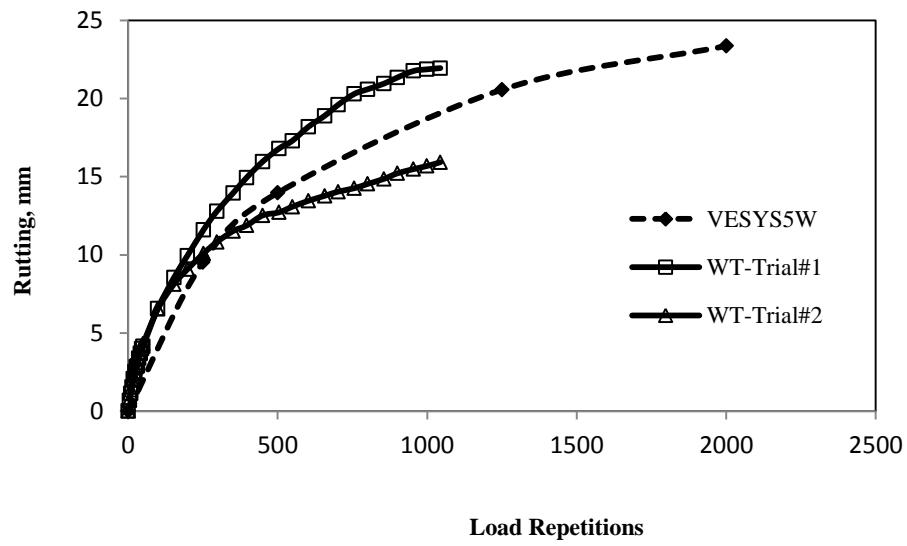


a) FA

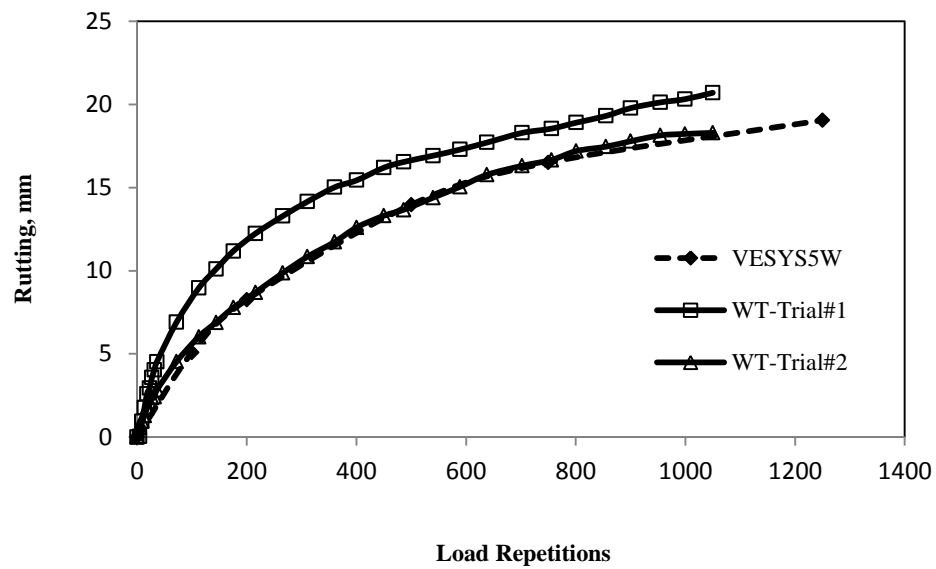


b) SFA

Figure 5-4: Measured and Predicted Rutting for Sabkha-FA/SFA Mixes.

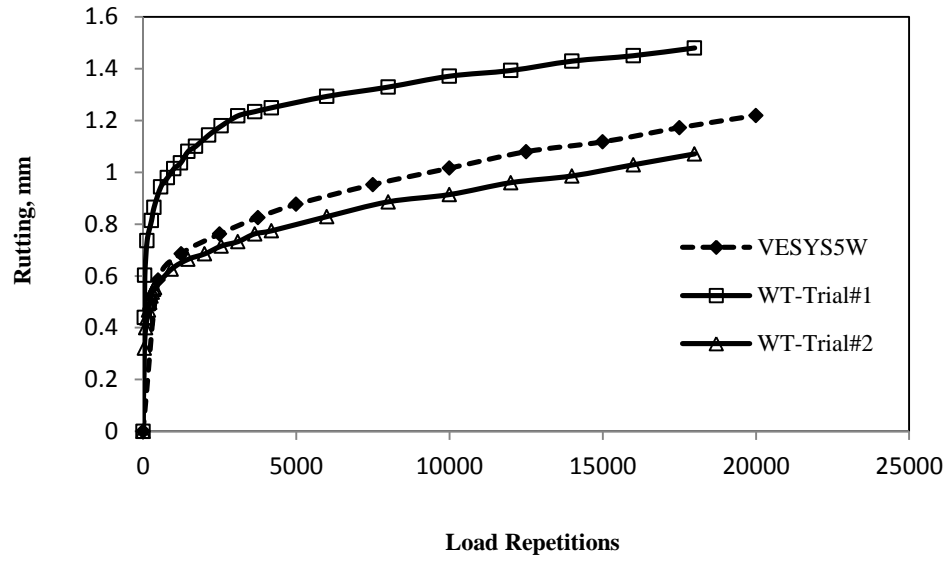


a) FA

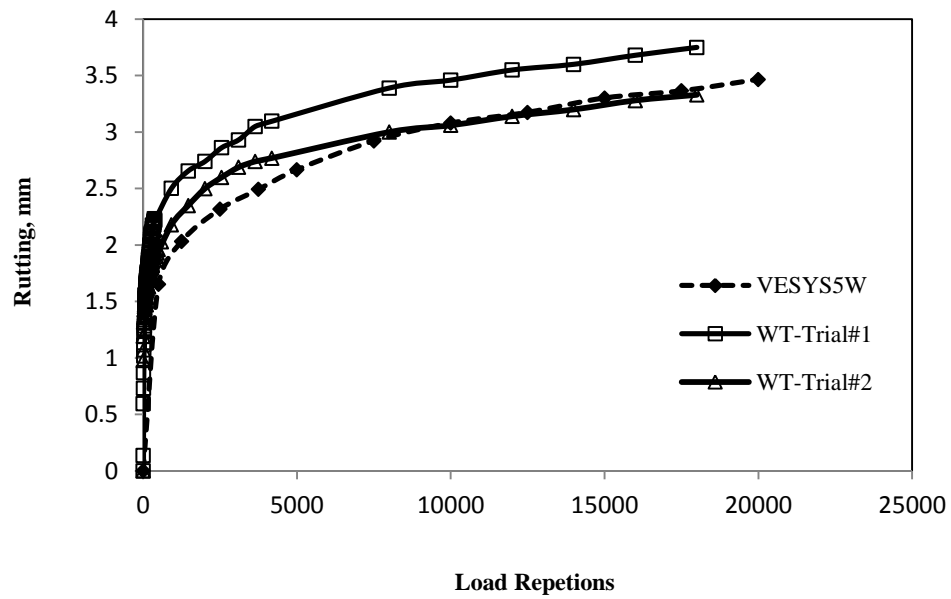


b) SFA

Figure 5-5: Measured and Predicted Rutting for Sand-FA/SFA Mixes.

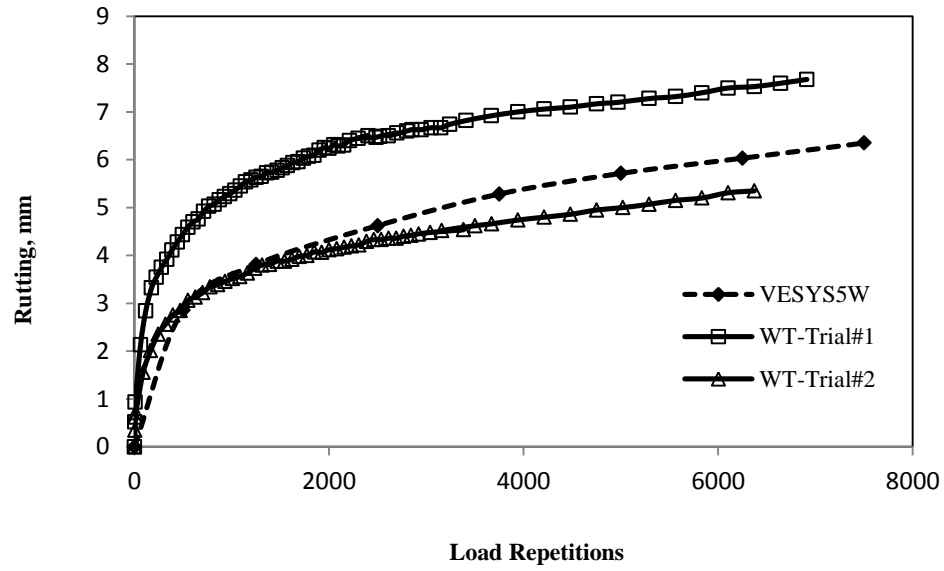


a) EA

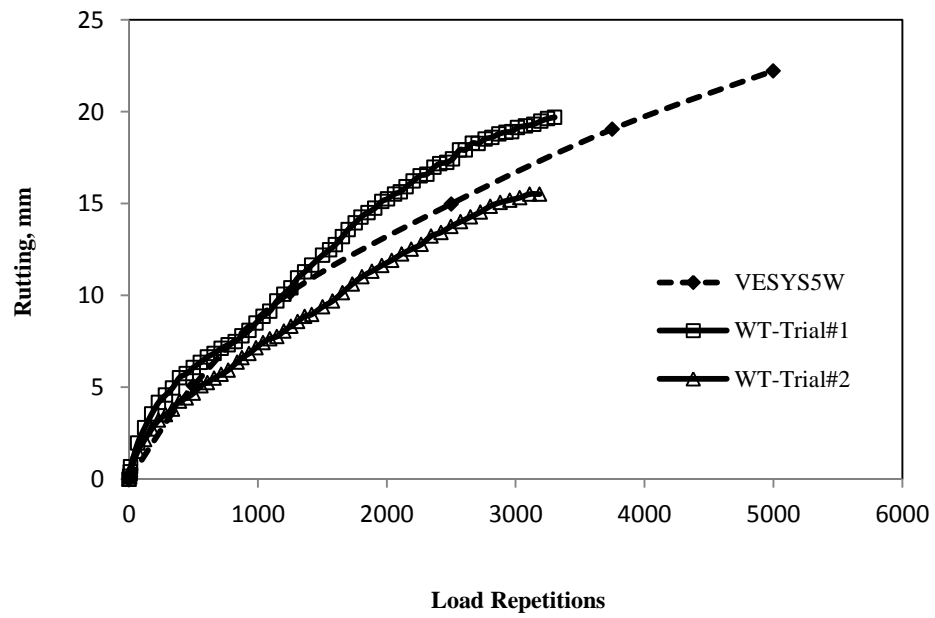


b) SEA

Figure 5-6: Measured and Predicted Rutting for Marl-EA/SEA Mixes.



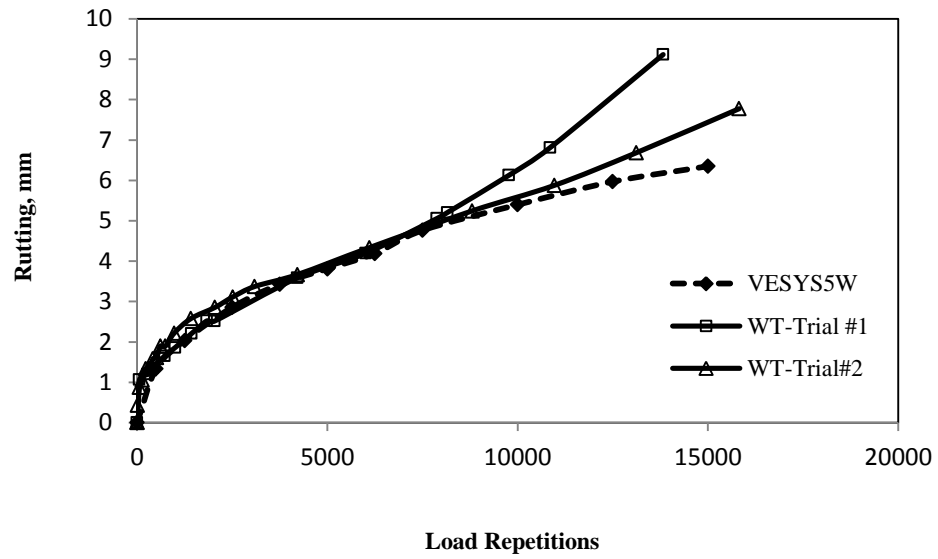
a) EA



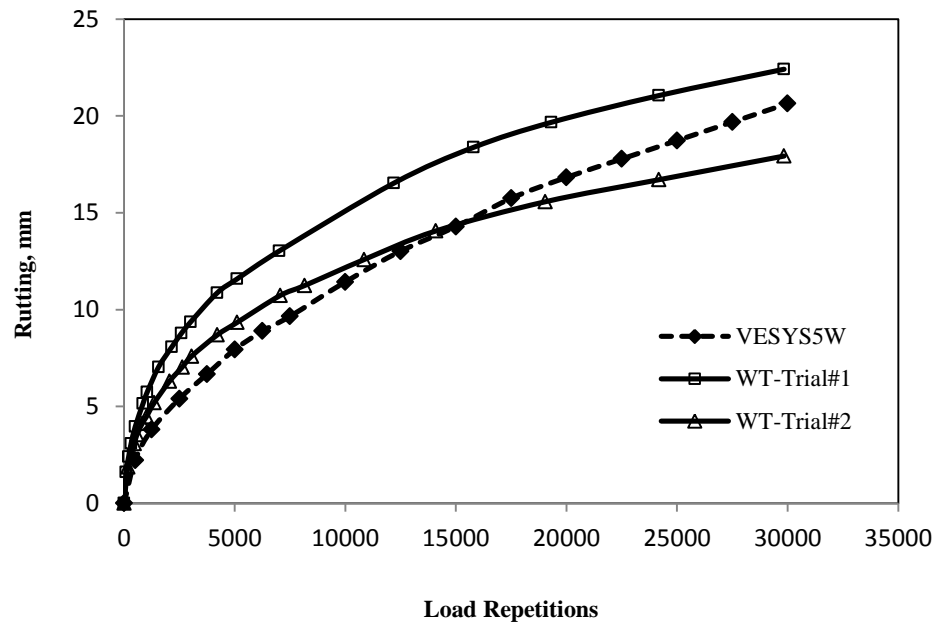
b) SEA

Figure 5-7: Measured and Predicted Rutting for Sabkha-EA/SEA Mixes.





a) EA



b) SEA

Figure 5-8: Measured and Predicted Rutting for Sand-EA/SEA Mixes.

## 5.3 Development of Pavement Thickness Design Charts

Design charts for pavement thickness design are developed in this section based on the modulus results presented in Chapter 4 and the calibrated rutting prediction models developed in the previous sections of this chapter. Only marl and sabkha soils treated with FA/SFA and EA/SEA were considered, since they gave a better permanent deformation resistance performance than sand soil mixes.

### 5.3.1 Cases Analyzed

Since most of the subgrade soils in the Kingdom of Saudi Arabia are usually marl, sabkha or dune sand, three different subgrade cases were selected and analyzed as follows:

#### i. Marl Subgrade

In this case a three layers system consisting of 2 inches of hot mix asphalt (HMA) layer for local street and a base course layer of stabilized marl with FA, SFA, EA and SEA on untreated marl subgrade with CBR of 25 % as shown in Figure 5.9. Since marl soil is more resistance to rutting and less permeable compared to others soils, there is no need for a subbase layer.

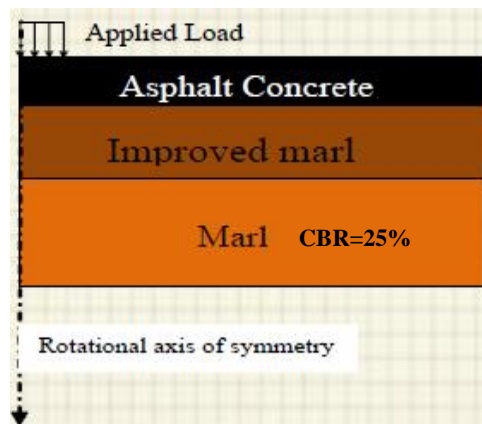


Figure 5-9: Case 1: Three Layers System-Marl Subgrade.

## ii. Sabkha Subgrade

This case has two combinations as shown in Figure 5.9. In the first combination (Figure 5.9 (a)) 6 inches layer of untreated sand with CBR of 15% was used on the sabkha subgrade with CBR of 10% as a subbase and drainage layer followed by a base layer of treated marl with FA, SFA, EA, and SEA and finally a 2 inches layer of HMA. The second combination (Figure 5.9 (b)) has the same structure as in the first combination with the base layer of treated sabkha with FA, SFA, EA and SEA instead of the treated marl.

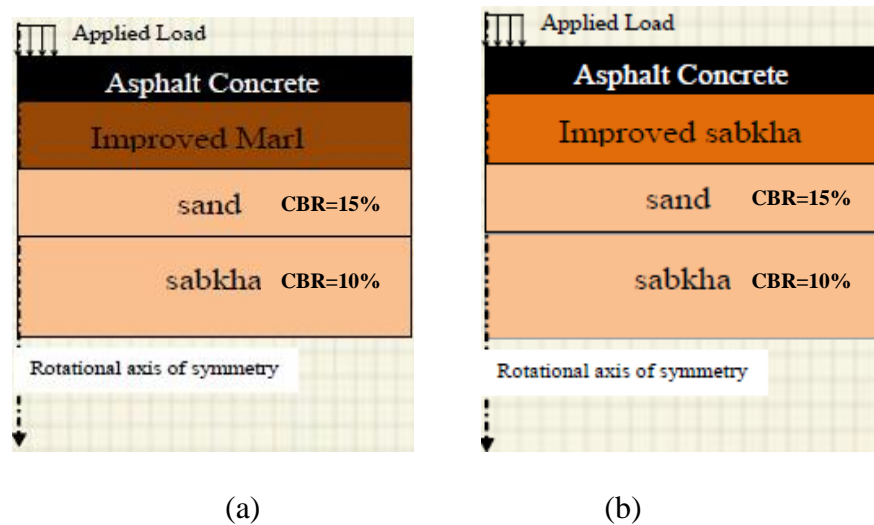


Figure 5-10: Case 2: Four Layers System-Sabkha Subgrade.

## iii. Sand Subgrade

For the sand subgrade case, four layers systems with two combinations as shown in Figure 5.11 were analyzed. Figure 5.11(a) shows the first combination which consists of a 2 inches HMA layer over a base layer of treated marl with FA, SFA, EA and SEA and 6 inch subbase layer of untreated sabkha (CBR= 10%) over a natural sand subgrade (CBR = 15%). Similarly, the second combination shown in

Figure 5.11(b) has the same structure as in the first combination (Figure 5.11(a)) except that sabkha treated with FA, SFA, EA and SEA was used in the base layer instead of treated marl. The reason of using untreated sabkha soil as a subbase layer instead of untreated marl soil is the availability of sabkha soil particularly in deserts and these areas located along the coastal line of Arabian Gulf and red sea as well. Using marl soil will increase the cost of such projects, thus, it will be economical to use available sabkha as a subbase layer as long as it is insulated from water damage.

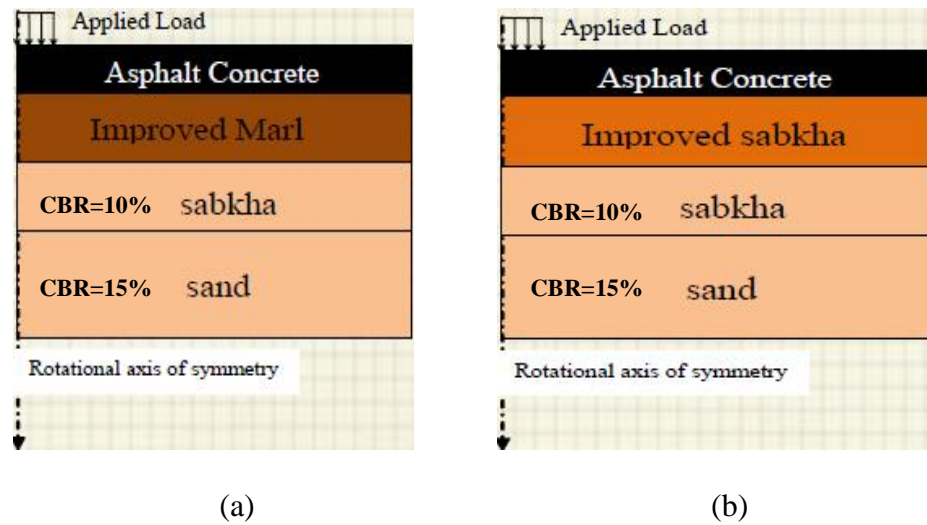


Figure 5-11: Case 3: Four Layers System- Sand Subgrade.

To develop the design charts for any combination explained above, the following steps were followed (see Appendix B):

- The Poisson ratio and resilient modulus for the asphalt concrete layer was taken as reported by Ramadhan [1988].

- The Poisson ratio for other layers was taken as 0.35 and in order to obtain the accurate values of the resilient modulus for the treated base materials, the base layer was divided into sub-layers and starting with assumed initial seed values of resilient modulus based on the results of resilient modulus test presented in Chapter 4.
- 3D move analysis finite element software was used to compute the stress state in each sub-layer under the standard single axle load 80 kN (18 kips), since it has the ability to subdivide the base layer to 10 sub-layers.
- The calculated average stress of the sub-layers was then used to recalculate the subsequent resilient modulus value and the process continued for a number of iteration until the difference between the assumed and calculated  $M_R$  was less than 1%.
- The calibrated models of the permanent deformation properties in Tables 5.3 and 5.4 were used to calculate  $\alpha$  and  $\mu$  for the stabilized base layer under the calculated applied stress and at a certain temperature (22 °C or 40 °C).
- The calibrated permanent deformation values  $\alpha$  and  $\mu$ , the resilient modulus and the Poisson ratio at both test temperatures (22 °C and 40 °C) were entered into VESYS 5W software to predict the layer and total rut depths for the pavement structure.
- By limiting the total pavement and subgrade deformation to 2.54 cm (1 inch), the rutting service life were determined in the form of equivalent axle load (EAL).
- The thickness of the stabilized base layer was then increased and the process was repeated.

- Finally, the results of this process were presented in the form of design charts. In these charts, the total traffic in the terms of equivalent 80 kN (18 kips) axle load (EAL) is plotted versus the stabilized layer thickness.

The developed design charts for the evaluated stabilized base materials in the different cases and combinations are presented in Figures 5.12 to 5.21. The results clearly reflect the performance of the treated materials (marl and sabkha) as they followed the same trend found from the laboratory dynamic triaxial tests and the verification test using wheel track. Thus, we can conclude that marl and sabkha soils with FA or SFA can be used for medium to high traffic volume roads, whereas, only marl treated with EA or SEA can be used for the same purpose. Sabkha stabilized with EA or SEA is suitable for a low to medium traffic volume roads.

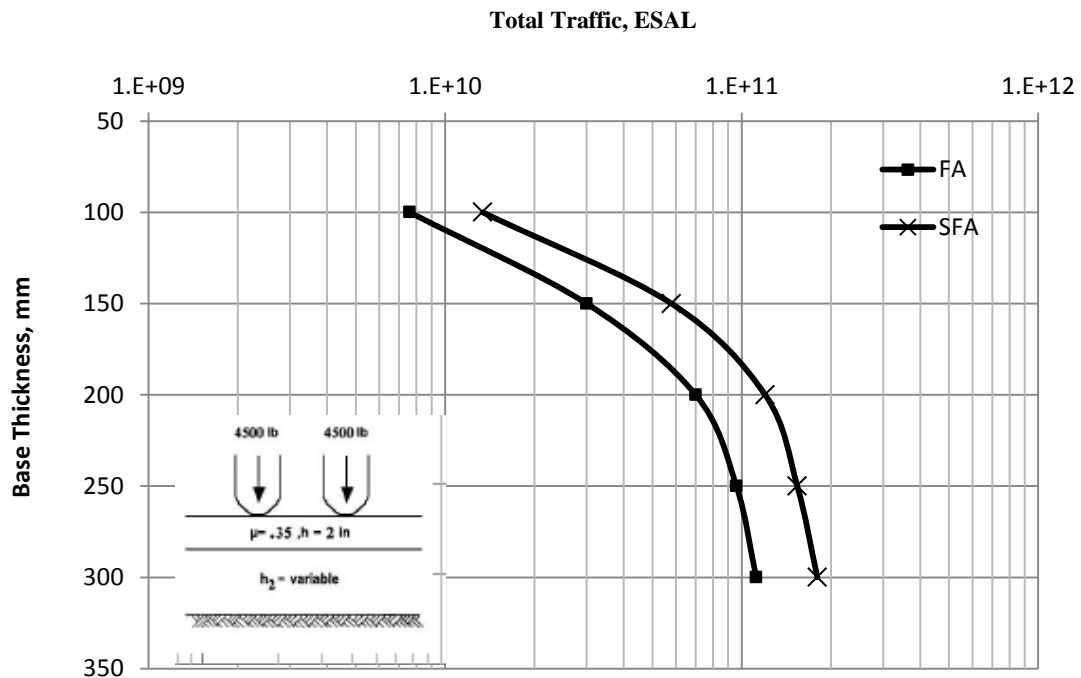


Figure 5-12: Relationship between Marl-Foamed Asphalt Base Thickness and Total Traffic-Case 1.

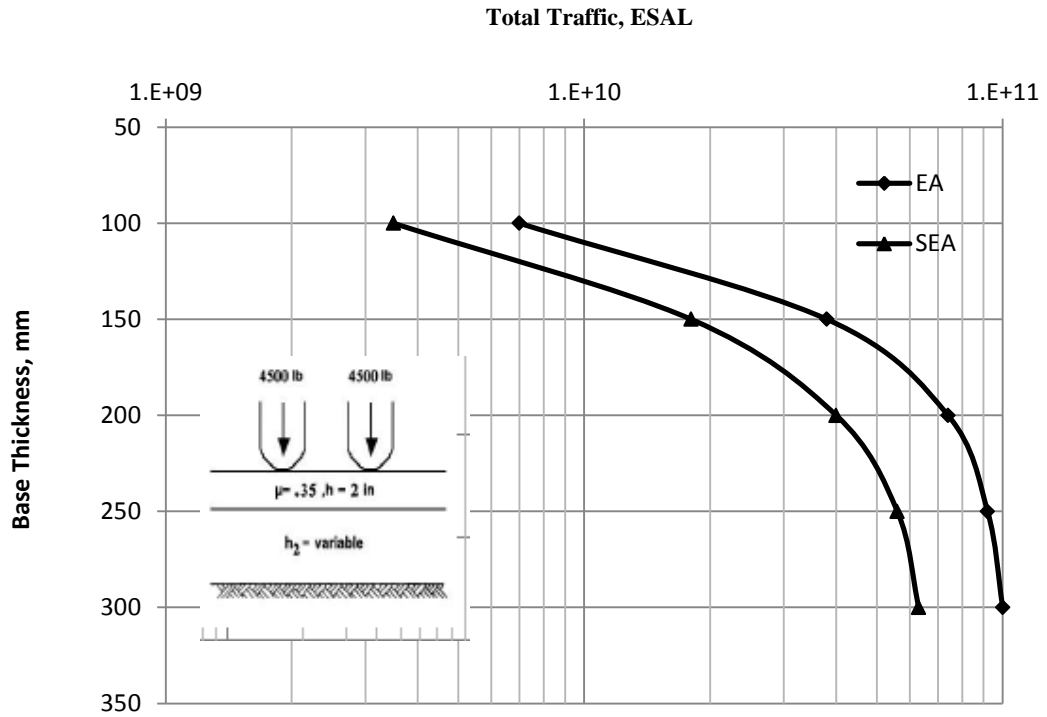


Figure 5-13: Relationship between Marl-Emulsified Asphalt Base Thickness and Total Traffic-Case 1.

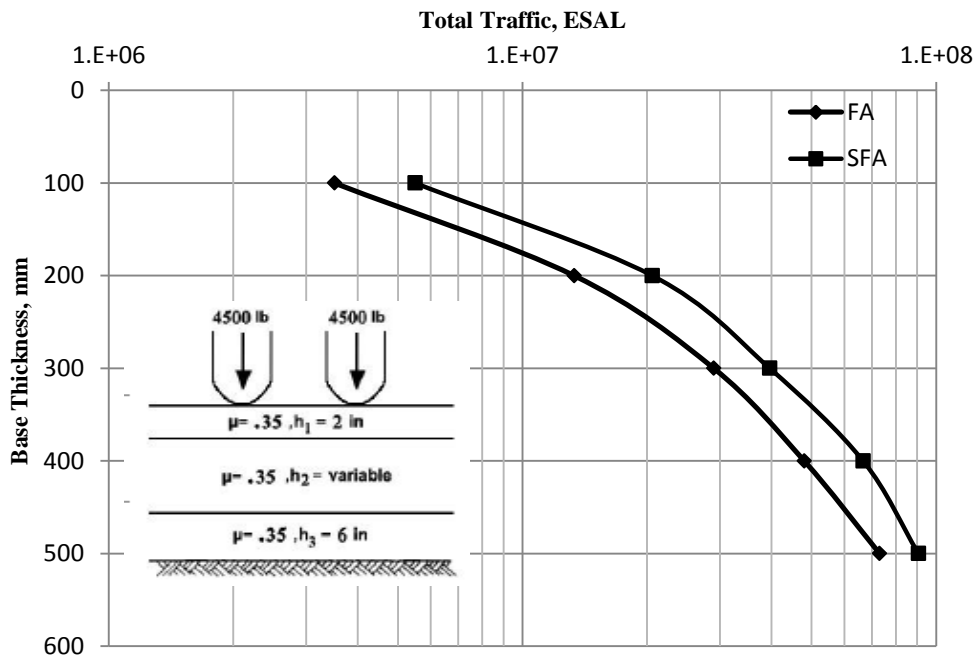


Figure 5-14: Relationship between Marl-Foamed Asphalt Base Thickness and Total Traffic-Case 2.

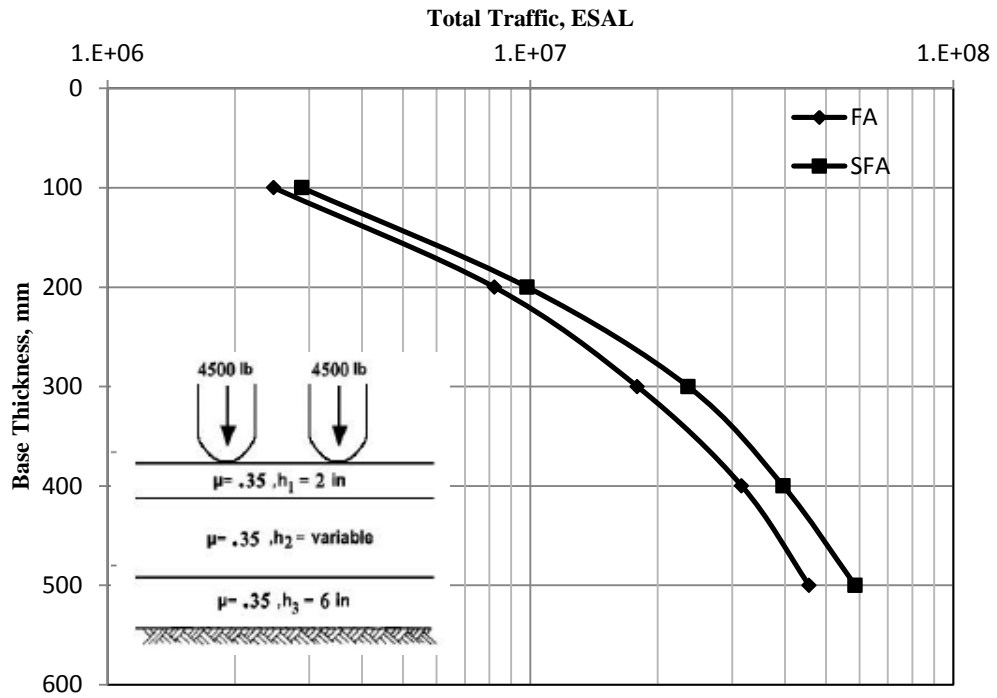


Figure 5-15: Relationship between Sabkha-Foamed Asphalt Base Thickness and Total Traffic-Case 2.

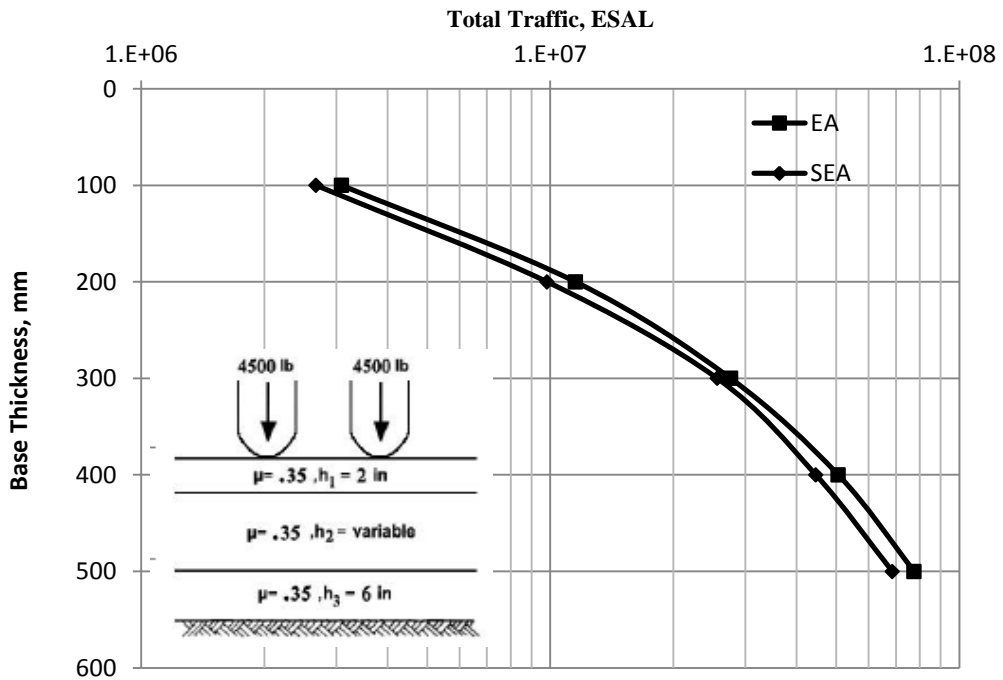


Figure 5-16: Relationship between Marl-Emulsified Asphalt Base Thickness and Total Traffic-Case 2.



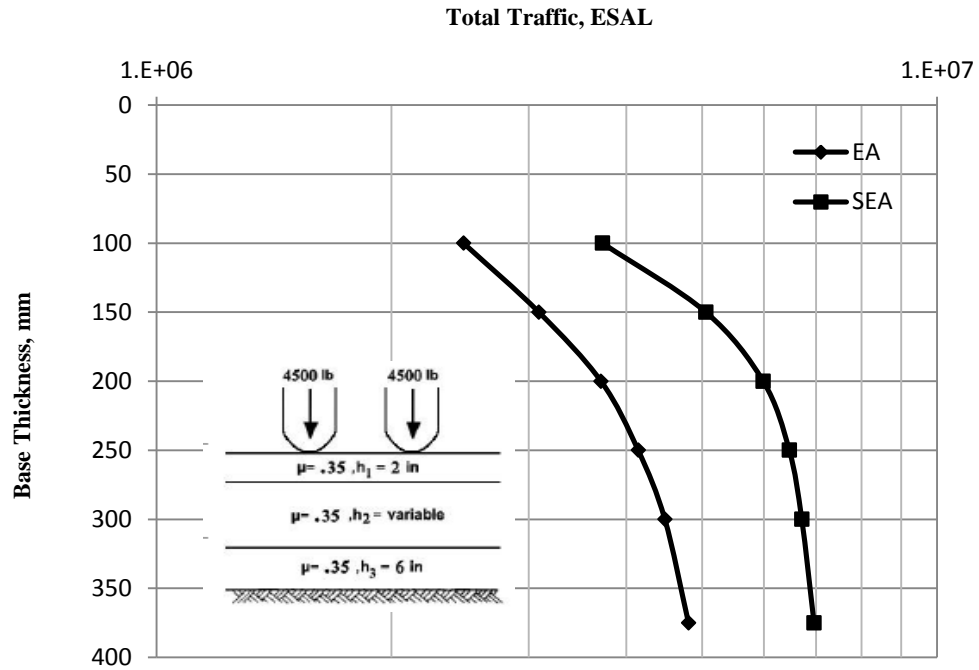


Figure 5-17: Relationship between Sabkha-Emulsified Asphalt Base Thickness and Total Traffic-Case 2.

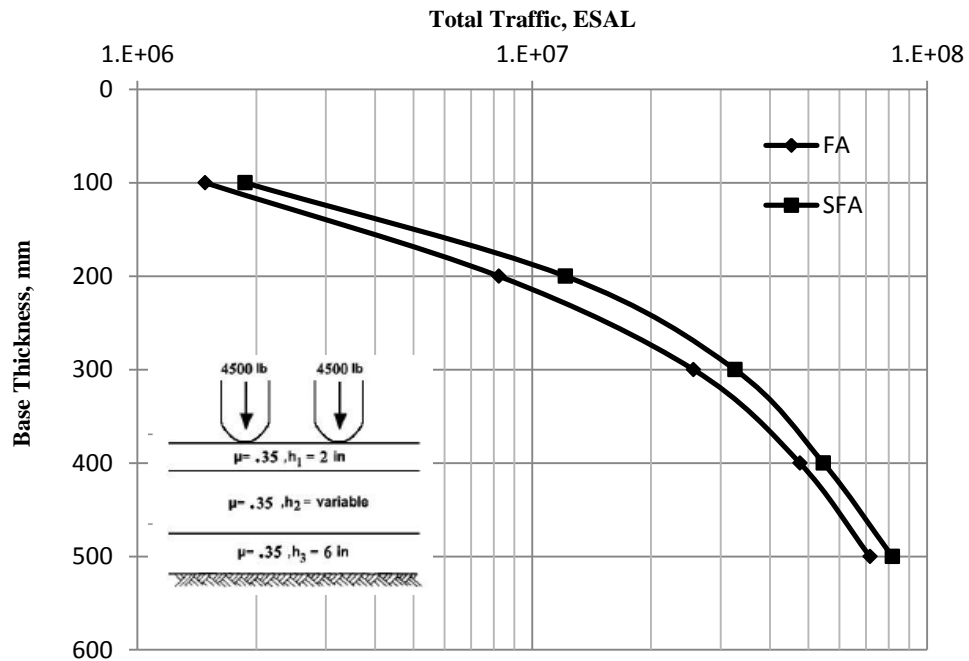


Figure 5-18: Relationship between Marl-Foamed Asphalt Base Thickness and Total Traffic-Case 3.

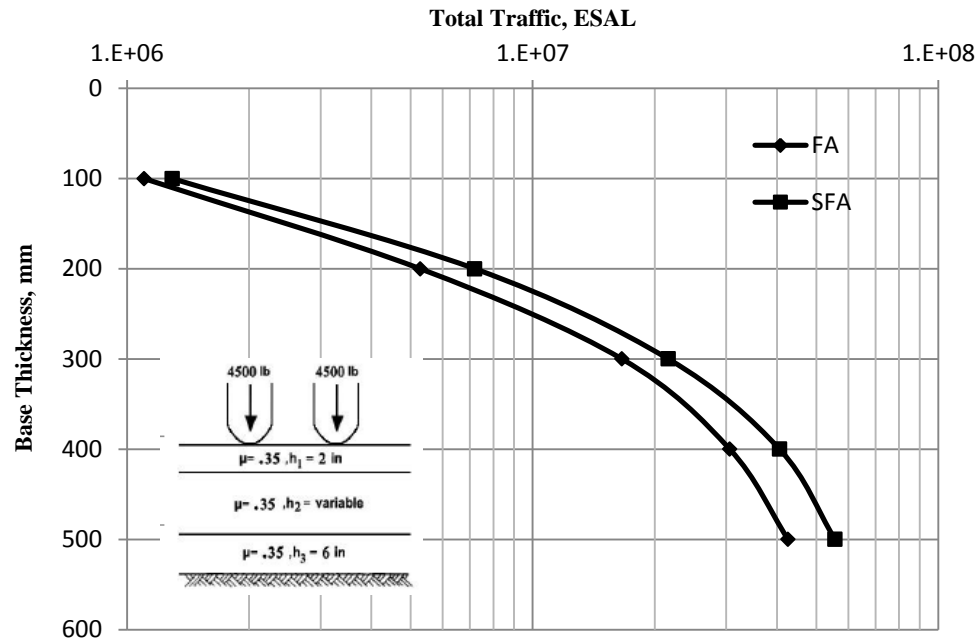


Figure 5-19: Relationship between Sabkha-Foamed Asphalt Base Thickness and Total Traffic-Case 3.

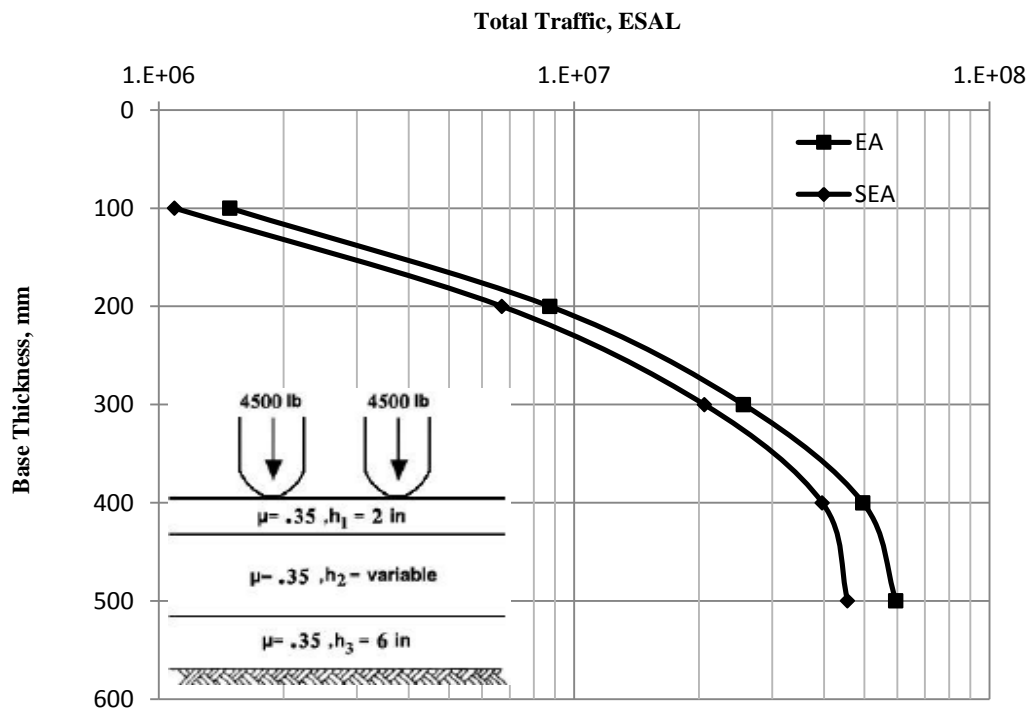


Figure 5-20: Relationship between Marl-Emulsified Asphalt Base Thickness and Total Traffic-Case 3.

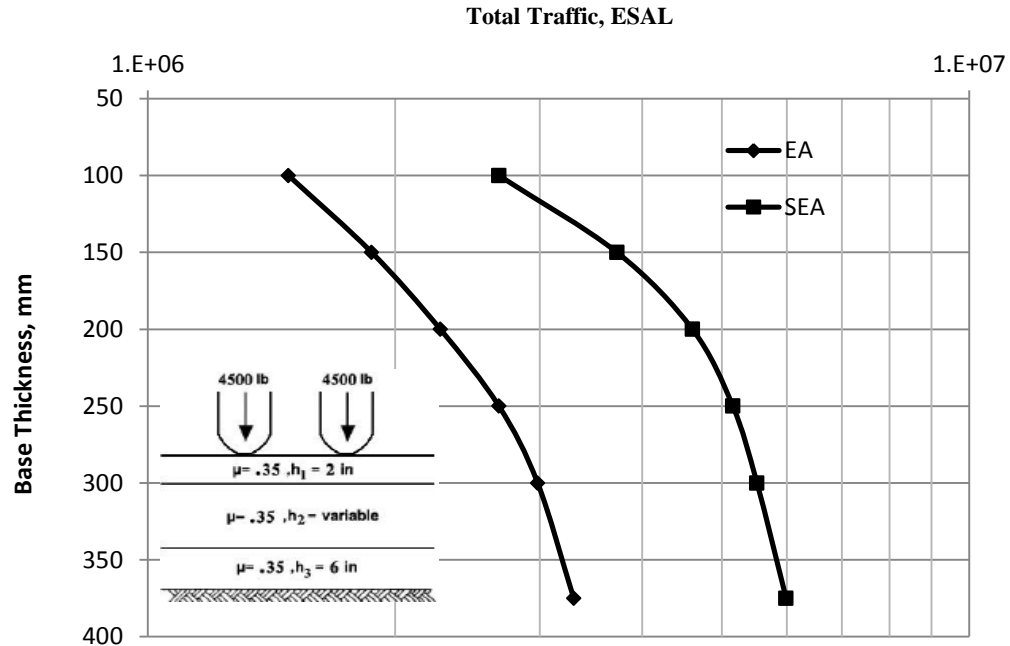


Figure 5-21: Relationship between Sabkha-Emulsified Asphalt Base Thickness and Total Traffic-Case 3.

### 5.3.2 Work Results Limitations

It is known that, many types of marl, sabkha and sand soils are available and each type has its own characteristic and engineering behavior depending on their physical and mechanical properties. Thus, it is worth mentioning that, the developed rutting prediction models and the pavement thickness design charts constructed for the cases analyzed in this study are restricted to the soils types whose characterizations and engineering properties are presented in Chapter 4 of this report.

## **CHAPTER 6**

# **SUMMARY, CONCLUSIONS AND RECOMMENDATIONS**

### **6.1 Summary**

This study was design to treat three eastern Saudi soils, namely marl, sabkha and dune sand. The potentiality of producing and using new asphaltic materials that are foam sulfur asphalt (SFA) and emulsion sulfur asphalt (SEA) in improving and enhancing the mechanical properties of these soils were investigated and compared with the conventional foam and emulsion asphalt (FA and EA) mixes.

Characterization of the investigated soils was performed including specific gravity, Atterberg limits, grain-size distribution and mineralogical composition. The optimum moisture content corresponding to the maximum dry density of the investigated soils was determined using modified Proctor compaction test. Soaked California bearing ratio (CBR) test was conducted on marl and sand specimens soaked in normal water, whereas, sabkha specimens were soaked in sabkha brine.

The evaluation of the mechanical properties of the conventional and improved mixes was performed by conducting Marshall stability, indirect tensile strength, durability, resilient modulus and static and dynamic triaxial test. Micro-characterization study using XRD and/or SEM devices were utilized to depict qualitatively the

mechanisms of improvement of some investigated soils mixes. Statistical analysis was also performed to test the significance of improvement in the mechanical properties under the effect of many factors. In addition to that, regression models were developed for predicting the mechanical properties such as, shear strength, resilient modulus and permanent deformation properties. The permanent deformation of the investigated conventional and modified mixes was also assessed by conducting dynamic triaxial and wheel tracking tests. Thereafter, the models of rutting prediction were developed and calibrated to the wheel tracking results and the pavement thickness design charts were constructed based on the calibrated models.

## **6.2 Conclusions**

Based on the analysis and interpretation of the results presented in this study, the following main conclusions could be drawn:

- Foamed sulfur asphalt (SFA) mixes were found to have higher stability than conventional foamed asphalt (FA) mixes and satisfied the requirement recommended by Asphalt Institute. On the other hand, emulsified sulfur asphalt were found to reduce the stability compared with standard emulsified asphalt, however, they still satisfied the Asphalt Institute requirements.
- SFA showed a significant effect on the ITS for marl and sand soils, while, in sabkha soil an insignificant effect was observed compared with FA.
- SEA increased ITS for marl and sabkha soils, while the inverse is true for sand soil. However, the increase in ITS was marginal.

- Results of ITS for FA, SFA, EA and SEA mixes, except dune sand mixes, satisfied the specifications assigned by SABITA [1998].
- SFA and SEA enhanced the durability of mixes against water damage effects and the stability loss was lower than conventional FA and EA mixes.
- SFA has a significant effect on shear strength (particularly cohesion) of the investigated soils. On the other hand, SEA reduced the shear strength of the soils mixes.
- The resilient moduli of SFA mixes are slightly less than FA mixes. However, the resilient moduli of SEA mixes are slightly higher than EA mixes.
- The resilient moduli for all mixes were found to increase with the increase in deviator stress and were slightly affected by the temperature increase which indicated that sulfur modified asphalt (SFA and SEA) mixes performed well at high temperature than conventional mixes (FA and EA).
- SFA mixes showed superior rutting resistance compared with FA mixes.
- SEA was found to increase the permanent deformation susceptibility of the soils mixes especially at 22 °C.
- Permanent deformation prediction models were developed for the investigated mixes at 22 °C and 40 °C .
- The developed models were calibrated with the wheel tracking test results at 22 °C and then the pavement thickness design charts were constructed for design purposes.

- VESYS 5W program is suitable to predict the rut depth since it can predict the layer rut depth and the total rut depth of the pavement structure with a reasonable degree of accuracy.

### **6.3 Recommendations**

- Among all investigated soils, marl treated with FA, SFA, EA or SEA has a superior resistance to permanent deformation and can be used for heavy traffic roads.
- Sabkha soil treated with FA and SFA also showed a high rutting resistance and can be used for medium to high traffic roads, whereas, sabkha treated with EA and SEA showed rutting susceptibility and can only be used for low to medium traffic roads.
- Dune sand treated with FA, SFA, EA and SEA are very sensitive to permanent deformation and showed a higher rutting, thus, it can only be used for light traffic roads such as agricultural roads.
- Modified foamed and emulsified sulfur asphalt mixes should be introduced in Saudi road specification as construction materials.

### **6.4 Future Research**

- Reinforce dune sand with the suitable percentage of marl soil and investigate the mechanical properties and permanent deformation susceptibility of the blend mixed with FA, SFA, EA and SEA.
- Construct 200 m test section with SFA or SEA treated marl base/subbase layer and monitor its performance in collaboration with Ministry of Transport (MOT).

## REFERENCES

- Abdullah, Gamil M. S. "Stabilization of Eastern Saudi Soils Using Heavy Fuel Oil Fly Ash and Cement Kiln Dus," *MSc Thesis, King Fahd University of Petroleum and Minerals*, Dhahran, Saudi Arabia, 2009.
- Aiban, S.A., Al-Abdul Wahhab; H. and Al-Amoudi, O.S.B. (1995), "Cement Stabilized Marl; Field Trial in Dammam. Area" , unpublished work.
- Aiban, S., Al-Abdul Wahhab, H. and Al-Amoudi, O. "Identification, Evaluation and Improvement of Eastern Saudi Soils for Constructional Purposes," *Final Report Submitted to KACST*, September, 1999.
- Aiban, S. A., Al-Amoudi, O.S.B., Ahmed, H. R. and Al-Abdul Wahhab, H. I. "Characterization and Stabilization of Eastern Saudi Calcareous Soils," *Proceedings of the Fourteenth International Conference on Soil Mechanics and Foundation Engineering*, Hamburg, pp. 13-16, 6-12 September, 1997.
- Al-Abdul Wahhab, H. I."Evaluation of Emulsified Asphalt for Use in Saudi Arabia,"*PhD. Dissertaion, Oregon State University*, 1985.
- Al-Abdul Wahhab, H. I."Evaluation of Emulsified Asphalt for Road Construction & Maintenance in Saudi Arabia," *Arabian Symposium on Roads Pavement Design Technology*, Amman, Jordan, 2-5 July, 1992.
- Al-Abdul Wahhab, H. I. and Abduljauwad, S. N.,(1989),"Study of Soil Satbilization in the Eastern Province of Saudi Arabia," *Proceedings of the 11<sup>th</sup> IRF World Meeting*, Seoul, Korea, , Vol.III, pp. 117-120,16-21 April 1989.
- Al-Abdul Wahhab, H. I., Ahmad, I., Aiban, S. A., and Al-Amoudi, O.S.B. " Stabilization of Al-Aziziyah (Eastern Saudi Arabia) Sabkha Soil," *Third Gulf Conference on Roads*, Muscat in March 6-8, 2006.
- Al-Abdul Wahhab, H. I. and Asi, I. M." Stabilization of a Saudi Sabkha Soil with Liquid Asphalts," *Proceeding of the First World Congress on Emulsion*, Paris, October 19-22, 1993.
- Al-Abdul Wahhab, H. I. and Asi, I. M."Stabilization of Eastern Saudi Marl and Dune Sand for Construction Purposes."The Fourth Saudi Engineering Conference, volume II, pp. 347-352, Nov., 1995.
- Al-Abdul Wahhab, H. I., Asi, I.M., and Al-Amoudi, O.S.B."Investigation on Stabilization of a Saudi Sabkha Soil," *Proceeding of the Second Geotechnical Engineering Conference*, Cairo Univ.,Vol. I, pp. 500-511, January 10-13, 1994.



- Al-Abdul Wahhab, H. I. and Baig, M. G. "Evaluation of Sulfur-Asphalt Technology for Local Applications." Evaluation of Foamed Asphalt for Road base Stabilization". Proceeding of 7th Saudi Engineering Conference, Riyadh, Saudi Arabia, Dec, 2007.
- Al-Abdul Wahhab, H. I., Baig, M. G., Mahmoud, I. A., and Kattan, H.M." Study of Road Bases Construction in Saudi Arabia Using Foam Asphalt" *Construction and Building Materials*; Vol. 26, pp. 113–121, 2012.
- Al-Abdul Wahhab, H. I., Baig, M. G., Mahmoud, I. A., and Kattan, H.M." Evaluation of Foamed Asphalt for Road base Stabilization". *Proceeding of 7th Saudi Engineering Conference*, Dec, 2007., Riyadh, Saudi Arabia.
- Al-Abdul Wahhab, H. I. and Hicks, R.G."Evaluation of Emulsified Asphalt Treated Mixes," Proceeding of the 3rd IRF Regional Conference, Riyadh, February, Vol.3, pp. 159-174, 1988.
- Al-Aghbari, M.Y. and Dutta, R.K."Effect of Cement and Cement By-Pass Dust on the Engineering Properties of Sand." *An International Conference on Geotechnical Engineering*, Vol.2, pp.425-431, 2008.
- Al-Amoudi, O.S.B." Usage of Cement Kiln Dust for the Stabilization of Eastern Saudi Soils." *An International Conference on Geotechnical Engineering* 11-13 December 2006, Singapore.
- Al-Amoudi, O.S.B., Abduljawwad, S.N., EI-Naggar, Z.R. and Rasheeduzzafar (1992a), "Response of Sabkha to Laboratory Tests: A Case Study, *Engineering Geology*, Vol. 33, pp.111-125.
- Al-Amoudi, O.S.B., Khan, K. and Al-Kahtani, N. S., "Stabilization of a Saudi Calcareous Marl Soil", *Construction and Building Materials*, Vol. 24, pp. 1848–1854, 2010.
- Al-Halhouli, A. A." Evaluation of Emulsified Asphalt Treated Sand for Road Bases" M.S thesis, *University of King Fahd University of Petroleum and Minerals*, 1986.
- Al-Khashab, N.M., and Al-Hayalee, T.M." Stabilization of Expansive Clayey Soil Modified by Lime with an Emulsified Asphalt Addition," *Eng. & Technology*, Vol.26 No.10, 2008.
- Arabiyat, T. S."Strength of Asphalt Emulsion Treated Marl for Road Bases" M.S thesis, *University of King Fahd University of Petroleum and Minerals*, 1985.
- Asi I.M." Stabilization of Sabkha Soil Using Foamed Asphalt Technology," *Journal of Materials in Civil Engineering*, Vol. 13, No. 5, September/October, 2001.

- Asi, I.M. and Al-Abdul Wahhab, H.I.”Stabilization of Eastern Saudi Marl and Dune Sand for Construction Purposes,” *Proceedings of the 4<sup>th</sup> Saudi Engineering Conference, KAU*, Vol.II, pp. 347-352, 5-8 November 1995.
- Asi I.M., Al-Abdul Wahhab H.I., Al-Amoudi O.S.B., and Siddiqui Z.U. Stabilization of dune sand using foamed asphalt. *Geotech Test J, ASTM* , Vol. 25, pp. 168-176, 2002.
- Asi I.M, Al-Abdul Wahhab H.I., Khan M.I., and Siddiqui Z.U.” Stabilization of Dune Sand for Base and Sub-base Applications Utilizing Foamed Asphalt Technology,” In: *1<sup>st</sup> international conference performance of roads, bridges and airport pavements in hot climates*, Dubai; April 28–29, 1998.
- Asi .I.M., Siddiqui Z.U., Al-Abdul Wahhab H.I., and Khan M.I.(1999),”. Stabilization of Sabkha Soil for Road Bases Using Foamed Asphalt Technology,” In: *Fifth Saudi engineering conference*; March, 1999.
- Asphalt Emulsion Manufacturers Association (AEMA), “A Basic Asphalt Emulsion Manual”, Manual Series (MS) No. 19, 2004.
- Asphalt Institute”State-of-Knowledge on the use of Sulfur-Extended Asphalt (SEA),”December, 2007.
- Baig, M. G., Al-Abdul Wahhab, H. I., Isam A . M., Al-Mehthel M., Al-Idi S.F., and Grosch, J.” Investigation of sulfur modified asphalt concrete mixes for road construction in the gulf.” *Efficient Transportation and Pavement Systems – Al-Qadi, Sayed, Alnuaimi & Masad (eds)*© 2009 Taylor & Francis Group, London, ISBN 978-0-415-48979-9.
- Barengberg, E.J. and M.R. Thompson.”Calibrated Mechanistic Structural Analysis Procedures for Pavements Phase 1 & II of NCHRP Project 1-26. National Cooperative Highway Research Program”. Transportation Research Board. Washington, DC, 1990.
- Beatty, T.L., Dunn, K., Harrigan, E.T., Stuart, K., and Weber, H.”Field Evaluation of Sulfur-Extended Asphalt Pavements” *Transportation Research Record* 1115, *Transportation Research Board*, Washington, DC, 1987.
- Behzadi, G. and Yandell, W.O.”Determination of Elastic and Plastic Subgrade Soil Parameters for Asphalt Cracking and Rutting Prediction.” *Transp. Res. Rec. 1540*, *Transportation Research Board*, Washington, D.C.,pp. 97-104, 1996.
- Brady, N. C. and Weil, R. R.” Elements of the Nature and Properties of Soils”, *3<sup>rd</sup> edition*, *Pearson Prentice Hall*, 2010.

- Brown E. R., Foo K. Y., *Evaluation of Variability in Resilient Modulus Test Results* (ASTM D 4123-82. NCAT Report No. 91-6, 1989.
- Bunga, E., Pallu, H.M.S, Selintung, M., and Thaha, M.A.” Stabilization of Sandy Clay Loam with Emulsified Asphalt.” *International Journal of Civil & Environmental Engineering IJCEE-IJENS* Vol: 11 No: 05, 2011 .
- Celard, B.” Sulfur Addition to Asphalt Paving Mixes.” *Eurobitume Seminar*. London, p. 318 ( 1978).
- Christopher, B. R., Schwartz, C., and Boudreau, R. “Geotechnical Aspects of Pavements,” *US Department of Transportation Publication No. FHWA NHI-05-037*. 2006
- Coklin, A. R., "Introduction to Soil Chemistry, Analysis and Instrumentation", *A John Wiley & Sons, Inc, Publication*, 2005.
- Cooper, S. B., Elseifi, M. A., Mohammad, L. N., and Hassan, M. “Performance and Cost Effectiveness of Sustainable Technologies in Flexible Pavements Using the Mechanistic-Empirical Pavement Design Guide.” *90<sup>th</sup> Transportation Research Board Annual Meeting, Transportation Research Board*, Washington, DC, 2011.
- Cooper, S. B., Mohammad L. N., and Elseifi, M.A.” Laboratory Performance Characteristics of Sulfur-Modified Warm-Mix Asphalt,” *Journal of Materials in Civil Engineering* © ASCE / September, 2011.
- Diylajee, V.A., and Raymond, G.P. “Repetitive Load Deformation of Cohesionless Soil,” *J.Geotech. Engrg. Div., ASCE*, 108(10), pp.1215-1229, 1982.
- Focus. Foamed asphalt – A Success on Federal Lands Highway. *US Department of Transportation, FHWA*; August 2003.
- Garba, R. “Permanent Deformation Properties of Asphalt Concrete Mixtures, PhD Thesis, *Norwegian University of Science and Technology*”, 2002.
- Gautam, B., Yuan, D., Abdallah, I., and Nazarian, S.” Guidelines for Using Local Materials for Roadway Base and Subbase,” *Research Report 0-5562-1, Center for Transportation Infrastructure Systems, The University of Texas at El Paso, El Paso, TX*, 2009.
- Gawel, I.” Sulphur-Modified Asphalts. In *Asphaltenes and Asphalts*; Yen, T. F.; Chilingarian, G. V., Eds.; Developments in Petroleum Science 40B; Elsevier Science B. V.: Amsterdam, The Netherlands, 2000; Vol. 2, Chapter 19.

- Hausmann, M. R. "Engineering principles of Ground Modification," *McGraw Hill Publishing Company*, 1990.
- He, Gui-ping and Wong, Wing-gun "Decay Properties of the Foamed Bitumens." *Construction and Building Materials* Vol. 20, PP: 866–877 (2006).
- Hornych, P., and El Abd, A. "Selection and Evaluation of Models for Prediction of Permanent Deformation of Unbound Granular Materials in Road Pavements", Work Package 5, Performance-based Specifications, Sustainable and Advanced Materials for Road Infrastructure (SAMARIS), Competitive and Sustainable Growth (GROWTH) Programme, 2004.
- [http://en.wikipedia.org/wiki/Asphalt\\_concrete](http://en.wikipedia.org/wiki/Asphalt_concrete)
- <http://www.fhwa.dot.gov/engineering/geotech/pubs/05037/07d.cfm>
- Huan, Y., Siripun, K., Jitsangiam, P., and Nikraz, H. "A Preliminary Study on Foamed Bitumen Stabilisation for Western Australian pavements." *Scientific Research and Essays* Vol. 5(23), pp. 3687-3700, 4 December, 2010.
- Hu, S., Zhou, FJ, and Scullion, T. "Development, Calibration, and Validation of a New M-E Rutting Model for HMA Overlay Design and Analysis", *Journal of Materials in Civil Engineering*; Vol. 23(2):pp.89–99, 2011
- Hussain, J., Wilson, D. J., Henning, T. F., and Alabaster, D. "Comparing Results Between the Repeated Load Triaxial Test and Accelerated Pavement Test on Unbound Aggregate". *Journal of Materials in Civil Engineering*, 2013.
- James, A. "Overview of Asphalt Emulsion." *Transportation Research Circular E-C102: Asphalt Emulsion Technology*, 2006.
- Kavussi, A., and Modarres, A. "Laboratory Fatigue Models for Recycled Mixes with Bitumen Emulsion and Cement." *Construction and Building Materials* Vol. 24, pp. 1920–1927, 2010.
- Kendall, M., Baker, B., Evans, P., and Ramanujan, J. "Foamed Bitumen Stabilization: The Queensland Experience," *20<sup>th</sup> Australian Road Research Conference*, March 2001.
- Kenis W.J. "Predictive Design Procedures, VESYS Users Manual, An Interim Design Method for Flexible Pavements Using the VESYS Structural Subsystem," *Final Report FHWA-RD-77-154, Federal Highway Administration*, Washington, D.C, 1977.

- Kennepohl, G.J., Logan, A. and Bean, D.C.”Conventional Paving Mixes with Sulfur-Asphalt Binders.” *Proc. Assoc. Asphalt Paving Technol.*, 44: 485, 1975.
- KFUPM.”Accelerated Testing Comparison of SAES-Q-006 Foam Asphalt and Aggregate/ Hot Asphalt Mix Asphalt Pavement Sections,” *Final Report Submitted to Saudi Aramco*, December, 2005.
- KFUPM.”Evaluation of the Potential of Using Sulfur Asphalt in Saudi Roads,” *Sixth Progress Report, Submitted to Saudi Aramco*, November, 2008.
- Khedr, S.A.”Deformation mechanism in asphaltic concrete.” *J. Transp. Engrg.* , ASCE,112(1), 29, 1986.
- Kowalski, T.E., and Starry, D.W.”Modern Soil Stabilization Techniques,” Presentation Paper at The *2007 Annual Conference of the Transportation Association of Canada Saskatoon*.
- Lee, D.Y.” Treating Marginal Aggregates and Soils with Foamed Bitumen,” *Proceedings, Association of Asphalt Paving Technologists*, vol.50, p.211, 1981.
- Lekarp F., Isacsson U., Dawson A. “State of the art – II : Permanent strain response of unbound aggregates”, *Journal of Transportation Engineering ASCE*, vol. 126, No.1, pp 76-83, 2000.
- Lewandowski, L.H.”Polymer Modification of Paving Asphalt Binders,” *Rubber Chemistry and Technology*, Volume 67, PP435- 447.1994.
- Li, P., and Liu, J. Characterization of Asphalt Treated Base Course Material (*No. FHWA-AK-RD-10-07*), 2010.
- Mahoney, J.P., Lary J.A., Balgunaim, F. and Lee, T.C., “Sulfur Extended Asphalt Laboratory Investigation, Mixture Characterization”, *Washington State Department of Transportation, Final Report WA-RD 53.2*, June 1982.
- Majidzadeh, K, S. Khedr, and H. Guirguis. “Implementation of a Pavement Design System”, volume 1 and 2 of the *final report. Research project EES 579. Ohio State Univeristy*. Columbus, OH,1981.
- Masegosa, R.M., Canamero, P., Cabezudo, M.S., Vinas, T., Salom, C., Prolongo, M.G. and Paez, M. A., "Thermal Behaviour of Bitumen Modified by Sulphur Addition", *5th Eurasphalt Eurobitume Congress*, 13-15th June 2012, Istanbul.
- McCarthy, J. E.”Soil Stabilization for Pavement.”*Department of the Army and Air Force. TM 5-822-14/AFJMAN 32-1019*, 5-9, 2005.

- Ministry of Public Works Republic of Indonesia."Paving Specifications Utilizing Bitumen Emulsions", Jakarta, 1990.
- Monismith, C.L."Rutting Prediction in Asphalt Concrete Pavements." Transp. Res. Rec. 616, *Transportation Research Board*, Washington, D.C., 2-8., 1976.
- Moore, R. K."Factors Affecting Unconfined Compressive Strength of Lime-Bituminous-Emulsion-Treated Clay," *Transportation Research Board*, TRP No. 843, pp. 85-88, 1982.
- Muthen, K.M."Foamed Asphalt Mixes Mix Design Procedure," *Contract Report CR-98/077*, Dec. 1998a *SABITA Ltd & CSIR Transportek* <http://foamasph.csir.co.za:81/>
- Muthen, K.M."Foamed Asphalt Mix Design Procedure," *Technical Report CSIR Transportek & SABITA Ltd.*, South Africa, 1998b.
- Oruc, S., Celik, F. and Akpinar, M. V."Effect of Cement on Emulsified Asphalt Mixtures." *Journal of Materials Engineering and Performance*, Vol. 16, pp. 578-583, 2007.
- Ramadhan, R. H."prediction of pavement rutting from laboratory characterization tests".MS thesis, *King Fahd University of Petroleum and Minerals*, 1988.
- Roberts, F. L., Engelbrecht, J. C., and Kennedy, T. W. "Evaluation of recycled mixtures using foamed asphalt." *Transportation Research Record 968*, Transportation Research Board, Washington, DC, 78-85,1984.
- SABITA Ltd. and CSIR Transportek. Foamed Asphalt Mixes: Mix Design Procedure. Contract Report CR-98/Draft; February 1998.
- Soter International."Foamed Asphalt Technology Transfer to the Kingdom of Saudi Arabia," Preliminary Proposal, Canada, 1994.
- Sreekrishnavilasam, A., Rahardja, S., Kmetz, R. and Santagata, M."Soil Treatment Using Fresh and Landfilled Cement Kiln Dust," *Construction and Building Materials*, Vol.21, pp. 318-327, 2007.
- Stephen, P., Yusu M., and Leslie, M. McCarthy., " Evaluation and Modeling of Repeated Load Test Data of Asphalt Concrete for Mechanistic-Empirical Pavement Design", *Journal of Materials in Civil Engineering, ASCE*, pp 993-999, Vol. 19, No. 11, November 2007.
- Strategic Highway Research Program, SHRP-A-404, "Fatigue Response of Asphalt-Aggregate Mixes", *National Research Council*, Washington DC, 1994.

- Strickland, D., Colange, J., Martin, M., and Deme, I. "Performance Properties of Sulphur Extended Asphalt Mixtures with Modified Sulphur Pellets," *Int. Society for Asphalt Pavements*, Lino Lakes, MN, 2008.
- Stuart, K.D. "Performance Evaluation of Sulfur-Extended Asphalt Pavements-Laboratory Evaluation. *Final Report*," *FHWA Report FHWA-RD-90-110*, *Federal Highway Administration*, Washington, DC, 1990.
- Sullivan, B. "Development of Flow Number and Flow Time Candidate Simple Performance Test for Asphalt Mixtures", MS Thesis. *Department of Civil and Environmental Engineering*, *Arizona State University*, Tempe 2002.
- Terrel, R. L., Epps, J. A., Barenberg, E.J., Mitchell, J. K. and Thompson, M. R. "Soil Stabilization in Pavement Structures- a user's manual, vol. I & II "Mixture Design Consideration", *Prepared for the Federal Highway Administration, Department*, Washington D.C. 20590, USA, Contract No. Dot-FH-11-9406, 1984.
- Thanaya, I. N. A. "Improving the performance of cold bituminous emulsion mixtures (CBEMs): incorporating waste". Ph.D thesis, *University of Leeds*, 2003.
- Timm, D., Tran, N., Taylor, A., Robbins, M., and Powell, B. "Evaluation of Mixture Performance and Structural Capacity of Pavements using Shell Thiopave, Phase I: Mix Design, Laboratory Performance Evaluation and Structural Pavement Analysis and Design." *NCAT Rep. 09-05*, *National Center for Asphalt Technology*, Auburn, AL, 2009.
- Tirado, C., Qing, Y., Carrasco, C., Nazarian, S., Osegueda, R. "A GIS Based Algorithm for Estimating Damage due to Superheavy Loads" *Report FHWA/TX-05/9-1502-01-6*, *Center for Transportation Infrastructure Systems, The University of Texas at El Paso*, El Paso, Texas, March 2006.
- Unified Facilities Criteria" Soil Stabilization for Pavement." *Department of the Army and Air Force. UFC 3-250-11*, 16 January 2004, TM 5-822-14/AFJMAN 32-1019.
- Vuong, B., and Armstrong, P. "Repeated load Triaxial testing on the Subgrade from Mulgrace ALF site," *Australian Road Research Board*, 1991.
- Wirtgen G. Cold recycling manual. 2nd ed. Germany: Windhaven; 2004. ISBN 3-00-936215-05-7.
- Xiao, F., Punith. V.S., Putman, B., and Amirkhanian, Serji N. "Utilization of Foaming Technology in Warm-Mix-Asphalt Mixtures Containing Moist Aggregates." *Journal of Materials in Civil Engineering* © ASCE / September, 2011.

Zaitsev, J.W. "Fatigue Response of Asphalt-Aggregate", Report SHRP-A-404, *National Research Council*, 1994.

Zhou, F., and Scullion, T." VESYS5 Rutting Model Calibrations with Local Accelerated Pavement Test Data and Associated Implementation," Report No. *FHWA/TX-03/9-1502-01-2*, *Texas Transportation Institute, College Station, TX*, 2002.

Zhou F. and Scullion T."Asphalt Pavement Performance Analysis Tool:VESYS5W," Report 9-1502-01-5, *Texas Transportation Institute, College Station, TX*, 2005.



## APPENDIX A

### MINITAB PRINTOUT OF RESULTS ANALYSIS OF VARIANCE (ANOVA)

#### 1) Foamed Asphalt Mixes

##### Minitab ANOVA Printout: Marl Soil

##### Two-way ANOVA: Dry ITS versus Type of additive, % Residual Asphalt

Source	DF	SS	MS	F	P
Type of additives	1	17228	17228.0	13.29	0.022
% Residual Asphalt	4	197094	49273.6	38.00	0.002
Error	4	5186	1296.6		
Total	9	219509			

S = 36.01    R-Sq = 97.64%    R-Sq(adj) = 94.68%

##### Two-way ANOVA: Soaked ITS versus Type of additive, % Residual Asphalt

Source	DF	SS	MS	F	P
Type of additives	1	17831	17831.2	28.95	0.006
% Residual Asphalt	4	154863	38715.9	62.85	0.001
Error	4	2464	616.0		
Total	9	175159			

S = 24.82    R-Sq = 98.59%    R-Sq(adj) = 96.83%

##### Two-way ANOVA: Dry Stability versus Add. Type, Res. %

Source	DF	SS	MS	F	P
Add. Type	1	24.000	24.0000	48.00	0.020
Res. %	2	134.333	67.1667	134.33	0.007
Error	2	1.000	0.5000		
Total	5	159.333			

S = 0.7071    R-Sq = 99.37%    R-Sq(adj) = 98.43%

##### Two-way ANOVA: Soaked Stability versus Add. Type, Res. %

Source	DF	SS	MS	F	P
Add. Type	1	16.667	16.6667	0.27	0.652
Res. %	2	37.333	18.6667	0.31	0.765
Error	2	121.333	60.6667		
Total	5	175.333			

S = 7.789    R-Sq = 30.80%    R-Sq(adj) = 0.00%

##### General Linear Model: $M_R$ versus Temp., Type of Additive, ...

Factor	Type	Levels	Values
Temp.	fixed	2	1, 2
Type of Additive	fixed	2	1, 2

Confining Pressure	fixed	5	1, 2, 3, 4, 5
Dev. Stress	fixed	5	1, 2, 3, 4, 5

Analysis of Variance for  $M_R$ , using Adjusted SS for Tests

Source	DF	Seq SS	Adj SS	Adj MS	F	P
Temp.	1	104395	104395	104395	9.60	0.003
Type of Additive	1	339150	339150	339150	31.18	0.000
Confining Pressure	4	2954991	1146808	286702	26.36	0.000
Dev. Stress	4	5271593	5271593	1317898	121.16	0.000
Error	65	707016	707016	10877		
Total	75	9377145				

S = 104.294    R-Sq = 92.46%    R-Sq(adj) = 91.30%

### Minitab ANOVA Printout: Sabkha Soil

#### Two-way ANOVA: Dry ITS versus Type of additives, % Residual Asphalt

Source	DF	SS	MS	F	P
Type of additives	1	15966.0	15966.0	61.53	0.001
% Residual Asphalt	4	65667.1	16416.8	63.26	0.001
Error	4	1038.0	259.5		
Total	9	82671.1			

S = 16.11    R-Sq = 98.74%    R-Sq(adj) = 97.17%

#### Two-way ANOVA: Soaked ITS versus Type of additives, % Residual Asphalt

Source	DF	SS	MS	F	P
Type of additives	1	4243.6	4243.60	36.16	0.004
% Residual Asphalt	4	36664.9	9166.21	78.11	0.000
Error	4	469.4	117.35		
Total	9	41377.9			

S = 10.83    R-Sq = 98.87%    R-Sq(adj) = 97.45%

#### Two-way ANOVA: Dry Stability versus Add. Type, Res. %

Source	DF	SS	MS	F	P
Add. Type	1	0.0400	0.0400	0.00	0.972
Res. %	2	12.9360	6.4680	0.25	0.799
Error	2	51.5760	25.7880		
Total	5	64.5521			

S = 5.078    R-Sq = 20.10%    R-Sq(adj) = 0.00%

### Two-way ANOVA: Soaked Stability versus Add. Type, Res.%

Source	DF	SS	MS	F	P
Add. Type	1	0.1350	0.13500	0.02	0.910
Res. %	2	16.6606	8.33032	1.00	0.499
Error	2	16.6159	8.30795		
Total	5	33.4115			

S = 2.882    R-Sq = 50.27%    R-Sq(adj) = 0.00%

### General Linear Model: $M_R$ versus Temp., Type of Additive, ...

Factor	Type	Levels	Values
Temp.	fixed	2	1, 2
Type of Additive	fixed	2	1, 2
Confining Pressure	fixed	5	1, 2, 3, 4, 5
Dev. Stress	fixed	5	1, 2, 3, 4, 5

Analysis of Variance for  $M_R$ , using Adjusted SS for Tests

Source	DF	Seq SS	Adj SS	Adj MS	F	P
Temp.	1	90976	90976	90976	10.32	0.002
Type of Additive	1	267297	267297	267297	30.32	0.000
Confining Pressure	4	2731867	1067694	266923	30.27	0.000
Dev. Stress	4	4607476	4607476	1151869	130.64	0.000
Error	65	573117	573117	8817		
Total	75	8270733				

S = 93.8999    R-Sq = 93.07%    R-Sq(adj) = 92.00%

### Minitab ANOVA Printout: Sand Soil

#### Two-way ANOVA: Dry ITS versus Type of additives, % Residual Asphalt

Source	DF	SS	MS	F	P
Type of additives	1	128.14	128.135	9.23	0.038
% Residual Asphalt	4	2370.02	592.504	42.68	0.002
Error	4	55.53	13.884		
Total	9	2553.69			

S = 3.726    R-Sq = 97.83%    R-Sq(adj) = 95.11%

#### Two-way ANOVA: Soaked ITS versus Type of additives, % Residual Asphalt

Source	DF	SS	MS	F	P
Type of additives	1	171.48	171.480	52.91	0.002
% Residual Asphalt	4	1024.79	256.197	79.05	0.000
Error	4	12.96	3.241		
Total	9	1209.23			

S = 1.800    R-Sq = 98.93%    R-Sq(adj) = 97.59%

### Two-way ANOVA: Dry Stability versus Add. Type, Res. %

Source	DF	SS	MS	F	P
Add. Type	1	0.04167	0.04167	0.02	0.892
Res. %	2	5.29000	2.64500	1.50	0.400
Error	2	3.52333	1.76167		
Total	5	8.85500			

S = 1.327    R-Sq = 60.21%    R-Sq(adj) = 0.53%

### Two-way ANOVA: Soaked Stability versus Add. Type, Res. %

Source	DF	SS	MS	F	P
Add. Type	1	0.10667	0.10667	0.05	0.850
Res. %	2	0.72333	0.36167	0.16	0.865
Error	2	4.62333	2.31167		
Total	5	5.45333			

S = 1.520    R-Sq = 15.22%    R-Sq(adj) = 0.00%

### General Linear Model: $M_R$ versus Temp., Type of Additive, ...

Factor	Type	Levels	Values
Temp.	fixed	2	1, 2
Type of Additive	fixed	2	1, 2
Confining Pressure	fixed	5	1, 2, 3, 4, 5
Dev. Stress	fixed	5	1, 2, 3, 4, 5

Analysis of Variance for  $M_R$ , using Adjusted SS for Tests

Source	DF	Seq SS	Adj SS	Adj MS	F	P
Temp.	1	51158	51158	51158	7.33	0.009
Type of Additive	1	124339	124339	124339	17.81	0.000
Confining Pressure	4	2813944	1192499	298125	42.71	0.000
Dev. Stress	4	4511865	4511865	1127966	161.59	0.000
Error	65	453730	453730	6980		
Total	75	7955036				

S = 83.5491    R-Sq = 94.30%    R-Sq(adj) = 93.42%

## 2) Emulsified Asphalt Mixes

### Minitab ANOVA Printout: Marl Soil

#### Two-way ANOVA: Dry ITS versus Type of additives, % Residual Asphalt

Source	DF	SS	MS	F	P
Type of additives	1	1570	1570.4	3.84	0.107
% Residual Asphalt	5	295635	59127.0	144.49	0.000
Error	5	2046	409.2		
Total	11	299251			

S = 20.23    R-Sq = 99.32%    R-Sq(adj) = 98.50%

#### Two-way ANOVA: Dry Marshal Stability versus Type of additives; % Residual Asphalt

Source	DF	SS	MS	F	P
Type of additives	1	369.835	369.835	372.23	0.000
% Residual Asphalt	5	322.117	64.423	64.84	0.000
Error	5	4.968	0.994		
Total	11	696.920			

S = 0.9968    R-Sq = 99.29%    R-Sq(adj) = 98.43%

#### Two-way ANOVA: Soaked Marshal Stability versus Type of additives, % Residual Asphalt

Source	DF	SS	MS	F	P
Type of additives	1	301.277	301.277	96.25	0.001
% Residual Asphalt	4	241.785	60.446	19.31	0.007
Error	4	12.521	3.130		
Total	9	555.583			

S = 1.769    R-Sq = 97.75%    R-Sq(adj) = 94.93%

#### General Linear Model: $M_R$ versus Temp., TYPE OF ADD, Confining Pr., DEV.

Factor	Type	Levels	Values
Temp.	fixed	2	1, 2
TYPE OF ADD	fixed	2	1, 2
Confining Pressure	fixed	5	1, 2, 3, 4, 5
DEV	fixed	5	1, 2, 3, 4, 5

Analysis of Variance for  $M_R$ , using Adjusted SS for Tests

Source	DF	Seq SS	Adj SS	Adj MS	F	P
Temp.	1	34690	34690	34690	4.18	0.045
TYPE OF ADD	1	4440	4440	4440	0.54	0.467
Confining Pressure	4	3037049	1204065	301016	36.30	0.000
DEV	4	5540866	5540866	1385216	167.04	0.000
Error	65	539021	539021	8293		
Total	75	9156066				

S = 91.0639    R-Sq = 94.11%    R-Sq(adj) = 93.21%

### Minitab ANOVA Printout: Sabkha Soil

#### Two-way ANOVA: Dry ITS versus Type of additives, % Residual Asphalt

Source	DF	SS	MS	F	P
Type of additives	1	2646.3	2646.26	12.55	0.024
% Residual Asphalt	4	21984.9	5496.23	26.07	0.004
Error	4	843.2	210.80		
Total	9	25474.4			

S = 14.52    R-Sq = 96.69%    R-Sq(adj) = 92.55%

#### Two-way ANOVA: Dry Marshal Stability versus Type of additives, % Residual Asphalt

Source	DF	SS	MS	F	P
Type of additives	1	7.7536	7.75358	67.22	0.001
% Residual Asphalt	4	8.7960	2.19901	19.06	0.007
Error	4	0.4614	0.11535		
Total	9	17.0110			

S = 0.3396    R-Sq = 97.29%    R-Sq(adj) = 93.90%

#### Two-way ANOVA: Soaked Marshal Stability versus Type of additives, % Residual Asphalt

Source	DF	SS	MS	F	P
Type of additives	1	1.58958	1.58958	33.45	0.004
% Residual Asphalt	4	4.55402	1.13851	23.96	0.005
Error	4	0.19008	0.04752		
Total	9	6.33368			

S = 0.2180    R-Sq = 97.00%    R-Sq(adj) = 93.25%

#### General Linear Model: Mr versus Temp., TYPE OF ADD, Confining Pr., DEV.

Factor	Type	Levels	Values
Temp.	fixed	2	1, 2
TYPE OF ADD	fixed	2	1, 2
Confining Pressure	fixed	5	1, 2, 3, 4, 5
DEV	fixed	5	1, 2, 3, 4, 5

Analysis of Variance for Mr, using Adjusted SS for Tests

Source	DF	Seq SS	Adj SS	Adj MS	F	P
Temp.	1	45793	45793	45793	7.18	0.009
TYPE OF ADD	1	8100	8100	8100	1.27	0.264
Confining Pressure	4	2492297	993146	248287	38.94	0.000
DEV	4	4578132	4578132	1144533	179.51	0.000
Error	65	414441	414441	6376		
Total	75	7538763				

S = 79.8499    R-Sq = 94.50%    R-Sq(adj) = 93.66%

### Minitab ANOVA Printout: Sand Soil

#### Two-way ANOVA: Dry ITS versus Type of additives, % Residual Asphalt

Source	DF	SS	MS	F	P
Type of additives	1	3280.7	3280.69	17.06	0.014
% Residual Asphalt	4	7376.7	1844.17	9.59	0.025
Error	4	769.2	192.31		
Total	9	11426.6			

S = 13.87    R-Sq = 93.27%    R-Sq(adj) = 84.85%

#### Two-way ANOVA: Dry Marshal Stability versus Type of additives, % Residual Asphalt

Source	DF	SS	MS	F	P
Type of additives	1	10.5750	10.5750	56.25	0.002
% Residual Asphalt	4	34.4188	8.6047	45.77	0.001
Error	4	0.7519	0.1880		
Total	9	45.7457			

S = 0.4336    R-Sq = 98.36%    R-Sq(adj) = 96.30%

#### Two-way ANOVA: Soaked Marshal Stability versus Type of additives, % Residual Asphalt

Source	DF	SS	MS	F	P
Type of additives	1	5.1273	5.12729	63.49	0.001
% Residual Asphalt	4	19.3503	4.83758	59.91	0.001
Error	4	0.3230	0.08075		
Total	9	24.8006			

S = 0.2842    R-Sq = 98.70%    R-Sq(adj) = 97.07%

#### General Linear Model: $M_R$ versus Temp., TYPE OF ADD, Confining Pr., DEV.

Factor	Type	Levels	Values
Temp.	fixed	2	1, 2
TYPE OF ADD	fixed	2	1, 2
Confining Pressure	fixed	5	1, 2, 3, 4, 5
DEV	fixed	5	1, 2, 3, 4, 5

Analysis of Variance for  $M_R$ , using Adjusted SS for Tests

Source	DF	Seq SS	Adj SS	Adj MS	F	P
Temp.	1	27901	27901	27901	4.53	0.037
TYPE OF ADD	1	1731	1731	1731	0.28	0.598
Confining Pressure	4	2328459	935992	233998	38.02	0.000
DEV	4	4009368	4009368	1002342	162.86	0.000
Error	65	400048	400048	6155		
Total	75	6767506				

S = 78.4512    R-Sq = 94.09%    R-Sq(adj) = 93.18%

## APPENDIX B

### AN EXAMPLE OF PAVEMENT THICKNESS DESIGN CHART

#### DEVELOPMENT

- a) To show how permanent deformation parameters ( $\alpha$  and  $\mu$ ) were obtained, marl soil treated with SFA and tested at 40 °C under stress level of 60 psi is used as an example. The result of dynamic triaxial test (the straight portion in the second stage) was presented in the log-log scale as shown in Figure B-1 below and thereafter, the slope (b) and intercept (a) coefficients of the curve were obtained. Resilient strain was calculated according to Eq. 5.4. Finally  $\alpha$  and  $\mu$  were calculated using Eq. 5.2.

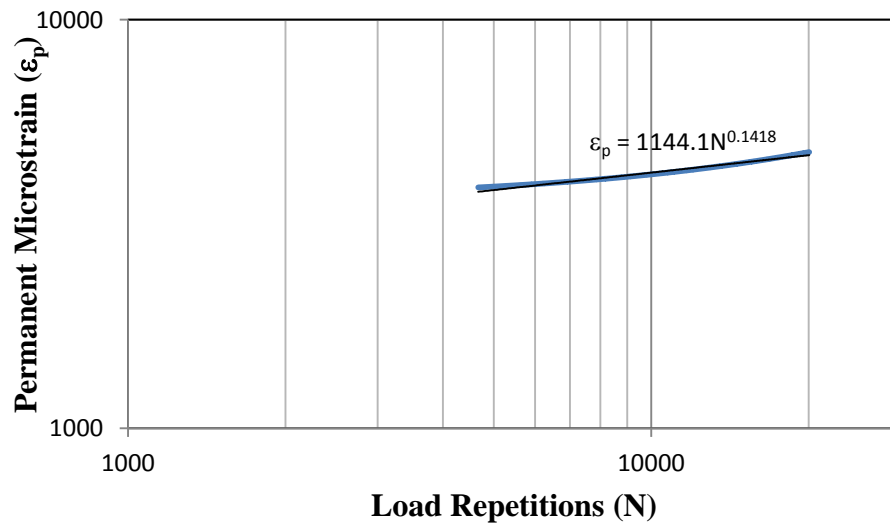


Figure B.1: Plot of Regression Coefficients a and b from Log Permanent Strain-Log Number of Loading Cycles.

Deviator stress = 413.68 kPa (60 psi)

Resilient modulus = 1683.2 Mpa (from Table 4.4)

Resilient Strain  $\epsilon_r = \frac{\sigma_d}{M_R} = 246$  microstrain

a = 1144 and b = 0.141 (from Figure B.1). Hence,  $\mu = \frac{ab}{\epsilon_r} = 0.653$  and  $b = 1 - \alpha = 0.859$



- b) To show how pavement thickness design charts for the stabilized materials were developed, the pavement structure shown in Figure B.2 where sabkha soil treated with foamed sulfur asphalt (SFA) as a base layer is used as an example (see cases analyzed in Chapter 5):

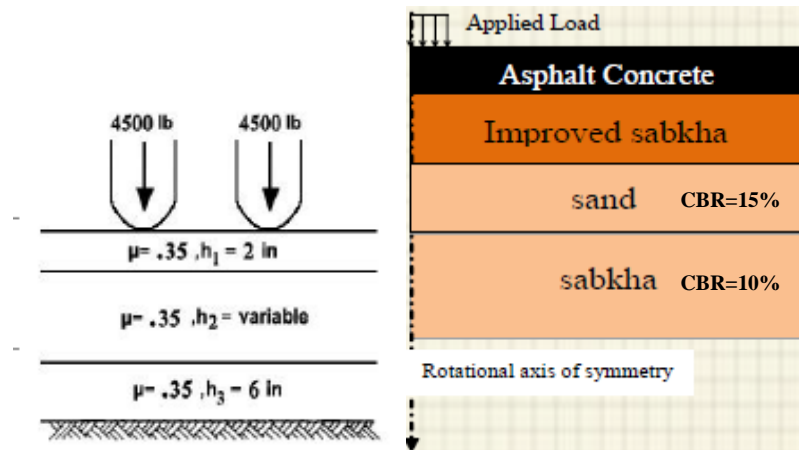


Figure B.2: Case 2(b): Four Layers System Sabkha Subgrade

- Case 2 (b) shown in Figure B.2 is a four layers system with AC layer (2 inch), stabilized sabkha base layer (variable thickness), sand subbase layer (6 inch) with CBR = 15% and sabkha subgrade soil with CBR = 10%. Poisson ratio = 0.35 for all layers.
- The thickness of AC layer (2 inch) and sand subbase layer (6 inch) were selected according to the specification of the Ministry of Transport.
- The purpose was to develop a thickness design chart for the SFA- sabkha base layer by changing its thickness and determined the corresponding rutting life for the pavement structure.
- By fixing the AC and sand subbase layers thicknesses and starting with 4 inch (100 mm) stabilized base layer thickness the following was performed:

- Resilient modulus for subgrade and subbase were calculated based on CBR value using formula  $M_R \text{ (psi)} = 2555 (\text{CBR})^{0.64}$  or  $M_R \text{ (MPa)} = 17.6 (\text{CBR})^{0.64}$

$$M_R \text{ (subgrade)} = 77 \text{ MPa} \quad M_R \text{ (subbase)} = 100 \text{ MPa}$$

- Using the procedure explained in Chapter 5 for resilient modulus calculation for the stabilized base layer the average stress calculated using 3D move FE software was 184 kPa (26.7 psi) at 22 °C and 215 kPa (31.2 psi) at 40 °C.
- Based on the calculated average stress and by using Table 4.4, the resilient modulus of the stabilized sabkha base layer:

$$M_R (22 \text{ } ^\circ\text{C}) = 757.1 \text{ MPa and } M_R (40 \text{ } ^\circ\text{C}) = 848 \text{ MPa}$$

- Using the calibrated rutting models (Table 5.3 and Table 5.5), the permanent deformation parameters of the stabilized sabkha base layer were calculated:

$$\text{At } 22 \text{ } ^\circ\text{C} : \mu = 0.001 \quad \text{and} \quad \alpha = 0.674$$

$$\text{At } 40 \text{ } ^\circ\text{C}: \mu = 0.212 \quad \text{and} \quad \alpha = 0.653$$

- Permanent deformation parameters for subgrade soils (Table 5.1):

$$\text{For sabkha: } \mu = 0.20 \quad \text{and} \quad \alpha = 0.85$$

$$\text{For sand: } \mu = 0.43 \quad \text{and} \quad \alpha = 0.80$$

- Permanent deformation parameters for AC layer:

$$\text{At } 22 \text{ } ^\circ\text{C}: \mu = 0.35 \quad \text{and} \quad \alpha = 0.78$$

$$\text{At } 40 \text{ } ^\circ\text{C}: \mu = 0.34 \quad \text{and} \quad \alpha = 0.63$$

- Using VESYS 5W software and input all structural information above for all pavement layers at the two seasons temperatures (22 °C and 40 °C), the total traffic in the terms of equivalent 80 kN (18 kips) axle load (EAL) required to cause total rutting failure (2.54 cm) was determined as ( $N = 2,883,110$ ) and plotted versus the stabilized layer thickness (4 inch = 100 mm). This is considered one point in the curve of the design chart.
- The thickness of the stabilized base layer was then increased and the process was repeated to get the remaining points.

## **Vitae**

Name : Gamil Mahyoub Saif Abdullah.

Nationality : Yemeni.

Date of Birth : October 10, 1975.

Email : aboashraf\_76@yahoo.com, saif.gamil@gmail.com.

Address : Taiz-Yemen.

Educational Qualifications :

1. Bachelor of Science in Civil Engineering (Water Resources Engineering) from University of Baghdad (June, 1997).
2. Master of Science in Civil Engineering (Geotechnical Engineering) from King Fahd University of Petroleum and Minerals (May, 2009).